RESEARCH ARTICLE

Contribution to the knowledge of the genus *Solskyia* Solsky, 1881 (Coleoptera, Tenebrionidae, Akidini) from China

Xing-Long Bai[1], Jing-Ze Liu[1], Guo-Dong Ren[2]

1 *Hebei Key Laboratory of Animal Physiology, Biochemistry and Molecular Biology, College of Life Sciences, Hebei Normal University, Shijiazhuang, Hebei 050024, China* **2** *The Key Laboratory of Zoological Systematics and Application, School of Life Sciences, Institute of Life Science and Green Development, Hebei University, Baoding, Hebei 071002, China*

Corresponding authors: Jing-Ze Liu (liujingze@hebtu.edu.cn), Guo-Dong Ren (gdren@hbu.edu.cn)

Citation: Bai X-L, Liu J-Z, Ren G-D (2022) Contribution to the knowledge of the genus *Solskyia* Solsky, 1881 (Coleoptera, Tenebrionidae, Akidini) from China. ZooKeys 1122: 1–18. https://doi.org/10.3897/zookeys.1122.86071

Abstract

Two new species of the genus *Solskyia*, *S. infossata* **sp. nov.** and *S. lhozhaga* **sp. nov.**, are described and illustrated from Xizang, China. *Solskyia lhasana* is redescribed and figured based on a male, and new material of *S. caporiaccoi* and *S. parvicollis* from China is documented. The ecology and biology of adults and larvae is briefly introduced. Furthermore, photographs of habitat, and a key to Chinese species are presented.

Keywords

Biology, darkling beetles, ecology, larvae, new species, Pimeliinae, redescription

Introduction

The tribe Akidini Billberg (Tenebrionidae, Pimeliinae) is divided into five genera: *Akis* Herbst, *Cyphogenia* Solier, *Morica* Dejean, *Sarothropus* Kraatz, and *Solskyia* Solsky (Bouchard et al. 2021). Two of them, *Cyphogenia* and *Solskyia*, are recorded from China (Iwan et al. 2020). *Cyphogenia* can be easily distinguished from *Solskyia* by the onychium, which is lobed ventrally.

Solskia used by Semenov (1891) and *Solskya* used by Semenov (1908) turned out to be incorrect subsequent spellings for *Solskyia* Solsky, 1881 (Bouchard et al. 2021), which have been followed by subsequent authors (e.g., Kaszab 1965; Ren and Yu 2000). To date, twelve species have been described in the genus *Solskyia* worldwide. Species of this genus are known to occur only in Asia, distributed from Central Asia to Kashmir and the Himalayas, and also found in China (Iwan et al. 2020). Most of them were mentioned in publications or monographs on tenebrionid beetles (e.g., Kraatz 1865; Reitter 1904; Español 1961; Medvedev 1968; Ren and Yu 2000), scientific reports of expeditions (e.g., Bates 1879; Della Beffa 1931; Gridelli 1934), and studies of regional faunas (e.g., Solsky 1881; Semenov 1889, 1891; Fairmaire 1891; Kaszab 1965, 1970). Among them, the contribution of Español (1961) was very valuable, including known previous species of the genus; two known species (i.e., *S. grombczewskii* Semenov, *S. parvicollis* Kraatz) were redescribed and two new species (i.e., *S. kaszabi* Español, *S. schmidi* Español) were described with line drawings of the habitus and male genitalia; an identification key to all known species of the genus was presented.

Three species of the genus *Solskyia* have been recorded from Xinjiang and Xizang, China until now (Ren and Yu 2000; Iwan et al. 2020). The first species, *Akis parvicollis* Kraatz, 1865, was mentioned in the publication of Kraatz's revision of the Old World tenebrionids [Kraatz (1865); from Lacordaire's group of Akisides]. The second species, *Solskyia caporiaccoi* Gridelli, 1934 was collected by the Italian expedition to Karakoram. The last species, *Solskyia lhasana* Ren & Yu, 2000, was described from Xizang, China based on a single female specimen.

This study aims to present an overview of the species belonging to the genus *Solskyia* in China, with a redescription of *S. lhasana* based on a male and the description of two new species from Xizang.

Materials and methods

The specimens were examined and dissected under a Nikon SMZ800 microscope, and photographs were taken using Canon EOS 5DSR camera. Aedeagi and ovipositors were detached from the body with insect pins, then glued to separate cards and pinned under the specimens. Specimens examined in this study are deposited in **HBUM** (Hebei University Museum, Baoding, China), and **IPPP** (Collection of Insect Prevention of The Potala Palace [布达拉宫防虫标本室], Lhasa, China). Larvae mentioned in this paper were collected along with adults in the same localities at the same time, with confirmed identity by emerging into adults by rearing in the laboratory. A single slash (/) separates data of different lines on a label, a double slash (//) separates data of different labels, authors' remarks are enclosed in brackets "[ ]".

Ecology and biology

Species of *Solskyia* live in the semi-deserts and mountains of Asia (Figs 15, 19, 23, 26, 30). Generational overlap is present in *Solskyia* species, and adults and larvae can be

found at the same time. Generally, they are hidden under stones, in crevices and caves (Figs 16, 23, 27, 30) during the day. In contrast, they are more frequent during the night, and can be found on the ground (Fig. 21), representing a large part of the local darkling beetle species abundance. Larvae can dig (Fig. 18). Adults secrete fluid from mouthparts when startled (Fig. 22), possibly as a form of defense.

A larva was collected from Günsa Township, Gar County, Xizang in August 24, 2015, and brought back to the laboratory for rearing. Eclosion into an adult occurred in late May 2016. The pupal stage was very short, just a few days.

Taxonomy

Genus *Solskyia* Solsky, 1881

Solskyia Solsky, 1881: 48; Gridelli 1934: 47; Español 1961: 123; Ren and Yu 2000: 325 (incorrect spelling as *Solskia*); Löbl et al. 2008: 127; Iwan et al. 2020: 138.

Type species. *Solskyia peregrina* Solsky, 1881, by monotypy.

Solskyia caporiaccoi Gridelli, 1934
Figs 15–22

Solskyia caporiaccoi Gridelli, 1934: 53; Español 1961: 131; Ren and Yu 2000: 326 (incorrect spelling as *Solskia*); Löbl et al. 2008: 127; Iwan et al. 2020: 138.

Material examined. China: 1♀ (HBUM), Burang County, Xizang, 1974-VIII-18, leg. Ji-Jun Li; 1♀ (HBUM), Burang County, Xizang, 2006-VIII-20, leg. Ming-Sheng Zhu; 1 ex. (HBUM), Burang County, Xizang, 30°17'11.8"N, 81°10'30.6"E, 3875 m, 2022-VII-8, leg. Jun-Sheng Shan; 3 ex. (HBUM), Burang County, Xizang, 30°16.5852'N, 81°11.4735'E, 4006 m, 2022-VII-10, leg. Guo-Dong Ren, Yi-Ping Niu, Xing-Long Bai, Kai-Xuan Liu; 2 ex. (HBUM), Qangzê Township, Zanda County, Xizang, 31°41.282'N, 79°46.610'E, 4420 m, 2015-VIII-24, leg. Guo-Dong Ren, Xing-Long Bai, Jun-Sheng Shan; 22 ex. (HBUM), Qangzê Township, Zanda County, Xizang, 31°49.779'N, 79°37.540'E, Alt. 4222 m, 2018-VIII-11, leg. Xing-Long Bai, Zi-Yuan Hu, Ming-Min Ma; 2 ex. (HBUM), Zanda Tulin, Zanda County, Xizang, 31°40.548'N, 79°44.382'E, Alt. 4047 m, 2018-VIII-11, leg. Xing-Long Bai, Zi-Yuan Hu, Ming-Min Ma; 1 ex. (HBUM), Zanda Tulin, Zanda County, Xizang, 31°33.846'N, 79°50.181'E, Alt. 4129 m, 2018-VIII-13, leg. Xing-Long Bai, Zi-Yuan Hu, Ming-Min Ma; 9 ex. (HBUM), Diyag Township, Zanda County, Xizang, 31°48.077'N, 78°50.666'E, Alt. 2956 m, 2018-VIII-12, leg. Xing-Long Bai, Zi-Yuan Hu, Ming-Min Ma; 61 ex. (HBUM), Diyag Township, Zanda County, Xizang, 31°47.026'N, 78°52.052'E, Alt. 2978 m, 2018-VIII-12, leg. Xing-Long Bai, Zi-Yuan Hu, Ming-Min Ma.

Distribution. China: Xizang; Kashmir.

Solskyia infossata sp. nov.
https://zoobank.org/DB08D547-1250-4800-B9CE-73A91270A069
Figs 1–5, 23–25

Type material. *Holotype*: ♂ (HBUM), 2018-VIII-6 / 西藏 林芝市朗县 [Nang County, Nyingchi City, Xizang] / 闫霞 [leg. Xia Yan] 3016 m / 西华师大标本馆 [Museum of China West Normal University]. *Paratypes*: 5 ex. (HBUM), 2018-VIII-6 / 西藏 林芝市朗县 [Nang County, Nyingchi City, Xizang] / 闫霞 [leg. Xia Yan] 3016 m / 西华师大标本馆 [Museum of China West Normal University]; 12 ex. (HBUM), 2019-VII-28 / 西藏加查加查镇奴巧村 [Nuqiao Village, Gyaca Town, Gyaca County, Xizang] / 潘昭 李秀敏 文明 王兰蕊 [leg. Zhao Pan, Xiu-Min Li, Ming Wen, Lan-Rui Wang] / 河北大学博物馆 [Hebei University Museum] // 29°08'19"N, 92°39'11"E / Alt. 3285 m / 河北大学博物馆 [Hebei University Museum].

Diagnosis. This new species closely resembles *S. lhozhaga* sp. nov., but can be distinguished from the latter by the following characters: (1) punctures on head finer (coarser in *S. lhozhaga*); (2) lateral sides of pronotum weakly "S" curved (arcuate in *S. lhozhaga*), posterior angles sharp and protruding outwards (weakly obtuse in *S. lhozhaga*). This new species is also somewhat similar to *S. lhasana*, it differs from the later by the following characters: (1) body wide-oval (elongate-oval in *S. lhasana*); (2) lateral margins of pronotum weakly "S" curved (arcuate in *S. lhasana*); (3) elytra wide and short (narrow and long in *S. lhasana*), base wider than pronotum (narrower in *S. lhasana*), lateral margins widest near middle (subparallel in *S. lhasana*), humeri rectangular-angled, rounded apically (widely obtuse in *S. lhasana*), surface of elytra and epipleura with punctures (granules in *S. lhasana*).

Distribution. China: Xizang.

Etymology. The species name is derived from its depressed dorsal side of the body.

Description. Total length 14.6–18.1 mm; width 8.0–9.2 mm. Wide-oval, dorsal side depressed, ventral side strongly convex. Body black, weakly shiny; labrum, palpi, antennomeres IX–XI and tarsi brown.

Head. Anterior margin of labrum nearly straight, with long setae, lateral margins parallel, distal part punctate, basal half smooth. Anterior margin of clypeus nearly straight at middle and serrate, lateral angles toothed and protruding forwards, with a deep incision between lateral angles and anterior part of genae; surface convex, sparsely and finely punctate. Clypeogenal suture indicated. Dorsal surface of head flat, lateral sides above eyes longitudinally carinate, shallowly, sparsely and finely punctate. Genal margins nearly right-angled protruding outwards before eyes, straightly converging forwards, strongly and arcuately narrowing backwards, sparsely and finely punctate. Eyes transverse. Temples behind eyes strongly and roundly narrowing backwards, punctures larger. Mentum transverse, anterior margin widely triangular emarginate, lateral margins subparallel and tilt up. Antennae slender and long, reaching beyond the pronotal base; basal part of antennomere I invisible in dorsal view, II very short, III very long, IV–VIII gradually shorter, X nearly spherical; XI sharped-oval, narrow and small, closely joint with X; III–VIII thicker at apex; apex of I–X with sparse setae and
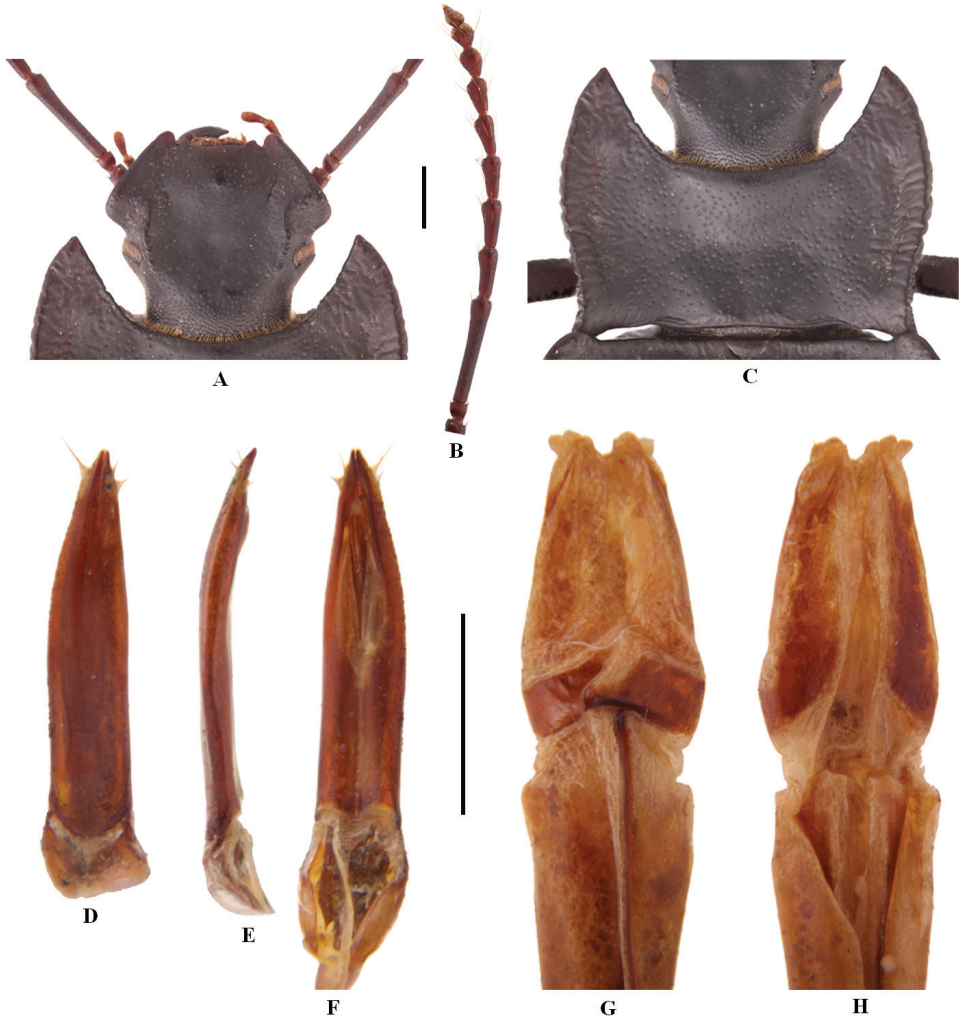
Figure 1. Characters of *Solskyia infossata* sp. nov. **A–F** male **A** head **B** antenna **C** pronotum **D–F** aedeagus in dorsal, lateral and ventral view, respectively **G, H** female: ovipositor in dorsal and ventral view, respectively. Scale bars: 3.5 mm (**A–C**); 1.0 mm (**D–H**).

gradually longer; inner side of apex of VIII, inner side and outside of apex of IX–X, apex of XI with sensilla.

Prothorax. Pronotum transverse, subcordiform, widest at middle, 2.4 times as wide as long, significantly wider than head; anterior margin deeply emarginate, beaded laterally; lateral margins weakly "S" curved, broadly beaded and strongly tilt up; posterior margin bisinuate, finely beaded; anterior angles sharp and protruding forwards, posterior angles sharp and protruding; lateral margins and sides wrinkled; surface strongly depressed with transverse depression in middle, weakly triangular convex in middle of anterior margin, shallowly, sparsely and coarsely punctate. Prothoracic hy-

Figure 2–5. Habitus of *Solskyia infossata* sp. nov. **2–3, 5** male (holotype) in dorsal, ventral and oblique view, respectively **4** female (paratype). Scale bars: 3.5 mm.

pomera depressed, smooth, shallowly and sparsely punctate. Prosternal process weakly sloping behind procoxae, apex blunt in lateral view.

Pterothorax. Elytra wide-oval, widest near middle, 1.1 times as long as wide; anterior margin nearly straight, base slightly wider than pronotum; lateral margins arcuate, weakly narrowing toward base and strongly narrowing toward apex from middle, lateral margins raised, humeri broad and wrinkled, right-angled, rounded apically; surface depressed, more deeply at base, but strongly convex near the middle of anterior margin, declivity sharply sloping downwards; sparsely and finely punctate, shallowly near base, lateral sides and apex, shallowly and coarsely wrinkled; epipleura wide, weakly convex, surface matte, shallowly, sparsely and finely punctate, shallowly and coarsely wrinkled. Scutellum triangular.

Abdomen. Ventrites strongly convex, densely and coarsely punctate, sparsely and shallowly near lateral sides and apex of the last ventrite; apical margin of the last ventrite widely rounded.

Legs. Slender and long; femora claviform, smooth; tibiae straight, rough; ventral surface of pro- and mesotarsomeres I–IV and metatarsomeres I–III with hairy tuft at apex; claws well developed.

Aedeagus. As in Fig. 1D–F. Length 2.6 mm, width 0.6 mm. Parameres length 2.0 mm, width 0.4 mm.

Ovipositor. As in Fig. 1G, H.

Sexual dimorphism. Females usually with slightly wider and more convex elytra, but in many cases, it is impossible to distinguish the two sexes without extracting the genitalia.

Solskyia lhasana **Ren & Yu, 2000**
Figs 6–9

Solskyia lhasana Ren & Yu, 2000: 325 (incorrect spelling as *Solskia*); Löbl et al. 2008: 127; Iwan et al. 2020: 138.

Type material. *Holotype*: ♀ (HBUM), 1979-V-10 / 西藏拉萨 [Lhasa, Xizang] / 李法圣 [leg. Fa-Sheng Li] / 河北大学博物馆 [Hebei University Museum] // HOLOTYPE.

Additional material. Cʜɪɴᴀ: 1♂ (HBUM), Zêtang Town, Shannan City, Xizang, 3538 m, 2018-VIII-13, leg. Liang Xiang; 1 ex. (IPPP), The Potala Palace, Lhasa, Xizang.

Distribution. China: Xizang.

Description of male. Length 17.9 mm; width 7.0 mm. Oval, elongated, dorsal side depressed, ventral side strongly convex. Body black, weakly shiny; labrum, palpi, antennomeres IX–XI and tarsi brown.

Head. Anterior margin of labrum nearly straight, with long setae, lateral margins parallel, distal part punctate, basal half smooth. Anterior margin of clypeus serrate, lateral angles weakly toothed and protruding forwards, with a shallow incision between lateral angles and anterior part of genae; surface convex, sparsely and finely punctate. Clypeogenal suture indicated. Dorsal surface of head flat, lateral sides above eyes longitudinally carinate, sparsely and finely punctate. Genal margins weakly obtuse-angled protruding outwards before eyes, straightly converging forwards, strongly and arcuately narrowing backwards, sparsely and finely punctate. Eyes transverse. Temples behind eyes strongly and roundly narrowing backwards, finely punctate. Mentum transverse, anterior margin widely triangularly emarginate, lateral margins arcuate and elevated. Antennae slender and long, reaching beyond the pronotal base; basal part of antennomere I invisible in dorsal view, II very short, III very long, IV–VIII gradually shorter, X nearly spherical; XI sharped-oval, narrow and small, closely joint with X; III–VIII thicker at apex; apex of I–X with sparse setae and gradually longer; inner side of apex of VIII, inner side and outside of apex of IX–X, apex of XI with sensilla.

Prothorax. Pronotum transverse, widest at middle, 2.2 times as wide as long, significantly wider than head; anterior margin deeply emarginate, beaded laterally; lateral margins arcuate, broadly beaded and strongly raised; posterior margin bisinuate, finely rimmed; anterior angles sharp and protruding forwards, posterior angles sharp and protruding outwards; lateral margins and sides wrinkled; surface strongly depressed with transverse depression in middle, weakly triangular convex in middle of anteri-
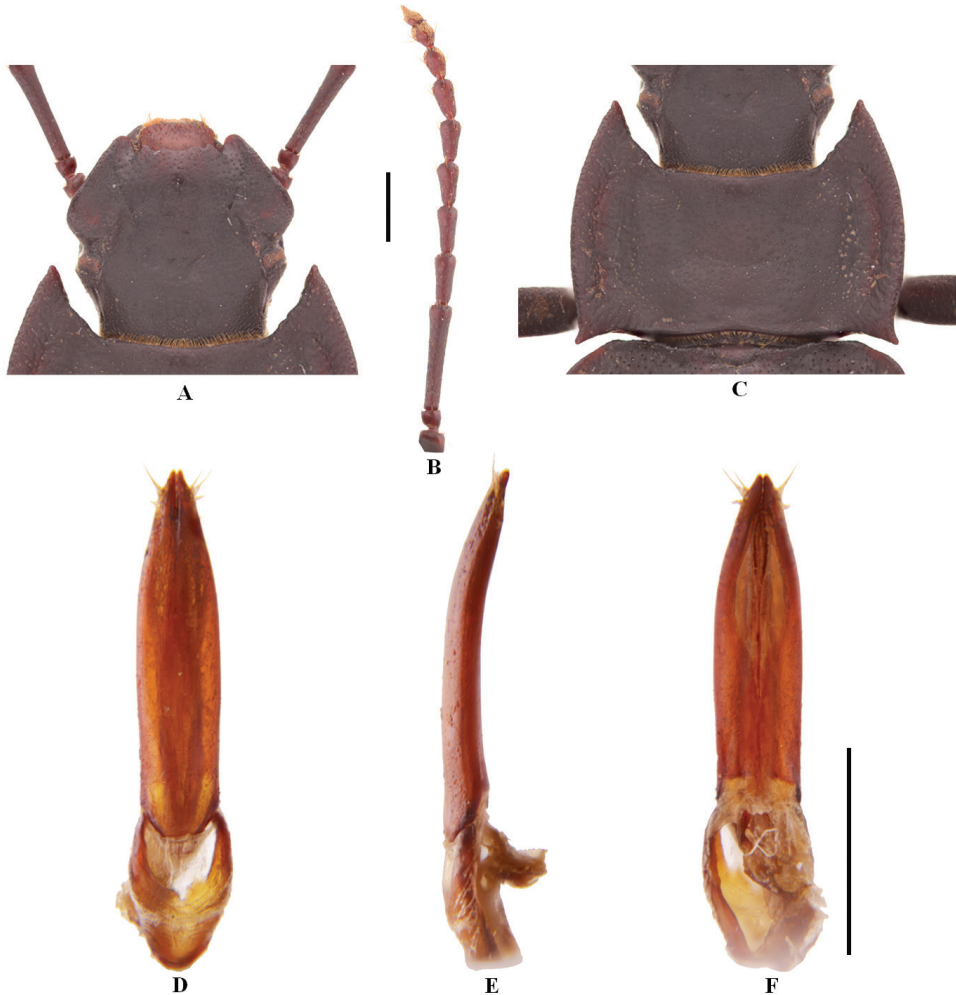
Figure 6. Characters of *Solskyia lhasana* Ren & Yu (male) **A** head **B** antenna **C** pronotum **D–F** aedeagus in dorsal, lateral and ventral view, respectively. Scale bars: 3.5 mm (**A–C**); 1.0 mm (**D–F**).

or margin, shallowly, sparsely and finely punctate. Prothoracic hypomera depressed, smooth, shallowly and sparsely punctate. Prosternal process weakly sloping behind procoxae, apex blunt in lateral view.

Pterothorax. Elytra oval elongated, widest near middle, 1.6 times as long as wide; anterior margin nearly straight, base narrower than pronotum; lateral sides subparallel, weakly narrowing toward base and strongly narrowing toward apex from middle, lateral margin raised; humeri widely obtuse-angled; surface depressed, deeper at base, declivity sharply sloping downwards; sparsely and finely granulated, shallowly and coarsely wrinkled; epipleura wide, weakly convex, sparsely and finely granulated, shallowly and coarsely wrinkled. Scutellum semicircular.
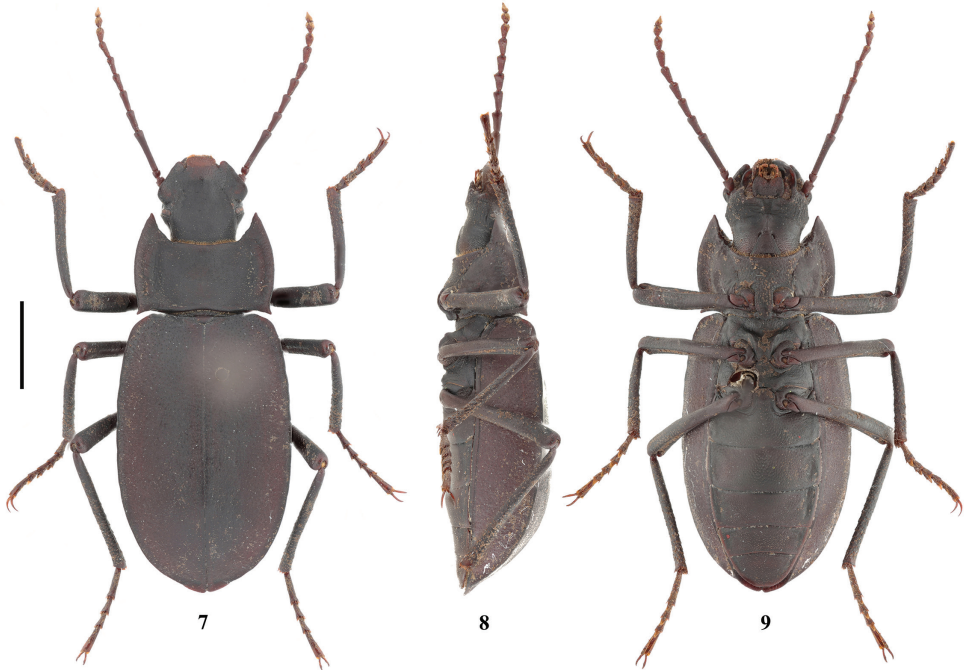
Figure 7–9. Habitus of *Solskyia lhasana* Ren & Yu (male) in dorsal, lateral and ventral view, respectively. Scale bars: 3.5 mm.

Abdomen. Ventrites strongly convex, shallowly punctate, gradually finer toward lateral sides and apex of the last ventrite; apical margin of the last ventrite widely rounded.

Legs. Slender and long; femora claviform, smooth; tibiae straight, rough; ventral surface of pro- and mesotarsomeres I–IV and metatarsomeres I–III with hairy tuft at apex; claws well developed.

Aedeagus. As in Fig. 6D–F. Length 2.4 mm, width 0.5 mm. Parameres length 1.8 mm, width 0.4 mm.

Solskyia lhozhaga sp. nov.

https://zoobank.org/72724339-6D66-44A5-AB0C-D2CA358CA483
Figs 10–14, 26–29

Type material. *Holotype*: ♂ (HBUM), 2014-VIII-7 / 西藏洛扎县生格乡 [Sênggê Township, Lhozhag County, Xizang] / 任国栋 白兴龙 单军生 [leg. Guo-Dong Ren, Xing-Long Bai, Jun-Sheng Shan] / 河北大学博物馆 [Hebei University Museum] // 28°12.752'N, 91°00.770'E / Alt. 3225 m / 河北大学博物馆 [Hebei University Museum]. *Paratypes*: 20 ex. (HBUM), 2014-VIII-7 / 西藏洛扎县生格乡 [Sênggê Township, Lhozhag County, Xizang] / 任国栋 白兴龙 单军生 [leg. Guo-Dong Ren,
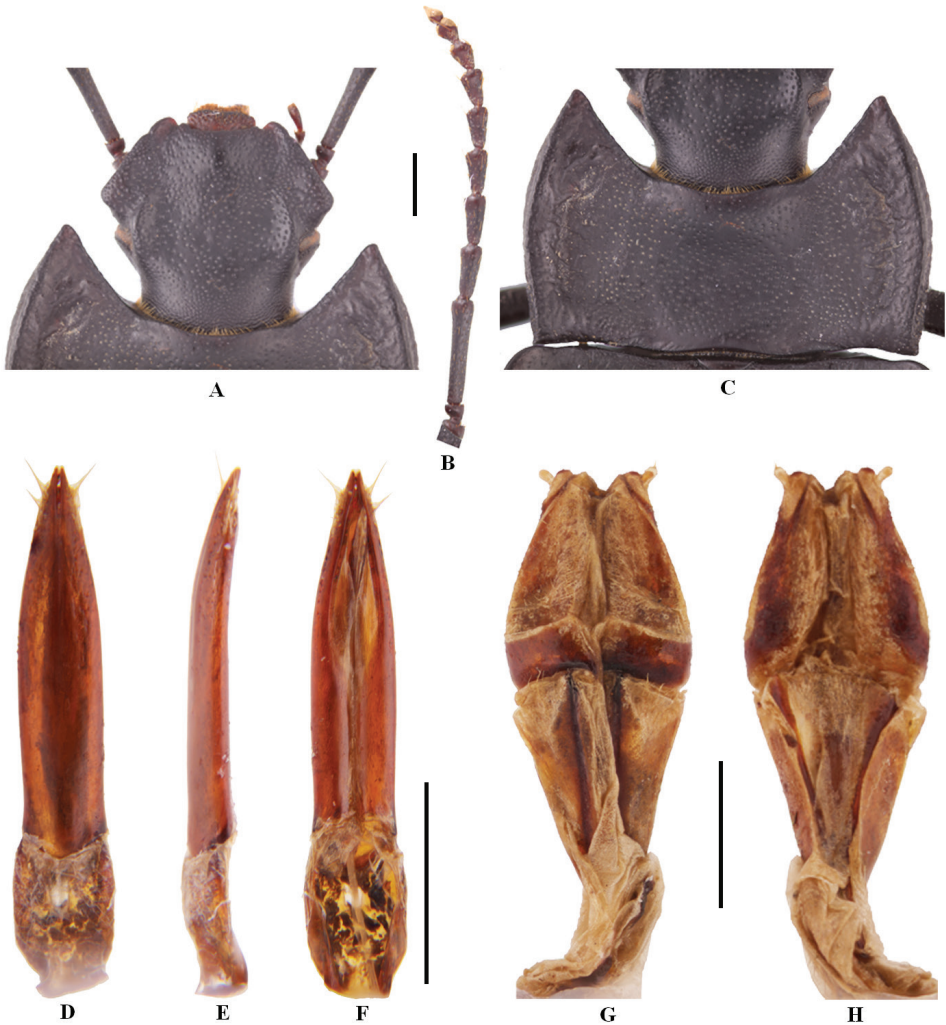
Figure 10. Characters of *Solskyia lhozhaga* sp. nov. **A–F** male **A** head **B** antenna **C** pronotum **D–F** aedeagus in dorsal, lateral and ventral view, respectively **G, H** female: ovipositor in dorsal and ventral view, respectively. Scale bars: 3.5 mm (**A–C**); 1.0 mm (**D–H**).

Xing-Long Bai, Jun-Sheng Shan] / 河北大学博物馆 [Hebei University Museum] // 28°12.752'N, 91°00.770'E / Alt. 3225 m / 河北大学博物馆 [Hebei University Museum]; 1 ex. (HBUM), 2022-VII-22 / 西藏洛扎拉康镇杰拉山 [Gyai La Shan, Lhakang Town, Lhozhag County, Xizang] / 任国栋 牛一平 白兴龙 刘凯璇 [leg. Guo-Dong Ren, Yi-Ping Niu, Xing-Long Bai, Kai-Xuan Liu] / 河北大学博物馆 [Hebei University Museum] // 28°08.0839'N, 91°09.3682'E / Alt. 3302 m / 河北大学博物馆 [Hebei University Museum].

Diagnosis. This new species closely resembles *S. infossata* sp. nov., but can be distinguished from the latter by the following characters: (1) punctures on head
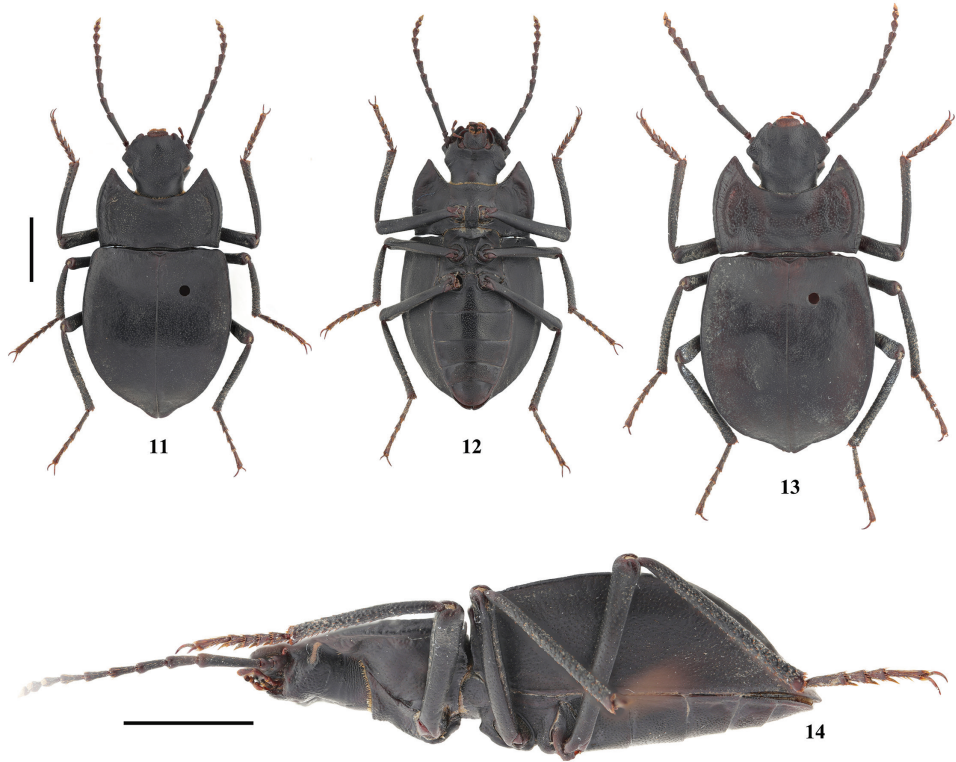
Figure 11–14. Habitus of *Solskyia lhozhaga* sp. nov. **11, 12, 14** male (holotype) in dorsal, ventral and lateral view, respectively **13** female (paratype). Scale bars: 3.5 mm.

coarser (finer in *S. infossata*); (2) lateral margins of pronotum arcuate (weakly "S" curved in *S. infossata*), posterior angles weakly obtuse (sharp and protruding outwards in *S. infossata*). This new species is also somewhat similar to *S. lhasana*, it differs from the later by the following characters: (1) body wide-oval (oval elongated in *S. lhasana*); (2) punctures on head coarser (finer in *S. lhasana*); (3) posterior angles of pronotum weakly obtuse (sharp and protruding outwards in *S. lhasana*), coarsely punctate (finely in *S. lhasana*); (4) elytra wide and short (narrow and long in *S. lhasana*), base wider than pronotum (narrower in *S. lhasana*), lateral margins widest near middle (subparallel in *S. lhasana*), humeri right-angled, rounded apically (widely obtuse in *S. lhasana*), surface of elytra and epipleura with punctures (granules in *S. lhasana*).

Distribution. China: Xizang.

Etymology. The species name is derived from the type locality – Lhozhag.

Description. Total length 16.6–19.2 mm; width 8.5–9.9 mm. Wide-oval, dorsal side depressed, ventral side strongly convex. Body black, weakly shiny; labrum, palpi, antennomeres IX–XI and tarsi brown.

Head. Anterior margin of labrum nearly straight, with long setae, lateral margins parallel, distal part punctate, basal half smooth. Anterior margin of clypeus nearly straight at middle and serrate, lateral angles weakly toothed and protruding forwards,

Figure 15–18. Habitat **15, 16** adult **17** and larva **18** of *Solskyia caporiaccoi* Gridelli in Qangzê Township, Zanda County, Xizang, China.

Figure 19–22. Habitat **19, 20** and adults **21, 22** of *Solskyia caporiaccoi* Gridelli in Diyag Township, Zanda County, Xizang, China.

Figure 23–25. Habitat **23** and adults **24, 25** of *Solskyia infossata* sp. nov. in Nuqiao Village, Gyaca Town, Gyaca County, Xizang, China (photograph by Zhao Pan).

with a shallow incision between lateral angles and anterior part of genae; surface convex, sparsely and coarsely punctate. Clypeogenal suture inconspicuous. Dorsal surface of head flat, lateral sides above eyes longitudinally carinate, sparsely and coarsely punctate. Genal margins nearly right-angled protruding outwards before eyes, straightly converging forwards, strongly and arcuately narrowing backwards, sparsely and coarsely punctate. Eyes transverse. Temples behind eyes strongly and roundly narrowing backwards, coarsely punctate. Mentum transverse, anterior margin widely triangularly emarginate, lateral margins subparallel and raised. Antennae slender and long, reaching beyond the pronotal base; basal part of antennomere I invisible in dorsal view, II

Figure 26–29. Habitat **26, 27** and adults **28, 29** of *Solskyia lhozhaga* sp. nov. in Sênggê Township, Lhozhag County, Xizang, China.

very short, III very long, IV–VIII gradually shorter, X nearly spherical; XI sharped-oval, narrow and small, closely joint with X; III–VIII thicker at apex; apex of I–X with sparse setae and gradually longer; inner side of apex of VIII, inner side and outside of apex of IX–X, apex of XI with sensilla.

Prothorax. Pronotum transverse, widest at middle, 2.6 times as wide as long, significantly wider than head; anterior margin deeply emarginate, beaded laterally; lateral margins arcuate, broadly beaded and strongly raised; posterior margin bisinuate, finely beaded; anterior angles sharp and protruding forwards, posterior angles weakly obtuse; lateral margins and sides wrinkled; surface strongly depressed with transverse depression in middle, weakly triangular convex in middle of anterior margin, sparsely and coarsely punctate. Prothoracic hypomera depressed, smooth, shallowly and sparsely punctate. Prosternal process weakly sloping behind procoxae, apex blunt in lateral view.

Pterothorax. Elytra wide-oval, widest near middle, 1.1 times as long as wide; anterior margin nearly straight, base slightly wider than pronotum; lateral sides arcuate, weakly narrowing toward base and strongly narrowing toward apex from middle, lateral margins raised, broad and wrinkled at base; humeri right-angled, rounded apically; surface depressed, with deeper depression at base, strongly convex in middle, declivity sharply sloping downwards; sparsely and finely punctate, shallowly near base, lateral sides and apex, inconspicuously wrinkled; epipleura wide, weakly convex, sparsely and finely punctate, inconspicuously wrinkled. Scutellum triangular.

Abdomen. Ventrites strongly convex, densely and coarsely punctate, sparsely and shallowly near lateral sides and apex of the last ventrite; apical margin of the last ventrite widely rounded.

Legs. Slender and long; femora claviform, smooth; tibiae straight, rough; ventral surface of pro- and mesotarsomeres I–IV and metatarsomeres I–III with hairy tuft at apex; claws well developed.

Aedeagus. As in Fig. 10D–F. Length 2.6 mm, width 0.5 mm. Parameres length 2.0 mm, width 0.4 mm.

Ovipositor. As in Fig. 10G, H.

Sexual dimorphism. Females usually with slightly wider and more convex elytra, but in many cases, it is impossible to distinguish the two sexes without extracting the genitalia.

Solskyia parvicollis (Kraatz, 1865)
Figs 30–33

Akis parvicollis Kraatz, 1865: 251.
Solskyia parvicollis: Gridelli 1934: 51; Español 1961: 127; Ren and Yu 2000: 325 (incorrect spelling as *Solskia*); Löbl et al. 2008: 127; Iwan et al. 2020: 138.
Cyphogenia plana Bates, 1879: 471.
Solskyia morawitzi Semenov, 1891: 363.
Solskya kuenluna Kaszab, 1965: 282.

Material examined. China: 2♂, 3♀ (HBUM), Yecheng County [Kargilik], Xinjiang, 1974-VII-12, leg. Xiang-Chu Yin, Ji-Jun Li; 1♀ (HBUM), Rutog County, Xizang, 1974-VII-11, leg. Xiang-Chu Yin, Ji-Jun Li; 5♂, 7♀ (HBUM), Rutog County, Xizang, 1974-VII-12, leg. Xiang-Chu Yin, Ji-Jun Li; 1♂, 1♀ (HBUM), Rutog County, Xizang, 1974-VII-13, leg. Xiang-Chu Yin, Ji-Jun Li; 7♂, 7♀ (HBUM), Shangqulong, Rutog County, Xizang, 1974-VII-12, leg. Xiang-Chu Yin, Ji-Jun Li; 1 ex. (HBUM), Banggong Co, Rutog County, Xizang, 33°26.714'N, 79°48.618'E, Alt. 4288 m, 2018-VIII-9, leg. Xing-Long Bai, Zhong-Hua Wei, Zi-Yuan Hu, Ming-Min Ma; 30 ex. (HBUM), Wüjang Village, Domar Township, Rutog County, Xizang, 33°37.204'N, 79°49.042'E, Alt. 4311 m, 2018-VIII-9, leg. Xing-Long Bai, Zhong-Hua Wei, Zi-Yuan Hu, Ming-Min Ma; 2♀ (HBUM), Shiquanhe Town, Xizang, 2004-VII-15, leg. Ai-Min Shi, Yi-Bin Ba; 1 ex. (HBUM), Shiquanhe Daban, Gar County, Xizang, 32°19.441'N, 80°00.444'E, 5014 m, 2015-VIII-25, leg. Guo-Dong Ren, Xing-Long Bai, Jun-Sheng Shan; 2 ex. (HBUM), Günsa Township, Gar County, Xizang, 31°54.310'N, 80°06.109'E, 4611 m, 2015-VIII-24, leg. Guo-Dong Ren, Xing-Long Bai, Jun-Sheng Shan; 3 ex. (HBUM), Gê'gyai County, Xizang, 32°23.394'N, 81°09.287'E, 4524 m, 2015-VIII-24, leg. Guo-Dong Ren, Xing-Long Bai, Jun-Sheng Shan.

Distribution. China: Xinjiang, Xizang; Kashmir, "Himalaya".

Figure 30–33. Habitat **30** adults **31, 32** and larva **33** of *Solskyia parvicollis* (Kraatz) in Wüjang Village, Domar Township, Rutog County, Xizang, China.

Key to known Chinese species of the genus *Solskyia*

1   Anterior margin of pronotum deeply emarginate, anterior angles sharp and protruding forwards, surface strongly depressed **2**
–   Anterior margin of pronotum slightly emarginate, anterior angles not sharp and not protruding forwards, surface weakly or not depressed **4**
2   Body oval elongated; elytra narrow and long, base narrower than pronotum, lateral margins subparallel, humeri widely obtuse-angled, surface of elytra and epipleura with granules ....*S. lhasana* **Ren & Yu, 2000**
–   Body wide-oval; elytra wide and short, base wider than pronotum, lateral margins arcuate, humeri right-angled, rounded apically, surface of elytra and epipleura with punctures..**3**
3   Lateral margins of pronotum arcuate, posterior angles weakly obtuse............ ....*S. lhozhaga* **sp. nov.**
–   Lateral margins of pronotum weakly "S" curved, posterior angles sharp and protruding ....*S. infossata* **sp. nov.**
4   Posterior angles of pronotum sharp and protruding; humeral carina of elytra elevated, humeri obtuse-angled ....*S. caporiaccoi* **Gridelli, 1934**
–   Posterior angles of pronotum not sharp and not protruding; humeral carina of elytra inconspicuous at base, humeri rounded.. ....*S. parvicollis* **(Kraatz, 1865)**

Acknowledgements

References

Bates F (1879) Characters of the new genera and species of Heteromera collected by Dr. Stoliczka during the Forsyth Expedition to Kashgar in 1873–74. Cistula Entomologica 2[1875–1882]: 467–484.

Bouchard P, Bousquet Y, Aalbu RL, Alonso-Zarazaga MA, Merkl O, Davies AE (2021) Review of genus-group names in the family Tenebrionidae (Insecta, Coleoptera). ZooKeys 1050: 1–633. https://doi.org/10.3897/zookeys.1050.64217

Della Beffa G (1931) Himalaia cashmiriano. Appendici scientifiche. Insetti del Kashmir raccolti dal dott. Cesare Calciati nelle spedizione Mario Piacenza (1913). Rizzoli & C., Milano, 173–187.

Español F (1961) Sobre alcunas *Solskyia* del Paquistán (Col. Tenebrionidae). Miscelánea Zoológica 1(4): 123–131.

Fairmaire L (1891) Descriptions de Coléoptères des montagnes de Kashmir. Comptes-Rendus des Séances de la Société Entomologique de Belgique 1891: lxxxviii–ciii.

Gridelli E (1934) Materiali zoologici raccolti dalla spedizione italiana al Karakoram (1929 – Anno vii). Coleoptera – Tenebrionidae. Atti del Museo Civico di Storia Naturale Trieste 12: 37–68. [pls. ix, x.]

Iwan D, Löbl I, Bouchard P, Bousquet Y, Chigray I, Egorov LV, Kamiński M, Merkl O, Nabozhenko M, Novák V, Ando K, Schawaller W, Soldati F (2020) Family Tenebrionidae Latreille, 1802: 104–475. In: Iwan D, Löbl I (Eds) Catalogue of Palaearctic Coleoptera. Volume 5. Tenebrionoidea. Revised and Updated Second Edition. Koninklijke Brill NV, Leiden-Boston, 945 pp. https://doi.org/10.1163/9789004434998

Kaszab Z (1965) Neue Tenebrioniden (Coleoptera) aus China. Annales Historico-Naturales Musei Nationalis Hungarici 57: 279–285.

Kaszab Z (1970) Beiträge zur Kenntnis der Fauna Afghanistans (Sammelergebniss von O. Jakeš 1963–64, D. Povolný & Fr. Tenora 1966, J. Šimek 1965–66, D, Povolný, J. Geiser, Z.

Šebek & Fr. Tenora 1967). Tenebrionidae, Col. Časopis Moravského Musea, Vědy přírodní 54(Supplementum): 5–182. [23 pls.]

Kraatz G (1865) Revision der Tenebrinoiden der alten Welt aus Lacordaire's Gruppen der Erodiides, Tentyriides, Akisides, Piméliides, und der europäischen Zophosis-Arten. Nicolai, Berlin, 393 pp. https://doi.org/10.5962/bhl.title.118624

Löbl I, Iwan D, Merkl O, Ando K, Bouchard P, Egorov LV, Lillig M, Masomuto K, Nabozhenko M, Novák V, Pettersson R, Schawaller W, Soldati F (2008) Family Tenebrionidae Latreille, 1802: 105–352. In: Löbl I, Smetana A (Eds) Catalogue of Palaearctic Coleoptera. Volume 5. Tenebrionoidea. Apollo Books, Stenstrup, 670 pp.

Medvedev GS (1968) New darkling beetles of the tribe Akidini (Coleoptera, Tenebrionidae). Entomologicheskoe Obozrenie 47: 892–898. [in Russian, English translation: Entomological Review 47: 544–548]

Reitter E (1904) Bestimmungs-Tabelle der Tenebrioniden-Unterfamilien: Lachnogyini, Akidini, Pedinini, Opatrini und Trachyscelini aus Europa und den angrenzenden Ländern. Verhandlungen des Naturforschenden Vereines in Brünn 42[1903]: 25–189.

Ren GD, Yu YZ (2000) On the darkling beetle tribe Akidini from China (Coleoptera: Tenebrionidae). Dong Wu Fen Lei Xue Bao 25(3): 320–329. [in Chinese, with English abstract]

Semenov AP (1889) Diagnoses Coleopterorum novorum ex Asia Centrali. Horae Societatis Entomologicae Rossicae 24: 193–226.

Semenov AP (1891) Diagnoses Coleopterorum novorum ex Asia centrali et orientali. Horae Societatis Entomologicae Rossicae 25[1890–91]: 262–382.

Semenov AP (1908) Analecta coleopterologica. XIV. Revue Russe d'Entomologie 7[1907]: 258–265.

Solsky SM (1881) New or little-known Coleoptera from the Russian Empire and neighboring countries. Trudy Russkago Entomologicheskago Obshchestva 13[1881–82]: 31–84. [in Russian]

RESEARCH ARTICLE

A peer-reviewed open-access journal
ZooKeys
Launched to accelerate biodiversity research

Phylogeography and ecology of bumble bees on Kolguev Island, a remote European Arctic landmass

Grigory S. Potapov[1], Yulia S. Kolosova[1], Alexander V. Kondakov[1],
Alena A. Tomilova[1], Boris Yu. Filippov[1], Natalia A. Zubrii[1], Vitaly M. Spitsyn[1],
Elizaveta A. Spitsyna[1], Alisa A. Zheludkova[1], Mikhail Yu. Gofarov[1],
Galina V. Bovykina[1], Ivan N. Bolotov[1]

1 *N. Laverov Federal Center for Integrated Arctic Research of the Ural Branch of the Russian Academy of Sciences, Northern Dvina Emb. 23, Arkhangelsk, 163069, Russia*

Corresponding author: Grigory S. Potapov (grigorij-potapov@yandex.ru)

Abstract

The bumble bee fauna of the Russian Arctic is rather poorly known. Kolguev Island, a remote insular territory in the Barents Sea, is one of the deficiently studied areas. In this study, material on Kolguev's bumble bees is re-examined, phylogeographic data analysed, putative scenarios explaining the origin of the bumble bee fauna on the island discussed, and the biology and phenology of these insular populations described. Five bumble bee species, i.e., *Bombus flavidus*, *B. lapponicus*, *B. jonellus*, *B. pyrrhopygus*, and *B. balteatus*, were recorded on this island. All of these species are widespread throughout the Eurasian Arctic. Bumble bee populations on Kolguev Island are characterised by a low level of molecular divergence from mainland populations. Based on paleogeographic reconstructions and phylogeographic patterns, it is hypothesised that the bumble bees appeared on this island in the Early Holocene. The lack of rodents (lemmings and voles) sharply decreases the number of available nesting places for bumble bees on Kolguev Island.

Keywords

Bumble bees, High Arctic,, island biogeography Pleistocene glaciations, mitochondrial DNA

Introduction

Kolguev Island is a remote insular territory on the continental shelf in the south-eastern part of the Barents Sea, with a total area of 5130 km² (Lavrinenko and Lavrinenko 2014). This island is composed of Quaternary sediments and is located approximately 70 km north of the coast of Eurasia (Lavrinenko and Lavrinenko 2014). Most of its area is occupied by an accumulative plain, with an average altitude of 20–30 m. However, the southern part of the island is covered by low-elevation wet tundra and peat bogs, while hilly landscapes with average elevations of 80–100 m prevail in its central part.

In the Late Pleistocene, during the period of maximum development of the Scandinavian Ice Sheet, Kolguev Island was a part of the continent due to lower sea levels (Velichko 2002). Available paleogeographic reconstructions reveal that the island area was covered by Arctic deserts (Velichko 2002) or even by massive ice sheets (Svendsen et al. 2004; Hughes et al. 2016). In the Early Holocene, Kolguev Island was isolated from the mainland due to rising sea levels and intense coastal erosion (Velichko 2002).

A review of published literature indicates that the insect fauna of the island may have originated in the Late Pleistocene or Early Holocene (Bolotov 2011). The species diversity of insects on Kolguev Island is rather poorly known, and most available works deal with Lepidoptera and Coleoptera (Buturlin 1903; Semenov 1904; Bolotov 2011; Kullberg et al. 2019; Spitsyn and Bolotov 2020; Potapov et al. 2021b). However, a few publications report on the fauna and species richness of bumble bees collected on Kolguev Island (Berezin 1995a; Kolosova and Potapov 2010, 2011; Potapov et al. 2014; Paukkunen and Kozlov 2020). None of the published entomological works contains data on the phylogeography and biogeographic affinities of insects from Kolguev, including bumble bees.

Bumble bees (genus *Bombus* Latreille) are well adapted to the harsh climatic conditions of the Arctic compared with other groups of bees (Panfilov 1968). The high adaptive capabilities of high-latitude bumble bees could be linked to more effective thermoregulation and shorter life cycle (Berezin 1990, 1995a, b; Radchenko and Pesenko 1994; Goulson 2010). In general, the bumble bee fauna of the Arctic is well studied, especially in Northern Europe and North America (Williams et al. 2014; Rasmont et al. 2021). Conversely, several remote, hard-to-reach areas of the European and Asian Arctic remain poorly studied, including Kolguev Island.

The bumble bee fauna of the Eurasian Arctic can be separated into three distinct groups of species: (1) the High Arctic taxa; (2) the Lower Arctic taxa; and (3) boreal species (Chernov 1978; Chernov and Matveeva 2002). The High Arctic species group contains *Bombus hyperboreus* Schönherr, 1809, *B. pyrrhopygus* Friese, 1902, and the polar relict species *B. glacialis* Friese, 1902 (Richards 1973; Chernov and Matveeva 2002; Williams et al. 2019; Potapov et al. 2021a). The latter species is endemic to the Novaya Zemlya Archipelago and Wrangel Island (Potapov et al. 2021a). The Lower Arctic group consists of a number of species such as *B. lapponicus* (Fabricius, 1793), *B. jonellus* (Kirby, 1802), *B. cingulatus* Wahlberg, 1854, and *B. balteatus* Dahlbom, 1832 (Chernov 1978; Chernov and Matveeva 2002). The expansion of boreal bumble

bee species associated with species-rich flowering plant associations through river valleys is a common means of enrichment of the Arctic fauna. The boreal species that may colonise the Arctic by this manner are *B. distinguendus* Morawitz, 1869, *B. hortorum* (Linnaeus, 1761), *B. flavidus* Eversmann, 1852, and others (Kolosova and Potapov 2011; Potapov et al. 2019). In general, the species richness of bumble bees in the Arctic and Subarctic regions ranges from two or three on islands to 12–14 at mainland sites (Potapov et al. 2014).

Most of the bumble bee species mentioned above have Palearctic distributions, with the exception of *B. jonellus*, *B. distinguendus*, and *B. flavidus* (Williams 1998). Currently, three Palearctic species of the subgenus *Alpinobombus*, i.e., *B. (A.) pyrrhopygus*, *B. (A.) balteatus*, and *B. (A.) hyperboreus*, are considered to be distinct species, and are closely related to the Nearctic *B. polaris* Curtis, 1835, *B. kirbiellus* Curtis, 1835, and *B. natvigi* Richards, 1931, respectively (Williams et al. 2015, 2019). However, a number of scholars consider that the Nearctic *B. polaris* and the Palearctic *B. pyrrhopygus* are conspecific and that the older name *B. polaris* should be used for this circumpolar taxon (Rasmont et al. 2021). At the same time, there are different opinions on the distribution of species belonging to the *Bombus* (*Pyrobombus*) *lapponicus*-complex (Sheffield et al. 2020).

This paper aims to (1) re-examine material on Kolguev's bumble bees using newly collected samples; (2) analyse phylogeographic data and discuss putative scenarios explaining the origin of the bumble bee fauna on Kolguev Island; and (3) describe ecological and phenological patterns for these insular populations.

Materials and methods

Data sampling, morphological study, and statistical tests

Samples of bumble bees from Kolguev Island were collected by Boris Yu. Filippov, Natalia A. Zubrii, Vitaly M. Spitsyn, Alisa A. Zheludkova, Aleksey G. Ardeev, and Grigory S. Potapov in 2009, 2018, and 2020 (total N = 287 specimens) (Suppl. material 1: Table S1). The bumble bees were collected in the southern part of the island, i.e., near the village of Bugrino (68.7819°N, 49.3087°E) and along a route from this village to Lake Krivoe (69.0194°N, 48.7211°E) (Fig. 1, Suppl. material 1: Table S1). In most cases, one sample represents a daily sampling effort of a single collector along a walked route of approximately 5 km.

The bumble bees were collected with an entomological net. In some cases, foraging plants of bumble bees were not accurately recorded or bumble bees were caught in flight. For this reason, it is impossible to give a detailed range of the bumble bee foraging resources on Kolguev Island. Our field research was carried out from July to August, allowing us to study phenological patterns for the most abundant species of bumble bees. However, the exact dates of the beginning of the bumble bee flight season on Kolguev Island are unknown because sampling was not possible in May and June.
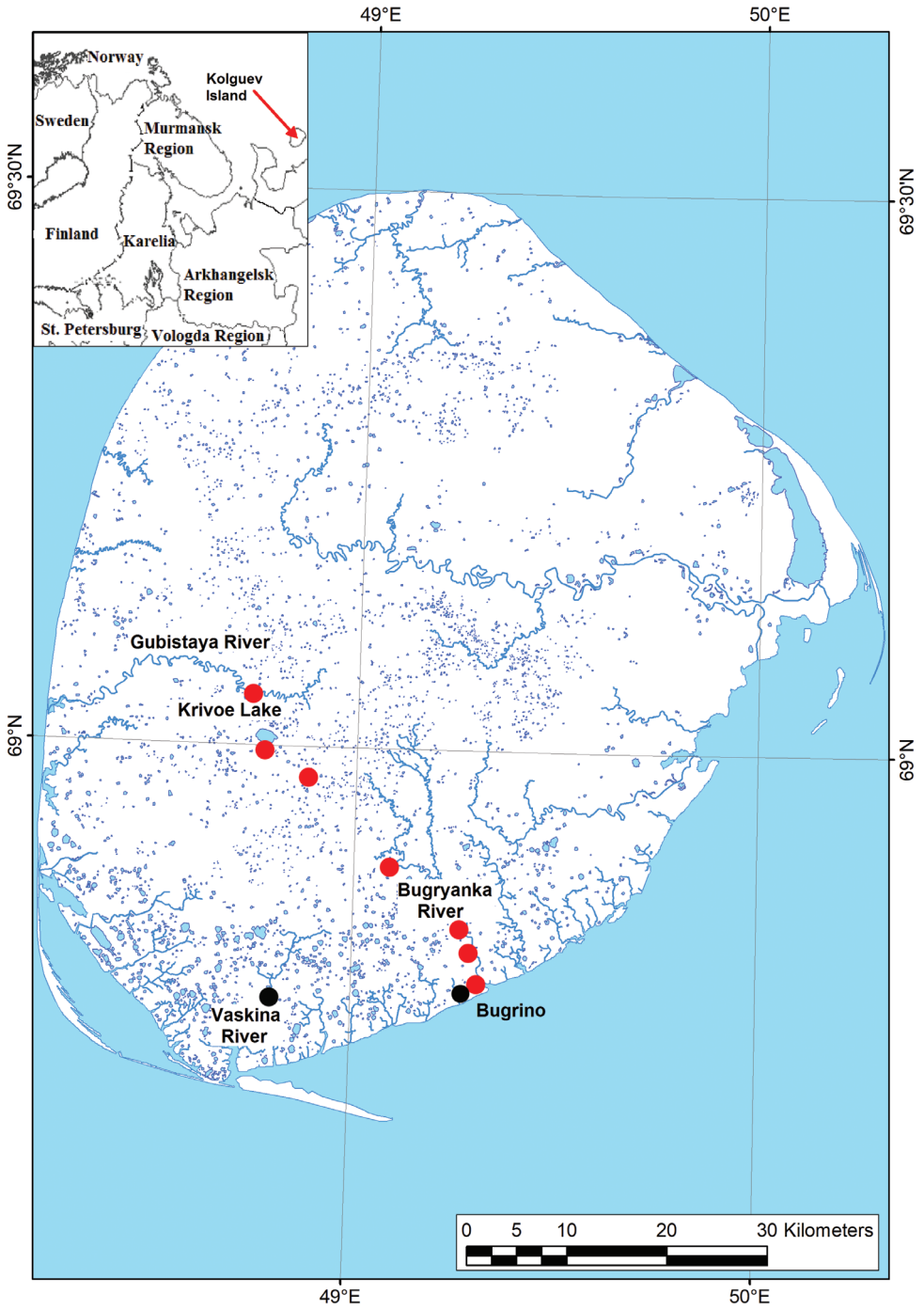
Figure 1. Map of localities on Kolguev Island, from which recent (red circles) and historical (black circles) samples of bumble bees were collected.

Specimens of bumble bees from Kolguev Island are deposited in the Russian Museum of the Biodiversity Hotspots (**RMBH**) of the N. Laverov Federal Center for Integrated Arctic Research of the Ural Branch of the Russian Academy of Sciences (Arkhangelsk, Russia). Additional material from the Chukotka and Yamal peninsulas were used for a comparative phylogeographic analysis (Suppl. material 1: Table S1). Only two specimens of bumble bees were found in historical samples from Kolguev Island collected by Buturlin's (1903) expedition (Suppl. material 1: Table S1). These two specimens were examined in the Zoological Institute of the Russian Academy of Sciences, St. Petersburg (**ZIN**).

Bumble bee specimens were studied using a stereomicroscope Solo 2070 (Carton Optical (Siam) Co., Ltd., Thailand). Bumble bees were identified following Løken (1973, 1984) and Williams et al. (2019). The nomenclature of species follows Williams (1998) and Williams et al. (2019). For the nest description and its measurements, we applied an approach described by Alford (1975) and Martinet et al. (2022).

Statistical procedures (Kolmogorov-Smirnov test for normality and Mann-Whitney test) for the analysis of relative abundance were performed with Statistica v. 13.3 (Stat Soft Inc., USA). We compared the parameters of relative abundance between Kolguev Island and the Novaya Zemlya Archipelago. Novaya Zemlya is the closest insular land to Kolguev Island (approximately 210 km) but differs by having a much larger total area (82,000 km^2) and harsher environmental conditions (Isachenko 1995).

Laboratory protocols

We generated new sequences of the cytochrome c oxidase subunit I (COI) gene from 15 bumble bee specimens (Table 1). The laboratory protocols followed those described in Potapov et al. (2018a, 2018b). Resulting COI gene sequences were checked manually using a sequence alignment editor (BioEdit v. 7.2.5; Hall 1999). The sequencing was carried out at the Engelhardt Institute of Molecular Biology of the Russian Academy of Sciences (Moscow, Russia) using the ABI PRISM BigDye Terminator v. 3.1 reagent kit.

Phylogeographic analyses

We used a median-joining network approach using Network v. 5.0.0.1 with default settings (Bandelt et al. 1999). Additional available COI sequences of *B. lapponicus*, *B. pyrrhopygus*, and *B. balteatus* were obtained from the BOLD (the Barcode of Life Data System; Ratnasingham and Hebert 2007) and GenBank databases (*N* = 35; Table 1). Each COI sequence of the aligned datasets was trimmed, leaving a 425-bp fragment for *B. lapponicus*, 455-bp fragment for *B. pyrrhopygus*, and 627-bp fragment for *B. balteatus*. The alignment of COI sequences was performed using the ClustalW algorithm implemented in MEGA7 (Kumar et al. 2016).

Results

Species richness

Five species of bumble bees were recorded on Kolguev Island, *B. flavidus*, *B. lapponicus*, *B. jonellus*, *B. pyrrhopygus*, and *B. balteatus* (Suppl. material 1: Table S1). During our studies in 2009, 2018, and 2020, *B. pyrrhopygus* and *B. lapponicus* were the most common and widespread taxa on the island (N = 124 and 123 specimens, respectively), while *B. balteatus* was observed less frequently (N = 43 specimens). Six specimens of *B. flavidus* were collected on this island and only one specimen of *B. jonellus* was sampled in 2009.

Relative abundance of bumble bees on Kolguev Island is 6.27±1.05 specimens per sample (mean ± s.e.; N = 48; in most cases, one sample represents a daily sampling effort of a single collector along a walked route of approximately 5 km), which is two times higher than that on Novaya Zemlya, with 3.11±0.46 specimens per sample (mean ± s.e.; N = 44; data from Potapov et al. 2019: table 1). The differences between these insular areas in relation to their relative bumble bee abundances are highly significant (Mann-Whitney test: U = 711, P = 0.0058). The mean number of recorded species per sample (± s.e.) on Kolguev Island and Novaya Zemlya is 1.94±0.13 (N = 48) and 1.43±0.10 (N = 44), respectively. This parameter is also higher on the first island (Mann-Whitney test: U = 707, P = 0.0029).

Phylogeography

We found that the sequenced *B. lapponicus* specimens from Kolguev Island belong to a single COI lineage (haplotype LP-1) that also occurs in the population from Yamal (Table 1, Fig. 2). *Bombus pyrrhopygus* shares two COI haplotypes on Kolguev, one of which is also known to occur in Norway, Novaya Zemlya, Chukotka, and Kamchatka (haplotype PY1). In contrast, the second haplotype of this species (PY10) was not recorded anywhere else but is genetically close to the first lineage. *Bombus balteatus* from Kolguev Island also shares two COI haplotypes (BL2 and BL3), which were not recorded anywhere else (Table 1, Fig. 2).

Colour variations

Bombus pyrrhopygus and *B. balteatus* are highly variable in their colour patterns (Løken 1973; Williams et al. 2019; Rasmont et al. 2021). The dark form of *B. pyrrhopygus*, which is known to occur in Scandinavia and the Kola Peninsula, was not recorded on Kolguev Island. Specimens of this species collected on Kolguev Island share a colour variation of tergites T4–T6. It ranges from a black coloration without ferruginous to a quite distinct ferruginous colouration. Regarding *B. balteatus*, the colour variation of T4–T6 from yellowish white to whitish occur in a series of specimens from Kolguev Island.
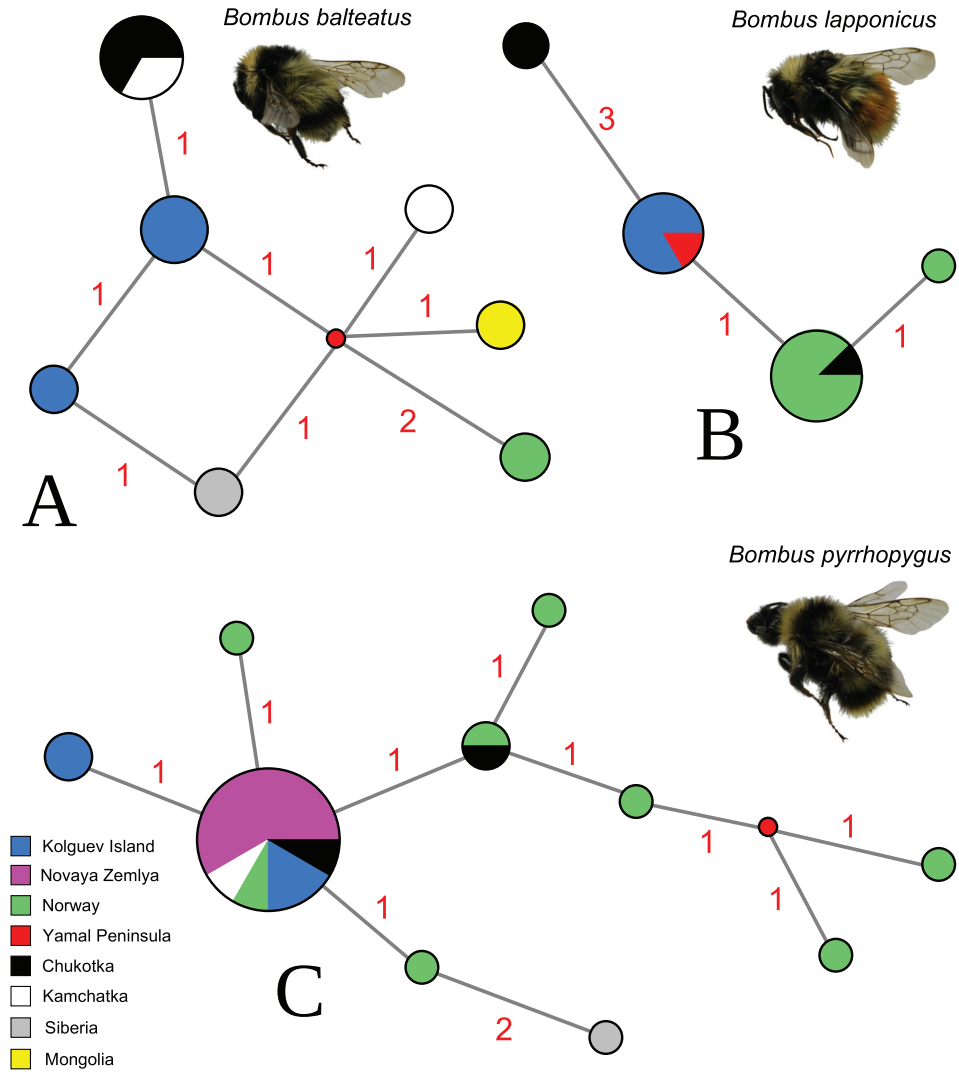
Figure 2. Median-joining haplotype networks of the available COI sequences of widespread bumble bees from Kolguev Island and other Arctic areas **A** *Bombus balteatus* **B** *B. lapponicus* **C** *B. pyrrhopygus*. The circle size is proportional to the number of available sequences belonging to a certain haplotype (smallest circle = one sequence). The small red dots indicate hypothetical ancestral haplotypes. Red numbers near branches indicate the number of nucleotide substitutions between haplotypes.

Bumble bee habitats, foraging resources, and phenological patterns

The main places of aggregation of foraging bumble bee individuals in the southern part of Kolguev Island are river valleys, where foraging resources and appropriate nesting places are concentrated (Fig. 3). Bumble bees rarely occur beyond these areas because

Table 1. List of COI sequences for bumble bee specimens used in phylogeographic analyses.

Species	COI haplotype code	COI GenBank/ BOLD IDS acc. no.	Specimen voucher	Locality	References
B. lapponicus	LP1	MT053066	RMBH BMB225	Kolguev Island	Potapov et al. (2021a)
B. lapponicus	LP1	MT053067	RMBH BMB226	Kolguev Island	Potapov et al. (2021a)
B. lapponicus	LP1	MT053068	RMBH BMB227	Kolguev Island	Potapov et al. (2021a)
B. lapponicus	LP1	MT053069	RMBH BMB228	Kolguev Island	Potapov et al. (2021a)
B. lapponicus	LP1	MT053070	RMBH BMB229	Kolguev Island	Potapov et al. (2021a)
B. lapponicus	LP1	OM666877	RMBH BMB102	Yamal: Syoyakha	This study
B. lapponicus	LP2	OM666878	RMBH BMB108	Chukotka: 13 km NE from Lorino	This study
B. lapponicus	LP3	OM666879	RMBH BMB109	Chukotka: Anadyr	This study
B. lapponicus	LP2	OM666880	RMBH BMB111	Chukotka: 13 km NE from Lorino	This study
B. lapponicus	LP3	GBHAP756-14	BOMBUS-001	Norway	Gjershaug et al. (2013)
B. lapponicus	LP3	GBHAP757-14	BOMBUS-002	Norway	Gjershaug et al. (2013)
B. lapponicus	LP3	GBHAP758-14	BOMBUS-006	Norway	Gjershaug et al. (2013)
B. lapponicus	LP3	GBHAP759-14	BOMBUS-008	Norway	Gjershaug et al. (2013)
B. lapponicus	LP4	GBHAP760-14	BOMBUS-010	Norway	Gjershaug et al. (2013)
B. lapponicus	LP3	GBHAP761-14	BOMBUS-014	Norway	Gjershaug et al. (2013)
B. lapponicus	LP3	GBHAP762-14	BOMBUS-020	Norway	Gjershaug et al. (2013)
B. lapponicus	LP3	GBHAP763-14	BOMBUS-033	Norway	Gjershaug et al. (2013)
B. pyrrhopygus	PY1	OM666883	RMBH BMB230	Kolguev Island	This study
B. pyrrhopygus	PY10	OM666884	RMBH BMB231	Kolguev Island	This study
B. pyrrhopygus	PY10	OM666887	RMBH BMB234	Kolguev Island	This study
B. pyrrhopygus	PY1	OM666888	RMBH BMB235	Kolguev Island	This study
B. pyrrhopygus	PY1	MK530667	RMBH BMB88	Novaya Zemlya: Malye Karmakuly	Potapov et al. (2019)
B. pyrrhopygus	PY1	MK530668	RMBH BMB90	Novaya Zemlya: Malye Karmakuly	Potapov et al. (2019)
B. pyrrhopygus	PY1	MK530679	RMBH BMB168	Novaya Zemlya: Bezymyannaya Bay	Potapov et al. (2019)
B. pyrrhopygus	PY1	MK530680	RMBH BMB169	Novaya Zemlya: Bezymyannaya Bay	Potapov et al. (2019)
B. pyrrhopygus	PY1	MK530681	RMBH BMB170	Novaya Zemlya: Bezymyannaya Bay	Potapov et al. (2019)
B. pyrrhopygus	PY1	MK530682	RMBH BMB171	Novaya Zemlya: Bezymyannaya Bay	Potapov et al. (2019)
B. pyrrhopygus	PY1	MK530684	RMBH BMB173	Novaya Zemlya: Bezymyannaya Bay	Potapov et al. (2019)
B. pyrrhopygus	PY6	OM698596	RMBH BMB199	Chukotka: Anadyr	This study
B. pyrrhopygus	PY1	OM698597	RMBH BMB202	Chukotka: Anadyr	This study
B. pyrrhopygus	PY1	AF279481	No data	Kamchatka	GenBank
B. pyrrhopygus	PY2	KF434342	BOMBUS-029	Norway	Gjershaug et al. (2013)
B. pyrrhopygus	PY1	NOAPI563-14	NOAPI563	Norway	BOLD [public record]
B. pyrrhopygus	PY3	NOAPI641-14	NOAPI641	Norway	BOLD [public record]
B. pyrrhopygus	PY4	WASPS403-14	CCDB-20945 B11	Siberia: Krasnoyarsky Kray	BOLD [public record]
B. pyrrhopygus	PY5	WASPS446-14	CCDB-20945 F06	Norway	BOLD [public record]
B. pyrrhopygus	PY6	WASPS456-14	CCDB-20945 G04	Norway	BOLD [public record]
B. pyrrhopygus	PY7	WASPS466-14	CCDB-20945 H02	Norway	BOLD [public record]
B. pyrrhopygus	PY8	WASPS467-14	CCDB-20945 H03	Norway	BOLD [public record]
B. pyrrhopygus	PY9	WASPS471-14	CCDB-20945 H07	Norway	BOLD [public record]
B. balteatus	BL2	OM666885	RMBH BMB232	Kolguev Island	This study

Species	COI haplotype code	COI GenBank/ BOLD IDS acc. no.	Specimen voucher	Locality	References
B. balteatus	BL2	OM666886	RMBH BMB233	Kolguev Island	This study
B. balteatus	BL3	OM666889	RMBH BMB236	Kolguev Island	This study
B. balteatus	BL1	OM666881	RMBH BMB200	Chukotka: Anadyr	This study
B. balteatus	BL1	OM666882	RMBH BMB201	Chukotka: Anadyr	This study
B. balteatus	BL4	BBWP355-09	1550F10-MON	Mongolia	BOLD [public record]
B. balteatus	BL5	NOAPI567-14	NOAPI567	Norway	BOLD [public record]
B. balteatus	BL6	WASPS398-14	CCDB-20945 B06	Siberia: Krasnoyarsky Kray	BOLD [public record]
B. balteatus	BL7	WASPS399-14	CCDB-20945 B07	Kamchatka	BOLD [public record]
B. balteatus	BL1	WASPS423-14	CCDB-20945 D07	Kamchatka	BOLD [public record]
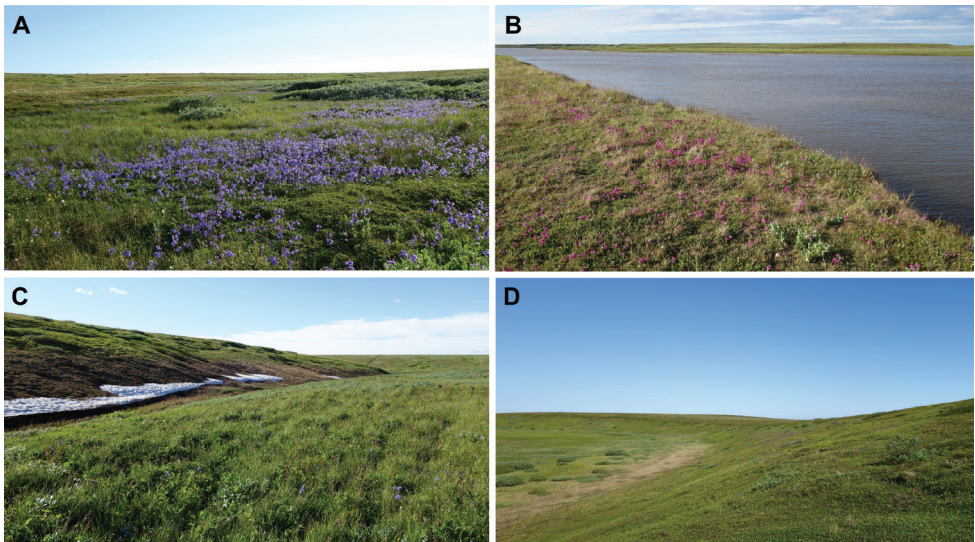
Figure 3. Habitats and foraging resources of bumble bees on Kolguev Island **A** willow-sedge tundra with *Polemonium acutiflorum*, 10.vii.2020 **B** meadow-like associations with *Pedicularis* sp., shore of the Bugryanka River, 10.vii.2020 **C** willow-sedge tundra with *Geum rivale* and *Polemonium acutiflorum* along a stream valley, 11.vii.2020 **D** willow-grass tundra on slopes with *Pedicularis* sp., 18.vii.2020.

continuous wet tundra and peat bog landscapes between river valleys are unfavourable for foraging and the establishment of colonies. Different species of bumble bees do not vary in their habitat preferences on Kolguev Island.

Bumble bees have been recorded on water avens (*Geum rivale*), whorled louse-wort (*Pedicularis verticillata*), hairy lousewort (*Pedicularis hirsuta*), tall Jacob's ladder (*Polemonium acutiflorum*), candle spur (*Delphinium elatum* var. *hirsutum*), cloudberry (*Rubus chamaemorus*), and on different willow species (*Salix* spp.).

Queens of bumble bees were recorded from early July to late August (Fig. 4). The majority of workers were collected in late July and early August, whereas males were caught in August. The final date when a bumble bee (*B. pyrrhopygus*) was recorded on Kolguev Island was 30 August (Suppl. material 1: Table S1).

Nest of *B. lapponicus*

One nest of *B. lapponicus* was found on Kolguev Island (15 August 2018, Bugryanka River valley, 68.802861°N, 49.299528°E, Potapov and Zheludkova leg.) (Fig. 5). This nest was located in a tundra site, the plant cover of which was dominated by cotton-grass (*Eriophorum* sp.), crowberry (*Empetrum nigrum*), cloudberry (*Rubus chamaemorus*), dwarf birch (*Betula nana*), and willows (*Salix* spp.). The nest was situated inside a tussock and contained 24 cocoons, of which 20 were empty. The mean size (± s.e.) of the measured cocoons is as follows: length 13±0.3 mm, width 10±0.2 mm (*N* = 8). The size of cocoons from the initial pupal clump is as follows: length 8±0.1 mm, width 7±0.1 mm (mean ± s.e.; *N* = 4). There were four living workers of *B. lapponicus* inside the nest, while four other workers were taken dead from cocoons. The length of living workers was 12, 11, 9, and 8 mm; the dead workers from cocoons were 13, 12, 12, and 8 mm long.

Discussion

Bumble bee fauna of Kolguev Island

The fauna of bumble bees on Kolguev Island with five species (*B. flavidus*, *B. lapponicus*, *B. jonellus*, *B. pyrrhopygus*, and *B. balteatus*) is similar to other species-poor Arctic faunas, dominated by cold-adapted bumble bee species (Potapov et al. 2019). The bumble bee fauna of Vaygach Island (the total area 3400 km^2, geographic distance approximately 340 km from Kolguev) is the most similar to the studied fauna. In particular, five bumble bee species occur on Vaygach Island, i.e., *B. flavidus*, *B. lapponicus*, *B. pyrrhopygus*, *B. balteatus*, and *B. hyperboreus* (see Potapov et al. 2017).

We have no reliable records of *B. hyperboreus* from Kolguev Island because earlier references to the existence of this species on the island (Kolosova and Potapov 2010, 2011; Rasmont et al. 2021) were incorrect. However, future records of *B. hyperboreus* on Kolguev Island can be expected, mainly in the central and northern part of this island, where the species richness of insects (e.g., Lepidoptera: Bolotov 2011) is higher due to the prevalence of hilly landscapes with richer plant diversity (Potapov et al. 2021b).

Only one specimen (queen) of *B. jonellus* was found on Kolguev Island in 2009. However, in subsequent studies, this species was not rediscovered there. As in the case of *B. hyperboreus*, additional research is needed in the central and northern parts of Kolguev Island. It is also possible that our solitary record of *B. jonellus* reflects an unsuccessful colonisation event because no workers and males of this species were recorded on Kolguev Island. It is well known that queens of bumble bees may migrate for quite considerable distances and that they are not deterred by larger water barriers (Fijen 2020). In the case of Kolguev Island, located 70 km from the mainland, the possibility of an accidental dispersal of a *B. jonellus* female to the island cannot be excluded. Earlier, two migrant butterfly species were recorded on Kolguev Island (Bolotov et al. 2021).
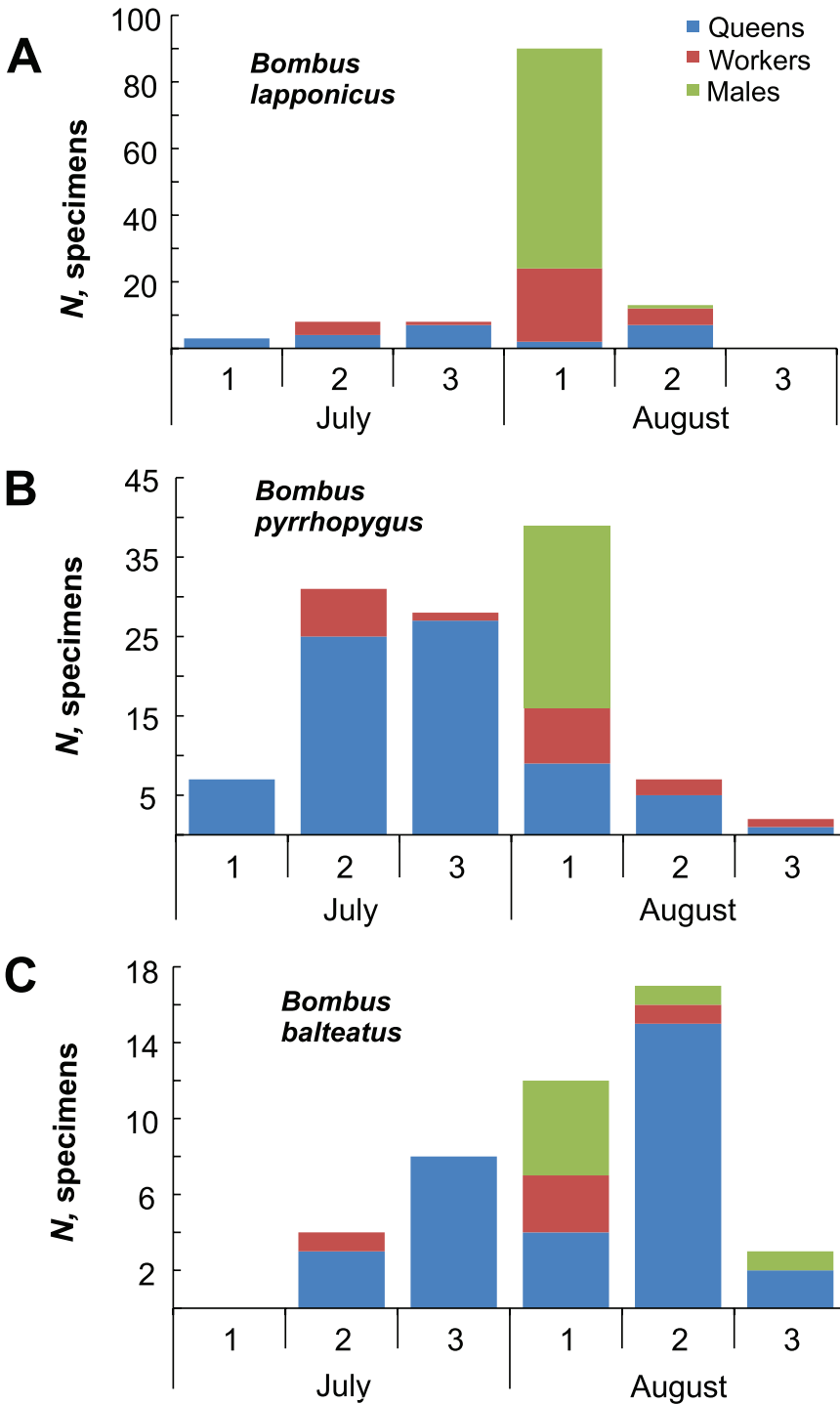
Figure 4. Phenology of bumble bees from Kolguev Island by ten-day periods **A** *Bombus lapponicus* (*N* = 122 specimens) **B** *B. pyrrhopygus* (*N* = 114 specimens) **C** *B. balteatus* (*N* = 44 specimens).
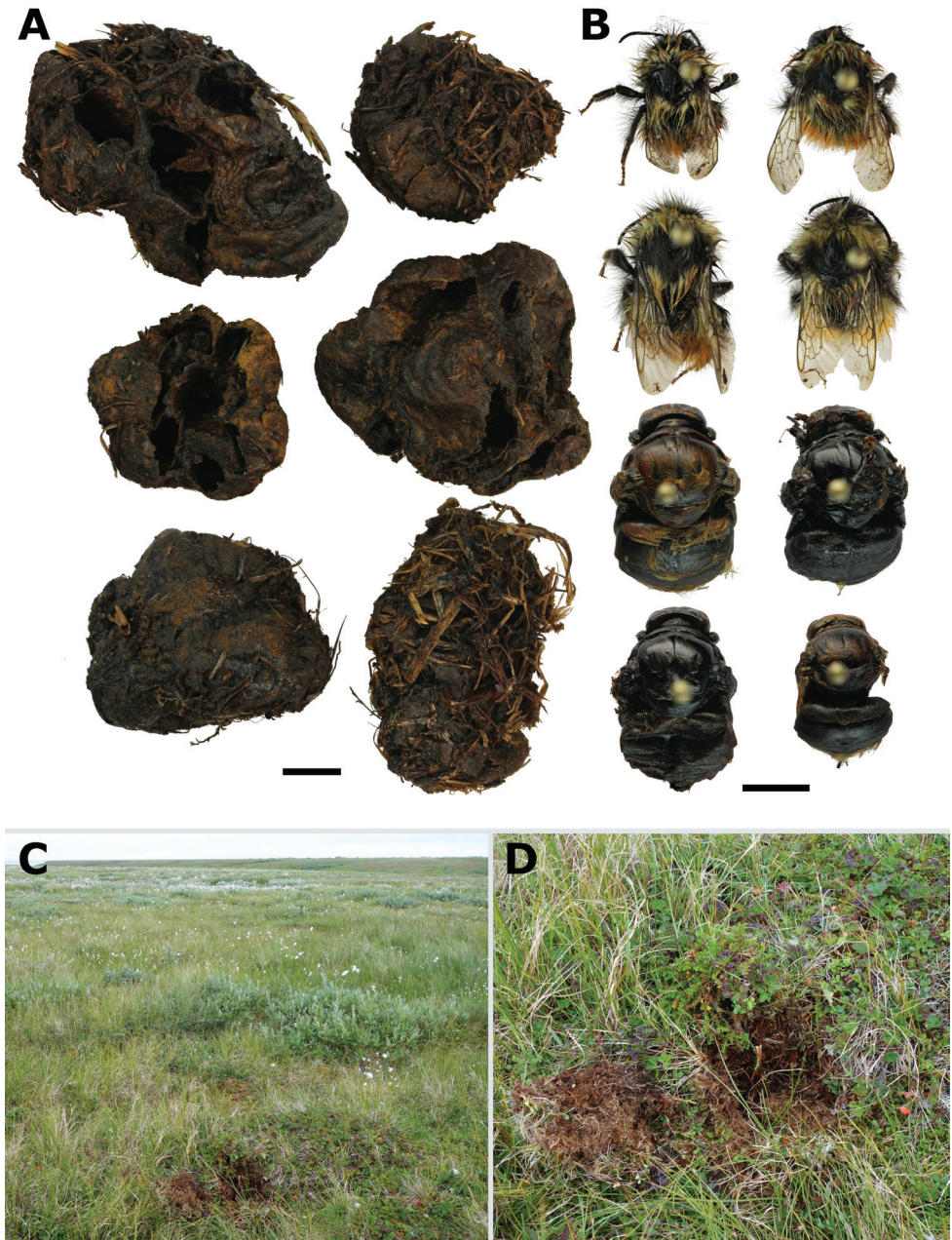
Figure 5. The nest of *Bombus lapponicus* on Kolguev Island **A** excavated nest **B** workers were found alive in the nest (four upper specimens), and those collected dead from cocoons (four lower specimens) **C** nesting site in tundra with cottongrass, crowberry, cloudberry, dwarf birch, and willows **D** tussock with the excavated nest. Scale bars: 5 mm.

A few specimens of *B. flavidus* were recorded on Kolguev Island, i.e., one female and five males. This cuckoo bumble bee is known as a social parasite of *B. lapponicus* (see Lhomme and Hines 2019), which is a common and widespread species on the island. Earlier reference to the record of *B. norvegicus*, another cuckoo bumble bee species, on Kolguev Island (Kolosova and Potapov 2010, 2011; Rasmont et al. 2021) is incorrect. It was based on a misidentification of a *B. flavidus* female. Hence, Kolguev's fauna contains only one species of cuckoo bumble bee, *B. flavidus*.

Finally, records of *B. glacialis* Friese, 1902 on Kolguev Island, mentioned by earlier scholars (Pittioni 1943), were not confirmed by our recent surveys (Potapov et al. 2021a). The latter species is a Pleistocene glacial relict and is endemic to Novaya Zemlya and Wrangel Island (Potapov et al. 2018a, 2019, 2021a). It is unlikely that *B. glacialis* is present on Kolguev Island due to the significant environmental differences between Kolguev and Novaya Zemlya.

Phylogeographic pattern in the populations of Kolguev's bumble bees and a prospective scenario of their expansion to this island

We analysed the COI sequences of three widespread species of bumble bees on Kolguev Island and found that they belong to common Northern Eurasian lineages. Kolguev's *B. lapponicus* reveals a single COI haplotype that also occurs in a population from Yamal and is close to the Norwegian lineage. *Bombus pyrrhopygus* shares two haplotypes, which are also known to occur in Norway, Novaya Zemlya, Chukotka, and Kamchatka. *Bombus balteatus* from Kolguev Island have two haplotypes, which were not recorded anywhere yet, but they are close to the COI lineage from Chukotka, Kamchatka, and Siberia. In summary, all three species from Kolguev share a low level of molecular divergence from mainland populations, which aligns with the results of earlier phylogeographic research on *B. hyperboreus* and *B. pyrrhopygus* from Novaya Zemlya (Potapov et al. 2019).

We hypothesise that *B. lapponicus*, *B. pyrrhopygus*, and *B. balteatus* spread across the emerged Eurasian shelf margin in the Late Pleistocene, with subsequent fragmentation of their continuous ranges in the Holocene. Taking into account the geological history of the region (Velichko 2002) and our data on bumble bee phylogeography, we conclude that the bumble bees appeared on Kolguev Island no earlier than the Early Holocene, as did some other animal species such as a tiger moth (Bolotov et al. 2015) and a freshwater fish (Artamonova et al. 2020). During the Last Glacial Maximum, Kolguev Island was covered by Arctic deserts or the ice sheet. After the Holocene Climate Optimum, the vegetation cover on the island shifted to tundra ecosystems (Velichko 2002), which are more suitable as habitats for cold-tolerant Arctic bumble bees.

The life cycle and ecology of the Kolguev's bumble bees

The three most common species of the insular fauna (*B. lapponicus*, *B. pyrrhopygus*, and *B. balteatus*) are widespread throughout Kolguev Island but *B. balteatus* occurs less

frequently. Obviously, the flight activity of bumble bees is dependent on weather conditions. Their flight season is typical for the Arctic territories with the maximum abundance of individuals in the warmest period. On Kolguev Island this period lasts from the second half of July to the first half of August and is characterised by a mean air temperature of 8 °C (Potapov et al. 2019, 2021a). We have no exact dates of the earliest emergence of bumble bee queens on Kolguev Island. As in the case of other Arctic islands, it should be sometime between mid-May and mid-June (Potapov et al. 2019, 2021a).

No bumble bee nests have been recorded on Kolguev Island prior to our recent discovery of a nest of *B. lapponicus*, described herein. This nest was found in mid-August, when the life cycle of *B. lapponicus* on Kolguev Island enters its final stage. Hence, we did not have the opportunity to examine several aspects of the species' development such as the emergence of the first-brood adults, behaviour of workers in the nest, and the emergence of males. From available data, we can only conclude that the nest on Kolguev is typical for this species (Martinet et al. 2022). The number of individuals in the colony was quite small, which is typical for bumble bee colonies from Arctic territories (Berezin 1990).

The complete absence of rodents (e.g., lemmings and voles) is a unique feature of Kolguev Island that influences the animal life of the island in several ways, especially by switching the Arctic predators from rodents to other prey resources (Pokrovsky et al. 2015). It is unknown how exactly the absence of lemmings affects the bumble bees of Kolguev Island, but in the Arctic, bumble bees frequently use lemming burrows as nesting sites. Hence, the abundance of bumble bees increases in areas with higher concentrations of lemmings and their burrows (Berezin 1990, 1995b; Potapov et al. 2021a). The lack of lemming burrows considerably limits the nesting places of bumble bees on Kolguev Island. It seems that bumble bees use every available resource such as tussocks, edges of river terraces, and human buildings to establish a nesting colony on the island.

The abundance of bumble bees on Kolguev Island is rather low but the mean value (number of specimens per sampling effort) is two times higher than that on Novaya Zemlya (Potapov et al. 2019, 2021a). The total and mean species richness of bumble bees on Kolguev Island is also higher compared with those on Novaya Zemlya. These differences could be explained by specific landscape and climatic features of Kolguev Island, which is a plain insular landmass, taking a more southern geographic position compared with that of the mountainous Novaya Zemlya Archipelago (Potapov et al. 2019, 2021a). However, a possible role of the interannual variability in weather conditions (sampling in the two areas was made in different years) may also be considered there.

Acknowledgements

References

Alford DV (1975) Bumblebees. Davis-Poynter, London, 325 pp.

Artamonova VS, Makhrov AA, Popov IY, Spitsyn VM (2020) European smelt (*Osmerus eperlanus* (Linnaeus, 1758)) on Kolguyev Island, Barents Sea, and factors limiting its spread through the Arctic. Contemporary Problems of Ecology 13(2): 127–131. https://doi.org/10.1134/S199542552002002X

Bandelt HJ, Forster P, Röhl A (1999) Median-joining networks for inferring intraspecific phylogenies. Molecular Biology and Evolution 16(1): 37–48. https://doi.org/10.1093/oxfordjournals.molbev.a026036

Berezin MV (1990) Ecology and nesting of bumble bees on Wrangel Island. In: Kipyatkov VE (Ed.) Proceedings of Colloquia of All-Union Entomological Society Section for the Study of Social Insects, 1st Colloquium, Leningrad (USSR), October 1990. VIEMS, Leningrad, 19–28. [In Russian]

Berezin MV (1995a) Geographical diversity, species correlation, population structure and cenotic interactions of Arctic bumble bees (Apidae, *Bombus*). Swedish-Russian Tundra Ecology-Expedition-94. Tundra Ecology-94. A Cruise Report. Swedish Polar Research Secretariat, Stockholm, 205–215.

Berezin MV (1995b) Shmeli v arkticheskih ekosistemah [Bumblebees in Arctic ecosystems]. In: Shilov IA (Ed.) Ecosystems of the North, structure, adaptations, stability: Proceedings of the Russian Symposium, Petrozavodsk (Russia), October, 1993. Moscow State University, Moscow, 43–57. [In Russian]

Bolotov IN (2011) Fauna and ecology of butterflies (Lepidoptera, Rhopalocera) from Kanin Peninsula and Kolguev Island. Zoologicheskii Zhurnal 90(11): 1365–1373. [In Russian]

Bolotov IN, Tatarinov AG, Filippov BY, Gofarov MY, Kondakov AV, Kulakova OI, Spitsyn VM (2015) The distribution and biology of *Pararctia subnebulosa* (Dyar, 1899) (Lepidoptera: Erebidae: Arctiinae), the largest tiger moth species in the High Arctic. Polar Biology 38(6): 905–911. https://doi.org/10.1007/s00300-014-1643-2

Bolotov IN, Mizin IA, Zheludkova AA, Aksenova OV, Kolosova YS, Potapov GS, Spitsyn VM, Gofarov MY (2021) Long-distance dispersal of migrant butterflies to the Arctic Ocean islands, with a record of *Nymphalis xanthomelas* at the northern edge of Novaya Zemlya (76.95°N). Nota Lepidopterologica 44: 73–90. https://doi.org/10.3897/nl.44.62249

Buturlin SA (1903) Predvaritelnyj kratkij otchet o poezdke na ostrov Kolguev letom 1902 goda. [Preliminary summary of a trip to Kolguev Island in the summer of 1902] Izvestia Imperatorskogo Russkogo Geograficheskogo Obshchestva 39: 228–248. [In Russian]

Chernov YuI (1978) Structure of the animal population in the Subarctic. Nauka, Moscow, 167 pp. [In Russian]

Chernov YuI, Matveeva NV (2002) Landscape-zonal distributions of species in the Arctic. Uspekhi sovremennoy biologii 1: 26–45. [In Russian]

Fijen TPM (2020) Mass-migrating bumblebees: An overlooked phenomenon with potential far-reaching implications for bumblebee conservation. Journal of Applied Ecology 58(2): 274–280. https://doi.org/10.1111/1365-2664.13768

Gjershaug JO, Staverløkk A, Kleven O, Ødegaard F (2013) Species status of *Bombus monticola* Smith (Hymenoptera: Apidae) supported by DNA barcoding. Zootaxa 3716(3): 431–440. https://doi.org/10.11646/zootaxa.3716.3.6

Goulson D (2010) Bumblebees. Behaviour, Ecology and Conservation. Oxford University Press, Oxford, 330 pp.

Hall TA (1999) BioEdit: a user-friendly biological sequence alignment editor and analysis program for Windows 95/98/NT. Nucleic Acids Symposium 41: 95–98.

Hughes AL, Gyllencreutz R, Lohne ØS, Mangerud J, Svendsen JI (2016) The last Eurasian ice sheets – a chronological database and time-slice reconstruction, DATED-1. Boreas 45(1): 1–45. https://doi.org/10.1111/bor.12142

Isachenko AG (1995) Fiziko-geograficheskaja harakteristika regiona [Physical and geographical characteristics of the region]. In: Frolov AK (Chief Editor) Sostojanie okruzhajushchej sredy Severo-Zapadnogo i Severnogo regionov Rossii [State of the environment of the North-Western and Northern regions of Russia]. Nauka, Saint-Petersburg, 7–30. [In Russian]

Kolosova YuS, Potapov GS (2010) Local fauna of bumble bees (Hymenoptera: Apidae, Bombini) of the European North of Russia: the delta of the Pechora River and the Kolguev Island. Vestnik Pomorskogo Universiteta. Seria Estestvennye nauki 3: 69–75. [In Russian]

Kolosova YuS, Potapov GS (2011) Bumblebees (Hymenoptera, Apidae) in the forest-tundra and tundra of Northeast Europe. Entomological Review 91(7): 830–836. https://doi.org/10.1134/S0013873811070049

Kullberg J, Filippov BY, Spitsyn VM, Zubrij NA, Kozlov MV (2019) Moths and butterflies (Insecta: Lepidoptera) of the Russian Arctic islands in the Barents Sea. Polar Biology 42(2): 335–346. https://doi.org/10.1007/s00300-018-2425-z

Kumar S, Stecher G, Tamura K (2016) MEGA7: Molecular Evolutionary Genetics Analysis Version 7.0 for Bigger Datasets. Molecular Biology and Evolution 33(7): 1870–1874. https://doi.org/10.1093/molbev/msw054

Lavrinenko OV, Lavrinenko IA (2014) The plant cover of reindeer pastures on the Kolguev Island: succession of research and current approaches. In: Geltman DV (Ed.) Botany: history, theory, practice (on the 300th anniversary of the founding of the V.L. Komarov

Botanical Institute of the Russian Academy of Sciences): Proceedings of the International scientific Conference, St. Petersburg (Russia), June 2014. St. Petersburg State Electrotechnical University named after V.I. Ulyanov (Lenin), St. Petersburg, 124–130. [In Russian]

Lhomme P, Hines HM (2019) Ecology and evolution of cuckoo bumble bees. Annals of the Entomological Society of America 112(3): 122–140. https://doi.org/10.1093/aesa/say031

Løken A (1973) Studies of Scandinavian bumble bees (Hymenoptera, Apidae). Norsk Entomologisk Tidsskrift 20(1): 1–218.

Løken A (1984) Scandinavian species of the genus *Psithyrus* Lepeletier (Hymenoptera, Apidae). Entomologica Scandinavica 23: 1–45.

Martinet B, Przybyla K, Atkins J, Bosiger Y, Evrard D, Gill P, van Alphen J, Whyte G, Rasmont P (2022) Description of nest architecture and ecological notes on the bumblebee *Bombus* (*Pyrobombus*) *lapponicus* (Hymenoptera: Apidae: Bombini). Insectes Sociaux 69: 131–135. https://doi.org/10.1007/s00040-022-00849-5

Panfilov DV (1968) Obshchij obzor naselenija pchelinyh Evrazii [General overview of the communities of bees in Eurasia]. Sbornik trudov Zoologicheskogo muzeja Moskovskogo universiteta 11: 18–35. [In Russian]

Paukkunen J, Kozlov MV (2020) Stinging wasps, ants and bees (Hymenoptera: Aculeata) of the Nenets Autonomous Okrug, northern Russia. Annales Zoologici Fennici 57(1–6): 115–128. https://doi.org/10.5735/086.057.0112

Pittioni B (1943) Die boreoalpinen Hummeln und Schmarotzerhummeln (Hymen., Apidae, Bombinae). Teil 2. Mitteilungen aus den Königlichen Naturwissenschaftlichen Instituten in Sofia 16: 1–78.

Pokrovsky I, Ehrich D, Ims RA, Kondratyev AV, Kruckenberg H, Kulikova O, Mihnevich J, Pokrovskaya L, Shienok A (2015) Rough-legged buzzards, Arctic foxes and red foxes in a tundra ecosystem without rodents. PLoS ONE 10(2): e0118740. https://doi.org/10.1371/journal.pone.0118740

Potapov GS, Kolosova YuS, Gofarov MY (2014) Zonal distribution of bumblebee species (Hymenoptera, Apidae) in the North of European Russia. Entomological Review 94(1): 79–85. https://doi.org/10.1134/S0013873814010096

Potapov GS, Kolosova YS, Zubriy NA, Filippov BY, Vlasova AA, Spitsyn VM, Bolotov IN, Kondakov AV (2017) New data on bumblebee fauna (Hymenoptera: Apidae, *Bombus* Latr.) of Vaygach Island and the Yugorsky Peninsula. Arctic Environmental Research 17(4): 346–354. https://doi.org/10.17238/issn2541-8416.2017.17.4.346

Potapov GS, Kondakov AV, Spitsyn VM, Filippov BY, Kolosova YS, Zubrii NA, Bolotov IN (2018a) An integrative taxonomic approach confirms the valid status of *Bombus glacialis*, an endemic bumblebee species of the High Arctic. Polar Biology 41(4): 629–642. https://doi.org/10.1007/s00300-017-2224-y

Potapov GS, Kondakov AV, Kolosova YS, Tomilova AA, Filippov BY, Gofarov MY, Bolotov IN (2018b) Widespread continental mtDNA lineages prevail in the bumblebee fauna of Iceland. ZooKeys 774: 141–153. https://doi.org/10.3897/zookeys.774.26466

Potapov GS, Kondakov AV, Filippov BY, Gofarov MY, Kolosova YS, Spitsyn VM, Tomilova AA, Zubrii NA, Bolotov IN (2019) Pollinators on the polar edge of the Ecumene: Taxonomy,

phylogeography, and ecology of bumble bees from Novaya Zemlya. ZooKeys 866: 85–115. https://doi.org/10.3897/zookeys.866.35084

Potapov GS, Berezin MV, Kolosova YS, Kondakov AV, Tomilova AA, Spitsyn VM, Zheludkova AA, Zubrii NA, Filippov BY, Bolotov IN (2021a) The last refugia for a polar relict pollinator: Isolates of *Bombus glacialis* on Novaya Zemlya and Wrangel Island indicate its broader former range in the Pleistocene. Polar Biology 44(8): 1691–1709. https://doi.org/10.1007/s00300-021-02912-6

Potapov GS, Spitsyna EA, Spitsyn VM (2021b) The first record of *Boloria frigga* (Lepidoptera: Nymphalidae) on Kolguev Island, Arctic Russia. Travaux du Muséum National d'Histoire Naturelle. Grigore Antipa 64(2): 103–108. https://doi.org/10.3897/travaux.64.e65131

Radchenko VG, Pesenko YuA (1994) Biology of bees (Hymenoptera, Apoidea). Zoological Institute RAS, Saint-Petersburg, 351 pp. [In Russian]

Rasmont P, Ghisbain G, Terzo M (2021) Bumblebees of Europe and neighbouring regions. Hymenoptera of Europe 3. N.A.P. Editions, Verrières-le-Buisson, 628 pp.

Ratnasingham S, Hebert PDN (2007) BOLD: The Barcode of Life Data System. Molecular Ecology Notes 7(3): 355–364. https://doi.org/10.1111/j.1471-8286.2007.01678.x

Richards KW (1973) Biology of *Bombus polaris* Curtis and *B. hyperboreus* Schönherr at Lake Hazen, Northwest territories (Hymenoptera: Bombini). Quaestiones Entomologicae 9: 115–157.

Semenov A (1904) Contribution à la faune de l'île Kolgujev. Coleoptera. Horae Societatis Entomologicae Rossicae 37: 116–126. [In Russian]

Sheffield CS, Oram R, Heron JM (2020) *Bombus* (*Pyrobombus*) *johanseni* Sladen, 1919, a valid North American bumble bee species, with a new synonymy and comparisons to other "red-banded" bumble bee species in North America (Hymenoptera, Apidae, Bombini). ZooKeys 984: 59–81. https://doi.org/10.3897/zookeys.984.55816

Spitsyn VM, Bolotov NI (2020) First record of *Syngrapha diasema* (Lepidoptera: Noctuidae) from Kolguev Island, Arctic Russia. Biharean Biologist 14(1): 52–53.

Svendsen JI, Alexanderson H, Astakhov VI, Demidov I, Dowdeswell JA, Funder S, Gataullin V, Henriksen M, Hjort C, Houmark-Nielsen M, Hubberten HW, Ingolfsson O, Jakobsson M, Kjær KH, Larsen E, Lokrantz H, Lunkka JP, Lyså A, Mangerud J, Matiouchkov A, Murray A, Möller P, Niessen F, Nikolskaya O, Polyak L, Saarnisto M, Siegert C, Siegert MJ, Spielhagen RF, Stein R (2004) Late Quaternary ice sheet history of northern Eurasia. Quaternary Science Reviews 23(11–13): 1229–1271. https://doi.org/10.1016/j.quascirev.2003.12.008

Velichko AA (2002) Dynamics of terrestrial landscape components and inland and marginal seas of Northern Eurasia during the last 130000 years. Atlas-monograph "Evolution of landscapes and climates of Northern Eurasia. Late Pleistocene – Holocene – elements of prognosis. II. General paleogeography". GEOS, Moscow, 296 pp. [In Russian]

Williams PH (1998) An annotated checklist of bumble bees with an analysis of patterns of description (Hymenoptera: Apidae, Bombini). Bulletin of the Natural History Museum Entomology Series 67: 79–152. [updated at] https://www.nhm.ac.uk/research-curation/research/projects/bombus/

Williams PH, Thorp RW, Richardson LL, Colla SR (2014). Bumble Bees of North America: An Identification Guide. Princeton University Press, Princeton, 208 pp.

Williams PH, Byvaltsev AM, Cederberg B, Berezin MV, Ødegaard F, Rasmussen C, Richardson LL, Huang J, Sheffield CS, Williams ST (2015) Genes Suggest Ancestral Colour Polymorphism are Shared Across Morphologically Cryptic Species in Arctic Bumblebees. PLoS ONE 10(12): e0144544. https://doi.org/10.1371/journal.pone.0144544

Williams PH, Berezin MV, Cannings SG, Cederberg B, Ødegaard F, Rasmussen C, Richardson LL, Rykken J, Sheffield CS, Thanoosing C, Byvaltsev AM (2019) The arctic and alpine bumblebees of the subgenus *Alpinobombus* revised from integrative assessment of species' gene coalescents and morphology (Hymenoptera, Apidae, *Bombus*). Zootaxa 4625(1): 1–68. https://doi.org/10.11646/zootaxa.4625.1.1

Supplementary material 1

Table S1

Authors: Grigory S. Potapov, Yulia S. Kolosova, Alexander V. Kondakov, Alena A. Tomilova, Boris Yu. Filippov, Natalia A. Zubrii, Vitaly M. Spitsyn, Elizaveta A. Spitsyna, Alisa A. Zheludkova, Mikhail Yu. Gofarov, Galina V. Bovykina, Ivan N. Bolotov

Data type: Specimen data

Explanation note: Specimens of bumble bees examined under this study.

  Link: https://doi.org/10.3897/zookeys.1122.82993.suppl1

RESEARCH ARTICLE

A peer-reviewed open-access journal

ZooKeys

Launched to accelerate biodiversity research

Long-term stability in the winter diet of the Japanese serow (Artiodactyla, Caprinae)

Mitsuko Hiruma[1], Kahoko Tochigi[1], Ryosuke Kishimoto[2], Misako Kuroe[3], Bruna Elisa Trentin[4], Shinsuke Koike[5]

1 *Graduate School of Agriculture, Tokyo University of Agriculture and Technology, 3-5-8 Saiwai-Cho, Fuchu, Tokyo 183-8509, Japan* **2** *Institute of Mountain Science, Shinshu University, 8304 Minami-minowa, Kamiina-gun, Nagano 399-4511, Japan* **3** *Nagano Environmental Conservation Research Institute, 2054-120 Kitagou, Nagano 381-0075, Japan* **4** *Department of Ecology, UNESP São Paulo State University, Botucatu, São Paulo 18610-034, Brazil* **5** *Institute of Agriculture, Tokyo University of Agriculture and Technology, 3-5-8 Saiwai-Cho, Fuchu, Tokyo 183-8509, Japan*

Corresponding author: Shinsuke Koike (koikes@cc.tuat.ac.jp)

Citation: Hiruma M, Tochigi K, Kishimoto R, Kuroe M, Trentin BE, Koike S (2022) Long-term stability in the winter diet of the Japanese serow (Artiodactyla, Caprinae). ZooKeys 1122: 39–51. https://doi.org/10.3897/zookeys.1122.76486

Abstract

The winter diets of northern ungulates are sensitive to changes in environmental conditions and ungulate population densities. We hypothesized that the winter diets of smaller browser ungulates might not readily change in response to fluctuating environmental conditions. We analyzed long-term trends in the winter diet of the Japanese serow (*Capricornis crispus*) by analyzing rumen contents of 532 individuals over a span of 16 years among five populations along with changes in the population densities of sika deer (*Cervus nippon*) in Nagano Prefecture, central Japan. The winter diet composition of the serow was stable over the long term despite the increase in deer population density. The little-flexible nature of the serow diet may explain the long-term stability in the winter diets.

Keywords

browser, *Capricornis crispus*, *Cervus nippon*, population dynamics, sika deer, ungulate

Introduction

The winter diets of northern ungulates are sensitive to changes in environmental conditions, and the compositions of their diets undergo change to adapt to the nutritional restrictions of winter (e.g., Matinka 1968; Coblentz 1970; Morrison et al. 2002). Thus, nutrition is a critical link between environmental and population density in northern populations of free-ranging ungulates (Skogland 1985; Garroway and Broders 2005). Nevertheless, research on the winter food habits of northern free-ranging ungulates has mostly been limited to short-term studies.

Previous long-term studies on the winter diet of white-tailed deer (*Odocoileus virginianus*) have shown that changes in vegetation alongside changing population densities and increasing snow depth can influence the winter diet (McCullough 1985; Tremblay et al. 2005; DelGiudice et al. 2012). Annual variations in the winter diet affect the deer's nutritional intake, body condition, and population dynamics (Delgiudice et al. 2001). For sika deer (*Cervus nippon*), population density, snow depth, and habitat quality (e.g., vegetation structure) are critical factors that influence the composition of the winter diet (Seto et al. 2015). According to these studies, both grazers (northern sika deer) and browsers (white-tailed deer) can alter their winter diets according to changes in environmental conditions and population density (McCullough 1985; Tremblay et al. 2005; DelGiudice et al. 2012; Seto et al. 2015). White-tailed deer are medium-sized (50–130 kg) browsers that live in various habitats, such as forests and grasslands. They are nonterritorial, gather in herds, consume grasses, and migrate to areas that are rich in food resources (Smith 1991; VerCauteren and Hygnstrom 1998). However, smaller browsers tend to be solitary, territorial, inhabit forests, generally possess a higher-quality diet, and are highly selective in terms of food items and foraging areas (Jarman 1974; Hofmann 1989). We hypothesized that the winter diet of smaller and forest-dwelling browsers might not readily change in response to fluctuating environmental conditions.

The Japanese serow (*Capricornis crispus*) is an endemic ungulate species in Japan. The Japanese serow was designated as a Special National Treasure in 1955; hunting this animal is illegal. In the early 20th century, the number of serows decreased dramatically due to poaching, but their populations gradually recovered after protective legislation was passed after World War II (Tokida 2019). In the 1970s, their expanded distribution and increased population sparked conflicts with the forestry industry because serows eat the twigs and leaves of young trees in conifer plantations in the winter. Consequently, partial and facultative culling has been permitted since 1979 in damaged forest areas, and since 1990 in some damaged agricultural regions. Serows are small (30–50 kg) members of the family Bovidae and mainly inhabit forests. They are solitary, monogamous, and territorial. The habitat areas of male and female serows overlap; however, individual territories that are scent-marked with parotid gland secretions do not overlap with those of the same sex (Ochiai 2009). Serows are browsers

that selectively feed on high-quality plant material; they mainly subsist on the leaves of deciduous broad-leaved trees and forbs from spring to fall and deciduous broad-leaved winter buds in the winter when food availability is low (Ochiai 1999). Depending on their habitat, they may also feed on evergreen conifers, evergreen shrubs, grasses, and sedges (Ochiai 1999; Jiang et al. 2008; Kobayashi and Takatsuki 2012; Asakura et al. 2014; Yamashiro et al. 2019). The leaves of conifers and broad-leaved evergreens can also serve as significant food resources for the serow (Jiang et al. 2008).

We examined the changes in serow food habits by analyzing long-term (2000–2015) trends in winter food habits in central Japan along with changes in the environmental conditions. Particularly, we focused on the population density of sika deer as an environmental condition. The serow is a browser that mainly feeds on woody plants and is considered to have a narrow food habit, whereas the sika deer is considered an "intermediate feeder" among cervid species with a very flexible food habit (Hofmann 1985). Thus, a previous study indicated that there is potential competition for food sources between serows and sika deer, and serows might not switch to alternative foods due to their narrow food habits if the number of deer populations becomes overabundant (Tokida 2019). Moreover, the study pointed out that this phenomenon may decrease the density of serows (Tokida 2019). However, it has not been definitively confirmed that the food habits of serows remain unchanged as the density of sika deer increases. We hypothesized that the winter food habits of serows do not change as the sika deer increases, because the serow is a small-sized, solitary, territorial, and forest-dwelling browser that is characterized by highly selective foraging habits. We examined the annual variation in winter diets of serows in Nagano Prefecture, central Japan, as well as the potential key variables that influence serow inhabitation.

Methods

Study area and population status of serow

Nagano Prefecture, Japan (35°11'–37°01'N, 137°19'–138°44'E) (Fig. 1), covers a wide latitudinal area, with a climate that differs markedly from north to south. The annual mean temperature, precipitation, and snow accumulation for the years 2005–2015 were 12.2 °C, 81.3 mm, and 14.4 cm depth, respectively, in the northern region (36°39'N, 138°11'E); 11.4 °C, 107.7 mm, and 7.7 cm depth, respectively, in the central region (36°02'N, 138°06'E); and 13.0 °C, 138.6 mm, and 5.4 cm depth, respectively, in the southern region (35°31'N, 137°49'E) (Japan Meteorological Agency 2019). No statistically significant trend was highlighted in long-term changes in the annual greatest snow depth in Nagano Prefecture (Shinshu Monitoring Network for Climate Change 2018).

The estimated total serow population in Nagano Prefecture was 9340 ± 1630 in 2000 but has hovered around 7738 ± 6420 in 2018 using the block-count method (Nagano Prefecture 2020). There has been little change in the distribution area of serows over the past 20 years (Nagano Prefecture 2020). There are seven local serow populations in Nagano Prefecture: Echigo–Nikko–Mikuni (EN), South Alps (SA), North Alps (NA), Central Alps (CA), Yatsugatake (YA), Kanto Mountains, and Northern Nagano (Nagano Prefecture 2020). The Kanto Mountains and Northern Nagano populations were excluded from this study because the sample numbers of the populations were too small for data analysis. The results of an official national survey using the block-count method (Maruyama and Furubayashi 1983) after fall defoliation revealed gradual long-term declines from 2000 to 2014 in all populations. The densities (serows / km² ± SD) of the populations in 2000, 2004, and 2014, are shown in Table 1 (Nagano Prefecture 2000, 2020).
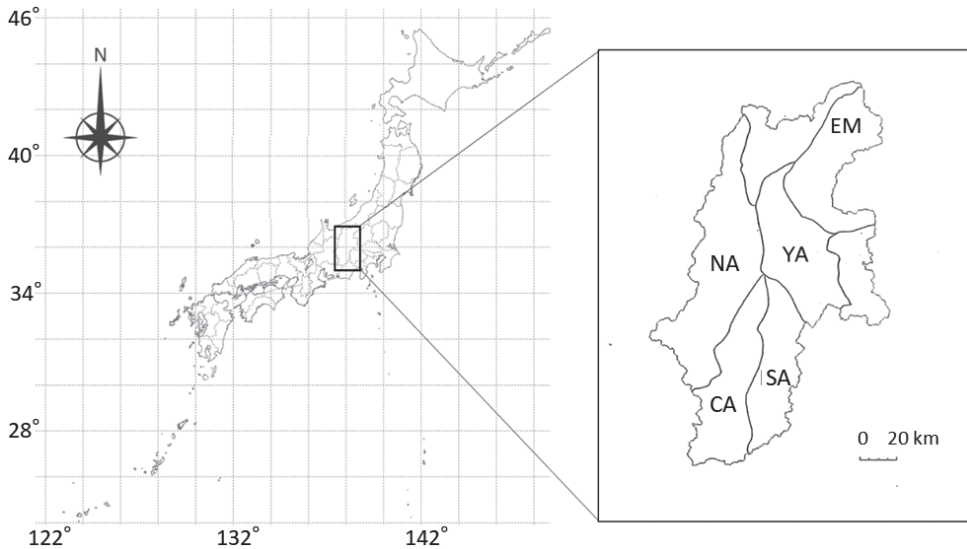
Figure 1. Location of Nagano Prefecture and location of the five serow populations analyzed: Echigo–Nikko–Mikuni (EM), South Alps (SA), North Alps (NA), Central Alps (CA), and Yatsugatake (YA).

Table 1. Estimated densities (serows / km² ± SD) of the serow populations in 2000, 2004, and 2014 (Nagano Prefecture 2000, 2020).

	EM	SA	YA	NA	CA
2000	2.48 ± 3.43	0.57 ± 0.83	0.47 ± 1.04	1.70 ± 1.99	4.16 ± 3.23
2004	0.51	0.33 ± 0.67	0.46 ± 0.73	0.51 ± 0.61	2.40 ± 2.37
2014	0.83 ± 1.11	0.25 ± 0.70	0.28 ±0.49	0.59 ± 1.00	2.22 ± 2.84

Echigo–Nikko–Mikuni (EM), South Alps (SA), Yatsugatake (YA), North Alps (NA), and Central Alps (CA).
Estimated number and density (number/km²) based on the block count method.

Serow rumen samples

Since 2000, approximately 10% of the rumen contents has been collected randomly from each culled serow for monitoring purposes (Fig. 2). We used rumen content samples from serows culled in forest areas from 2000 to 2015 for analysis. The sample numbers for each population are as follows: EN, 99; SA, 71; NA, 148; CA, 160; and YA, 54. In total, we analyzed 532 samples.

We analyzed the reported frequencies as percentages of each food group using the point-frame method (Stewart 1967), which estimates the percentage composition according to the surface area and is easier to conduct than weight-based methods. We randomly selected subsamples from each sample, spread them over 5 mm grids, and then identified the plant fragments touching each intersection point along a transect. We evaluated each subsample at 400 points or more per transect. Since we could not identify most plant fragments to the species level, we categorized them into six food groups: i.e., leaves of deciduous broad-leaved trees, leaves of broad-leaved evergreens trees, leaves of planted conifers, leaves of natural conifers, leaves of graminoids, and other materials. The other food materials include woody fibers, woody buds, fruits, ferns, and unknown items. Planted conifers refer to *Cryptomeria japonica* and *Chamaecyparis obtusa*, whereas natural conifers comprise other conifer species.
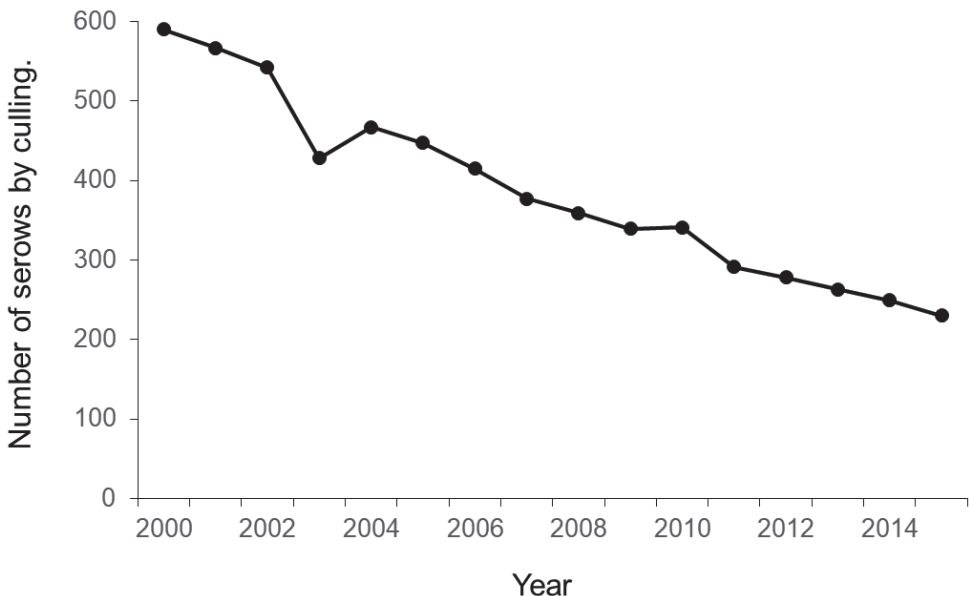
Figure 2. Number of serows through culling from 2000 to 2014 (Nagano Prefecture 2020).

Deer density

For data regarding sika deer population density, we referred to the official surveys conducted by Nagano Prefecture (Table 2) (Nagano Prefecture 2016). These surveys grouped deer into seven populations that nearly overlap with the serow populations; therefore, we used the deer density for the deer population (hereafter, deer density) that corresponded to the target serow population. We used the values for the years that the survey was conducted (1999, 2010, and 2015) to estimate a regression model in which the value for the no-survey years was the dependent variable and the value for the recorded year was the explanatory variable. We then used the value estimated by the said regression model (theoretical value on the regression line) as the assigned value.

The results of an official survey using the block count and fecal pellet count methods in the fall of each year (1999–2015) revealed that there was a gradual long-term increase in the deer population in YA, whereas the densities of the SA population remained stable, and the densities of the NA, CA, and EN populations remained low. Additionally, most areas were not inhabited by deer until the 2000s (Fig. 3) (Nagano Prefecture 2016).

Table 2. Estimated number and density (median values) of sika deer in each area of Nagano Prefecture in 1999, 2010, and 2015 (Nagano Prefecture 2016).

	YA	SA	Other
1999	8,657 (6.2)	18,858 (11.2)	–
2010	48,527 (20.7)	33,787 (11.4)	8,644 (3.9)
2015	128,598 (51.4)	30,812 (12.7)	19,795 (5.2)

Yatsugatake (YA) and South Alps (SA)
Estimated number and density (number/km²) based on the block count and fecal pellet methods.
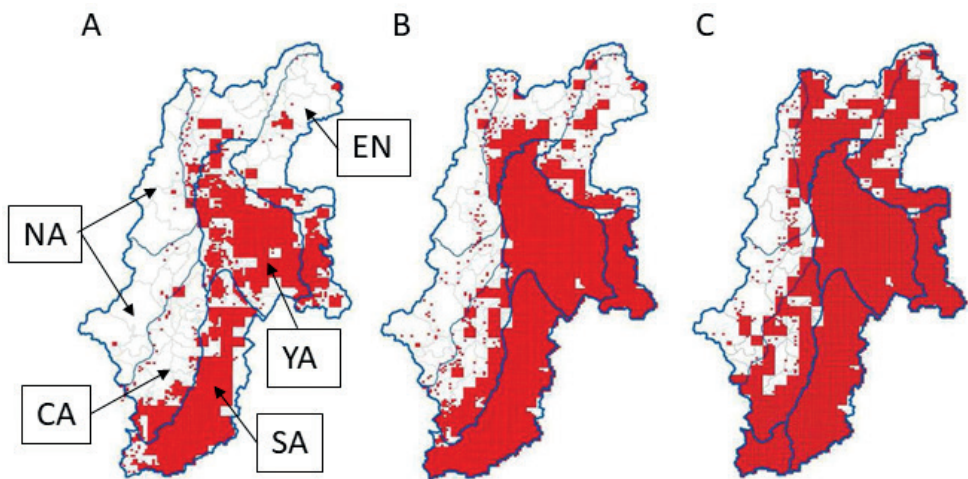
Figure 3. Distribution of sika deer in Nagano Prefecture in 2003 (**A**), 2010 (**B**), and 2015 (**C**). Red area: the distribution meshes (1 km²: 1 km × 1 km) of the existence or non-existence of sika deer based on a questionnaire completed by local people and hunting statistic data (Nagano Prefecture 2016).

Statistical analysis

For analysis, years potentially have both a direct effect through the decrease of food availability and an indirect effect thorough deer density on the winter diet of serows. We employed Bayesian regression models with paths to verify the existence or non-existence of this relationship.

First, we converted the food item frequency of each food group to proportions and modeled them with Dirichlet regression to account for the composition data. Since the number of rumen content counts at cross-sectional points is equal to the discrete level, and the total number of counts for each subsample is summed up to a fixed number, the probability of the occurrence of one group is influenced by increases or decreases in other groups (i.e., multivariate analysis). A disadvantage of this transformation is that the information from the data is changed or lost when skewing the data structure. In contrast, the Dirichlet distribution is appropriate for count-based data summed up to a fixed value.

To build a model for estimating the factors influencing diets of serows, we set the proportion of the six food groups as the response variables. In food groups, we set leaves of deciduous broad-leaved trees as the reference category. We defined year (the years 2000–2015 were converted to years 1–16) and deer density as the explanatory variables. Food composition is possibly different among serow populations due to differences in vegetation and food availability. Therefore, we included the serow population as a random effect. We assumed that response variables follow a Dirichlet distribution.

To build a model for estimating annual changes in deer density, we set the deer density as a response variable and year as an explanatory variable. Density may differ among deer populations due to differences in hunting pressure and food availability. Therefore, we included the serow population as a random effect. We assumed that response variables follow a normal distribution.

To evaluate whether there are significant paths among serow dietary composition, year, and deer density, we checked whether 95% credible intervals (CIs) for estimate values of each variable were greater than zero. We standardized the estimated unstandardized coefficients to compare the impact of factors in which the unit and size differed. We used a Bayesian approach, implemented using the BRMS (Bayesian Regression Model Stan) package (Bürkner 2018) in R (R Core Team 2021). We used the BRMS default priors for each regression. We set the number of iterations to 30,000 and discarded the first 20,000 steps as burn-in. Then, we thinned the remaining 10,000 steps every 50 steps to give 1000 samplings per chain. Subsequently, we ran four chains with randomly selected initial values for each model. Finally, we evaluated whether MCMC converged well from visual assessment using the Gelman–Rubin diagnostic (1.00–1.08) (Gelman et al. 2003).

Results

According to the model analysis results, the 95% CIs of coefficients of year and deer density on all food groups had zero overlap (Table 3). In other words, the composition of food in the serow rumens did not change linearly over the years and was not affected
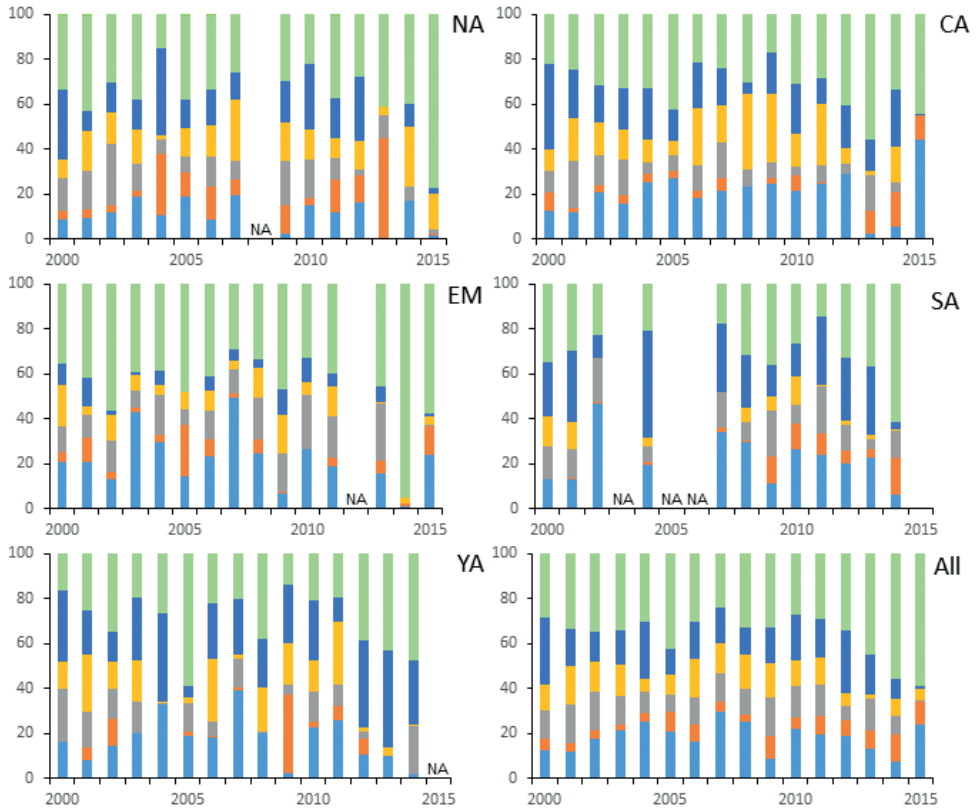
Figure 4. Percent composition of the six major food groups in Japanese serow rumen samples of the six populations in Nagano Prefecture, pooled across the populations from 2000 to 2015. The leaves of different plants are depicted as follows. Aqua: deciduous broad-leaved trees, orange: broad-leaved evergreens trees, gray: planted conifers, yellow: natural conifers, blue: graminoids, yellow: other plant foods. The populations are North Alps (NA), Central Alps (CA), Echigo–Nikko–Mikuni (EN), South Alps (SA), Yatsugatake (YA), and pooled across all populations (All).

by deer density (Fig. 4). The effect of year on deer density was significant (unstandardized mean = 0.058; 95% CI: 0.039, 0.075, Table 3). Therefore, only the direct path of year to deer density was significant. These results are due to the fact that we had to estimate the no-survey years of deer density by regression imputation. The direct path of the year to serow diets and the indirect path of the year through deer density to serow food composition were not significant (Fig. 5).

Discussion

The serows' winter diet did not readily change in response to increasing deer density. This may be a result of their ecological characteristics, such as small size, solitary na-

Table 3. Model coefficients for six the food plat groups of the serow rumen modeled with Dirichlet distribution for deer density and with normal distribution. Leaves of deciduous broad-leaved trees were set as the reference category. We presented estimates in 95% credible intervals (CIs) for each model parameters. All response variables had a random effect on population. Estimated coefficients were standardized to have zero mean with a standard deviation 1.

Response variables	Parameter	Estimate	SE	Lower CI	Upper CI	Standardized estimate
Fixed effect						
Leaves of broad-leaved evergreen trees	Intercept	–1.032	0.163	–1.360	–0.737	0.000
	Year	0.019	0.014	–0.008	0.046	0.640
	Deer density	–0.004	0.010	–0.024	0.017	–0.217
Leaves of planted conifers	Intercept	–0.342	0.135	–0.628	–0.085	0.000
	Year	–0.013	0.014	–0.042	0.013	–0.326
	Deer density	0.008	0.010	–0.011	0.028	0.317
Leaves of natural conifers trees	Intercept	–0.734	0.211	–1.139	–0.320	0.000
	Year	0.024	0.014	–0.003	0.051	0.559
	Deer density	–0.003	0.010	–0.021	0.017	–0.094
Leaves of graminoids	Intercept	–0.312	0.243	–0.792	0.210	0.000
	Year	–0.005	0.014	–0.031	0.022	–0.095
	Deer density	0.008	0.010	–0.012	0.027	0.250
Other food material	Intercept	0.491	0.166	0.139	0.789	0.000
	Year	0.013	0.012	–0.011	0.038	0.246
	Deer density	–0.003	0.010	–0.022	0.017	–0.085
Deer density	Intercept	1.033	0.888	–0.964	2.780	0.000
	Year	0.058	0.009	0.039	0.075	0.037
Random effect						
SD (Leaves of broad-leaved evergreen trees)	Intercept	0.187	0.189	0.011	0.705	
SD (Leaves of planted conifers trees)	Intercept	0.129	0.114	0.005	0.407	
SD (Leaves of natural conifers)	Intercept	0.317	0.208	0.083	0.873	
SD (Leaves of graminoids)	Intercept	0.421	0.277	0.134	1.200	
SD (Other food material)	Intercept	0.219	0.195	0.015	0.760	
SD (Deer density)	Intercept	1.864	0.898	0.800	4.204	
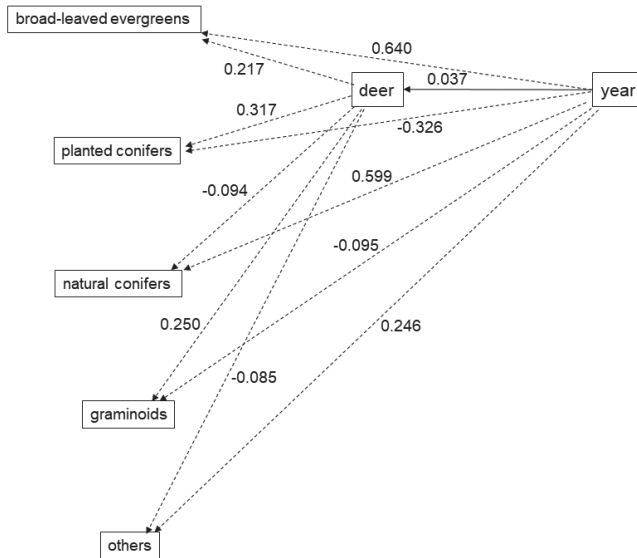
Figure 5. Directed acyclic graph depicting the year and deer density that are not important in the path analysis of serow food habits. Solid lines: 95% credible intervals (CIs) whose path coefficients do not overlap with zero (see Table 2). Dash lines: coefficients whose 95% CIs overlap with zero. The larger the absolute value of the coefficient, the stronger the effect.

ture, and territoriality, which characterized highly selective foraging habits. Therefore, the results support our hypothesis.

It is well known that when deer density rises, vegetation, particularly forest floor vegetation, declines or disappears (Takatsuki 2009). In Nagano Prefecture, there is evidence that the forest ground vegetation is decreasing due to the increasing deer population (Nagano Prefecture 2016). Previous studies on the degree of dietary overlap between serows and sika deer revealed the existence of a dietary partition between the two species (Kobayashi and Takatsuki 2012). However, due to the vast range and flexibility of feeding habits in deer, they expanded their diet to include coniferous tree needles and twigs and bark of deciduous trees only during severe winters that is limited food resources season (Koganezawa 1999). As a result, their diet overlapped with that of the serows during these winters, possibly resulting in a rapid depletion of the serows' restricted food supply due to the expanded consumption of food items of sika deer. In accordance with the findings from the previous studies, the results of this study suggest the following two possibilities by deer density increase for serows' response occurs separately or simultaneously.

First, spatial partitioning between sika deer and serows may progress. Although there are some regions where the diets of both species overlap, distinctions in habitat use between the two species are also known (Yamashiro et al. 2019). Specifically, there are differences in habitat use between the two species; serows utilized steep rocky slopes, whereas sika deer appeared more frequently in grasslands (Yamashiro et al. 2019; Takada et al. 2020). Due to this spatial partitioning, increase of sika deer population might not have affected the winter diet of serow populations. Second, as serows strictly defend their home ranges as intrasexual territories and are very sedentary (Kishimoto and Kawamichi 1996), it is assumed that serows may respond to decrease food amount caused by an increase deer density by expanding their territorial range. This is supported by the positive correlation between food amount and serows density and negative correlation between food amount and serows' territorial range size (Sone et al. 1999; Ochiai et al. 2010). Therefore, if food availability deteriorates to the point where the serows cannot maintain territory, serows may need to move into the more inhospitable region. The occurrence of these two events may have caused a long-term decline in serow population.

In this study, we could not clearly evaluate the relationship between the increase in deer and the decrease in serows because we did not investigate changes in the vegetation structure and winter food habits of deer and serows' behavior. However, decrease in serow food supply as a result of increased sika deer density could have resulted in a spatial partitioning between sika deer and serow or decrease in serow density.

Acknowledgements

References

Asakura G, Kaneshiro Y, Takatsuki S (2014) A comparison of the fecal compositions of sympatric populations of sika deer and Japanese serow on Mt. Sanrei in Shikoku, southwestern Japan. Mammal Study 39(2): 129–132. https://doi.org/10.3106/041.039.0201

Bürkner P (2018) Advanced Bayesian multilevel modeling with the R package brms. The R Journal 10(1): 395–411. https://doi.org/10.32614/RJ-2018-017

Coblentz BE (1970) Food habits of George Reserve deer. The Journal of Wildlife Management 34(3): 535–540. https://doi.org/10.2307/3798859

Delgiudice GD, Moen RA, Singer FJ, Riggs MR (2001) Winter nutritional restriction and simulated body condition of Yellowstone elk and bison before and after the fires of 1988. Wildlife Monographs 147: 1–60.

DelGiudice GD, Sampson BA, Giudice J (2012) A long-term assessment of the effect of winter severity on the food habits of white-tailed deer. The Journal of Wildlife Management 77(8): 1664–1675. https://doi.org/10.1002/jwmg.616

Garroway CJ, Broders HG (2005) The quantitative effects of population density and winter weather on the body condition of white-tailed deer (Odocoileus virginianus) in Nova Scotia, Canada. Canadian Journal of Zoology 83(9): 1246–1256. https://doi.org/10.1139/z05-118

Gelman A, Carlin JB, Stern HS, Rubin DB (2003) Bayesian Data Analysis. 2nd Edn. Champan & Hall/CRC, London, 668 pp. https://doi.org/10.1201/9780429258480

Hofmann RR (1985) Digestive physiology of deer: their morphophysiological specialization and adaption. In: Drew K, Fennessy P (Eds) Biology of deer production. Royal Society of New Zealand Bulletin 22: 393–407.

Hofmann RR (1989) Evolutionary steps of ecophysiological adaptation and diversification of ruminants: A comparative view of their digestive system. Oecologia 78(4): 443–457. https://doi.org/10.1007/BF00378733

Japan Meteorological Agency (2019) Endangered species database. 2005–2014. http://www.data.jma.go.jp/obd/stats/etrn/index.php [Accessed 6 September 2020]

Jarman PJ (1974) The social organization of antelope in relation to their ecology. Behaviour 48(1–4): 215–266. https://doi.org/10.1163/156853974X00345

Jiang Z, Torii H, Takatsuki S, Ohba T (2008) Local variation in diet composition of the Japanese serow during winter. Zoological Science 25(12): 1220–1226. https://doi.org/10.2108/zsj.25.1220

Kishimoto R, Kawamichi T (1996) Territoriality and monogamous pairs in a solitary ungulate, the Japanese serow, Capricornis crispus. Animal Behaviour 52(4): 673–682. https://doi.org/10.1006/anbe.1996.0212

Kobayashi K, Takatsuki S (2012) A comparison of food habits of two sympatric ruminants of Mt. Yatsugatake, central Japan: Sika deer and Japanese serow. Acta Theriologica 57(4): 343–349. https://doi.org/10.1007/s13364-012-0077-x

Koganezawa M (1999) Changes in the population dynamics of Japanese serow and sika deer as a result of competitive interactions in the Ashio Mountains, central Japan. Biosphere Conservation 2: 35–44. https://doi.org/10.20798/biospherecons.2.1_35

Maruyama N, Furubayashi K (1983) Preliminary examination of block count method for estimating numbers of sika deer in Fudakake. Journal of the Mammalogical Society of Japan 9: 274–278. https://doi.org/10.11238/jmammsocjapan1952.9.274

Matinka CJ (1968) Habitat relationships of white-tailed deer and mule deer in northern Montana. The Journal of Wildlife Management 32(3): 558–565. https://doi.org/10.2307/3798936

McCullough DR (1985) Variables influencing food-habits of whitetailed deer on the George Reserve. Journal of Mammalogy 66(4): 682–692. https://doi.org/10.2307/1380794

Morrison SF, Forbes GJ, Young SJ (2002) Browse occurrence, biomass, and use by white-tailed deer in a northern New Brunswick deer yard. Canadian Journal of Forest Research 32(9): 1518–1524. https://doi.org/10.1139/x02-081

Nagano Prefecture (2000) Specified Wildlife Conservation and Management Plan (Japanese Serow). Nagano Prefecture, Japan, 42 pp. [In Japanese]

Nagano Prefecture (2016) Specified Wildlife Conservation and Management Plan (Sika Deer). Nagano Prefecture, Japan, 72 pp. [In Japanese]

Nagano Prefecture (2020) Specified Wildlife Conservation and Management Plan (Japanese Serow). Nagano Prefecture, Japan, 62 pp. [In Japanese]

Ochiai K (1999) Diet of the Japanese serow (Capricornis crispus) on the Shimokita Peninsula, northern Japan, in reference to variations with a 16-year interval. Mammal Study 24(2): 91–102. https://doi.org/10.3106/mammalstudy.24.91

Ochiai K (2009) *Capricornis crispus* (Temminck, 1945). In: Ohdachi SD, Ishibashi Y, Iwasa MA, Saitoh T (Eds) The Wild Mammals of Japan. Shoukadoh Book Sellers, Kyoto, 306–309.

Ochiai K, Susaki K, Mochizuki T, Okasaka Y, Yamada Y (2010) Relationships among habitat quality, home range size, reproductive performance and population density: Comparison of three populations of the Japanese serow (Capricornis crispus). Mammal Study 35(4): 265–276. https://doi.org/10.3106/041.035.0406

R Core Team (2021) R: a language and environment for statistical computing. R Foundation for Statistical Computing, Vienna, Australia.

Seto T, Matsuda N, Okahisa Y, Kaji K (2015) Effects of population density and snow depth on the winter food composition of two contrasting sika deer populations. The Journal of Wildlife Management 79: 243–253. https://doi.org/10.1002/jwmg.830

Shinshu Monitoring Network for Climate Change (2018) The report of Shinshu Monitoring Network for Climate Change 2015. https://shinshu-moninet.org/wp-content/uploads/2018/02/report2015_full.pdf [Accessed 29 July 2021]

Skogland T (1985) The effects of density-dependent resource limitations on the demography of wild reindeer. Journal of Animal Ecology 54(2): 359–374. https://doi.org/10.2307/4484

Smith WP (1991) Odocoileus virginianus. Mammalian Species 388(388): 1–13. https://doi.org/10.2307/3504281

Sone K, Okumura H, Abe M, Kitahara E (1999) Biomass of food plants and density of Japanese serow, Capricornis crispus. Memoirs of the Faculty of Agriculture. Kagoshima University 35: 7–16.

Stewart DRM (1967) Analysis of plant epidermis in faeces: A technique for studying the food preferences of grazing herbivores. Journal of Applied Ecology 4(1): 83–111. https://doi.org/10.2307/2401411

Takada H, Ohuchi R, Watanabe H, Yano R, Miyaoka R, Nakagawa T, Zenno Y, Minami M (2020) Habitat use and the coexistence of the sika deer and the Japanese serow, sympatric ungulates from Mt. Asama, central Japan. Mammalia 84(6): 503–511. https://doi.org/10.1515/mammalia-2019-0150

Takatsuki S (2009) Effects of sika deer on vegetation in Japan: A review. Biological Conservation 142(9): 1922–1929. https://doi.org/10.1016/j.biocon.2009.02.011

Tokida K (2019) Japanese serows. In: Koike S, Yamaura Y, Taki H (Eds) Forest and wildlife. Kyoritsu Shuppan., Tokyo, 50–60. [In Japanese]

Tremblay JP, Thibault I, Dussault C, Huot J, Cote SD (2005) Long- term decline in white-tailed deer browse supply: Can lichens and litterfall act as alternative food sources that preclude density-dependent feedbacks. Canadian Journal of Zoology 83(8): 1087–1096. https://doi.org/10.1139/z05-090

VerCauteren KC, Hygnstrom SE (1998) Effects of agricultural activities and hunting on home ranges of female white-tailed deer. The Journal of Wildlife Management 62(1): 280–285. https://doi.org/10.2307/3802289

Yamashiro A, Kaneshiro Y, Kawaguchi Y, Yamashiro T (2019) Dietary overlap but spatial gap between sympatric Japanese serow (Capricornis crispus) and sika deer (Cervus nippon) on Eastern Shikoku, Japan. Mammal Study 44(4): 261–226. https://doi.org/10.3106/ms2018-0072

RESEARCH ARTICLE

A new species of *Racelda* Signoret, with taxonomical notes and a key to the males of the genus (Hemiptera, Reduviidae, Ectrichodiinae, Ectrichodiini)

Hélcio R. Gil-Santana[1], Jader Oliveira[2,3]

1 *Laboratório de Diptera, Instituto Oswaldo Cruz, Av. Brasil, 4365, 21040-360, Rio de Janeiro, RJ, Brazil*
2 *Universidade de São Paulo, Faculdade de Saúde Pública, Laboratório de Entomologia em Saúde Pública, São Paulo, SP, Brazil* 3 *Laboratório de Parasitologia, Universidade Estadual Paulista "Julio de Mesquita Filho", Faculdade de Ciências Farmacêuticas UNESP/FCFAR, Rodovia Araraquara Jaú, KM 1, 14801-902, Araraquara, SP, Brazil*

Corresponding author: Hélcio R. Gil-Santana (helciogil@uol.com.br, helciogil@ioc.fiocruz.br)

Citation: Gil-Santana HR, Oliveira J (2022) A new species of *Racelda* Signoret, with taxonomical notes and a key to the males of the genus (Hemiptera, Reduviidae, Ectrichodiinae, Ectrichodiini). ZooKeys 1122: 53–79. https://doi.org/10.3897/zookeys.1122.84424

Abstract

Racelda ottoi Oliveira & Gil-Santana, **sp. nov.**, belonging to the tribe Ectrichodiini in the subfamily Ectrichodiinae, is described based on males from northeastern Brazil. Photographs of the male types of *Racelda alternans* Signoret, 1863, *R. moerens* Breddin, 1898, and *R. spurca* (Stål, 1860) are presented. A summary of and notes on the taxonomic history of the genus and a key to males are provided.

Keywords

Introduction

The subfamily Ectrichodiinae in the New World includes 24 genera and more than 100 described species (Gil-Santana and Baena 2009; Gil-Santana et al. 2013, 2015, 2020; Gil-Santana 2014, 2015, 2019, 2020a, 2020b; Forthman and Weirauch 2017; Schuh and Weirauch 2020; Forthman and Gil-Santana 2021). A summary of the taxonomy of New World Ectrichodiinae was also provided by Gil-Santana et al. (2015).

Forthman and Weirauch (2017) created two new tribes, Ectrichodiini and Tribelocodiini, resulting in a new composition of Ectrichodiinae (*sensu novum*) in the New World. Ectrichodiini now includes all the genera formerly belonging to Ectrichodiinae, except *Ectrichodiella* Fracker & Bruner, 1924 which has been transferred to Tribelocodiini. The latter also includes *Tribelocodia* Weirauch, 2010 (which previously belonged to Tribelocephalinae, now a junior synonym of Ectrichodiinae). An updated key to the genera of this group considering this new arrangement of Ectrichodiinae was presented by Forthman and Gil-Santana (2021).

Because of the lack of consensus of previous authors about the validity or recognition of some genera of Ectrichodiini (Dougherty 1995; Carpintero and Maldonado 1996), there is a need of a taxonomic revision and a phylogenetic analysis of all these genera (Gil-Santana et al. 2015, 2020). For instance, *Pseudoracelda* Carpintero, 1980 was considered to be a junior synonym of *Racelda* Signoret, 1863 by Dougherty (1995) but a valid genus by Carpintero and Maldonado (1996), Forero (2004), Gil-Santana et al. (2013, 2015, 2020), and Forthman and Gil-Santana (2021). It is noteworthy that in this case, Dougherty (1995: 175) justified her synonymization of these genera by stating that *Pseudoracelda* would have been erected by Carpintero (1980) for a female "whose character description fits well within the diversity seen in the sexual dimorphism of the genus *Racelda*." She also stated that *P. macrocephala* Carpintero, 1980 "is retained as a species of *Racelda* because the unique specimen is unavailable for study." In Ectrichodiinae, the sexual dimorphism ranges from slight (e.g., body size, development of the hemelytron, and eye and ocellar size) to extreme, where females exhibit brachyptery to aptery in both pairs of wings and major modifications in other parts of the body (Forthman and Weirauch 2017). Sexual dimorphism in *Racelda* is regarded as being strongly developed (Dougherty 1995) or extreme (Forthman and Weirauch 2017). The females are apterous, their external structures are so strongly modified that it is impossible to associate females to a species, except if associated with the respective males (Dougherty 1995). In *Racelda*, the apterous females have small eyes, the ocellar tubercle obsolete, and ocelli lacking; the posterior lobe of pronotum and the scutellum may be atrophied (Carpintero and Maldonado 1996). *Pseudoracelda*, however, was described based on a male holotype and, more importantly, also on a winged female ("allotype female") with well-developed ocelli (Carpintero 1980), what justifies considering it valid, until a taxonomic revision and a phylogenetic analysis of all the Ectrichodiinae (or at least Ectrichodiini) genera are produced (Gil-Santana et al. 2015).

Currently, *Racelda* has six species (Carpintero and Maldonado 1996; Bérenger and Gil-Santana 2005; Gil-Santana et al. 2015).

Materials and methods

Photographs of paratypes of *Racelda ottoi* sp. nov. (Figs 12, 16–21, 25) were taken by the junior author (JO) using a stereoscope microscope (Leica 205A) with a digital camera.

Photographs of the male syntype (Figs 3–5) and other potential (?) male syntype (Figs 6–8) of *Racelda alternans* Signoret, 1863, deposited in the Natural History Museum, Vienna, Austria (**NHMW**), were taken by Harald Bruckner and provided by him and Herbert Zettel. Images of the male syntype of *Racelda spurca* Stål, 1860 (Figs 58–60), deposited in the Swedish Museum of Natural History, Stockholm, Sweden (**NHRS**) (freely accessible at: http://www2.nrm.se/en/het_nrm/s/racelda_spurca. html) were provided by Gunvi Lindberg.

The holotype and paratypes of *R. ottoi* sp. nov. (Figs 11, 39); holotype of *Racelda moerens* Breddin, 1898 (Figs 9, 10), and non-type specimens of *Racelda aberlenci* Bérenger & Gil-Santana, 2005 (Figs 1, 2), *R. robusta* Bérenger & Gil-Santana, 2005 (Figs 56, 57), and *R. spurca* (Figs 61, 62) were directly examined and imaged by the first author (HRG-S). Photographs were taken using digital cameras (Nikon D5200 or D5600 with a Nikon 105 mm macro lens). The respective types, depositories, and curators, who kindly allowed examining specimens, are as follows: type specimens of *R. alternans*: **NHMW**, Herbert Zettel; male holotype of *R. moerens* Breddin, 1898: Senckenberg Deutsches Entomologisches Institut, Müncheberg, Germany (**SDEI**), Stephan M. Blank.

Scanning electron microscopy images (Figs 13–15, 22–24, 26–38, 40–42, 45, 46) were obtained by the second author (JO). Two male paratypes of *R. ottoi* sp. nov. were cleaned in an ultrasound machine. Subsequently, the samples were dehydrated in alcohol, dried in an incubator at 45 °C for 20 min, and fixed in small aluminum cylinders with transparent glaze. Sputtering metallization was then performed on the samples for 2 min at 10 mA in an Edwards sputter coater. After this process, the samples were studied and photographed using a high-resolution field emission gun scanning electron microscope (SEM; JEOL, JSM-6610LV), similarly as described by Rosa et al. (2010, 2014).

The figure of the abdominal segment VIII (Fig. 43) and most figures of the male genitalia of *R. ottoi* sp. nov. (Figs 44, 47–55) were produced by the first author (HRG-S). Dissections of the male genitalia were made by first removing the pygophore from the abdomen with a pair of forceps and then clearing it in 20% NaOH solution for 24 h. The dissected structures were studied and photographed in glycerol using digital cameras (Sony DSC-W570 and DSC-W830). Drawings were made using a camera lucida. Images were edited using Adobe Photoshop CS6.

Observations were made using a stereoscope microscope (Zeiss Stemi) and a compound microscope (Leica CME). Measurements were made using a micrometer eyepiece. General morphological terminology mainly follows Schuh and Weirauch (2020). The (visible) segments of labium are numbered as II to IV, given that the first segment is lost or fused to the head capsule in Reduviidae (Weirauch 2008). In case of terms applied particularly to the Ectrichodiinae, the terminology of general morphology follows Dougherty (1995) and Forthman et al. (2016). In general, to genitalia terms, Forthman et al. (2016) are followed.

All type specimens of *Racelda ottoi* sp. nov. were collected by members of the team of the "Diversity and conservation of Hemiptera (Insecta) from the Caatinga" Project, funded by the Brazilian "Conselho Nacional de Desenvolvimento Científico e Tec-

nológico", process 421413/2017-4, and authorized through the Biodiversity Authorization and Information System (SISBIO), collection permit number 62159.

The type specimens of *Racelda ottoi* sp. nov. will be deposited as follows: male holotype, 2 male paratypes in the "Coleção Zoológica do Maranhão" (**CZMA**) of the "Centro de Estudos Superiores da Universidade Estadual do Maranhão", Caxias, Maranhão, Brazil; 1 male paratype in the "Coleção Entomológica do Instituto Oswaldo Cruz" (**CEIOC**), Rio de Janeiro, Brazil, and 2 male paratypes used to obtain SEM images will be deposited in the Dr Jose Maria Soares Barata Triatominae Collection (**CTJMSB**) of the São Paulo State University, Julio de Mesquita Filho, School of Pharmaceutical Sciences, Araraquara, São Paulo, Brazil. Additional non-type specimens of other species were or will be deposited in the Entomological Collection of the Museu Nacional da Universidade Federal do Rio de Janeiro, Rio de Janeiro, Brazil (**MNRJ**).

When describing label data, a slash (/) separates the lines and a double slash (//) different labels, and comments or translations to English of the label data are provided in square brackets ([ ]). All measurements are in millimeters (mm).

Results

Taxonomy

Subfamily Ectrichodiinae

Genus *Racelda* Signoret, 1863

Signoret (1863) created *Racelda* for the species he was describing, *R. alternans* Signoret, 1863, providing a short description of the genus. Dougherty (1995) and Carpintero and Maldonado (1996) provided redescriptions of *Racelda*. Dougherty (1995) stated that the pronotum of *Racelda* has the mid-longitudinal furrow well developed anteriorly and obsolete posteriorly, and the anterolateral corners are squared. Carpintero and Maldonado (1996) stated that the longitudinal sulcus extends along both lobes of pronotum, the circular spiracles and the short prongs on the triangular scutellum would be diagnostic of males of the genus. Forero (2004) considered the main diagnostic characteristics of *Racelda* to be: the first visible labial segment longer than the second, longitudinal sulcus of pronotum continuous on the two lobes, prolongations of the scutellum short, and strong sexual dimorphism.

With the exception of *Racelda monstrosa* Carpintero, 1980, described based only on the female holotype, all other species of *Racelda*, *R. aberlenci* Bérenger & Gil-Santana, 2005, *R. alternans*, *R. moerens* Breddin, 1898, *R. robusta* Bérenger & Gil-Santana, 2005, and *R. spurca* (Stål, 1860) were described based only on male specimens (Signoret 1863; Stål 1860; Breddin 1898; Carpintero 1980; Bérenger and Gil-Santana 2005).

There are no formal descriptions of the females of any of these species in the literature, only the figures of the dorsal habitus of the females of *R. alternans* (Carpintero and Maldonado 1996; Melo and Faúndez 2015) and *R. spurca* (Forthman and Weirauch 2017) exist. Because of that, the comments about the characteristics of the species, most of which with their females unknown or not well characterized, are based or focused only on the respective males.

Racelda aberlenci Bérenger & Gil-Santana, 2005
Figs 1, 2

Material examined. French Guiana, Bélizon, vii.2001, H. Gaspard leg., 2 males (MNRJ).

Racelda aberlenci was described based on males from French Guiana and Brazil (Amazonian region) (Bérenger and Gil-Santana 2005).

Racelda alternans Signoret, 1863
Figs 3–8

Type material examined. *Racelda alternans*. **Male syntype:** *alternans* [handwritten] / det. Signoret. [printed] // Chile [handwritten] / Coll. Signoret. [printed] // [printed red label]: Typus / Racelda /alternans Signoret, 1863 / etik. Hecher 1996 / REDV. 102/1; Male [potential] syntype: *alternans* [handwritten] / det. Signoret. [printed] // Chile [handwritten] / Coll. Signoret. [printed] // [printed red label]: Typus? / etik. Hecher 1996 (NHMW).

Racelda alternans was described from Chile (Signoret 1863), and it is the type species of *Racelda* by monotypy (Maldonado 1990). It was also recorded from Argentina by Dougherty (1995).

A male syntype is deposited in NHMW (Figs 3–5). Besides this syntype, another male deposited in the same collection and with same data is considered as a potential (probable) or doubtful ("?") syntype of *R. alternans* (Sehnal 2000) (Figs 6–8). The position of uncertainty of Sehnal (2000) about this potential syntype was based mainly on the supposed divergence between the coloration of the pronotum of this specimen and the original description of *R. alternans* by Signoret (1863). His description stated the following: prothorax [pronotum] brownish with two large lateral yellow markings, which meet almost at level of anterior furrow. This description seems to be in accordance with both specimens, possibly, even more with that which was considered as a doubtful syntype by Sehnal (2000) (Fig. 6). In the recognized syntype there are only lateral pale markings on hind lobe of pronotum which are far from meeting at the level of the transverse furrow (Fig. 3), while in the doubtful syntype, besides similar lateral pale markings on hind lobe, the fore lobe is almost completely pale, a coloration only interrupted by the mid-longitudinal furrow (Fig. 6). It is noteworthy that the drawing of the habitus (dorsal
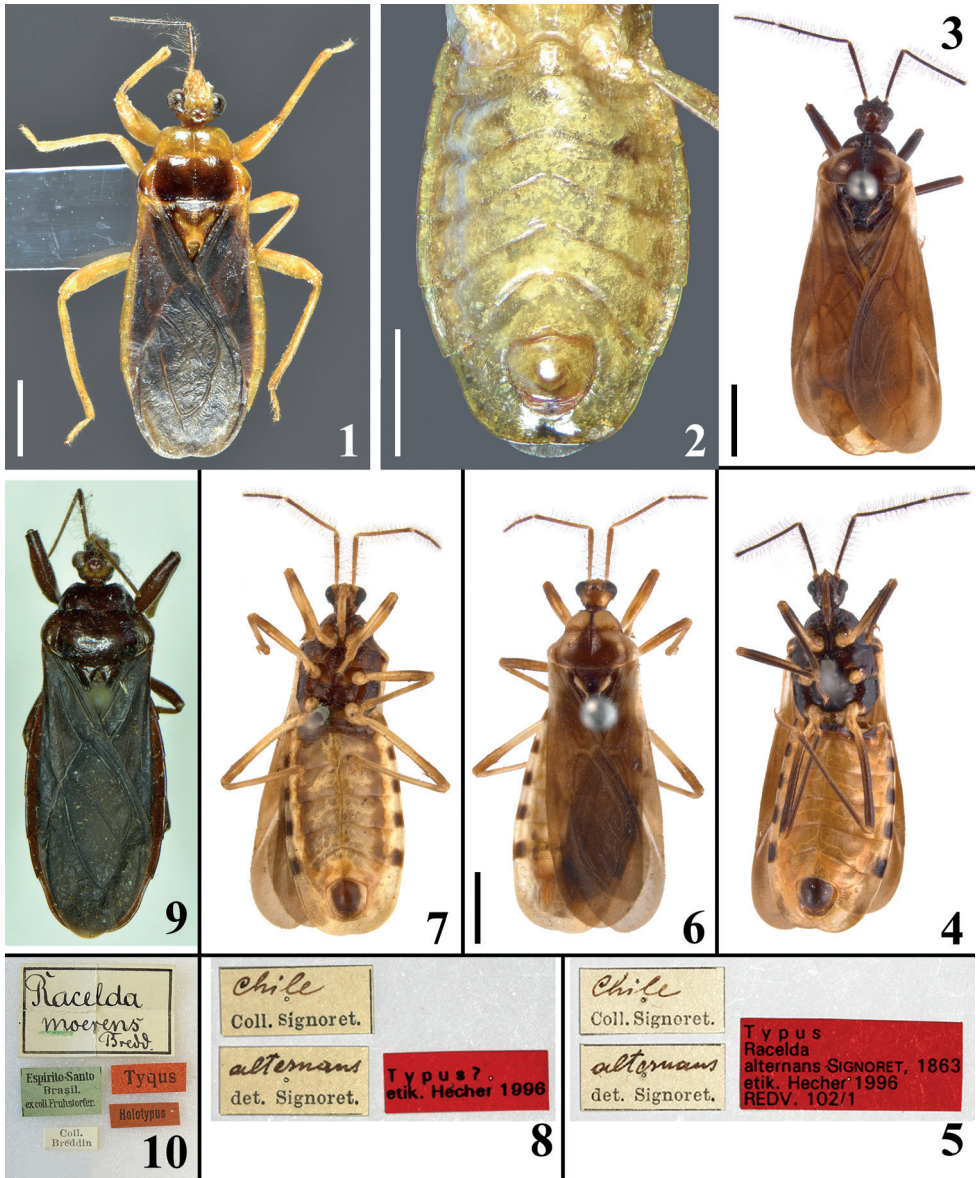
Figures 1–10. 1, 2 *Racelda aberlenci* Bérenger & Gil-Santana, 2005, male from French Guiana. **1** dorsal view **2** abdomen, ventral view. **3–8** *Racelda alternans* Signoret, 1863, male specimens deposited in NHMW. **3–5** syntype **3** dorsal view **4** ventral view **5** labels **6–8** potential syntype **6** dorsal view **7** ventral view **8** labels. **9, 10** *Racelda moerens* Breddin, 1898, male holotype deposited in SDEI **9** dorsal view **10** labels. Scale bars: 2.0 mm (**2, 3, 6**); 1.0 mm (**1**).

view) of *R. alternans* which accompanies the original description ("fig. 6") clearly shows a pair of pale rounded markings on fore lobe of pronotum, although smaller than what is seen in the "?" syntype, in which almost all the fore lobe (except the median sulcus) is pale (Fig. 6). It is possible that more than these two type specimens existed when Signo-

ret described the species, but the figure makes it clear that another specimen, with pale portions on the fore lobe of the pronotum, which are not observed in the syntype recognized by Sehnal (2000), was drawn and therefore considered by Signoret (1863) as belonging to this species. On the other hand, it is noteworthy that the quality of details and precision of the drawings in Signoret's paper are not those required today for a scientific drawing of a specimen. Thus, it is possible that the pale markings of the pronotum had not been well depicted and the pale markings were represented smaller than they are in the "?" syntype. The lack of precision in the mentioned drawing is suggested by the pattern of the lateral pale markings of the hind lobe, which were drawn as a pair of parallel lines meeting at their apices, while in reality they are continuous markings at each side of hind lobe. Therefore, this evidence and the fact that the original labels of both type specimens are very similar and with the same handwriting (Figs 5, 8), suggest that both specimens should be considered and possibly recognized as syntypes of *R. alternans*.

Melo and Faúndez (2015) argued that *R. alternans* could be easily distinguished by the characteristic coloration of the thorax of the males. The pronotum of the male photographed by them (their fig. 11) presented a general dark coloration with a relatively large median pale marking on each side of fore lobe and the hind lobe with lateral pale markings similar to those of the syntype considered as doubtful by Sehnal (2000) (Fig. 6).

Racelda moerens Breddin, 1898
Figs 9, 10

Type material examined. Male holotype: *Racelda* / *moerens* [letters "*mo*" underlined with green] / Bredd. [handwritten label] // Espirito-Santo / Brasil. / ex coll. Fruhstorfer. [printed green label] // Tyqus [*sic*] [printed red label] // Holotypus [printed red label] // Coll. / Breddin [printed label] (SDEI).

According with the original description (Breddin 1898), *R. moerens* was described based on a unique male from state of Espírito Santo, Brazil (Breddin 1898). It is deposited in SDEI and bears two red labels, one reading "Tyqus" [certainly meaning "Typus", a mere typo] and other "Holotypus" (Figs 9, 10). Gaedike (1971) listed this type specimen as the holotype of the species. It is known that several type specimens described in that time currently bear "typus", holotypus" or "paratypus" labels, although these were not attached by the author of the species, but subsequently in curatorial practice. In any case, taking into account that the evidence supports that Breddin's description was based on this single specimen, even not stated as the holotype in the original publication, it is considered fixed as such by monotypy (ICZN, Art. 73.1.2) and also in accordance with Gaedike (1971).

Dougherty (1995) recorded a large variation in the size of males of *R. moerens*, with a range in total length from 9.5 to 18.2 mm, although the individuals were otherwise identical. The collecting of variously sized individuals on the same date and at the same locality implies that they belonged to the same population (Dougherty 1995).

Racelda moerens has been recorded so far only from Brazil (Maldonado 1990; Dougherty 1995).

Racelda ottoi Oliveira & Gil-Santana, sp. nov.
http://zoobank.org/57A592A5-8D05-4EAD-B8ED-B7F9C2ADAE15
Figs 11–55

Type material. Brazil, Pernambuco State, Catimbau National Park: Tupanatinga, Estrada do Gado [Cattle Road], 08°29'11.8"S, 37°20'25.5"W, 663 m alt., 19.iii.19, light trap, R. Carrenho leg., ***holotype***, male, 1 male paratype; light trap with white cloth, J.M.S. Rodrigues leg., 1 male paratype (CZMA); Buíque, ICMBio grounds, 08°33'54.9"S, 37°14'20.2"W, 730 m alt., 17.iii.19, light trap with white cloth, J.M.S. Rodrigues leg., 2 male paratypes (CTJMSB), 1 male paratype (CEIOC).

Diagnosis. *Racelda ottoi* sp. nov. can be separated from other species of the genus by the combination of characters presented in the key below. *Racelda ottoi* sp. nov. shares similarities in coloration with *R. robusta* and *R. aberlenci* such as possessing both the fore lobe of pronotum and the abdomen, including the connexivum, mostly pale, while in the other species of the genus, these parts are mostly dark or at least, in case of the connexivum, it has well-defined dark markings on most segments. However, *R. ottoi* sp. nov. can be separated from *R. robusta* and *R. aberlenci* based on the coloration of the head and the legs, which are mostly blackish and with larger dark markings on femora and tibiae, respectively, in the former species, while in the latter two species, the head is completely pale, and the femora and tibiae are almost completely pale with the apices of femora and extremities of tibiae variably faintly dark marked or not marked. Additionally, while the longitudinal sulcus of pronotum is continuous on the two lobes in *R. robusta* and *R. aberlenci*, it is interrupted at the level of transverse sulcus in *R. ottoi* sp. nov.

Description. Male. Figs 11–55. Measurements are given in Table 1.

Coloration: general coloration pale to pale yellowish to orange with darkened to brownish or blackish portions or markings (Figs 11, 12, 25, 39). **Head**, including neck, mostly blackish (Figs 11, 12); pale whitish to pale yellowish ventrally between the level of inner margin of eyes; a thin reddish line around ocelli, sometimes partially interrupted as in the holotype; a somewhat paler medial marking behind ocellar tubercle and on neck, variable in size, both present in the holotype and alternatively absent in some of the paratypes; base of neck paler in variable extension or completely dark as in the holotype; close to base of labium, on pale whitish ventral area, a small blackish marking as a thin transverse line or as a pair of separate markings; antennal segments (Figs 16–21) mostly dark with basal portion of scape and intersegmental joints pale; scape, pedicel and basiflagellomeres blackish to brownish black; distiflagellomeres somewhat paler, brownish; labrum paler on its distal half; labium pale to pale yellowish with apex of first visible segment darkened and faintly, irregularly marked with variably darkened portions such as a basoventral marking on segment II (first visible) and lateral and dorsal portions of segments III–IV; the latter entirely faintly darkened in one paratype. **Thorax** (Figs 11, 25): pronotum mostly pale orange, faintly darkened at collar, inferior portion of anterolateral angles, median portion of basal half of hind lobe and, in one paratype, medially to distal portion of humeral angles; scutellum blackish; propleura orange with a dark irregular marking extending above and/or anteriorly to fore supracoxal lobe, reaching prosternum at anterior portion, including their rounded
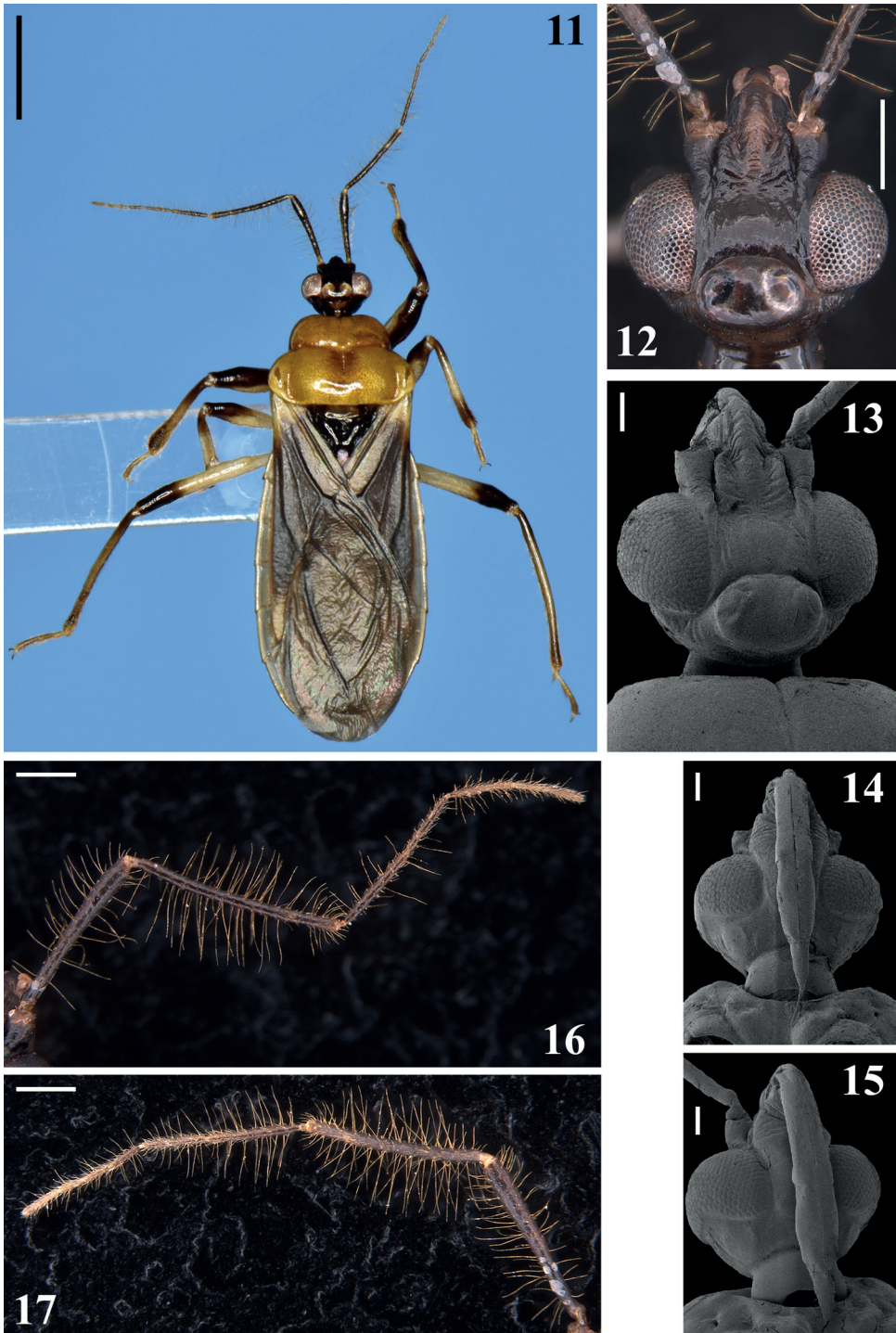
Figures 11–17. *Racelda ottoi* Oliveira & Gil-Santana, sp. nov. **11** holotype, dorsal view **12–15** head **12, 13** dorsal view **14** ventral view **15** ventrolateral view **16, 17** antenna, dorsal view **16** right **17** left. Scale bars: 2.0 mm (**11**); 0.5 mm (**12, 16, 17**); 0.2 mm (**13–15**).
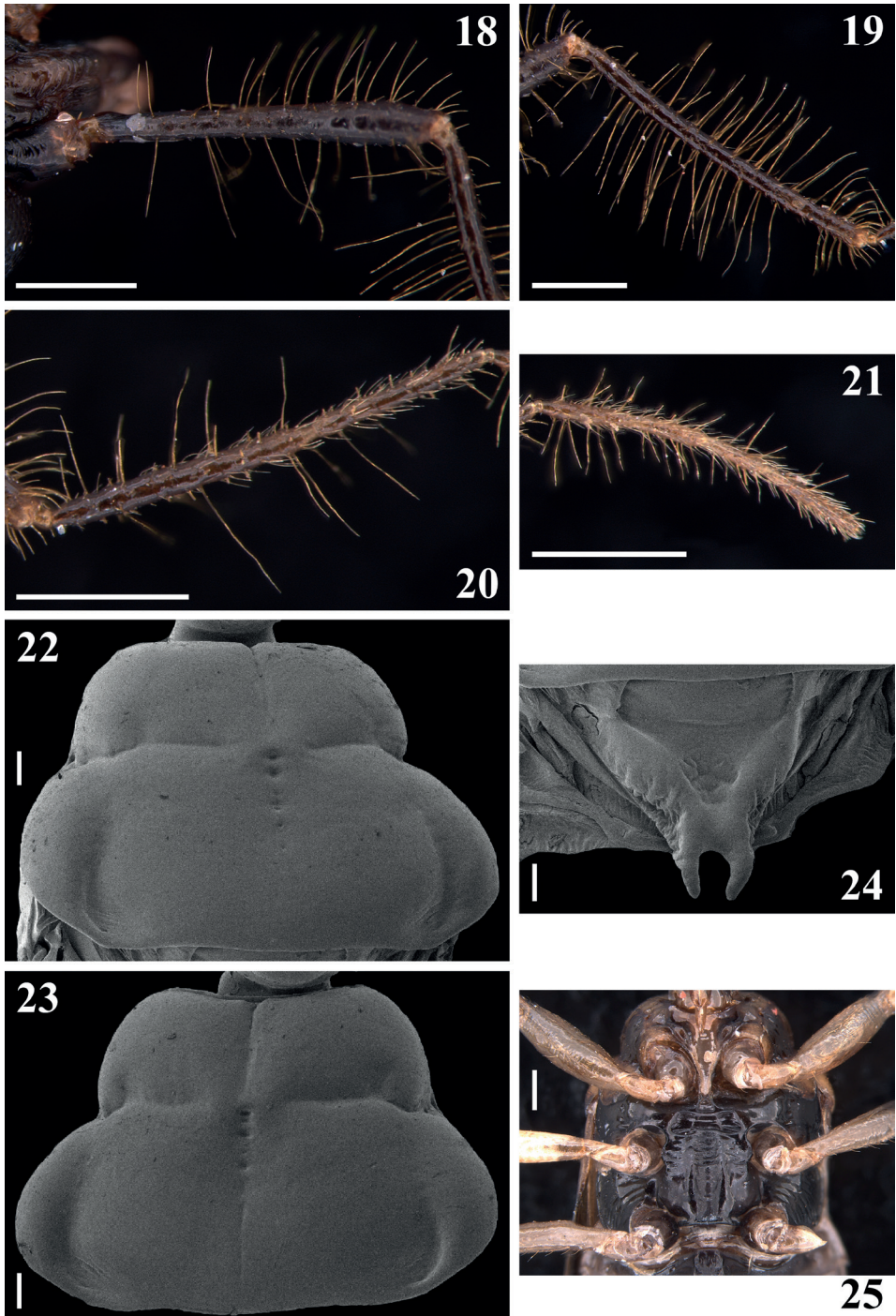
Figures 18–25. *Racelda ottoi* Oliveira & Gil-Santana, sp. nov. **18–24** dorsal view **18–21** antennal segments **18** scape and basal portion of pedicel **19** apical portion of scape and pedicel **20** basiflagellomeres **21** distiflagellomeres **22, 23** pronotum, different paratypes **24** scutellum **25** thorax, ventral view. Scale bars: 0.5 mm (**18–21, 25**); 0.2 mm (**22–24**).

Table 1. Measurements (in mm) of type specimens (*N* = 6) of *Racelda ottoi* sp. nov.

	Holotype	Mean	SD	Minimum	Maximum
Length to tip of abdomen	9.0	9.6	0.51	9.0	10.5
Length to tip of hemelytra (*N* = 5)[1]	9.2	9.73	0.56	9.2	10.6
Head length excluding neck	1.6	1.56	0.05	1.5	1.6
Head width across eyes	1.4	1.48	0.07	1.4	1.6
Synthlipsis	0.6	0.58	0.04	0.5	0.6
Eye width	0.4	0.41	0.04	0.4	0.5
Ocellar tubercle width	0.6	0.6	0.0	0.6	0.6
Ocellus width	0.2	0.24	0.04	0.2	0.3
Scape length	1.4	1.5	0.06	1.4	1.6
Pedicel length	1.6	1.67	0.10	1.6	1.8
Basiflagellomere I length	0.7	0.73	0.05	0.7	0.8
Basiflagellomere II length	0.4	0.47	0.05	0.4	0.5
Distiflagellomere I length (*N* = 5)[2]	0.25	0.27	0.02	0.25	0.3
Distiflagellomere II length (*N* = 5)[2]	0.2	0.2	0.0	0.2	0.2
Distiflagellomere III length (*N* = 5)[2]	0.15	0.19	0.02	0.15	0.2
Distiflagellomere IV length (*N* = 5)[2]	0.25	0.31	0.02	0.25	0.4
Labial segment II length	0.9	1.03	0.10	0.9	1.2
Labial segment III length	0.6	0.58	0.04	0.5	0.6
Labial segment IV length	0.3	0.41	0.09	0.3	0.5
Fore lobe of pronotum length	0.6	0.61	0.04	0.6	0.7
Fore lobe of pronotum max. width	2.0	2.0	0.0	2.0	2.0
Hind lobe of pronotum length	1.2	1.18	0.04	1.1	1.2
Hind lobe of pronotum max. width	2.9	2.95	0.05	2.9	3.0
Fore femur length	1.8	1.88	0.09	1.8	2.0
Fore tibia length	1.9	1.9	0.0	1.9	1.9
Fore tarsus length	0.7	0.7	0.0	0.7	0.7
Middle femur length	1.8	1.81	0.04	1.8	1.9
Middle tibia length	1.9	1.8	0.08	1.7	1.9
Middle tarsus length	0.7	0.68	0.04	0.6	0.7
Hind femur length	2.9	2.96	0.05	2.9	3.0
Hind tibia length	3.1	3.03	0.10	2.9	3.2
Hind tarsus length	1.0	1.01	0.04	1.0	1.1
Abdomen length*	5.4	5.51	0.17	5.3	5.7
Abdomen maximum width	3.3	3.63	0.20	3.3	3.9

[1, 2] Distal portion of hemelytra and distiflagellomeres absent in one specimen.

* Measured on ventral view, at midline, from anterior margin of sternite II to posterior border of last segment.

processes; margins of prosternal process and its apex dark; meso- and metapleura and sterna mostly blackish; a small pale orange marking on median and distal portion of middle and hind supracoxal lobes, respectively. Legs: fore coxa whitish, pale with anterior surface variably darkened; middle and hind coxae from mostly pale to mostly darkened and paler only at distal margin; trochanters pale to pale yellowish; femora pale whitish, blackish on dorsal surface of fore (except at its base) and approximately distal third to distal fourth of middle and hind femora, respectively; fore femora also variably darkened at apex on lateral surfaces or even around segment; distal markings on middle and hind femora variably somewhat shorter on ventral surface; in one paratype blackish markings on middle and hind femora smaller, occupying only approxi-
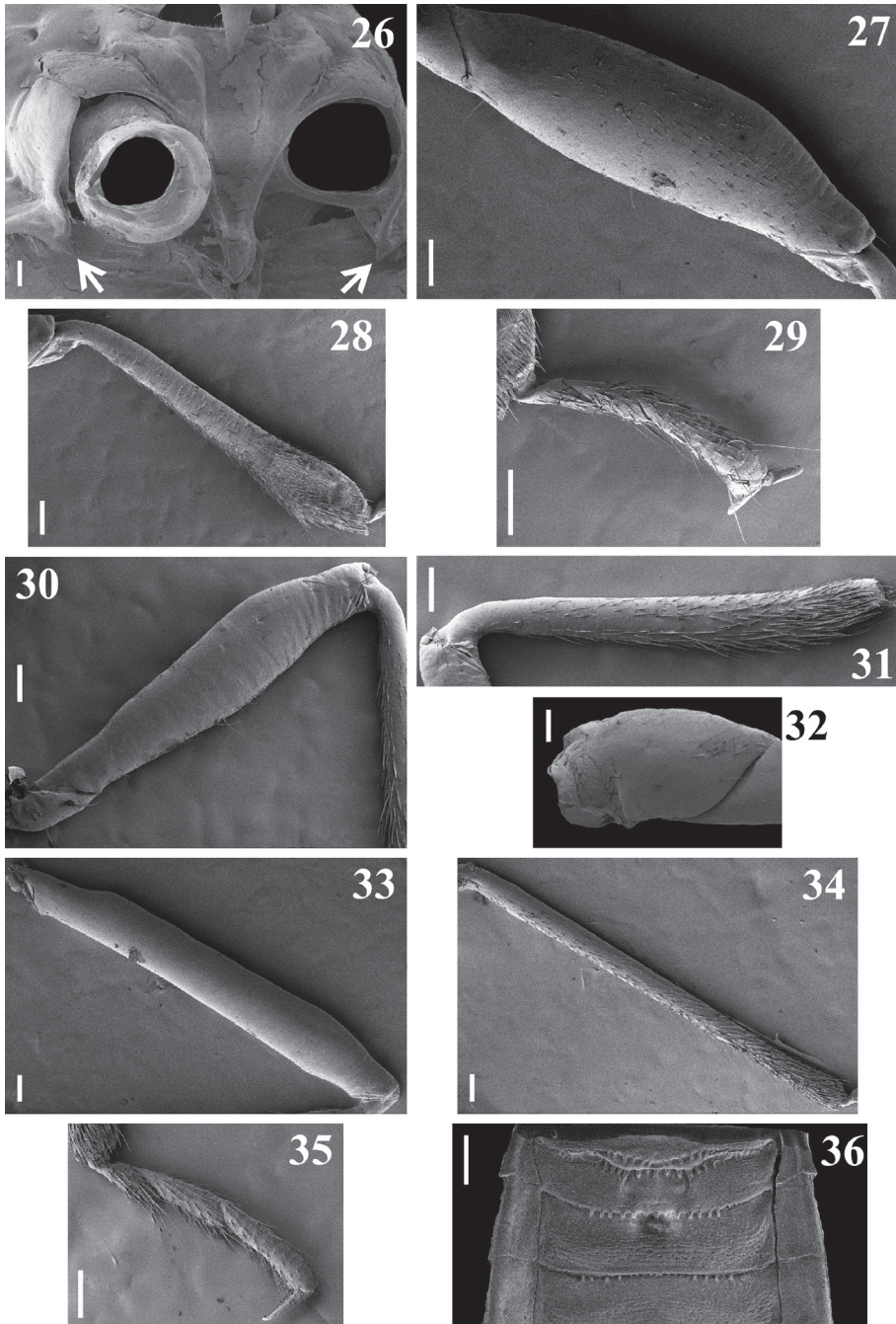
Figures 26–36. *Racelda ottoi* Oliveira & Gil-Santana, sp. nov. **26** prothorax, ventral view, arrows point to posteroventral elongate processes of propleura **27–29** fore leg **27, 28** lateral view, inner surface **27** femur **28** tibia **29** tarsus, dorsal view **30–35** lateral view, inner surface **30, 31** middle leg **30** trochanter, femur and basal half of ventral surface of tibia **31** tibia **32–35** hind leg **32** trochanter **33** femur **34** tibia **35** tarsus **36** abdomen, segments I–IV, except distal portion of the latter, dorsal view. Scale bars: 0.5 mm (**36**); 0.2 mm (**27–31, 33–35**); 0.1 mm (**26, 32**).

mately distal fifth of segment; tibiae dark, brownish to blackish, with approximately their median portion variably paler, pale coloration occupying approximately median third on fore and middle tibiae and one-half on hind tibiae; pale coloration varying from almost as dark as dark extremities of segment, pale brownish to pale whitish; tarsi pale brownish. Hemelytra blackish; pale on base of dorsal surface, laterally, and on basal lateral portion; also slightly paler on apex of corium. *Abdomen* (Figs 11, 39): mostly pale whitish to pale yellowish; apex of connexival posterolateral angle of segment II somewhat darkened; in one paratype, connexival segment II completely darkened; sternite II mostly dark to blackish, except at posterolateral portion where it is pale in variable extension; intersternite furrow between between segments II–III and adjacent anterior portion of latter segment darker in one paratype (Fig. 39); midlateral subrounded shallow depressed areas on sternites III–VII faintly darkened; area posterior to genital capsule, on last sternite, darkened in most specimens, dark coloration varying in extension laterally; exposed portions of genital capsule and parameres dark to blackish. *Structure*: Body integument mostly shiny. *Head* (Figs 11–21): shorter than pronotum (including neck); subtriangular in dorsal and lateral views. Vertex not elevated; minimum distance between eyes in dorsal view (synthlipsis) approximately 1.5–1.6 times longer than width of each eye. Antenna inserted proximal to midpoint between anterior margin of eyes and apex of head. Anteocular portion approximately twice as long as postocular portion (excluding neck); total length (excluding neck) of head longer than its maximum width across eyes; integument generally with coarsely transverse subparallel sulci or wrinkled; smooth on ocellar tubercle and neck. Clypeus moderately elongated, not elevated, rounded in lateral view, slightly wider at basal portion, its integument with transverse subparallel sulci. Antenna (Figs 16–21): scape somewhat curved and enlarged towards apex, slightly shorter than pedicel; the latter somewhat curved at midportion; flagellum slender, divided in pseudosegments, two basiflagellomeres and four distiflagellomeres; basiflagellomeres thinner than pedicel, first basiflagellomere longer than second; distiflagellomeres somewhat thinner than basiflagellomeres, first three subequal in length, last a little longer. Labium (Figs 14, 15) moderately thick, segment II (first visible) straight, somewhat thicker towards apex, approximately 1.5 times longer than the segment III, its apex approximately at level of anterior half of eyes in lateral view; segment III somewhat thicker; segment IV, shorter, tapering, reaching stridulatory sulcus approximately at its anterior third. Gula with lateral shallow longitudinal ridges, between which is a furrow narrower than labium, almost imperceptible in some individuals. Constriction between postocular portion and neck distinct (Fig. 13). Eyes large, prominent, subhemisphaerical in dorsal view, reniform in lateral view; transverse sulcus curved, reaching inner posterior angle of the eye (Figs 12, 13). Ocellar tubercle prominent, large, undivided, ocelli rounded, the distance between them somewhat closer than the diameter of each ocellus (Figs 12, 13). *Thorax* (Figs 11, 22–35): integument shiny; collar very thin; anterolateral angles pointed and small; fore lobe rounded on anterior and lateral margins, shorter and narrower than hind lobe; mid-longitudinal sulcus on fore lobe thin and narrow, ending somewhat above a median slightly elevated portion at median portion of transverse sulcus, with the remaining posterior part of the mid-longitudinal sulcus represented by
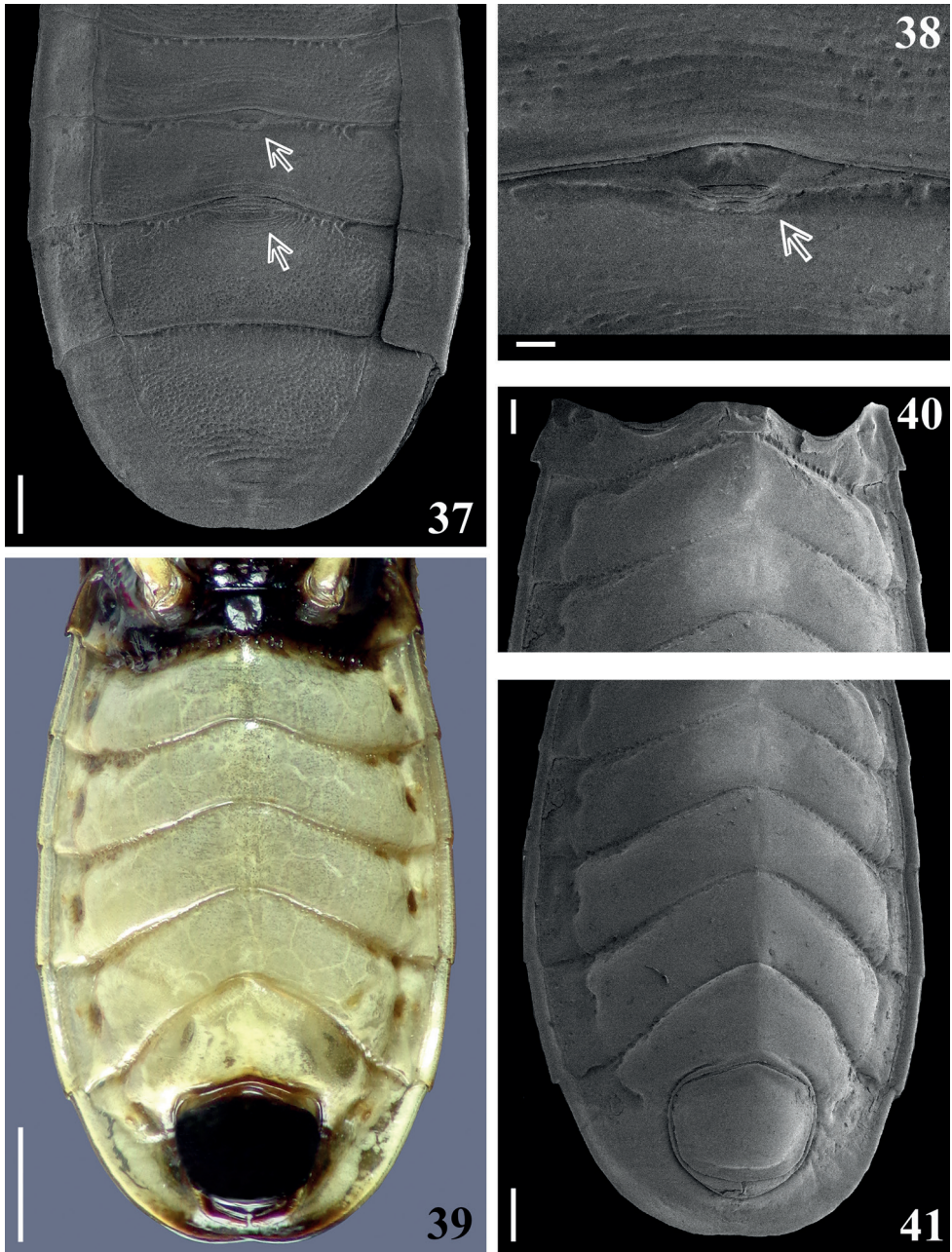
Figures 37–41. *Racelda ottoi* Oliveira & Gil-Santana, sp. nov., abdomen. **37, 38** dorsal view **37** distal portion of segment III and segments IV–VII, arrows point to the **dag** on tergites V and VI **38 dag** on basal portion of tergite V (pointed by an arrow) (**dag**: scar of dorsal abdominal gland opening) **39–41** ventral view **40** segments II–III, IV, except laterodistal portion, and midanterior portion of segment V **41** segments III (except basal portion), IV–VII. Scale bars: 1.0 mm (**39**); 0.5 mm (**37, 41**); 0.3 mm (**40**); 0.1 mm (**38**).

few punctations, about half a dozen, two or three more anterior ones somewhat deeper and larger, followed by progressively smaller and shallower punctations towards posterior margin, shortly or not exceeding the distal half of hind lobe (Figs 22, 23), sometimes posterior to punctations, a very thin median longitudinal line ending short of posterior margin (Fig. 23); transverse furrow distinct, interrupted at median portion by the median elevated portion, sinuous, curved forward at lateral portion (Figs 22, 23), continuing laterally, on propleura, forming a somewhat curved lateral furrow, with short shallow ridges on anterior portion of its inferior margin, ending at posterior margin of propleura; posterolateral furrows of pronotum distinct; humeral angles rounded (Figs 11, 22, 23). Scutellum with a shallow median depression; scutellar prongs moderately short and curved, narrowly separated at base and convergent towards their apices (Fig. 24). Integument of pro- and mesopleura mostly smooth; faintly wrinkled by a few linear subparallel thin shallow linear impressions on supracoxal lobes; integument of metapleura with several linear subparallel irregular ridges, its superior margin thickened and curved. Supracoxal lobes of propleura somewhat prominent, those of meso- and metapleura not. Propleura with posteroventral elongate processes, apices acute, directed posteromedially, just posterior to laterodistal third of fore coxa, above lateral portion of anterior margins of mesosternum (Fig. 26). Anterior margin of mesopleura with a median small process, projecting anteriorly, rounded at apex which meets posterior margin of propleura. Prosternum wider on approximately anterior half, moderately large, prolonged between fore coxae, apex rounded, reaching mesosternum, with its median portion occupied by stridulitrum (Fig. 26). Mesosternum anteriorly to middle coxa mostly flattened and with smooth integument; on its median portion, just posterior to apex of process of prosternum, a small oval depression on midline, with elevated borders, below and laterally to which, a pair of subrounded small depressions; middle coxae bordered by slightly elevated margins anteriorly and medially. Between middle and hind coxae, a moderately elevated area with integument marked by few shallow transverse sulci and a pair of submedian shallow longitudinal ridges somewhat more elevated at distal half (Fig. 25). Fore coxae close, separated by a shorter distance than approximately half the width of each of them; middle and hind coxae distant from each other by a distance approximately equivalent to somewhat more than twice and approximately 1.7 times the width of each of them, respectively (Fig. 25). Fore and middle femora and tibiae subequally long; fore femora somewhat thickened, except at basal and distal portions (Fig. 27); middle femora thickened subapically (Fig. 30); hind femora and tibiae longer, slender, femora somewhat thickened subapically (Fig. 33). Tibiae straight, slightly longer than the correspondent femora; fore tibiae thicker at apex, in which the anterior margin is prominent and with a mesal comb (Fig. 28); middle and hind tibiae slightly thicker subapically and at apex, respectively (Figs 31, 34); spongy fossae on apices of fore and middle tibiae very small. All tarsi slender, three-segmented (Figs 29, 35). Hemelytra generally dull; moderately shiny on base of dorsal surface, laterally, and on lateral portion, basally (the same portions in which the coloration is pale) (Fig. 11). ***Abdomen*** (Figs 11, 36–41, 43): Tergite I narrow, carinulate
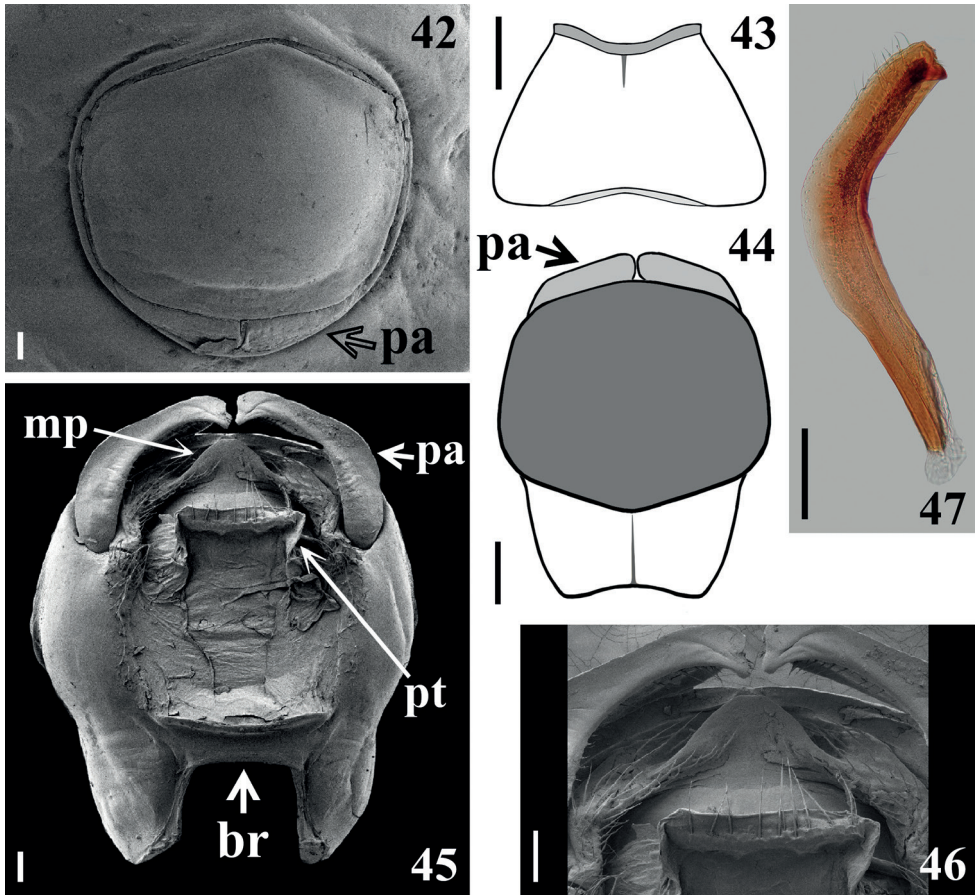
Figures 42–47. *Racelda ottoi* Oliveira & Gil-Santana, sp. nov., male genitalia. **42** genital capsule "in situ", ventral view **43, 44** schematic outline, ventral view **43** abdominal segment VIII, **44, 45** pygophore **45, 46** parameres slightly moved apart, dorsal view **46** apical portions of parameres and proctiger and medial process of pygophore **47** right paramere. Abbreviations: **br**: transverse bridge; **mp**: medial process of pygophore; **pa**: paramere; **pt**: proctiger Scale bars: 0.3 mm (**43, 44**); 0.2 mm (**47**); 0.1 mm (**42, 45, 46**).

on median portion of posterior margin (Fig. 36); other tergites shortly carinulate on posterior margin, except lateral portion, the ridges shorter on tergite IV, very faint on tergite VII (Figs 36, 37). Tergite II with its anteromedian portion bordered by a pair of longer curved longitudinal ridges (Fig. 36). Shallow and small punctations irregularly distributed on tergites III–VII; inner portion of respective connexival dorsal segment with few punctations (Figs 36, 37). Scars of dorsal abdominal glands openings (dag) on median anterior margins of tergites V and VI, that on the latter larger than that on tergite V; these tergites are carinulate only between the scars and lateral portion (Figs 37, 38). Connexivum with posterolateral angles of segments II–VI prominent, that of segment II somewhat more than the others (Figs 11, 36, 39–41). Sternites with shiny and generally smooth integument (Fig. 39); sternite II narrower than following segments,

its median portion elevated (Figs 39, 40); sternites II and III separated by shallow canaliculae, which are absent at lateral portions; other intersternite furrows with small, shallow punctations, absent in midline, sparser or absent towards lateral portions and less numerous on last interstenite furrow; sternites III–VII with smooth integument and midlateral subrounded shallow flat depressions, anterior portion of the latter close and medial to the respective spiracles (Figs 39–41). Spiracles round and small. Posterior margin of segment VII slightly curved anteriorly at its midportion (Fig. 39). Segment VIII not visible externally, sclerotized on ventral portion, which is translucent; segment becomes wider towards posterior margin; both basal and distal margins of ventral portion curved, the former more than the latter and more sclerotized than remaining part of segment (Fig. 43); dorsal portion membranous and narrower; spiracles on dorsal margin of ventral portion. **Vestiture:** integument generally mostly glabrous. **Head:** some long moderately curved pale setae scattered on the anterior and lateral portions of base of first visible labial segment; several long, erect, pale setae on apical portion of second visible labial segment and scattered on last labial segment. Antenna (Figs 16–21): scape with some and pedicel with few short, oblique, thin setae, and both segments covered by long pubescence formed by numerous long, erect, stout, pale setae, approximately twice as long as width of scape and 4–5 times as long as width of pedicel, except at distal portion, where these setae are shorter; flagellomeres covered by very numerous short, oblique, curved, thin pale setae, forming a short dense pubescence, except on approximately basal half of first basiflagellomere, where setae are less numerous; flagellomeres also covered by long stout, erect pale setae; those on first basiflagellomere almost as long and numerous than those of pedicel, becoming progressively shorter and less numerous on following flagellomeres. **Thorax:** pronotum with a tuft of golden stout setae on inner margin of posterior border of pronotum beside lateral margin of scutellar base. Borders of posterior prolongation of prosternum with thin, longer, dark golden setae; some scattered pale thin setae on postacetabular area of prosternum laterally to the prosternal process. Legs: coxa with some stout, curved, pale or somewhat darkened, thin setae on apical margin; trochanters and ventral surface of femora with several curved, stout and curved pale, thin setae (Figs 30, 32); fore trochanter and fore femur with also at least one thinner, longer subbasal seta; some scattered similar long setae on dorsal, lateral and ventral surfaces of femora, on fore femora some rows of curved, thin, pale, shorter setae on dorsal surface (Fig. 27); tibiae glabrous at approximately basal third to two-thirds of dorsal surface, with a mid-ventral fringe of short, straight, somewhat stouter, pale brownish setae; at approximately distal third, all tibiae generally covered by pale brownish to darkened setae, which become somewhat more numerous towards apex, where they are longer on ventral and lateral surfaces (Figs 28, 31, 34); tarsi covered with numerous yellowish and golden setae, which are longer on ventral surface (Figs 29, 35).

Male genitalia. Pygophore, in ventral and lateral views: exposed portion of pygophore subpentagonal (Figs 39, 41, 42, 44) and rounded, respectively, integument smooth and shiny; only pigmented (blackish) in the exposed portion (Figs 39, 44); in dorsal view (Fig. 45): between anterior and posterior genital openings, a moderately
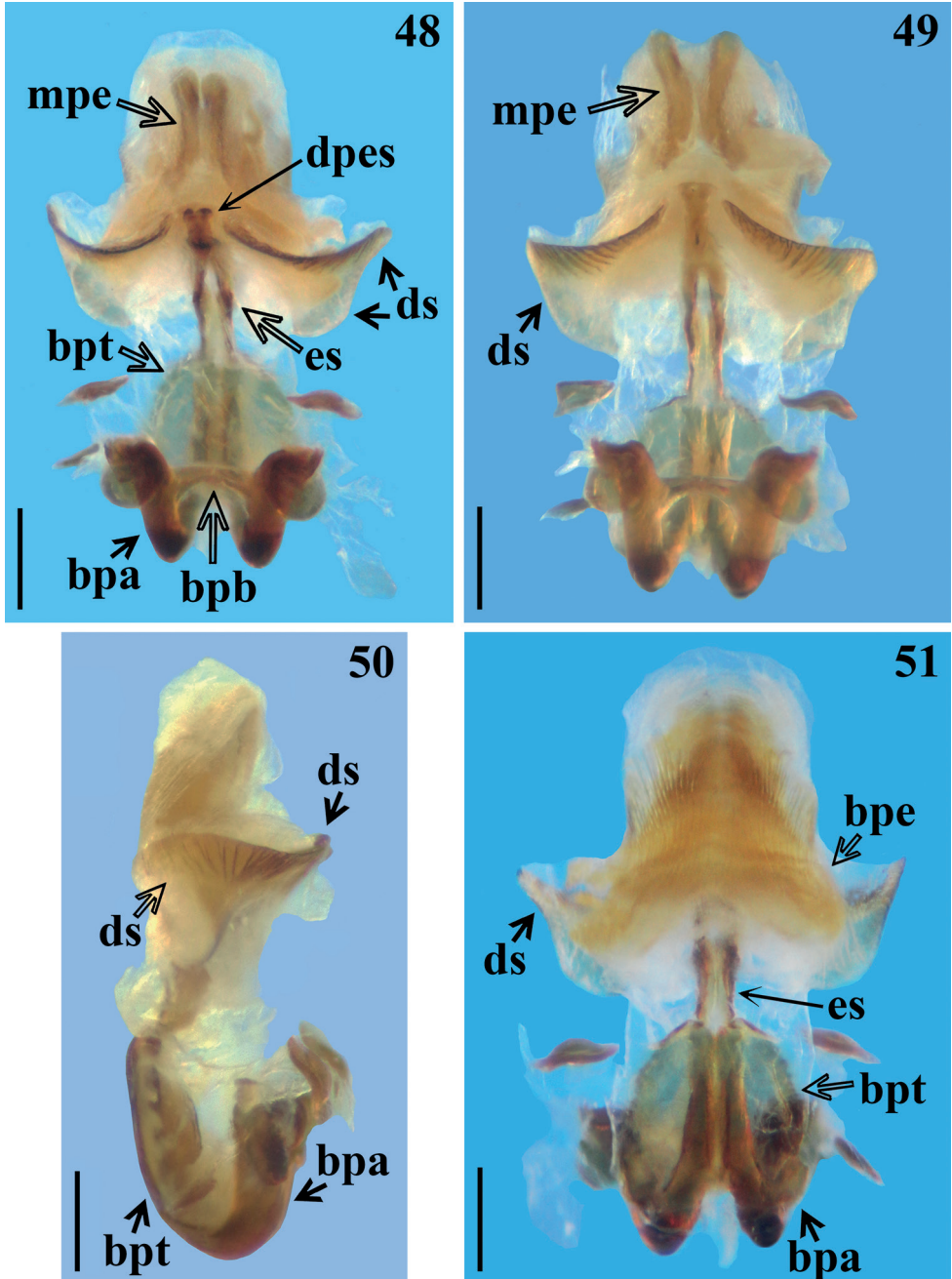
Figures 48–51. *Racelda ottoi* Oliveira & Gil-Santana, sp. nov., male genitalia, phallus. **48, 49** dorsal view **50** lateral view **51** ventral view. Abbreviations: **bpa**: basal plate arm; **bpb**: basal plate bridge; **bpe**: basal process of endosoma; **bpt**: basal plate extension; **dpes**: dorsal phallothecal sclerite-endosomal struts fusion; **ds**: dorsal phallothecal sclerite; **es**: endosomal struts; **mpe**: median process of endosoma. Scale bars: 0.3 mm (**48–51**).
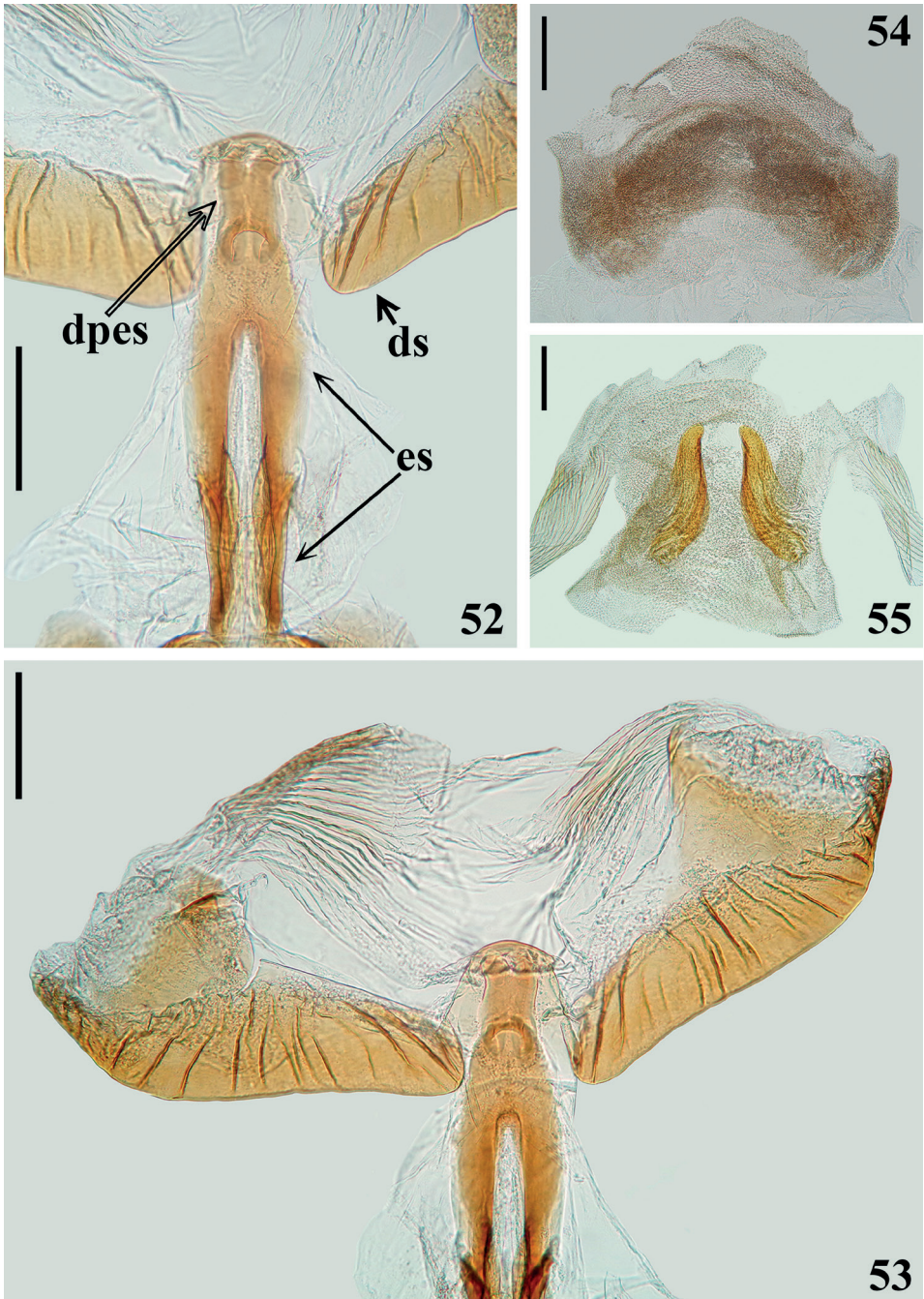
Figures 52–55. *Racelda ottoi* Oliveira & Gil-Santana, sp. nov., male genitalia, dorsal view. **52** endosomal struts (**es**), dorsal phallothecal sclerite-endosomal struts fusion (**dpes**) and median portions of distal thickened margin of dorsal phallothecal sclerite (**ds**) **53** distal half of endosomal struts, dorsal phallothecal sclerite-endosomal struts fusion and dorsal phallothecal sclerite **54** basal process of endosoma **55** median process of endosoma. Scale bars: 0.2 mm (**52–55**).

broad, slightly sclerotized dorsal (transverse) straight bridge (br); membranous areas of posterior genital opening smooth; proctiger (pt) subsquared, posterior margin almost straight, with a subapical single row of few long straight setae (Figs 45, 46). Medial process of pygophore (mp) sclerotized, subrounded, apical margin almost straight (Figs 45, 46). Parameres (pa) mildly exposed when genital capsule is in situ (Fig. 42) their apices in contact in resting position (Figs 42, 44); symmetrical, elongated, curved at approximately middle third, where they are somewhat larger; apex truncated, with a rounded subapical tooth in inferior margin; mostly glabrous, with some rows of long setae on inner surface, a few subapical short somewhat stout setae on upper surface and a row of somewhat curved very short setae above the subapical tooth (Figs 46–47). Phallus: articulatory apparatus with basal plate extension (bpt) enlarged, longer than basal plate, the latter with moderately short and curved basal plate arms (bpa), connected by a narrow basal plate bridge (bpb) (Figs 48–51). Dorsal phallothecal sclerite (ds) symmetrical, enlarged to apex; distal margin thickened and more sclerotized, with several linear grooves interrupted at midportion beside apex of struts and dorsal phallothecal sclerite–endosomal struts fusion (dpes) (Figs 48, 49, 52, 53). Endosomal struts (es) formed by a pair of parallel arms, somewhat thinner at basal third, slightly enlarging toward apex, where they converge and become largely united, being continuous with dorsal phallothecal sclerite–endosomal struts fusion (dpes) (Fig. 52). Endosoma wall longitudinally striated on basal portion, ventrally (Fig. 51), smooth basally, and mostly very densely minutely, spiny towards apical portion (spines minute). Two processes of endosoma: a wide, arcuate, basal process (bpe) formed by diffuse thickening (Figs 51, 54) and a median process (mpe) at apical portion (Figs 48, 49). Median process formed by a pair of elongate, flat, somewhat curved, moderately sclerotized plates (Fig. 55).

Distribution. Brazil, state of Pernambuco.

Etymology. The new species is named in honor to Otto Pompeu Fusco de Oliveira, the beloved son of the junior author (JO).

Comments. The inclusion of *R. ottoi* sp. nov. in *Racelda* is in accordance with the characteristics assigned to the species of this genus by Dougherty (1995), Carpintero and Maldonado (1996), and Forero (2004). *Racelda ottoi* sp. nov. differs from the other species of the genus by the combination of characteristics stated in the key for males of *Racelda*, presented below and from the species to which it seems closest, *R. aberlenci* and *R. robusta*, by the set of features commented on in its diagnosis.

The antennae of most of the New World Ectrichodiinae males are pubescent on all segments with short setae but which are more abundant on the distal segments (Dougherty 1995). Dougherty (1995) also stated that in *Racelda* the antennae of males have long and short pubescence on all segments. In *R. ottoi* sp. nov., the setae of the long pubescence are longer and formed with more numerous elements on the scape and pedicel (Figs 16–19), becoming progressively shorter and less numerous on the following segments (flagellomeres), while the short pubescence is almost absent on the scape and pedicel and become progressively more numerous to very dense on the flagellomeres (Figs 16, 17, 20, 21). Yet, the males of the new species present large eyes and well-developed ocelli, and they are macropterous (Figs 11–13). Although all these
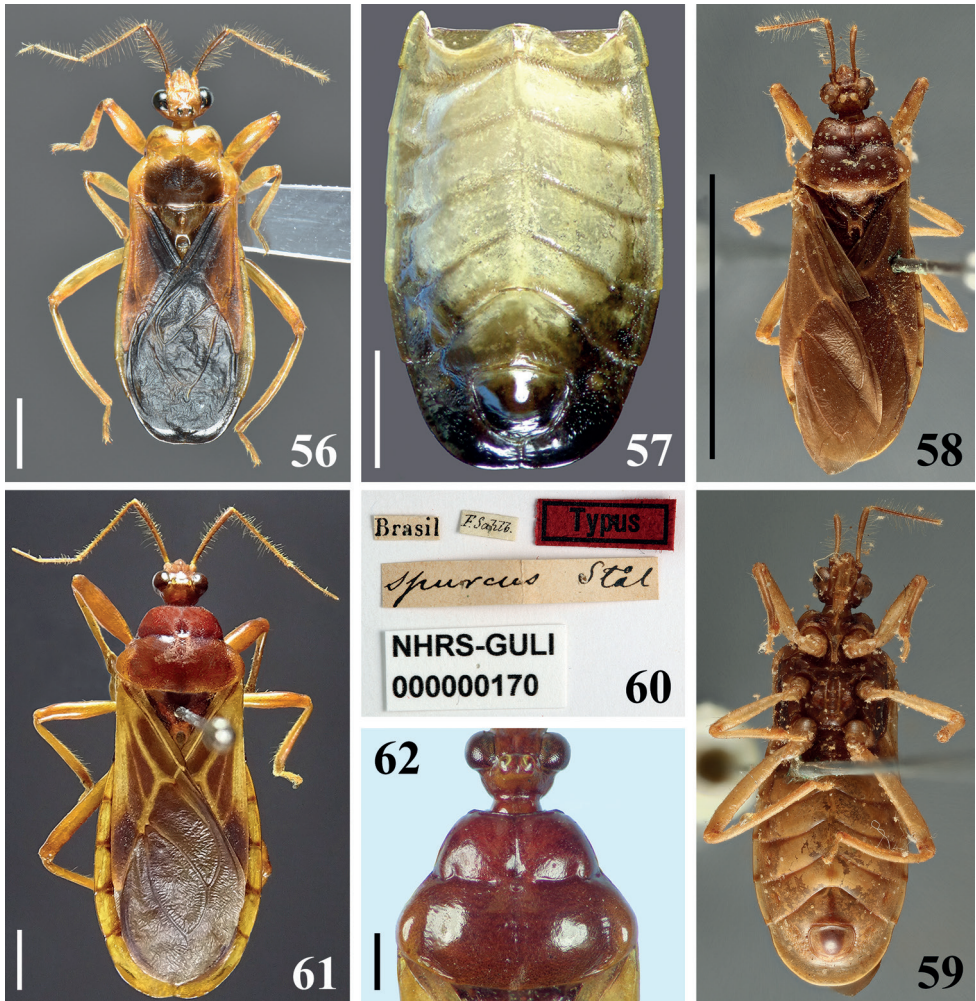
Figures 56–62. 56,57 *Racelda robusta* Bérenger & Gil-Santana, 2005, male from French Guiana **56** dorsal view **57** abdomen, ventral view **58–62** *Racelda spurca* (Stål, 1860) **58–60** male syntype deposited in NHRS, catalog number NHRS-GULI000000170, photographed by Gunvi Lindberg, © 2020 Naturhistoriska riksmuseet. Made available by the Swedish Museum of Natural History under Creative Commons Attribution 4.0 International Public License, CC-BY 4.0, https://creativecommons.org/licenses/by/4.0/legalcode **58** dorsal view, scale bar modified from original **59** ventral view **60** labels **61, 62** male from Brazil, dorsal view **62** distal portion of head and pronotum. Scale bars: 10.0 mm (**58**); 2.0 mm (**57,61**); 1.0 mm (**56,62**).

characteristics are similar to those presented by males of Ectrichodiinae and *Racelda* in contrast with conspecific females, which have very reduced eyes and ocelli and are apterous (Dougherty 1995; Carpintero and Maldonado 1996), because no females of *R. ottoi* sp. nov. were found, the extent of sexual dimorphism, including possible differences in coloration, will only be known if more specimens of both sexes become available in the future for examination.

Interestingly, the mid-longitudinal sulcus on hind lobe of pronotum was represented by a few punctations, about half a dozen, and the two or three more anterior ones were somewhat deeper and larger, scarcely or not exceeding the distal half of the hind lobe (Fig. 11), while after obtaining SEM images (Figs 22, 23), it was possible to record that sometimes, posterior to the punctations, there is also a very thin median longitudinal line ending short of posterior margin (Fig. 23). Therefore, there is an intraspecific variation in the extension and characteristics of the mid-longitudinal sulcus on the hind lobe in *R. ottoi* sp. nov.

Racelda robusta Bérenger & Gil-Santana, 2005
Figs 56, 57

Material examined. French Guiana, Bélizon, xi.2001, H. Gaspard leg., 2 males (MNRJ).

Racelda robusta was described based on a male from French Guiana (Bérenger and Gil-Santana 2005). Gil-Santana et al. (2013) recorded the species from Brazil (Amazonian region). They observed that while the holotype had the center of hind lobe of pronotum entirely blackish, the male from Brazil had a less extensive blackish coloration, with a pale portion below the transverse sulcus. In the males from French Guiana examined here, the area below the tranverse sulcus is also pale to some extent, except at medially (Fig. 56), suggesting intraspecific rather than geographic variation in the size of this blackish marking.

Racelda spurca (Stål, 1860)
Figs 58–62

Material examined. Brazil, São Paulo State: *RACELDA* / *spurca* (Stål [handwritten] / J.C.M. Carvalho. det. 1991 [printed; except two latter numbers, which were handwritten] // [handwritten label]: 20.XI.1955 / Barueri / K. Lenko leg., 1 male (MNRJ).

Racelda spurca was described based on an unspecified number of male specimens from Rio de Janeiro, Brazil. Stål (1860, 1872) cited "Mus. Holm." (NHRS) as the depository of the type specimen(s). Currently, there is only one type specimen of *R. spurca* deposited there (G. Lindberg pers. comm.) (Figs 58–60). The possibility that the species was described based on more than one specimen cannot be excluded and, following Art. 73.2 and the Recommendation 73F of the ICZN, this specimen is therefore considered as a syntype.

Some characteristics of a non-type male specimen examined here (Figs 61, 62) are noteworthy, such as the presence of pale veins on the coria of hemelytra (Fig. 61) and the longitudinal sulcus of the pronotum, which is clearly interrupted at the level of transverse sulcus (Fig. 62) and not continuous along the two lobes.

Discussion

Considering the fact that the females of most species of *Racelda* are unknown, it is possible that *Racelda monstrosa*, described based only on a female, may be conspecific with one of the species of *Racelda* in which only the males are known so far. However, this possibility seems unlikely for *R. aberlenci*, *R. ottoi* sp. nov., and *R. robusta* because of the large differences in general coloration and size. While *R. monstrosa* is generally dark and larger (total length to the tip of abdomen 20 mm) (Carpintero 1980), the other species have several pale portions and are quite smaller, with the following total length: *R. aberlenci* (11 mm), *R. ottoi* sp. nov. (9–10.5 mm), and *R. robusta* (13.5 mm) (Bérenger and Gil-Santana 2005; this work).

It is noteworthy that some of the diagnostic characteristics of *Racelda* stated by previous authors were not present in some species or specimens studied here. The longitudinal sulcus has been described as extending along both lobes of pronotum, i.e., as continuous on the two lobes (Carpintero and Maldonado 1996; Forero 2004), but it may be interrupted at the level of transverse sulcus (e.g., in *R. ottoi* sp. nov. (Figs 22, 23) and *R. spurca* (Fig. 62)). Yet, in *R. ottoi* sp. nov., SEM images of two different specimens showed intraspecific variation, in which, posterior to the punctations on anterior portion of hind lobe, sometimes there is also a very thin median longitudinal line ending short of posterior margin (Fig. 23). Therefore, it is plausible to consider that in other species such variation in the extension of longitudinal sulcus on hind lobe may occur; more specimens need investigation to determine this. In this case, it is more appropriate to generally consider the mid-longitudinal sulcus simply as being well developed anteriorly and obsolete posteriorly as stated by Dougherty (1995). On the other hand, Dougherty (1995) in her key to Ectrichodiinae genera stated that in *Racelda* the anterolateral corners of pronotum would always be squared. However, although in many species they really seem roughly squared (e.g., *R. aberlenci*, *R. moerens*, *R. robusta*, and *R. spurca*) (Figs 1, 9, 56, 58), in *R. alternans*, the type species of the genus, they are definitively rounded (Figs 3, 6). Therefore, although this characteristic might be maintained among features presented by species of *Racelda*, it must not be posited as the deciding factor for including specimens/species in *Racelda* as stated in the Dougherty's key. It may be necessary in the future to redefine the genus *Racelda* to accommodate these variations.

Key to the species of *Racelda* Signoret, 1863 (males only)

1   Connexivum with alternating pale and dark portions on segments III–VI...**2**
–   Connexivum without alternating pale and dark portions **3**
2   Fore femora only slightly thickened (Figs 4, 7); connexival dark markings on segments III–VI, occupying approximately the distal half to distal third of these segments (Figs 4, 6, 7)...................................***alternans* Signoret, 1863**
–   Fore femora clearly thickened (Fig. 61); connexival dark markings on segments III–VI occupying only distal margin of these segments (Figs 58, 61) ..
       .... ***spurca* (Stål, 1860)**

3   Pronotum, connexivum and sternites mostly darkened (Fig. 9)....................
         .... *moerens* Breddin, 1898
–   Most part of pronotum (or at least its fore lobe and humeral angles), con-
         nexivum and sternites mostly or completely pale **4**
4   Coria of hemelytra mostly dark yellow to orange (Fig. 56); segments VI–VII
         of connexivum, lateral portions of sternites V–VI and sternite VII almost or
         completely dark to blackish (Fig. 57) ....
         .... *robusta* Bérenger & Gil-Santana, 2005
–   Coria of hemelytra mostly dark to blackish, with only the basolateral portion
         pale and sometimes the apex faintly paler; connexival segments III–VII and
         sternites III–VI pale (Figs 1, 2, 11, 39); sternite VII sometimes somewhat
         darkened only on the portion posterior to genital capsule (Fig. 39), otherwise
         completely pale too **5**
5   Head completely pale (Fig. 1); pronotum: mid-longitudinal sulcus of pro-
         notum continuous on two lobes; fore lobe pale, hind lobe mostly dark, with
         portions lateral to postero-lateral furrows pale or with faint dark markings
         (Fig. 1); legs mostly pale with femoro-tibial joints and apices of tibiae variably
         faintly darkened (Fig. 1); sternite II pale (Fig. 2) ....
         .... *aberlenci* Bérenger & Gil-Santana, 2005
–   Head mostly blackish (Figs 11, 12), pale to whitish ventrally, between level
         of inner portion of eyes; pronotum: mid-longitudinal sulcus on fore lobe
         interrupted somewhat above a median elevated portion of transverse sulcus
         (Figs 22, 23); mostly orange, faintly darkened at median portion of basal
         half of hind lobe (Fig. 11); legs: fore femora extensively blackish dorsally,
         middle and hind femora blackish on their distal half and distal third, re-
         spectively; tibiae darkened with their median portion paler (Fig. 11); ster-
         nite II almost completely dark (Fig. 39) ....
         .... *ottoi* Oliveira & Gil-Santana, sp. nov.

Acknowledgements

References

Bérenger J-M, Gil-Santana H (2005) Nouveau genre et nouvelles espèces d'Ectrichodiinae d'Amérique du Sud (Heteroptera, Reduviidae). Bulletin de la Société Entomologique de France 110(4/5): 509–516. https://doi.org/10.3406/bsef.2005.16271

Breddin G (1898) Studia hemipterologica. IV. Jahresberichte und Abhandlungen des Naturwissenschaftlichen Vereins in Magdeburg 1896–1898: 149–163.

Carpintero DJ (1980) Nuevos Ectrichodiinae americanos (Insecta–Hemiptera–Reduviidae). Acta Scientifica. Serie Entomología 14: 3–33.

Carpintero DJ, Maldonado J (1996) Diagnostic characters and key to the genera of American Ectrichodiinae (Heteroptera, Reduviidae). Caribbean Journal of Science 32(2): 125–141.

Dougherty V (1995) A review of the New World Ectrichodiinae genera (Hemiptera: Reduviidae). Transactions of the American Entomological Society 121(4): 173–225.

Forero D (2004) Capítulo 5. Diagnosis de los gêneros neotropicales de la família Reduviidae (Hemiptera: Heteroptera), y su distribución em Colombia (excepto Harpactorinae). In: Fernández F, Andrade G, Amat G (Eds) Insectos de Colombia, Vol. 3. Universidad Nacional de Colombia, Bogotá, DC, 128–275.

Forthman M, Gil-Santana HR (2021) Two new species of *Rhiginia* Stål, 1859, with taxonomical notes on species in the "*cruciata*-group" of this genus and an updated key to the New World genera of Ectrichodiinae (Heteroptera, Reduviidae). Zootaxa 4952(2): 201–234. https://doi.org/10.11646/zootaxa.4952.2.1

Forthman M, Weirauch C (2017) Millipede assassins and allies (Heteroptera: Reduviidae: Ectrichodiinae, Tribelocephalinae): total evidence phylogeny, revised classification and evolution of sexual dimorphism. Systematic Entomology 42(3): 575–595. https://doi.org/10.1111/syen.12232

Forthman M, Chłond D, Weirauch C (2016) Taxonomic monograph of the endemic millipede assassin bug fauna of Madagascar (Hemiptera: Reduviidae: Ectrichodiinae). Bulletin of the American Museum of Natural History 400: 1–152. https://doi.org/10.1206/amnb-928-00-01.1

Gaedike H (1971) Katalog der in den Sammlungen des ehemaligen Deutschen Entomologischen Institutes aufbewahrten Typen—V. Beiträge zur Entomologie 21: 79–159. https://doi.org/10.21248/contrib.entomol.21.1-2.79-159

Gil-Santana HR (2014) *Pothea berengeri* sp. nov. from Brazil, with taxonomic notes on *Pothea furtadoi* Gil-Santana & Costa and *Pothea jaguaris* (Carpintero) and reinstatement of *Parapothea* Carpintero as junior synonym of *Pothea* Amyot & Serville (Hemiptera: Heteroptera: Reduviidae: Ectrichodiinae). Zootaxa 3826(3): 497–516. https://doi.org/10.11646/zootaxa.3826.3.4

Gil-Santana HR (2015) First record of the genus *Pseudopothea* from South America, with description of a new species from Brazil (Hemiptera: Heteroptera: Reduviidae: Ectrichodiinae). Zootaxa 3904(4): 541–552. https://doi.org/10.11646/zootaxa.3904.4.3

Gil-Santana HR (2019) New records, taxonomic notes, and the description of a new species of Reduviidae (Hemiptera: Heteroptera) from Ecuador. Zootaxa 4613(3): 502–520. https://doi.org/10.11646/zootaxa.4613.3.5

Gil-Santana HR (2020a) A new species of *Pothea*, with new records and taxonomic notes on other species of the genus (Hemiptera: Heteroptera: Reduviidae). Zootaxa 4778(3): 439–470. https://doi.org/10.11646/zootaxa.4778.3.2

Gil-Santana HR (2020b) New synonymies among species of *Brontostoma* (Hemiptera: Heteroptera: Reduviidae). Zootaxa 4869(3): 301–325. https://doi.org/10.11646/zootaxa.4869.3.1

Gil-Santana HR, Baena M (2009) Two new species of *Brontostoma* Kirkaldy (Hemiptera: Heteroptera: Reduviidae: Ectrichodiinae) from Bolivia, with description of the male genitalia of two other species of the genus, and description of the female of *B. doughertyae* Gil-Santana, Lopes, Marques & Jurberg. Zootaxa 1979(1): 41–52. https://doi.org/10.11646/zootaxa.1979.1.4

Gil-Santana HR, Baena M, Grillo H (2013) *Berengeria* Gil-Santana & Coletto-Silva, a junior synonym of *Ectrichodiella* Fracker & Bruner, with new records and taxonomic notes on Ectrichodiinae from Brazil, and with keys to Ectrichodiinae and Reduviinae genera of the New World (Hemiptera: Heteroptera: Reduviidae). Zootaxa 3652(1): 60–74. https://doi.org/10.11646/zootaxa.3652.1.2

Gil-Santana HR, Forero D, Weirauch C (2015) Assassin bugs (Reduviidae excluding Triatominae). In: Panizzi AR, Grazia J (Eds) True Bugs (Heteroptera) of the Neotropics, Entomology in Focus 2. Springer Science+Business Media, Dordrecht, 307–351. https://doi.org/10.1007/978-94-017-9861-7_12

Gil-Santana HR, Oliveira J, Bérenger J-M (2020) A new genus and a new species of Ectrichodiinae from French Guiana and an updated key to the genera of the New World (Hemiptera, Reduviidae). ZooKeys 968: 85–109. https://doi.org/10.3897/zookeys.968.54291

ICZN [International Commission on Zoological Nomenclature] (1999) International Code of Zoological Nomenclature. Fourth Edition. The International Trust for Zoological Nomenclature, London. https://www.iczn.org/the-code/

Maldonado CJ (1990) Systematic catalogue of the Reduviidae of the world. Caribbean Journal of Science, Special Publication No. 1, University of Puerto Rico. University of Puerto Rico, Mayagüez, 694 pp.

Melo MC, Faúndez E (2015) Synopsis of the family Reduviidae (Heteroptera: Cimicomorpha) from Chile. Revista de la Sociedad Entomológica Argentina 74(3–4): 153–172.

Rosa JA, Mendonça VJ, Rocha CS, Gardim S, Cilense M (2010) Characterization of the external female genitalia of six species of Triatominae (Hemiptera, Reduviidade) by scanning electron microscopy. Memórias do Instituto Oswaldo Cruz 105(3): 286–292. https://doi.org/10.1590/S0074-02762010000300007

Rosa JA, Mendonça VJ, Gardim S, Carvalho DB, Oliveira J, Nascimento JD, Pinotti H, Pinto MC, Cilense M, Galvão C, Barata JMS (2014) Study of the external female genitalia of 14 *Rhodnius* species (Hemiptera, Reduviidae, Triatominae) using scanning electron microscopy. Parasites & Vectors 7(1): e17. https://doi.org/10.1186/1756-3305-7-17

Schuh RT, Weirauch C (2020) True bugs of the world (Hemiptera: Heteroptera). Classification and Natural History. Second Edition. Siri Scientific Press, Manchester, 767 pp. [+ 32 pls]

Sehnal C (2000) Typencatalog der Reduviidae des Naturhistorischen Museums in Wien (Insecta: Heteroptera). – Kataloge der wissenschaftlichen Sammlungen des Naturhistorischen Museums in Wien, Band 14: Entomologie. Naturhistorischen Museums Wien, Vienna, 126 pp.

Signoret V (1863) Révision des Hémiptères du Chili. Annales de la Société Entomologique de France 4(3): 541–588.

Stål C (1860) Bidrag till Rio de Janeiro-Traktens Hemipter-fauna. Kongliga Svenska Vetenskaps-Akademiens Handlingar 2: 1–84.

Stål C (1872) Enumeratio Hemipterorum. Bidrag till en förteckning öfver alla hittills kända Hemiptera, jemte systematiska meddelanden. 2. Kongliga Svenska Vetenskaps-Akademiens Handlingar 10(4): 1–159.

Weirauch C (2008) From four- to three- segmented labium in Reduviidae (Hemiptera: Heteroptera). Acta Entomologica Musei Nationalis Pragae 48(2): 331–344.

RESEARCH ARTICLE

Three new deep-sea species of *Marphysa* (Annelida, Eunicida, Eunicidae) from Papua New Guinea (Bismarck and Solomon seas)

Nicolas Lavesque[1], Guillemine Daffe[2], Christopher Glasby[3,4],
Stéphane Hourdez[5], Pat Hutchings[4,6]

1 *CNRS, Université de Bordeaux, Bordeaux INP, EPOC, UMR 5805, Station Marine d'Arcachon, Arcachon, France* **2** *CNRS, Université de Bordeaux, Observatoire Aquitain des Sciences de l'Univers, UMS 2567 POREA, Pessac, France* **3** *Museum and Art Gallery Northern Territory, Darwin, Australia* **4** *Australian Museum Research Institute, Australian Museum, 1 William Street, Sydney, NSW 2010, Australia* **5** *CNRS, Sorbonne Université, Laboratoire d'Ecogéochimie des Environnements Benthiques, LECOB, Banyuls, France* **6** *Department of Biological Sciences, Macquarie University, North Ryde NSW 2109, Australia*

Corresponding author: Nicolas Lavesque (nicolas.lavesque@u-bordeaux.fr)

Abstract

Three new species of *Marphysa* Quatrefages, 1866, *Marphysa banana* **sp. nov.**, *Marphysa papuaensis* **sp. nov.**, and *Marphysa zanolae* **sp. nov.** are described from deep-sea sunken vegetation off Papua New Guinea, using both morphology and molecular data (for two species). With the presence of compound spinigers only and the branchiae present over many chaetigers, *Marphysa banana* **sp. nov.** belongs to the group B2. This species is characterised by the presence of eyes, the presence of branchiae starting from chaetiger 20, and by the presence of three types of pectinate chaetae and bidentate subacicular hooks starting from chaetigers 13–52. With the presence of compound falcigers only and the branchiae restricted to a short anterior region, *Marphysa papuaensis* **sp. nov.** belongs to the group C1. This species has a bilobed prostomium but no eyes, has branchiae from chaetigers 7 to 14–16 with up to 16 filaments. *Marphysa papuaensis* **sp. nov.** is also characterised by the presence of bidentate subacicular hooks from chaetiger 20 and by a single type of pectinate chaetae. Finally, *Marphysa zanolae* **sp. nov.** belongs to the group C2, with the presence of compound falcigers only and the branchiae present over many chaetigers. This species is characterised by the absence of eyes, by the presence of branchiae with a single long filament starting from chaetiger 31, by unidentate subacicular hooks starting from chaetiger 28 and finally by one type of pectinate chaetae with very long outer teeth.

Introduction

Situated in the Coral Triangle, Papua New Guinea is considered a marine biodiversity hotspot and shows a high level of endemism. Although the terrestrial and shallow water fauna is well known, the deep-sea fauna has rarely been studied (Pante et al. 2012). Indeed, the historical expeditions of 'Siboga' and the HMS 'Challenger', which both sampled the deep sea, did not pay much attention to this area, and only the 'Galathea' and RV 'Vityaz' expeditions carried out benthic sampling in the deep sea (hadal zone) (Pante et al. 2012; Corbari et al. 2019). Only a few taxonomic studies on polychaetes have been conducted in the region, in coastal habitats (Dahlgren 1996; Rouse 1996; Britayev et al. 1999; Rouse 2012) and hydrothermal vents (Watson 2001; Reuscher et al. 2011) but data on other types of deep-sea habitats are still lacking. Between 2010–2014, the Muséum National d'Histoire Naturelle (MNHN) and the Institut de Recherche pour le Développement (IRD), in collaboration with the University of Papua New Guinea (UPNG) launched four sampling campaigns (BIOPAPUA 2010, PAPUA NIUGINI 2012 MADEEP, and KAVIENG 2014) aiming to explore the deep-sea biodiversity of this region, especially in the Bismarck and Solomon seas (Pante et al. 2012; Corbari et al. 2019).

Marphysa Quatrefages, 1866 is a very speciose genus with 83 accepted species (Read and Fauchald 2022), commonly found from intertidal shores to shallow waters (Glasby and Hutchings 2010). As far as we know, and unlike *Eunice* the other species-rich genus of the family, *Marphysa* species are never found in the deep sea. Except for the non-indigenous species *Marphysa victori* Lavesque, Daffe, Bonifácio & Hutchings, 2017 (Lavesque et al. 2020), most of the species show restricted distributions (Hutchings and Kupriyanova 2018; Lavesque et al. 2019) and are often very restricted to particular habitats (Hutchings and Karageorgopoulos 2003; Glasby and Hutchings 2010; Zanol et al. 2016; Lavesque et al. 2019). Following Fauchald (1970) and Glasby and Hutchings (2010), species of the genus *Marphysa* can be separated into five artificial groups based on the type of compound chaetae: no compound chaetae present (Group A), only compound spinigers present (Group B), only compound falcigers present (Group C), both compound spinigers and falcigers present (Group D), and compound spinigers only anteriorly and posterior segments only with simple limbate chaetae (Group E). Finally, each group can also then be divided into species having branchiae present over a short anterior region (subdivision 1) or branchiae present over many chaetigers (subdivision 2).

Until now, 15 species of *Marphysa* have been described from the Central Indo-Pacific Realm (sensu Spalding et al. 2007), two species belonging to Group A (*M. fijiensis* Molina-Acevedo & Idris, 2021 and *M. moribidii* Idris, Hutchings &

Arshad, 2014), nine species to Group B (*M. hongkongensa* Wang, Zhang & Qiu, 2018; *M. iloiloensis* Glasby, Mandario, Burghardt, Kupriyanova, Gunton & Hutchings, 2019; *M. maxidenticulata* Liu, Hutchings & Kupriyanova, 2018; *M. mullawa* Hutchings & Karageorgopoulos, 2003; *M. multipectinata* Liu, Hutchings & Sun, 2017; *M. orientalis* Treadwell, 1936; *M. tribranchiata* Liu, Hutchings & Sun, 2017; *M. tripectinata* Liu, Hutchings & Sun, 2017, and *M. bulla* Liu, Hutchings & Kupriyanova, 2018, which was recently synonymised with *M. victori* Lavesque, Daffe, Bonifácio & Hutchings, 2017 (Lavesque et al. 2020); two species belong to Group C (*M. bernardi* Rullier, 1972 and *M. soembaensis* Augener, 1933); and only one species belongs to each of groups D (*M. digitibranchia* Hoagland, 1920) and E (*M. fauchaldi* Glasby & Hutchings, 2010).

In this study, three new deep-sea species belonging to groups B2 (*Marphysa banana* sp. nov.), C1 (*Marphysa papuaensis* sp. nov.), and C2 (*Marphysa zanolae* sp. nov.) are described using both morphology and molecular data (for two of them). The type specimens were found in deep-sea sunken vegetation (decaying wood or cultivated plants leaves). It is not surprising, as this region is known to accumulate large quantities of decomposing vegetation, transiting from tropical forests to marine canyons (Pante et al. 2012), hosting original and diverse fauna (Samadi et al. 2007).

Materials and methods

Sampling and morphological analyses

Specimens were collected by beam trawl during the MADEEP cruise (see https://expeditions.mnhn.fr/campaign/madeep) and the KAVIENG cruise (https://expeditions.mnhn.fr/campaign/kavieng2014) in May–September 2014, in the Solomon Sea (Fig. 1). All material was sorted on board RV 'Alis' and fixed in 80% ethanol. A few parapodia were removed from several specimens for molecular analysis. Specimens were examined under a Nikon SMZ25 stereomicroscope and a Nikon Eclipse *Ci* microscope, and photographed with a Nikon DS-Ri 2 camera. Measurements were made with the NIS-Elements Analysis software. Drawings were made from pictures using Inkscape software. Width of all specimens was obtained by measuring chaetiger 10 with parapodia. Morphological terminology is based on Fauchald (1992) for general terms, Paxton (2000) for head appendages and Molina-Acevedo and Carrera-Parra (2015) for maxillary apparatus. Terminology of pectinate chaetae follows Glasby et al. (2019), based on a previous study of Molina-Acevedo & Carrera-Parra (2017): isodont means outer teeth much longer than internal teeth, anodont means outer teeth more or less same length as internal teeth, and heterodont when one long and one short (same length as internal teeth) lateral tooth are present. The width of the pectinate blade is wide when ≥ 30 μm and narrow below this. Finally, the size of the internal teeth is long when they measure 12 μm or more and thick when are 2 μm or more, below these values the teeth are defined as short and slender, respectively.
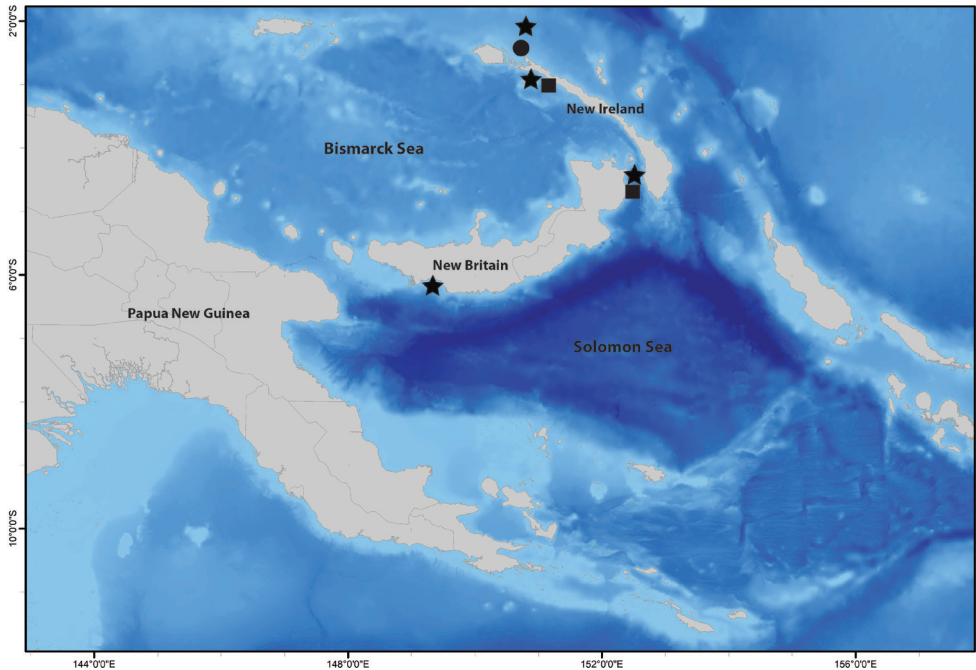
Figure 1. Sampling sites of type material of *Marphysa banana* sp. nov. (black circle), *Marphysa papuaensis* sp. nov. (black star), and *Marphysa zanolae* sp. nov. (black square) in Papua New Guinea.

Some parapodia along the body were removed from the type material of each species (see Material examined), dehydrated in ethanol, critical point dried, covered with 20 nm of gold, examined under the scanning electron microscope (JEOL JSM 6480LA) and imaged with a secondary detector at Macquarie University, Sydney, Australia.

The studied material is deposited at the Muséum National d'Histoire Naturelle, Paris (**MNHN**) and the Australian Museum, Sydney (**AM**). Additional material is lodged in the collection housed at the Arcachon Marine Station (**SMA**).

Molecular data and analyses

Extraction of DNA was done with ISOLATE II Genomic DNA kit (BIOLINE) following protocol supplied by the manufacturers. Approximately 600 bp of COI (cytochrome c oxidase subunit I) gene was amplified, using primers polyLCO and polyHCO COI (Carr et al. 2011). PCR (Polymerase Chain Reaction) was performed with Taq DNA Polymerase QIAGEN Kit in 20 μL mixtures containing: 2 μL of 10X CoralLoad PCR Buffer (final concentration of 1X), 1.5 μL of MgCl2 (25 Mm) solution, 1.5 μL of PCR nucleotide mix (final concentration of 0.2 mM each dNTP), 0.4 μl of each primer (final concentration of 0.2 μM), 0.1 μl of Taq DNA Polymerase (5U/μl), 1 μl template DNA and 13.1 μL of nuclease-free water. The temperature profile was as follows 94 °C / 60 s – (94 °C / 40 s – 45 °C / 40 s – 72 °C / 60 s)*5 cycles – (94 °C / 40 s – 51 °C/ 40 s – 72 °C / 60 s)*35 cycles – 72 °C / 300 s – 4 °C. PCR success was verified by electrophoresis in

a 1% p/v agarose gel stained with Gelred. Amplified products were sent to Macrogen Company to obtain sequences, using the same set of primers as used for PCR.

Fifty-nine COI sequences were downloaded from GenBank or obtained during this study, fifty-six COI sequences of *Marphysa* species and three outgroup species from closely related genera in the family Eunicidae (Table 1). During this study, one COI sequence was obtained both for *Marphysa papuaensis* sp. nov. and *Marphysa zanolae* sp. nov., but we failed to obtain a sequence for *Marphysa banana* sp. nov.

All COI sequences were aligned in Geneious Prime 2019.0.4 using the MUSCLE plugin and default settings. The AIC and BIC tests in jModeltest 2.2.10 (Darriba et al. 2012) were used to select the GTR + I + G model of molecular evolution as the best evolutionary model for the COI gene alignment. The phylogenetic analysis was performed in MrBayes v. 3.2.6 (Ronquist and Huelsenbeck 2003). The analysis was run for 10 million generations (sampled every 1000), 25% of the generations were discarded as burn-in and the standard deviation of split frequencies decreased below 0.01. FigTree v. 1.4.4 (Rambaut 2007) was used to visualise the majority-rule consensus tree displaying all nodes with a posterior probability > 0.5. Pair-wise Kimura 2-parameter (K2P) genetic distance was performed using MEGA v. 7.0.26.

Table 1. Terminal taxa used in the molecular part of the study (COI gene), with type localities, collection localities, GenBank accession numbers, and references.

Species	Type locality	Collection locality	GenBank accession number	Reference
Eunice cf. *violaceomaculata*	Tortugas, Caribbean	Carrie Bow Cay, Belize	GQ497542	Zanol et al. 2010
Palola viridis	Samoa, Pacific Ocean	Kosrae, Micronesia	GQ497556	Zanol et al. 2010
Leodice rubra	Saint Thomas, Caribbean	Ceara, Brazil	GQ497528	Zanol et al. 2010
M. aegypti	Suez Canal, Egypt	Suez Canal, Egypt	MF196969	Elgetany et al. 2018
M. bifurcata	WA, Australia	Qld, Australia	KX172177	Zanol et al. 2016
M. bifurcata	WA, Australia	Qld, Australia	KX172178	Zanol et al. 2016
M. brevitentaculata	Tobago	Quintana Roo, Mexico	GQ497548	Zanol et al. 2010
M. californica	California, USA	California, USA	GQ497552	Zanol et al. 2010
M. disjuncta	California, USA	California, USA	GQ497549	Zanol et al. 2010
M. chirigota	Bay of Cadiz, Spain	Bay of Cadiz, Spain	MN816442	Martin et al. 2020
M. chirigota	Bay of Cadiz, Spain	Bay of Cadiz, Spain	MN816443	Martin et al. 2020
M. chirigota	Bay of Cadiz, Spain	Bay of Cadiz, Spain	MN816444	Martin et al. 2020
M. fauchaldi	NT, Australia	NT, Australia	KX172165	Zanol et al. 2016
M. gaditana	Bay of Cadiz, Spain	Bay of Cadiz, Spain	MN816441	Martin et al. 2020
M. hongkongensa	Hong Kong	Hong Kong	MH598525	Wang et al. 2018
M. hongkongensa	Hong Kong	Hong Kong	MH598526	Wang et al. 2018
M. iloiloensis	Iloilo, Philippines	Tigbauan, Philippines	MN106279	Glasby et al. 2019
M. iloiloensis	Iloilo, Philippines	Tigbauan, Philippines	MN106280	Glasby et al. 2019
M. iloiloensis	Iloilo, Philippines	Tigbauan, Philippines	MN106281	Glasby et al. 2019
M. kristiani	NSW, Australia	NSW, Australia	KX172160	Zanol et al. 2016
M. kristiani	NSW, Australia	NSW, Australia	KX172161	Zanol et al. 2016
M. kristiani	NSW, Australia	NSW, Australia	KX172162	Zanol et al. 2016
M. kristiani	NSW, Australia	NSW, Australia	KX172158	Zanol et al. 2016
M. madrasi	Chennai, India	Chennai, India	MT813506	Hutchings et al. 2020
M. madrasi	Chennai, India	Chennai, India	MT813507	Hutchings et al. 2020
M. mossambica	Mozambique	Iloilo, Philippines	KX172164	Zanol et al. 2016
M. mullawa	Qld, Australia	NSW, Australia	KX172166	Zanol et al. 2016
M. mullawa	Qld, Australia	NSW, Australia	KX172167	Zanol et al. 2016

Species	Type locality	Collection locality	GenBank accession number	Reference
M. mullawa	Qld, Australia	NSW, Australia	KX172168	Zanol et al. 2016
M. mullawa	Qld, Australia	NSW, Australia	KX172176	Zanol et al. 2016
M. papuaensis sp. nov.	Papua New Guinea	Papua New Guinea	OP184050	This study
M. pseudosessiloa	NSW, Australia	NSW, Australia	KY605405	Zanol et al. 2010
M. pseudosessiloa	NSW, Australia	NSW, Australia	KY605406	Zanol et al. 2010
M. regalis	Bermuda	Ceara, Brazil	GQ497562	Zanol et al. 2010
M. sanguinea	Devon, UK	Callot Island, France	GQ497547	Zanol et al. 2010
M. sanguinea	Devon, UK	Cornwall, UK	MK541904	Lavesque et al. 2019
M. sanguinea	Devon, UK	Arcachon Bay, France	MK950853	Lavesque et al. 2019
M. sanguinea	Devon, UK	Brest, France	MK967470	Lavesque et al. 2019
M. tripectinata	Beihai, China	Beihai, China	MN106271	Glasby et al. 2019
M. sherlockae	Durban, South Africa	Strand, South Africa	MT840349	Kara et al. 2020
M. sherlockae	Durban, South Africa	Strand, South Africa	MT840350	Kara et al. 2020
M. sherlockae	Durban, South Africa	Strand, South Africa	MT840351	Kara et al. 2020
M. tripectinata	Beihai, China	Beihai, China	MN106272	Glasby et al. 2019
M. tripectinata	Beihai, China	Beihai, China	MN106273	Glasby et al. 2019
M. tripectinata	Beihai, China	Beihai, China	MN106274	Glasby et al. 2019
M. tripectinata	Beihai, China	Beihai, China	MN106275	Glasby et al. 2019
M. tripectinata	Beihai, China	Beihai, China	MN106276	Glasby et al. 2019
M. tripectinata	Beihai, China	Beihai, China	MN106277	Glasby et al. 2019
M. tripectinata	Beihai, China	Beihai, China	MN106278	Glasby et al. 2019
M. victori	Arcachon Bay, France	Arcachon Bay, France	MG384996	Lavesque et al. 2017
M. victori	Arcachon Bay, France	Arcachon Bay, France	MG384997	Lavesque et al. 2017
M. victori	Arcachon Bay, France	Arcachon Bay, France	MG384998	Lavesque et al. 2017
M. victori	Arcachon Bay, France	Arcachon Bay, France	MG384999	Lavesque et al. 2017
M. victori	Arcachon Bay, France	Mangoku-ura Inlet, Japan	LC467767	Abe et al. 2019
M. victori	Arcachon Bay, France	Sendai Bay, Japan	LC467769	Abe et al. 2019
M. victori	Arcachon Bay, France	Ena Bay, Japan	LC467772	Abe et al. 2019
M. victori	Arcachon Bay, France	China	MT012514	Lavesque et al. 2020
M. viridis	Florida, USA	Ceara, Brazil	GQ497553	Zanol et al. 2010
M. zanolae sp. nov.	Papua New Guinea	Papua New Guinea	OP184049	This study

Taxonomic account

Family Eunicidae Berthold, 1827

Genus *Marphysa* Quatrefages, 1866

Type species. *Nereis sanguinea* Montagu, 1813.

Marphysa banana sp. nov.
https://zoobank.org/36B09BD6-2080-4266-9945-98EA1CA40913
Figs 2–4

Material examined. *Holotype*: MNHN-IA-2015-1608, complete. *Paratypes*: AM W.53773, complete; AM W.53774, complete, some parapodia mounted for SEM; MNHN-IA-2021-725, anterior part only. All material collected from South Pacific Ocean, Papua New Guinea, New Ireland, CP4254, -2.483°S, 150.66°E, depth 273–324 m, April 2014.
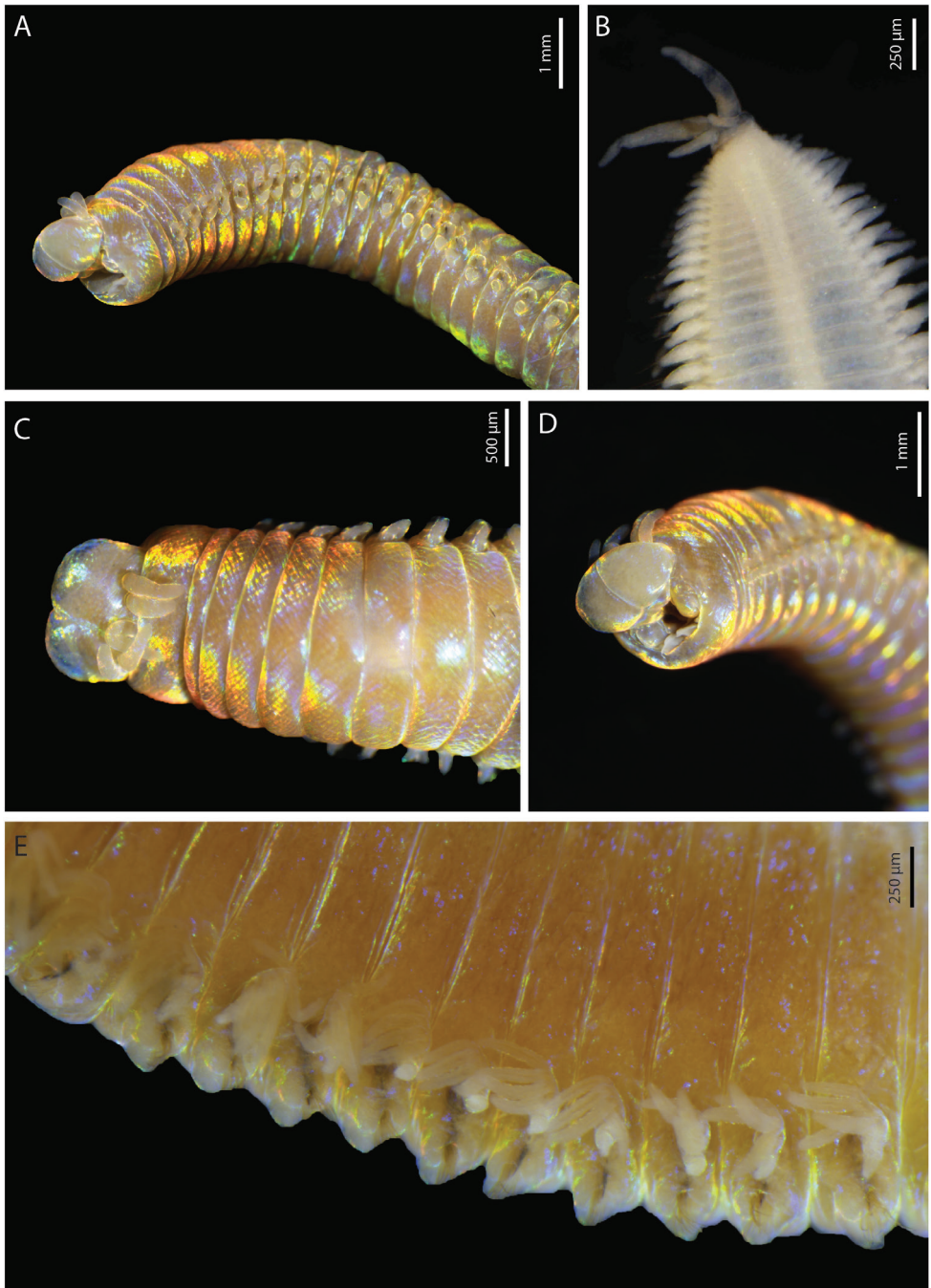
Figure 2. *Marphysa banana* sp. nov. holotype MNHN-IA-2015-1608 (**B**) paratype MNHN-IA-2021-725 (**A, C–E**): **A** anterior end, lateral view **B** pygidium, ventral view **C** anterior end, dorsal view **D** anterior end, frontal view **E** anterior chaetigers, dorso-lateral view.

Description (based on holotype, with variation in parentheses for paratypes). Preserved specimens strongly iridescent (Fig. 2A, C, D), ~ 230 (220) chaetigers, 112 mm (71–157) long, 3.3 mm (2.1–5.4) width at chaetiger 10, excluding parapodia. Body elongated and tapered gradually at posterior end (Fig. 2B).

Prostomium rounded anteriorly with two dorsoventrally flattened buccal lips an anterior notch between them, notch more visible ventrally (Fig. 2A, C, D). Two palps and three antennae slender and tapering, arranged in an arc on posterior margin of prostomium. Antennae more or less smooth, of equal length, longer than palps (same size), shorter (same size) than prostomium (Fig. 2C). Eyes present, one pair, brownish, very faint, present at posterior base between palps and lateral antennae. First peristomial ring ~ 3× longer than second one dorsally (Fig. 2C).

Maxillary apparatus (Fig. 3D, E) partially everted in holotype or paratypes. Formula as follows: MF = 1+1, 5+5, 6+0, 4+9, 1+1. MI ~ 2× longer than maxillary carrier, rectangular anteriorly, triangular posteriorly, with a pair of rounded wings situated at posterolateral margins. MI forceps-like, without attachment lamellae, sub-right-angle falcal arch. Closing system ~ 4× shorter than MI. Ligament between MI and MII golden. MII without attachment lamella, teeth triangular, distributed in less than half of plate length. Ligament between MII and MIII absent (or not sclerotized). MIII, single, longer than left MIV, curved, with equal-sized triangular teeth; short attachment lamella situated in the centre of posterior edge of maxilla, thin, dark. Left MIV short (less than half the size of right MIV) with wide, rounded base, left-most teeth longer than right-most ones; attachment lamella dark, semi-circular. Right MIV long, with teeth triangular, decreasing in size posteriorly; attachment lamella wide, semi-circular, dark. MV, paired, as long as high, with a dorsal curved tooth. Mandibles light brown, concentric stripes not visible; longer than MI; cutting plates whitish, without dorsal teeth (Fig. 3E).

First few parapodia located below middle line of body wall, but gradually positioned dorsally to approximately midline in subsequent segments (Fig. 2A). Notopodial cirri slender, tapering, slightly longer than ventral cirri, thinner posteriorly (Fig. 3A–C). Chaetal lobes comprising a low pre-chaetal lip and a globular post-chaetal lobe. Ventral cirri bluntly conical, with rounded tip, shorter than post-chaetal lobes anteriorly, thereafter slightly longer than post-chaetal lobes (Fig. 3A–C). Branchiae pectinate, commencing from chaetiger 20 (18–19) and continuing to near end, very short anteriorly, longer in medium chaetigers but not reaching mid-dorsal line; number of filaments increasing from 1–3 anteriorly to 4–6 in mid-body, decreasing to 3–4 in last several chaetigers (Figs 2E, 3A–C).

Aciculae black with paler blunt tips, approximately three or four per parapodium in anterior chaetigers, one or two per parapodium in middle chaetigers, and one per parapodium in posterior chaetigers. Supra-acicular chaetae with limbate capillaries and pectinates; capillaries present from first chaetiger to near pygidium, numbering up to 20 in anterior chaetigers (Fig. 3A–C).

Pectinate chaetae commencing from approximately chaetiger 20 to near end, three types identified. Type 1 from anterior parapodia to mid-body: isodont-narrow-slender (INS), having ~ 20 short internal teeth, each tooth prolonged by a thin filament (Fig. 4A, B). Types 2 and 3 from posterior parapodia only (Fig. 4C, D):
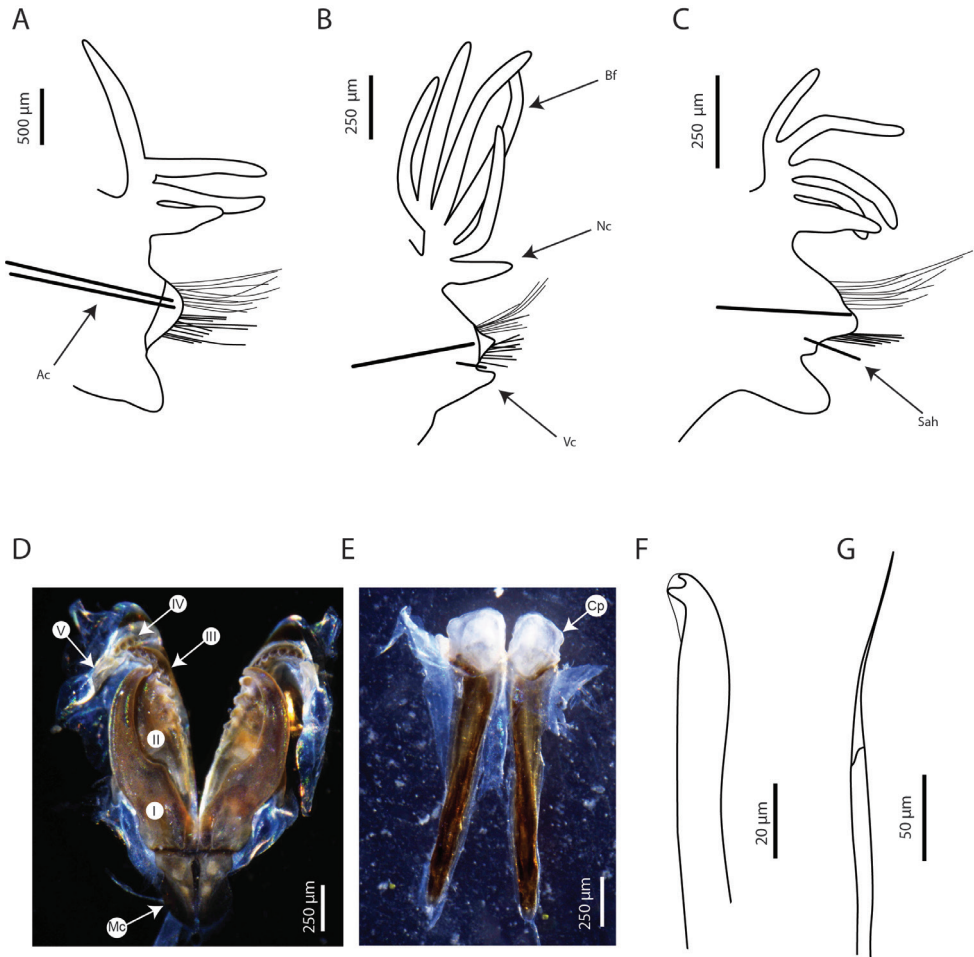
Figure 3. *Marphysa banana* sp. nov. holotype MNHN-IA-2015-1608 (**A–C, F–G**), paratype MNHN-IA-2021-725 (**D, E**): **A** parapodia from anterior chaetiger (chaetiger 29) **B** parapodia from mid-body (chaetiger 100) **C** parapodia from posterior chaetiger (chaetiger 190) **D** maxilla, dorsal view **E** mandibles, dorsal view **F** subacicular hook from mid-body (chaetiger 100) **G** spiniger from chaetiger 29. Abbreviations: MI to MV, maxillae I to V; Ac, aciculae; Bf, branchial filament; Cp, cutting plate; Mc, maxillary carrier; Nc, notopodial cirri; Sah, subacicular hook; Vc, ventral cirri. **A–C** Sah and Ac are illustrated schematically to indicate position.

type 2 asymmetrical, anodont-wide-thick (AWT), having ˷ 10 thick internal teeth, each tooth prolonged by a thin filament; type 3 asymmetrical, anodont-wide-slender (AWS), having ˷ 20 internal teeth, each tooth prolonged by a thin filament (Fig. 4D).

Subacicular chaetae with compound spinigers and subacicular hooks (Fig. 3F). Compound spinigers commencing from first chaetiger to near pygidium, with long, tapered blade. Subacicular hooks transparent, commencing from anterior chaetigers 43–52 (range for type material) to near end and inferior to bundle of spinigers, one per parapodium; much thinner than aciculae; subacicular hooks bidentate (Fig. 3F).
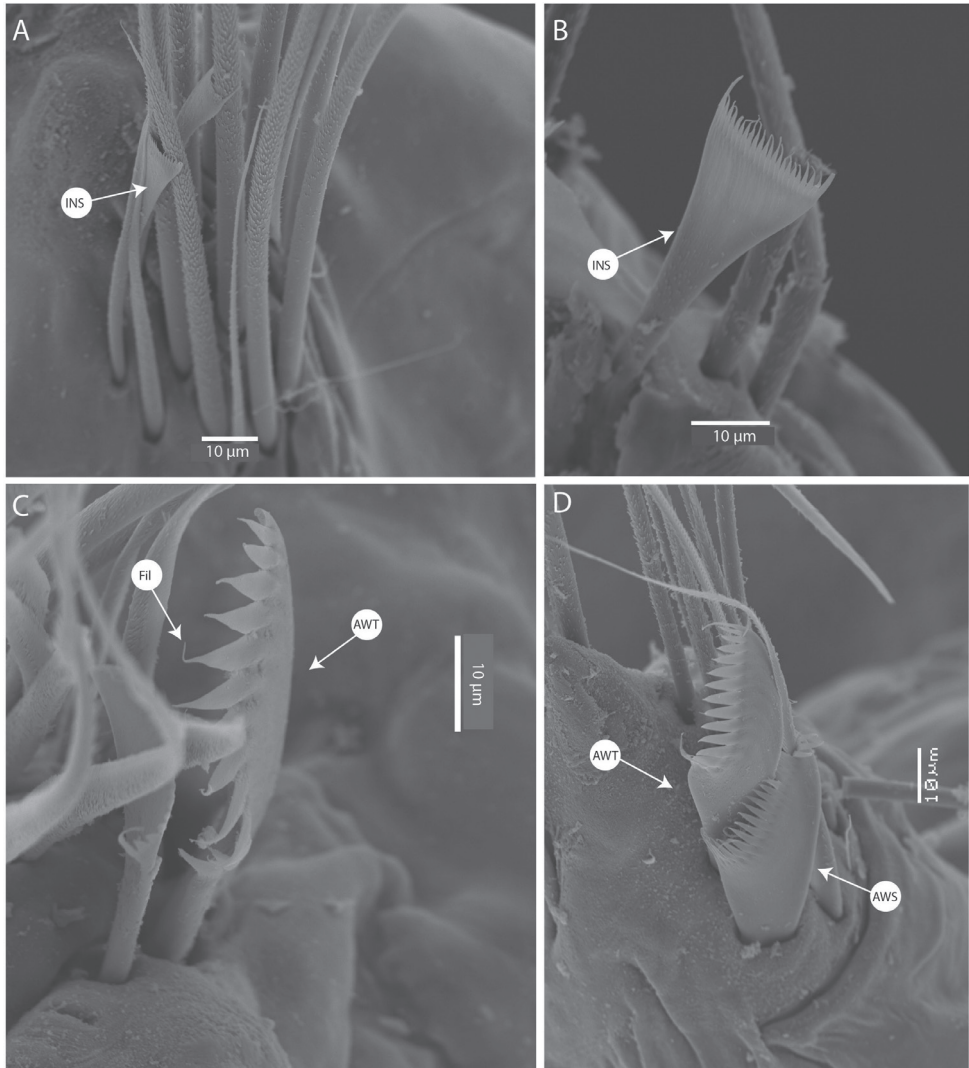
Figure 4. SEM images of pectinate chaetae of *Marphysa banana* sp. nov. paratype AM W.53774 **A** chaetiger 35 **B** chaetiger 67 **C** chaetiger 99 **D** chaetiger 131. Abbreviations: AWS, anodont-wide-slender; AWT, anodont-wide-thick; INS, isodont-narrow-slender; Fil, filament.

Pygidium round, with crenulated margin, dorsally positioned, with two pairs of tapering pygidial cirri attached at ventral edge, dorsal pair 2–3× length of ventral pair (Fig. 2B).

Etymology. The species name refers to the decomposing banana leaves among which all the specimens were found.

Type locality. South Pacific, Papua New Guinea, New Ireland.

Distribution. Only known from type locality.

Habitat. Between 273 and 324 m, found inside banana leaves that presumably have been entrained from river runoff via coastal waters.

Remarks. With the presence of compound spinigers only and the branchiae present over many chaetigers *Marphysa banana* sp. nov. belongs to the group B2, also known as the *sanguinea*-group Quatrefages, 1866. Among the nine species of this group occurring in the Central Indo-Pacific Realm, *M. banana* sp. nov. is similar to *M. hongkongensa*, *M. iloiloensis*, and *M. mullawa* by the presence of subacicular hooks starting from chaetigers 30–50 and the branchiae commencing from chaetigers 14–20.

However, *M. banana* sp. nov. differs from *M. hongkongensa* by the presence of pectinate chaetae starting from around chaetiger 20 instead of starting from the first few chaetigers as found for *M. hongkongensa*; and by the presence of three different types of pectinate chaetae instead of four types as found in *M. hongkongensa*. Moreover, *M. banana* sp. nov. has eyes whereas *M. hongkongensa* does not have any. The subacicular hooks of *M. banana* sp. nov. are bidentate while those of *M. hongkongensa* are unidentate and the maximum number of branchial filaments reaches six for *M. banana* sp. nov., while it can be ten for *M. hongkongensa*. Finally, *M. hongkongensa* lives in the lower intertidal of the Hong Kong region, while *M. banana* sp. nov. is a deep-sea species found inside banana leaves.

Marphysa banana sp. nov. differs from *M. iloiloensis* by the presence of four and nine teeth on the maxillary MIV, while *M. iloiloensis* has three and five teeth respectively. The two species show three different types of pectinate chaetae but not the same ones, as *M. banana* sp. nov. has INS, AWT and AWS with the first ones starting from chaetiger 20 while *M. iloiloensis* has INS, IWS and ANT, with first ones commencing from the first few chaetigers. The subacicular hooks are also different as they are bidentate for *M. banana* sp. nov. and unidentate for *M. iloiloensis*. Finally, *M. iloiloensis* lives in the brackish waters of the Philippines region, which is a very different habitat from the deep-sea habitat of *M. banana* sp. nov.

Marphysa banana sp. nov. differs from *M. mullawa* by the presence of pectinate chaetae starting from around chaetiger 20 instead of commencing from the first few chaetigers for *M. mullawa*, and the anterior chaetae numbering ~ 20 internal teeth instead of 10 for *M. mullawa*. The two species differ by their maxillary formulae, especially for maxillary MII (7+7 for *M. mullawa*, 5+5 for *M. banana* sp. nov.) and MIII (8+0 for *M. mullawa*, 6+0 for *M. banana* sp. nov.). Another difference concerns the shape of anterior branchiae, which are palmate for *M. mullawa* and pectinate for *M. banana* sp. nov. Once again, the two species live in very different habitats as *M. mullawa* is found in intertidal and shallow waters only, on mud or in seagrass beds.

Marphysa papuaensis sp. nov.

https://zoobank.org/991E2117-4921-4A7F-83B8-8F30EF6CA73C
Figs 5–7

Material examined. *Holotype*: MNHN-IA-2015-1559, complete, South Pacific Ocean, Papua New Guinea, New Britain, CP4264, -4.6°S, 152.4°E, depth 430–523 m, April 2014. *Paratypes*: MNHN-IA-2015-1415, complete, South Pacific Ocean, Papua New Guinea, New Britain, CP4337, -6.083°S, 149.316°E, depth 287–447 m,
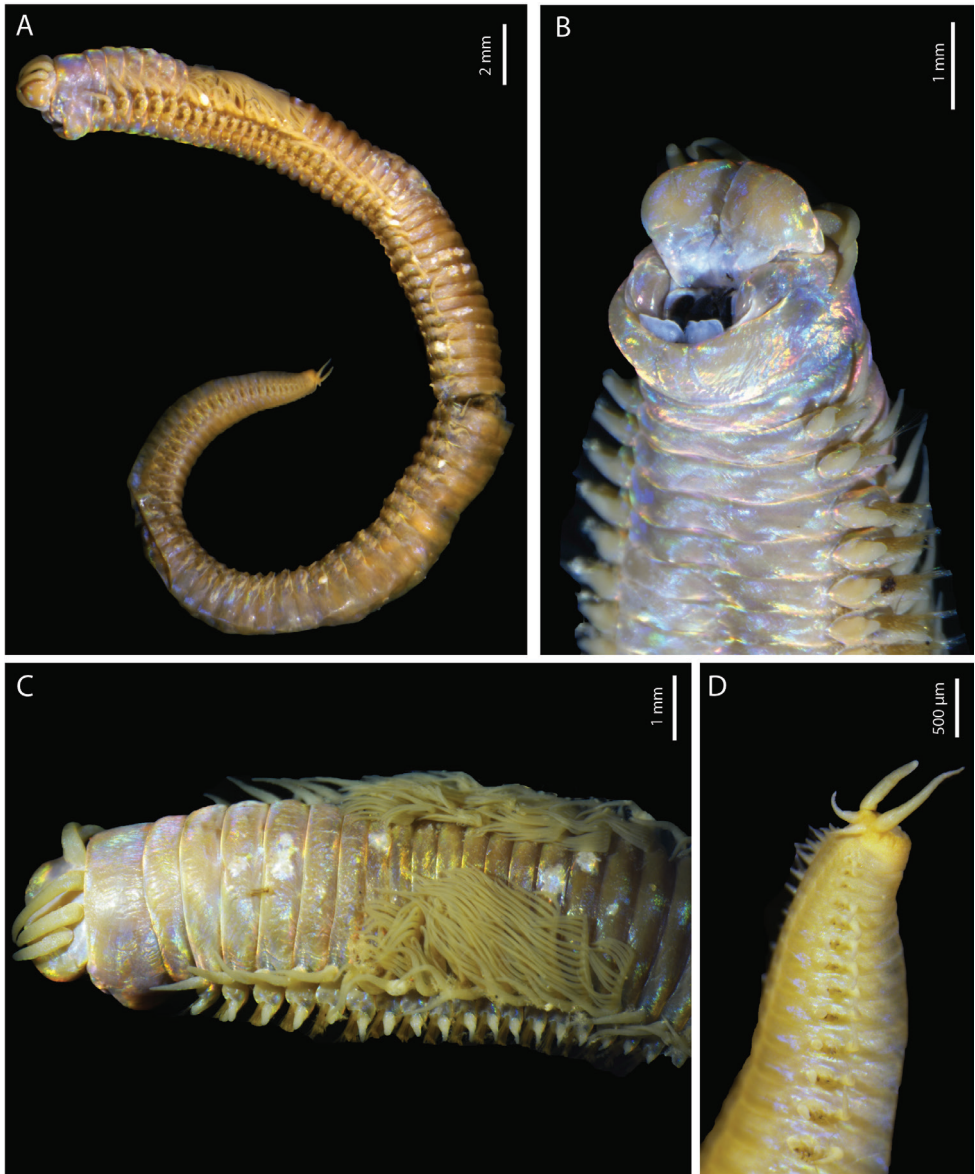
Figure 5. *Marphysa papuaensis* sp. nov. holotype MNHN-IA-2015-1559: **A** entire specimen, lateral view **B** anterior end, ventral view **C** anterior end, dorsal view **D** pygidium, lateral view.

May 2014; MNHN-IA-2015-1593, anterior part only, South Pacific Ocean, Papua New Guinea, New Britain, CP4329, -6.133°S, 149.166°E, depth 250–500 m, May 2014; AM W.53770, complete (several parapodia mounted for SEM), South Pacific Ocean, Papua New Guinea, New Britain, CP4264, 4.6°S, 152.4°E, depth 430–523 m, April 2014; AM W.53771, anterior part only, mounted for SEM, South Pacific Ocean,

Papua New Guinea, New Britain, CP4334, -6.116°S, 149.166°E, depth 430–620 m, May 2014; AM W.53772, complete, gravid, South Pacific Ocean, Papua New Guinea, New Britain, CP4266, -4.6166°S, 152.416°E, depth 575–616 m, April 2014.

Additional material. MNHN-IA-2015-1610, anterior part only, gravid, South Pacific Ocean, Papua New Guinea, New Ireland, CP4260, -2.9°S, 151.1°E, depth 350–847 m, April 2014; MNHN-IA-2015-1949, anterior part only, South Pacific Ocean, Papua New Guinea, New Ireland, CP4434, -2.25°S, 150.8°E, depth 1066–1200 m, August 2014; MNHN-IA-2015-1615, anterior part only, few parapodia used for molecular analysis, South Pacific Ocean, Papua New Guinea, New Hanover, CP4482, -2.683°S, 150.116°E, depth 761–825 m, September 2014.

Description (based on holotype, with variation in parentheses for paratypes). Specimens strongly iridescent (Fig. 5B), 88 (89) chaetigers, 45 mm (41–80) long, 3.6 mm (2.5–2.8) width at chaetiger 10, excluding parapodia. Body elongated and tapered gradually at posterior end, anteriorly not flattened (Fig. 5A).

Prostomium bilobed, with buccal lips separated by a ventral notch only (Fig. 5B). Two palps and three antennae slender and tapering, palpophores not visible, arranged in an arc on posterior margin of prostomium. Antennae more or less smooth, of equal length, slightly longer than palps and prostomium (same size) (Figs 5C, 7A). Eyes absent. First peristomial ring ~ 1.8× longer than second one dorsally (Figs 5C, 7A).

Maxillary apparatus (Fig. 6D, E) partially everted in holotype or paratypes. Formula as follows: MF = 1+1, 5(6)+5(6), 7+0, 4(3)+10(11), 1+1. MI ~ 2.5× longer than maxillary carrier, rectangular anteriorly, triangular posteriorly, with a pair of rounded wings situated at posterolateral margins. MI forceps-like, without attachment lamellae, sub-right-angle falcal arch. Closing system ~ 4–5× shorter than MI. Ligament between MI and MII rectangular, dark. MII without attachment lamella, teeth triangular, distributed in less than half of plate length. Ligament between MII and MIII absent (or not sclerotized). MIII, single, longer than left MIV, curved, with equal-sized triangular teeth; short attachment lamella situated in the centre of posterior edge of maxilla, oval, dark. Left MIV short (half the size of right MIV) with wide, rounded base, two left teeth longer than right-most ones; attachment lamella dark, semi-circular. Right MIV long, with teeth triangular, decreasing in size posteriorly; attachment lamella wide, semi-circular, dark. MV, paired, longer than wide, with a long tooth pointed ventrally, and a rounded dorsal margin (Fig. 6D). Mandibles dark with golden tips, with fine concentric stripes visible dorsally and ventrally, same size as MI; cutting plates whitish, with distinct growth rings, with three dorsal teeth (Fig. 6E).

Notopodial cirri very long, slender and, tapering (Fig. 6A–C), 2–3× longer than ventral cirri in all chaetigers. Pre-chaetal lobe inconspicuous. Post-chaetal lobe digitiform in the two or three first chaetigers, triangular with tapering tip from chaetiger 4, reducing in size from chaetiger 17, almost inconspicuous from chaetiger 28 (21) (Fig. 6A–C). Ventral cirri (Fig. 6A–C) bluntly conical, with slightly expanded bases and rounded tips from chaetigers 1–22, subconical and thinner thereafter. Branchiae pectinate (Figs 5C, 6A, 7A), starting from chaetiger 7 (7) and continuing for a limited number of segments, until chaetiger 16 (14); with 8–16 long filaments.
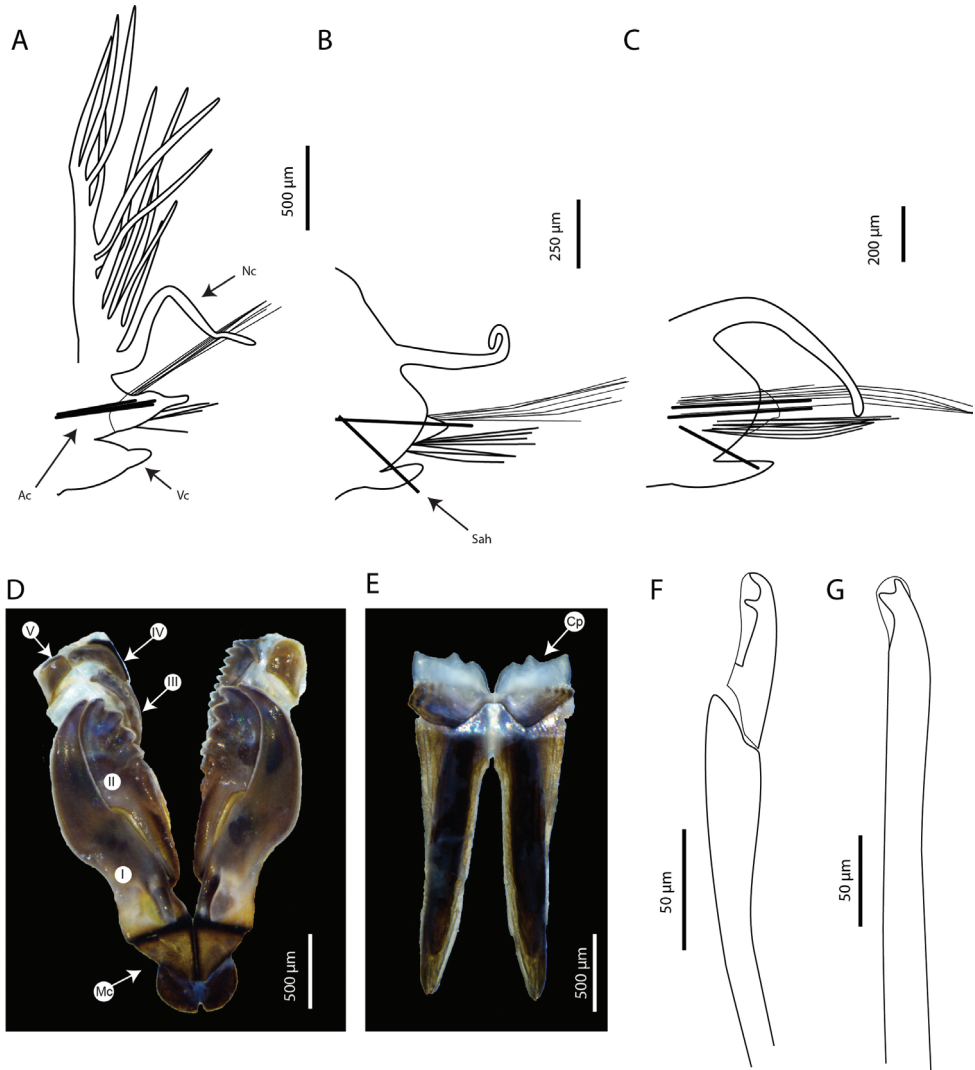
Figure 6. *Marphysa papuaensis* sp. nov. paratypes MNHN-IA-2015-1415 (**A–C, F, G**), MNHN-IA-2015-1593 (**D, E**): **A** parapodia from anterior chaetiger (chaetiger 12) **B** parapodia from mid-body (chaetiger 36) **C** parapodia from posterior chaetiger (chaetiger 74) **D** maxilla, dorsal view **E** mandibles, dorsal view **F** compound falcigers from anterior chaetiger (chaetiger 12) **G** subacicular hook from mid-body (chaetiger 36). Abbreviations: MI to MV, maxillae I to V; Ac, aciculae; Cp, cutting plate; Mc, maxillary carrier; Nc, notopodial cirri; Sah, subacicular hook; Vc, ventral cirri. **A–C** Sah and Ac are illustrated schematically to indicate position.

Aciculae black with paler blunt tips, 2–4 per parapodium along the body. Supra-acicular chaetae with limbate capillaries and pectinates; capillaries present from first chaetiger to near pygidium, numbering up to 20 in anterior chaetigers. Pectinate chaetae commencing from first few chaetigers to near end, one type identified as
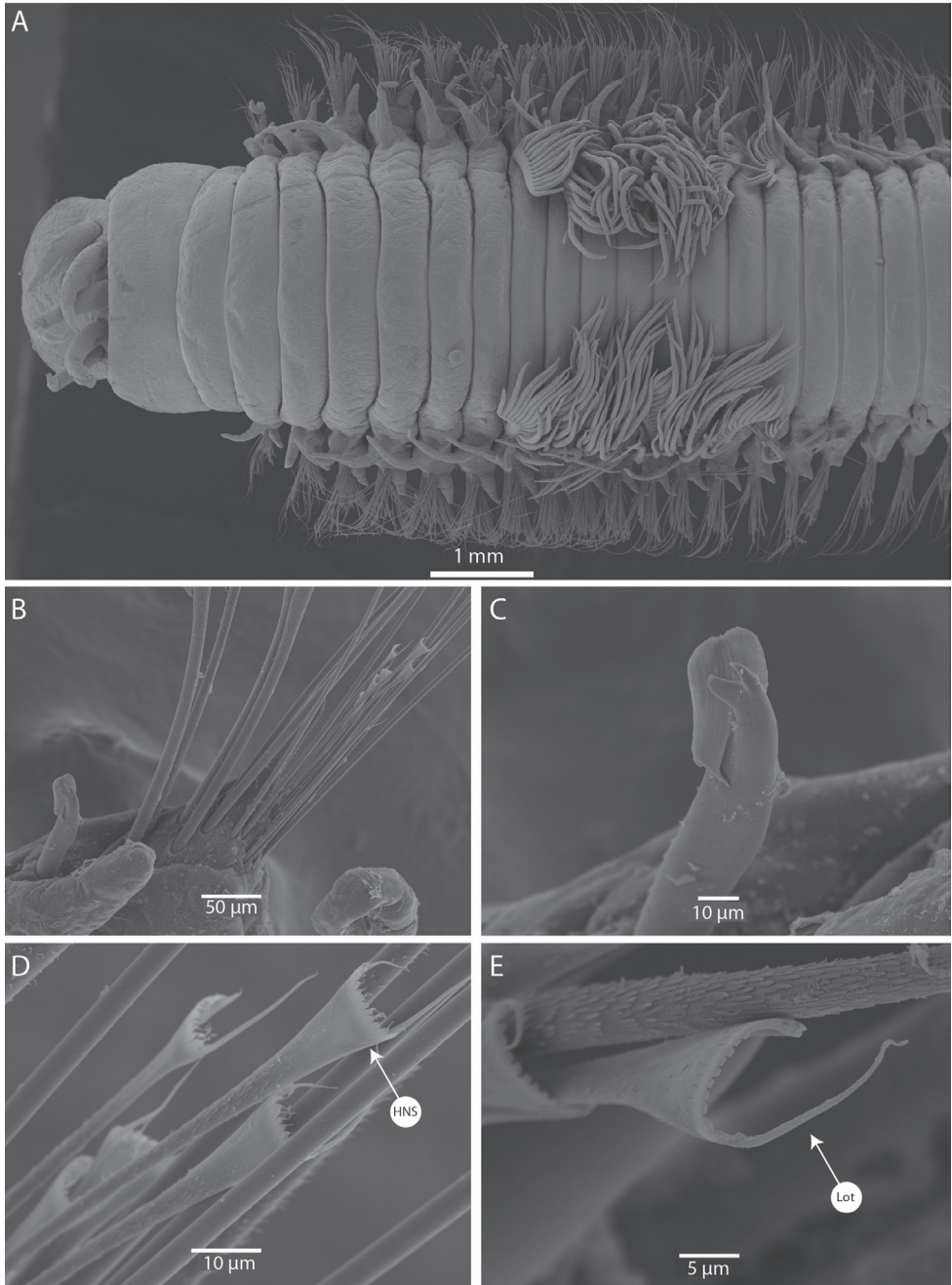
Figure 7. SEM images of *Marphysa papuaensis* sp. nov. paratypes AM W.53771 (**A**), AM W.53770 (**B–E**) **A** anterior end, dorsal view **B** parapodia, chaetiger 79 **C** subacicular hook, chaetiger 79 **D** pectinate chaetae, chaetiger 79 **E** pectinate chaetae, chaetiger 41. Abbreviations: HNS, heterodont-narrow-slender; Lot, Long outer tooth.

heterodont-narrow-slender (HNS; Fig. 7B, D, E), one outer tooth very long (Fig. 7E), having nine or ten short internal teeth, each tooth prolonged by a thin filament.

Subacicular chaetae with compound falcigers and subacicular hooks (Figs 6F, G, 7B, C). Compound falcigers bidentate, with short blade and large teeth, commencing from first chaetiger to near pygidium, with more than 50 chaetae within a parapodium in anterior part, with ~ 10 chaetae in mid-body and ~ 3–5 in last chaetigers (Fig. 6F). Subacicular hooks black with pale yellow tip, commencing from anterior chaetiger 20 (24) to end, most of the body with one hook per parapodia, but some posterior chaetigers with two, subacicular hooks bidentate (Figs 6G, 7B, C).

Pygidium round and crenulated, dorsally positioned, with two pairs of tapering pygidial cirri attached at ventral edge, dorsal pair 2 (3) × length of ventral pair (Fig. 5D).

Etymology. This species name refers to the type locality and geographical distribution of this species.

Type locality. Papua New Guinea, Solomon Sea, New Britain.

Distribution. Papua New Guinea, Solomon Sea (New Britain) and Bismarck Sea (New Ireland).

Habitat. Between 250 and 1200 m, mostly found inside sunken wood.

Remarks. Within the Central Indo-Pacific Realm, a single species with only compound falcigers present and branchiae restricted in a short region (group C1) has been described: *M. bernardi* Rullier, 1972 (type locality in New Caledonia). However, this species differs from *M. papuaensis* sp. nov. by the presence of a prostomium that is not bilobed, of antennae that are articulated and the absence of eyes. In contrast, *M. papuaensis* sp. nov. has smooth antennae, no eyes and a bilobed prostomium. The branchiae of *M. bernardi* are present from chaetiger 3, instead of chaetiger 7 for *M. papuaensis* sp. nov. and apparently *M. bernardi* has no pectinate chaetae, while *M. papuaensis* sp. nov. has pectinates commencing from first few chaetigers to near end. Finally, *M. bernardi* was collected in a bay from 7–8 m depth while *M. papuaensis* sp. nov. occurs only in deep sea, at 1200 m depth.

Marphysa zanolae sp. nov.

https://zoobank.org/EAB90680-0FDD-4B21-8FB9-DD43F378A119
Figs 8, 9

Material examined. *Holotype*: MNHN-IA-2015-1519, entire, few parapodia used for molecular analysis, South Pacific Ocean, Papua New Guinea, New Ireland, CP4260, -2.9°S, 151.1°E, depth 350–847 m, April 2014. *Paratype*: MNHN-IA-2015-1607, anterior part only, South Pacific Ocean, Papua New Guinea, New Britain, CP4266, -4.616°S, 152.25°E, depth 575–616 m, April 2014.

Description (based on holotype, with variation in parentheses for paratype). Preserved specimens 197 (85 ant. part only) chaetigers, 101 mm (36 mm) long, 4.1 mm (2.8 mm) wide at chaetiger 10, excluding parapodia. Body elongated, slightly tapering at posterior end.
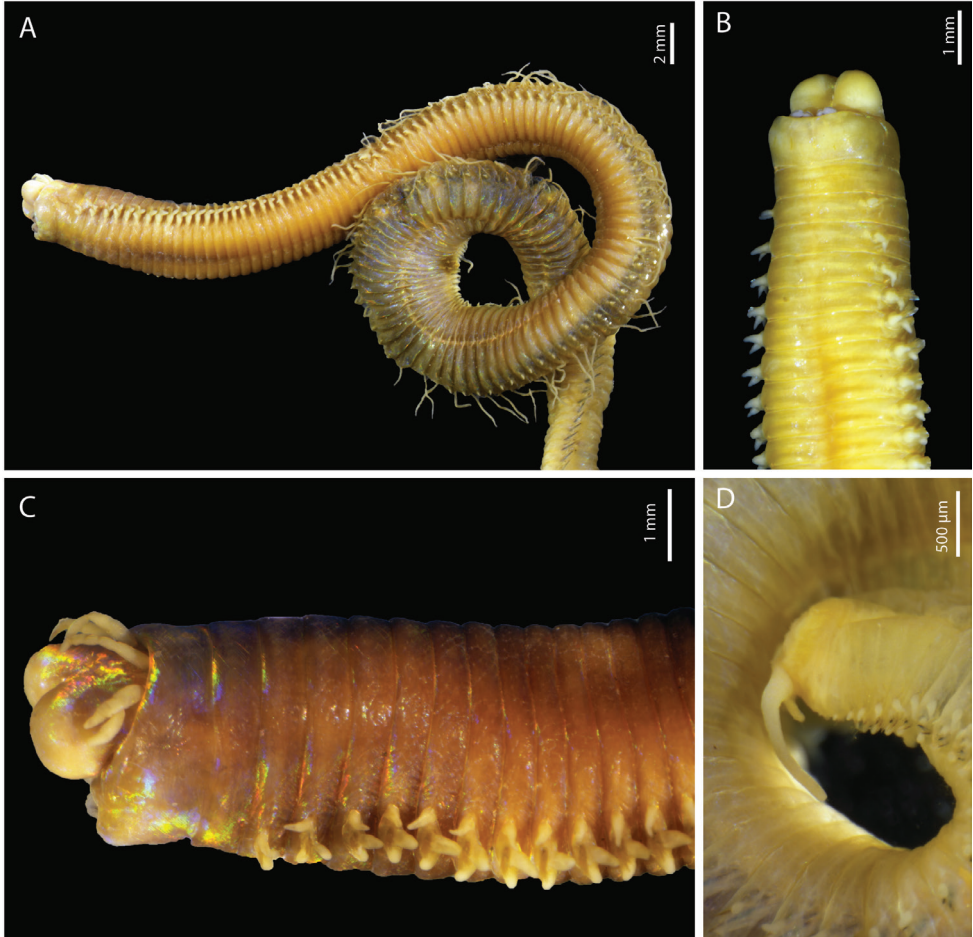
Figure 8. *Marphysa zanolae* sp. nov. holotype MNHN-IA-2015-1519 (**A, C, D**), paratype MNHN-IA-2015-1607 (**B**): **A** anterior end, lateral view **B** anterior end, ventral view **C** anterior end lateral view **D** pygidium.

Prostomium strongly bilobed with two dorsoventrally flattened buccal lips and an anterior notch between them (Fig. 8B, C). Two palps and three antennae slender and tapering, arranged in an arc on posterior margin of prostomium. Antennae more or less smooth, of equal length, shorter than prostomium (slightly longer for PNG012), slightly longer than palps (palps very short for paratype PNG12, but probably broken) (Fig. 8C). Eyes absent. First peristomial ring approximately the same size as second one dorsally (Fig. 8C).

Maxillary apparatus yellow to golden brown, partially everted in holotype and paratype. Maxillae with carriers and four paired elements and one single one, formula as follows (Fig. 9F): MF = 1+1, 4+4, 5+0, 3+6, 1+1. MI ~ 2× longer than maxillary carrier, rectangular anteriorly, triangular posteriorly, with a pair of oval

wings situated at posterolateral margins. MI forceps-like, without attachment lamellae; well-developed falcal arch. Closing system ~ 4–5× shorter than MI. MII wide, without attachment lamella, teeth triangular, recurved, and distributed in less than half of plate length. Ligament between MII and MIII absent (or not sclerotized). MIII, single, slightly shorter than right MIV, curved forming part of distal arc; with left four teeth recurved, equal-sized and triangular, two right teeth shorter and blunt, without attachment lamella. Left MIV short (half the size of right MIV) with wide, triangular base, left 2 teeth longer than right-most one; attachment lamella dark, semi-circular. Right MIV with teeth triangular, recurved, decreasing in size posteriorly; attachment lamella large, wide, best developed centrally. MV, paired, rectangular (longer than wide), with a broad cutting edge, and no clearly defined teeth (but following tradition to score as 1+1). Mandibles (Fig. 9G) yellow to golden brown, slightly shorter than MI plus carriers; cutting plates whitish, with distinct growth rings.

First two parapodia located below middle line of body wall, but gradually positioned dorsally to approximately midline in subsequent segments (Fig. 8A). Notopodial cirri with large base and slender, tapering tip from anterior to mid-body chaetigers, digitiform cirri in posterior chaetigers; same size as neuropodial cirri, but shorter than post-chaetal lobe in anterior chaetigers (Fig. 9A–C). Chaetal lobes comprising a low pre-chaetal lip and a large tongue-like post-chaetal lobe from first chaetiger to approximately chaetiger 25, almost inconspicuous thereafter. Ventral cirri bluntly conical until chaetiger 25, digitiform with bulbous base thereafter (Fig. 9A–C).

Branchiae with a long single filament (Figs 8A, 9B), commencing from chaetiger 31 (32) and continuing to mid-body (i.e., chaetiger 118 for holotype).

Aciculae black with paler blunt tips, ~ four per parapodium in anterior chaetigers, two or three per parapodium in middle chaetigers, and one or two per parapodium in posterior chaetigers. Supra-acicular chaetae with limbate capillaries and pectinates; capillaries present from first chaetiger to near pygidium, numbering up to 20 in anterior chaetigers. Pectinate chaetae commencing from first few chaetigers to near end, one type only (Fig. 9H, I), with two or three pectinate chaetae per parapodium in anterior body, up to seven from posterior chaetigers, isodont-wide-thick (IWT) having 11–20 long teeth (Fig. 9H, I).

Subacicular chaetae compound falcigers and subacicular hooks (Fig. 9D, E). Compound falcigers bidentate, with long blades and short teeth, commencing from first chaetiger to near pygidium, with more than 30 chaetae within a parapodium in anterior part, with ~ 20 chaetae in mid-body and ~ 5–7 in last chaetigers (Fig. 9D). Subacicular hooks amber to black, with much paler tip, commencing from anterior chaetiger 28 (chaetiger 30) to near end, one per parapodium in anterior and posterior parts, few chaetigers with two hooks in middle body; slightly thinner than aciculae; subacicular hooks unidentate, with blunt tip (Fig. 9E).

Pygidium round, dorsally positioned, with two pairs of tapering pygidial cirri attached at ventral edge, dorsal pair 3× length of ventral pair (Fig. 8D).

Etymology. This species is dedicated to Joana Zanol for her great contributions to the knowledge of Eunicidae and *Marphysa*, and her friendship to PH.
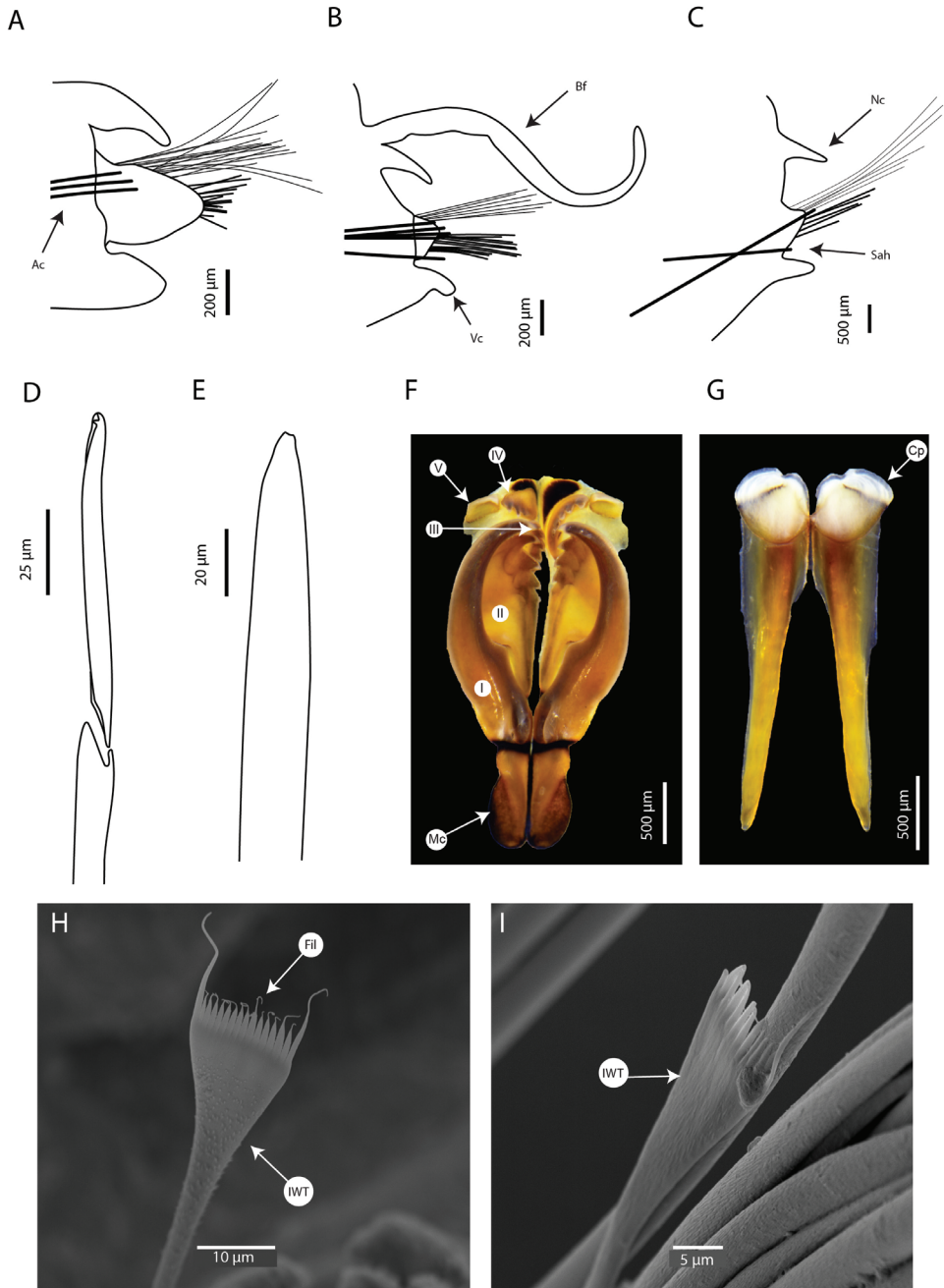
Figure 9. *Marphysa zanolae* sp. nov. holotype MNHN-IA-2015-1519 (**A–E**), paratype MNHN-IA-2015-1607 (**F,G**): **A** parapodia from anterior body (chaetiger 8) **B** parapodia from mid-body (chaetiger 31) **C** parapodia from posterior body **D** compound falcigers from anterior chaetiger (chaetiger 12) **E** subacicular hook from mid-body (chaetiger 43) **F** maxilla, dorsal view **G** mandibles, dorsal view **H** pectinate chaeta, chaetiger 48 **I** pectinate chaeta, chaetiger 33. Abbreviations: MI to MV, maxillae I to V; Ac, aciculae; Bf, branchial filament; Cp, cutting plate; Fil, filament; IWT, isodont-wide-thick; Mc, maxillary carrier; Nc, notopodial cirri; Sah, subacicular hook; Vc, ventral cirri. **A–C** Sah and Ac are illustrated schematically to indicate position.

Figure 10. Majority-rule consensus tree of *Marphysa* species from Bayesian analysis using COI. Asterisk indicates posterior probability > 80%. Text in red indicates specimens used in this study.

Type locality. Solomon Sea, Papua New Guinea, New Britain and New Ireland.

Distribution. Only known from type locality.

Habitat. Between 350 to 616 m depth, among pumice rocks, inside sunken wood.

Remarks. Within the Central Indo-Pacific Realm, only one species having only compound falcigers present and branchiae present in a long region (group C2) occurs: *M. soembaensis* Augener, 1933 (type locality in Pulau Sumba, South Indonesia). However, this species differs from *M. zanolae* sp. nov. by the presence of poorly developed branchiae with two or three branchial filaments instead of well-developed branchiae with a single long filament only for *M. zanolae* sp. nov. These branchiae start from chaetiger 40 for *M. soembaensis* and from chaetiger 31 for *M. zanolae*. Moreover, *M. soembaensis* has bidentate subacicular hooks while they are unidentate for *M. zanolae* sp. nov. Finally, *M. zanolae* sp. nov. has pectinate chaetae with very long outer teeth, which are not present in *M. soembaensis*. The blade of the compound falcigers is very short for *M. soembaensis* compared to those of *M. zanolae* sp. nov. Finally, specimens of *M. soembaensis* were sampled intertidally in a bay in Indonesia while *M. zanolae* sp. nov. occurs in deep-sea environments in Papua New Guinea.

Genetic data

COI gene was successfully sequenced and published at NCBI GenBank for two species: *M. papuaensis* sp. nov. and *M. zanolae* sp. nov. (Table 1, Fig. 10). Unfortunately, despite several attempts, sequences could not be obtained for the third species *M. banana* sp. nov. The two species *M. papuaensis* sp. nov. and *M. zanolae* sp. nov. are very different from all other species of *Marphysa* for which COI data are available and are relatively close to *M. regalis* Verrill, 1900 described from Bermuda (Fig. 10). The Pair-wise Kimura 2-parameter (K2P) between *M. papuaensis* sp. nov. and *M. zanolae* sp. nov. equal to 18.8% is relatively important and confirms the separation between these two species.

References

Abe H, Tanaka M, Taru M, Abe S, Nishigaki A (2019) Molecular evidence for the existence of five cryptic species within the Japanese species of *Marphysa* (Annelida: Eunicidae) known as "Iwamushi". Plankton & Benthos Research 14(4): 303–314. https://doi.org/10.3800/pbr.14.303

Berthold AA (1827) Latreille's Natürliche Familien des Thierreichs. Aus dem Französischen, mit Anmerkungen und Zusätzen. Verlage Landes-Industrie-Comptoirs, Weimar, 606 pp. https://doi.org/10.5962/bhl.title.11652

Britayev TA, Doignon G, Eeckhaut I (1999) Symbiotic polychaetes from Papua New Guinea associated with echinoderms, with descriptions of three new species. Cahiers de Biologie Marine 40(4): 359–374.

Carr CM, Hardy SM, Brown TM, Macdonald T, Hebert PDN (2011) A tri-oceanic perspective: DNA barcoding reveals geographic structure and cryptic diversity in Canadian polychaetes. PLoS ONE 6(7): e22232. https://doi.org/10.1371/journal.pone.0022232

Corbari L, Frutos I, Sorbe JC (2019) *Dorotea* gen. nov., a new bathyal genus (Amphipoda, Eusiridae) from the Solomon Sea (Papua New Guinea). Zootaxa 4568(1): 69–80. https://doi.org/10.11646/zootaxa.4568.1.4

Dahlgren TG (1996) Two species of *Dysponetus* (Polychaeta: Chrysopetalidae) from Italy and Papua New Guinea. Proceedings of the Biological Society of Washington 109(3): 575–585.

Darriba D, Taboada GL, Doallo R, Posada D (2012) jModelTest 2: More models, new heuristics and parallel computing. Nature Methods 9(8): 772–772. https://doi.org/10.1038/nmeth.2109

Elgetany AH, El-Ghobashy AE, Ghoneim AM, Struck TH (2018) Description of a new species of the genus *Marphysa* (Eunicidae), *Marphysa aegypti* sp. n., based on molecular and morphological evidence. Invertebrate Zoology 15(1): 71–84. https://doi.org/10.15298/invertzool.15.1.05

Fauchald K (1970) Polychaetous annelids of the families Eunicidae, Lumbrineridae, Iphitimidae, Arabellidae, Lysaretidae and Dorvilleidae from western Mexico. Allan Hancock Monograph in Marine Biology 5: 1–335.

Fauchald K (1992) A review of the genus *Eunice* (Polychaeta: Eunicidae) based upon type material. Smithsonian Contributions to Zoology 523: 1–422. https://doi.org/10.5479/si.00810282.523

Glasby CJ, Hutchings PA (2010) A new species of *Marphysa* Quatrefages, 1865 (Polychaeta: Eunicida: Eunicidae) from northern Australia and a review of similar taxa from the Indo-West Pacific, including the genus *Nauphanta* Kinberg, 1865. Zootaxa 2352(1): 29–45. https://doi.org/10.11646/zootaxa.2352.1.2

Glasby CJ, Mandario MAE, Burghardt I, Kupriyanova E, Gunton LM, Hutchings PA (2019) A new species of the *sanguinea*-group Quatrefages, 1866 (Annelida: Eunicidae: *Marphysa*) from the Philippines. Zootaxa 4674(2): 264–282. https://doi.org/10.11646/zootaxa.4674.2.7

Hoagland RA (1920) Polychaetous annelids collected by the United States fisheries steamer Albatross during the Philippine expedition of 1907–1909. Bulletin – United States National Museum 100(1): 603–635.

Hutchings P, Karageorgopoulos P (2003) Designation of a neotype of *Marphysa sanguinea* (Montagu, 1813) and a description of a new species of *Marphysa* from eastern Australia. Hydrobiologia 496(1–3): 87–94. https://doi.org/10.1023/A:1026124310552

Hutchings PA, Kupriyanova E (2018) Cosmopolitan polychaetes – fact or fiction? Personal and historical perspectives. Invertebrate Systematics 32(1): 1–9. https://doi.org/10.1071/IS17035

Hutchings P, Lavesque N, Priscilla L, Malathi E, Daffe G, Glasby CJ (2020) A new species of *Marphysa* (Annelida: Eunicida: Eunicidae) from India, with notes on previously described or reported species from the region. Zootaxa 4852(3): 285–308. https://doi.org/10.11646/zootaxa.4852.3.2

Idris I, Hutchings P, Arshad A (2014) Description of a new species of *Marphysa* Quatrefages, 1865 (Polychaeta: Eunicidae) from the west coast of Peninsular Malaysia and comparisons with species from *Marphysa* Group A from the Indo-West Pacific and Indian Ocean. Memoirs of the Museum of Victoria 71: 109–112. https://doi.org/10.24199/j.mmv.2014.71.11

Kara J, Molina-Acevedo I, Zanol J, Simon C, Idris I (2020) Morphological and molecular systematic review of *Marphysa* Quatrefages, 1865 (Annelida: Eunicidae) species from South Africa. PeerJ 8: e10076. https://doi.org/10.7717/peerj.10076

Lavesque N, Daffe G, Bonifácio P, Hutchings PA (2017) A new species of the *Marphysa sanguinea* complex from French waters (Bay of Biscay, NE Atlantic) (Annelida, Eunicidae). ZooKeys 716: 1–17. https://doi.org/10.3897/zookeys.716.14070

Lavesque N, Daffe G, Grall J, Zanol J, Gouillieux B, Hutchings PA (2019) Guess who? On the importance of using appropriate name: Case study of *Marphysa sanguinea* (Montagu, 1803). ZooKeys 859: 1–15. https://doi.org/10.3897/zookeys.859.34117

Lavesque N, Hutchings P, Abe H, Daffe G, Gunton LM, Glasby CJ (2020) Confirmation of the exotic status of *Marphysa victori* Lavesque, Daffe, Bonifácio & Hutchings, 2017 (Annelida) in French waters and synonymy of *Marphysa bulla* Liu, Hutchings & Kupriyanova, 2018. Aquatic Invasions 15(3): 355–366. https://doi.org/10.3391/ai.2020.15.3.01

Liu Y, Hutchings PA, Sun S (2017) Three new species of *Marphysa* Quatrefages, 1865 (Polychaeta: Eunicida: Eunicidae) from the south coast of China and redescription of *Marphysa sinensis* Monro, 1934. Zootaxa 4263(2): 228–250. https://doi.org/10.11646/zootaxa.4263.2.2

Liu Y, Hutchings PA, Kupriyanova E (2018) Two new species of *Marphysa* Quatrefages, 1865 (Polychaeta: Eunicida: Eunicidae) from northern coast of China and redescription for *Marphysa orientalis* Treadwell, 1936. Zootaxa 4377(2): 191–215. https://doi.org/10.11646/zootaxa.4377.2.3

Martin D, Gil J, Zanol J, Meca MA, Perez-Portela R (2020) Digging the diversity of Iberian bait worms *Marphysa* (Annelida, Eunicidae). PLoS ONE 15(1): e0226749. https://doi.org/10.1371/journal.pone.0226749

Molina-Acevedo IC, Carrera-Parra LF (2015) Reinstatement of three species of the *Marphysa sanguinea* complex (Polychaeta: Eunicidae) from the Grand Caribbean Region. Zootaxa 3925(1): 37–55. https://doi.org/10.11646/zootaxa.3925.1.3

Molina-Acevedo IC, Carrera-Parra LF (2017) Revision of *Marphysa* de Quatrefages, 1865 and some species of *Nicidion* Kinberg, 1865 with the erection of a new genus (Polychaeta: Eunicidae) from the Grand Caribbean. Zootaxa 4241(1): 1–62. https://doi.org/10.11646/zootaxa.4241.1.1

Molina-Acevedo IC, Idris I (2021) Unravelling the convoluted nomenclature of *Marphysa simplex* (Annelida, Eunicidae) with the proposal of a new name and the re-description of species. Zoosystematics and Evolution 97(1): 121–139. https://doi.org/10.3897/zse.97.59559

Montagu G (1813) Descriptions of several new or rare animals, principally marine, found on the south coast of Devonshire. Transactions of the Linnean Society of London 11(1): 18–21. https://doi.org/10.1111/j.1096-3642.1813.tb00035.x

Pante E, Corbari L, Thubaut J, Chan TY, Mana R, Boisselier MC, Bouchet P, Samadi S (2012) Exploration of the deep-sea fauna of Papua New Guinea. Oceanography 25(3): 214–225. https://doi.org/10.5670/oceanog.2012.65

Paxton H (2000) Family Eunicidae. In: Beesley PL, Ross GJB, Glasby CJ (Eds) Polychaetes & Allies. The Southern Synthesis. Fauna of Australia. Vol 4A. Polychaeta, Myzostomida, Pogonophora, Echiura, Sipuncula. CSIRO Publishing, Melbourne, 94–96.

Quatrefages A (1866) Histoire naturelle des Annelés marins et d'eau douce. Annélides et Géphyriens. Tome second. Librairie Encyclopédique de Rôret, Paris, 337–794. https://doi.org/10.5962/bhl.title.122818

Rambaut A (2007) FigTree. http://tree.bio.ed.ac.uk/software/figtree [accessed 20 July 2022]

Read G, Fauchald K (2022) *Marphysa* Quatrefages, 1866. In: Read G, Fauchald K (Eds) World Polychaeta database. www.marinespecies.org/aphia.php?p=taxdetails&id=129281 [accessed 01 July 2022]

Reuscher M, Fiege D, Wehe T (2011) Terebellomorph polychaetes from hydrothermal vents and cold seeps with the description of two new species of Terebellidae (Annelida: Polychaeta) representing the first records of the family from deep-sea vents. Journal of the Marine Biological Association of the United Kingdom 92(5): 997–1012. https://doi.org/10.1017/S0025315411000658

Ronquist F, Huelsenbeck JP (2003) MRBAYES 3: Bayesian phylogenetic inference under mixed models. Bioinformatics 19(12): 1572–1574. https://doi.org/10.1093/bioinformatics/btg180

Rouse G (1996) New *Fabriciola* and *Manayunkia* species (Fabriciinae: Sabellidae: Polychaeta) from Papua New Guinea. Journal of Natural History 30(12): 1761–1778. https://doi.org/10.1080/00222939600771031

Rouse G (2012) A new species of *Perkinsiana* (Sabellidae, Polychaeta) from Papua New Guinea; with a description of larval development. Ophelia 45(2): 101–114. https://doi.org/10.1080/00785326.1996.10432465

Rullier F (1972) Annélides polychètes de Nouvelle-Calédonie recueillies par Y. Plessis et B. Salvat. Expédition Française sur les Récifs Coralliens de la Nouvelle-Calédonie 6: 6–169.

Samadi S, Quéméré E, Lorion J, Tillier A, von Cosel R, Lopez P, Cruaud CA, Couloux A, Boisselier-Dubayle M (2007) Molecular phylogeny in mytilids supports the wooden steps to deep-sea vents hypothesis. Comptes Rendus Biologies 330(5): 446–456. https://doi.org/10.1016/j.crvi.2007.04.001

Spalding MD, Fox HE, Allen GR, Davidson N, Ferdaña ZA, Finlayson M, Halpern BS, Jorge MA, Lombana AL, Lourie SA, Martin KD, McManus E, Molnar J, Recchia CA, Robertson J (2007) Marine ecoregions of the world: A bioregionalization of coastal and shelf areas. Bioscience 57(7): 573–583. https://doi.org/10.1641/B570707

Treadwell AL (1936) Polychaetous annelids from Amoy, China. Proceedings of the United States National Museum 83(2984): 261–279. https://doi.org/10.5479/si.00963801.83-2984.261

Verrill AE (1900) Additions to the Turbellaria, Nemertina, and Annelida of the Bermudas, with revisions of some New England genera and species. Transactions of the Connecticut Academy of Arts and Sciences 10(2): 595–671. https://doi.org/10.5962/bhl.part.7035

Wang Z, Zhang Y, Qiu JW (2018) A New Species in the *Marphysa sanguinea* Complex (Annelida, Eunicidae) from Hong Kong. Zoological Studies 57(48): 1–13.

Watson C (2001) New genus and species of Chrysopetalidae (Polychaeta) from hydrothermal vents (south-western Pacific). The Beagle. Records of the Museums and Art Galleries of the Northern Territory 17: 57–66. https://doi.org/10.5962/p.286291

Zanol J, Halanych KM, Struck TH, Fauchald K (2010) Phylogeny of the bristle worm family Eunicidae (Eunicida, Annelida) and the phylogenetic utility of noncongruent 16S, COI and 18S in combined analyses. Molecular Phylogenetics and Evolution 55(2): 660–676. https://doi.org/10.1016/j.ympev.2009.12.024

Zanol J, da Silva T dos SC, Hutchings P (2016) Integrative taxonomy of *Marphysa* (Eunicidae, Polychaeta, Annelida) species of the *S*anguinea-group from Australia. Invertebrate Biology 135(4): 328–344. https://doi.org/10.1111/ivb.12146

RESEARCH ARTICLE

Geographic differentiation in male calling song of *Isophya modestior* (Orthoptera, Tettigoniidae, Phaneropterinae)

Slobodan Ivković[1], Dragan Chobanov[2], Laslo Horvat[3],
Ionuț Ștefan Iorgu[4], Axel Hochkirch[1]

1 *Trier University, Department of Biogeography, Universitätsring 15, 54296 Trier, Germany* **2** *Institute of Biodiversity and Ecosystem Research, Bulgarian Academy of Sciences, Tsar Osvoboditel Blvd. 1, 1000 Sofia, Bulgaria* **3** *Ruwerer Str. 39, 54292 Trier, Germany* **4** *"Grigore Antipa" National Museum of Natural History, Kiseleff Blvd. 1, 011341 Bucharest, Romania*

Corresponding author: Slobodan Ivković (s6slivko@uni-trier.de)

Citation: Ivković S, Chobanov D, Horvat L, Iorgu IŞ, Hochkirch A (2022) Geographic differentiation in male calling song of *Isophya modestior* (Orthoptera, Tettigoniidae, Phaneropterinae). ZooKeys 1122: 107–123. https://doi.org/10.3897/zookeys.1122.85721

Abstract

We studied the songs and morphology of the stridulatory file of *Isophya modestior* across its complete geographic range, in order to test our hypothesis that the male calling song of the species shows strong differentiation between the northern (Pannonian) and southern (Balkan) parts of its distribution range, reflecting its disjunct distribution. Our analyses confirm this hypothesis, separating analyzed specimens of *I. modestior* into two main groups - one present in the central part of the Balkan Peninsula (representing *Isophya modestior sensu stricto*), with the second group occurring in the Pannonian Basin, Dinarides, Slovenia and NE Italy. The most reliable difference between the groups is the duration of the main syllable, the number of stridulatory teeth and number of pulses in the main syllable, where all values are higher in specimens from the Balkan Peninsula. Additional analyses showed that within the second group, there are differences in analyzed characters between specimens from the Pannonian Basin and specimens from the Dinaric area, the latter ones having intermediate song characteristics, closer to the group from the Balkan Peninsula. Our study shows that detailed bioacoustic analyses can help to unravel patterns of intraspecific differentiation and thus provide a useful tool for taxonomic studies.

Introduction

Acoustic signals are a major channel for many animal species in order to provide various information (Bradbury and Vehrencamp 2011). Such signals can contain detailed information about the individual's identity, the position of the singing animal, body size, age, or physiological condition. Acoustic communication has been studied in many animal groups, such as fishes (Tricas and Boyle 2014), frogs (Xie et al. 2018; Filer et al. 2021), birds (Ng and Rheindt 2016), mammals (Bernstein et al. 2016) and many arthropods (Gogala and Popov 1997; Sweger and Uetz 2016). In crickets and katydids, acoustic communication is widespread and has, therefore, been studied for many decades (Faber 1928; Jacobs 1953). Fossils of Orthoptera possessing stridulatory organs exist from the Triassic and Jurassic periods (Béthoux and Nel 2002; Gorochov and Rasnitsyn 2002; Senter 2008), placing them among the first organisms with fossilized sound-producing structures.

Bioacoustic communication is one of the main characteristics of mating systems among Orthoptera (Hall and Robinson 2021). In general, male orthopterans produce a calling song and, in some groups, females respond acoustically to the male (Heller and von Helversen 1986; Heller et al. 2018). In the majority of the male Tettigoniidae (bush-crickets), the acoustic signal is produced with the stridulatory organ, which is placed at the base of the tegmina, where a toughened edge (*plectrum*) of the right tegmina is scraped against a file of teeth (*pars stridens*) on the underside of the left tegmina (Ragge and Reynolds 1998). The calling songs and the morphology of the stridulatory files are known to be reliable traits for the identification of a cryptic species that may otherwise be very difficult to identify due to high morphological similarity (Heller et al. 2004; Orci et al. 2005).

Zhantiev and Dubrovin (1977) published the first study on the stridulatory morphologies and song patterns in the genus *Isophya* Brunner von Wattenwyl, 1878, establishing that both characters are strictly species-specific within the genus and effective in discriminating cryptic species. These results were confirmed by Heller (1988) and Heller et al. (2004), resulting in the description of various new cryptic taxa within the genus *Isophya* (Orci et al. 2010; Iorgu 2012; Iorgu et al. 2017; Sevgili 2020) and resolving some identification problems in widely distributed species (Heller 1988).

Isophya modestior Brunner von Wattenwyl, 1882 is an interesting model species to study intraspecific variation in song and morphology of the stridulatory file across its range, as it has a disjunct distribution and shows some substantial morphological variability (Heller 1988; Heller 1990; Ingrisch 1991; Heller et al. 2004; Ingrisch and Pavićević 2010; Ingrisch and Pavićević 2012; Chobanov et al. 2013; Brizio et al. 2020). The body color of the species is green with white side keels on the pronotum and the reddish band on the upper part (Fig. 1). The male fore wing is green with dark spots and they are usually as long as the pronotum. Cerci are strongly curved in their distal third, while ovipositor is slightly curved. *I. modestior* usually inhabits bushes on the forest edges and clearings, but also can be found on mesic and semi-dry grasslands. The species is widespread in Europe, occurring from eastern Austria and northern
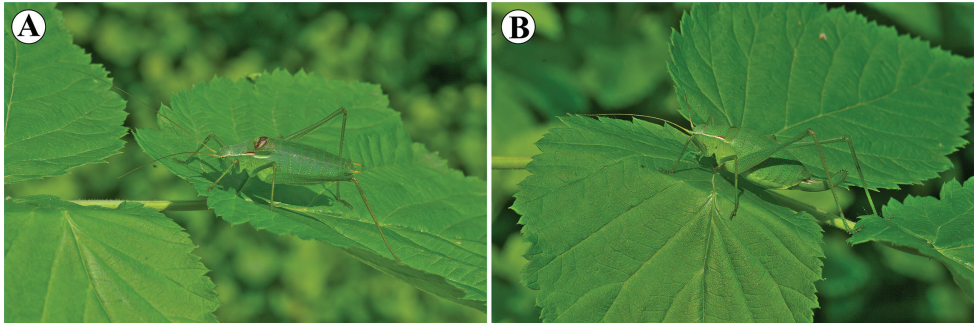
Figure 1. Habitus of *Isophya modestior* **A** male (Serbia: Beočin, 19 V 2018) **B** female (Serbia: Beočin, 19 V 2018).

Italy through to Bulgaria, but the distribution range is separated by a gap into two parts. The southern part of its distribution is in the NW Balkans (SW Romania, NW Bulgaria, N North Macedonia, inland part of Montenegro, Bosnia and Herzegovina, Kosovo, N Albania and Serbia), while the northern part of the range covers scattered populations in Croatia, Hungary, Slovakia, Austria, Slovenia and NE Italy (Chobanov et al. 2013; Hochkirch et al. 2016; Krištín et al. 2020) (Fig. 2).

We hypothesized that the male calling song of *I. modestior* shows strong differentiation between the northern (Pannonian) and southern (Balkan) parts of its range, reflecting its disjunct distribution. Therefore, we studied songs and the morphology of the stridulatory file of *I. modestior* across its complete range, complemented by data available in the literature. We analyzed the bioacoustic and morphological data for intraspecific differentiation.

Material and methods

Sample collection

Adults of *Isophya modestior* were collected in natural habitats throughout their range (Fig. 2) and brought to the laboratory, where their songs were recorded. In some instances, specimens were collected as nymphs, matured in a laboratory and recorded several days after maturation. Besides our own data, we used all published data on the song of the species (Heller 1988; Ingrisch 1991; Fontana 1998; Fontana et al. 2002; Nagy et al. 2003; Heller et al. 2004; Orci et al. 2005; Ingrisch and Pavićević 2010; Ingrisch and Pavićević 2012; Iorgu and Iorgu 2012; Chobanov et al. 2013; Brizio et al. 2020) and recordings deposited at Orthoptera Species File (Cigliano et al. 2021).

For our own sound recordings, we used Roland R-05, Edirol R-09HR and ZOOM H2 digital audio recorders. The majority of recordings were made at night, when the males actively sing. Sound analyses and oscillograms were made with Adobe Audition CC 2015 and Audacity. Parts of the stridulatory files were studied with

Figure 2. Distribution map of *Isophya modestior* (dotted line from Hochkirch et al. 2016) showing the localities from where songs were analyzed (for detailed locality data see Suppl. material 1); white symbol with black dot literature data; white symbol new, unpublished data. Groups are defined on the basis of the differentiation in the analysed characters (male calling song and morphology of the stridulatory file).

a scanning electron microscope (JEOL JSM 6460 LV) at the UCEM-NS (University Center for Electron Microscopy, Novi Sad), while other material was studied under a stereomicroscope.

Bioacoustic terminology

In this study, we follow the terminology by Heller et al. (2004) and Ragge and Reynolds (1998):

- Calling song: spontaneous song produced by an isolated male.
- Main syllable duration: the sound produced by one complete up (opening) and down (closing) stroke of the tegmina.
- Pulse: a simple, undivided, transient train of sound waves (here: the highly damped sound impulse arising as the impact of one tooth of the stridulatory file).
- After-click: pulse produced with considerable delay after the main pulse group.

Since most of our recordings were more than one hour long, we analyzed 5–10 minutes of each recording after which characteristics in 10 syllables per specimen were

chosen as an unbiased random sample. Detailed data on song recordings presented in this paper are provided in the Suppl. material 1.

Two published songs were excluded from this study:

1. Gomboc and Šegula (2014): the oscillogram does not match *I. modestior*;
2. Heller et al. (2004): inaccurate locality (either 20 km southwest of Ptuj or Kocara (Kozara?) national park (northern Bosnia).

In total, calling songs of 64 specimens from the complete distribution range were analyzed (Suppl. material 1, Fig. 2). For our study, we focused on the following characters: main syllable duration, number of pulses in main syllable and number of stridulatory teeth. To visualize the relationship between analyzed characters and populations, we ran a PCA (Principal Component Analysis) using the missMDA package in R (Version 4.1.2; R Core Team 2021). Based upon the results of preliminary studies, we assigned each individual to two groups (see results) and analyzed the three main characters for significant differences among those groups using AN-COVAs with temperature as covariate. To adjust the data to the model assumptions, we transformed the data using Box-Cox transformation using the MASS package (Venables and Ripley 2002). To test for song similarity in a multivariate context, we used Fisher's discriminant analysis (FDA) calculated in the mda package for R (Hastie and Tibshirani 2020). Due to a high linear correlation between the number of stridulatory teeth and pulses ($R^2 = 0.72$), we ignored the number of stridulatory teeth and deleted all individuals with missing data in one of the song traits.

Results

The calling song was relatively similar among populations and consisted of a train of single diminuending syllables, usually repeated in short sequences composed of two, rarely more than 13 syllables (Fig. 3). After-clicks were present in some specimens, varying from one to two, rarely three after-clicks (Fig. 3: A2, A3, B3, C2, C3, D3, E3, F3, G3 and H2).

The two groups (Balkan vs. Pannonian) differed mainly in:

(i) the duration of the main syllable;
(ii) the number of teeth on a stridulatory file in left tegmina;
(iii) the number of pulses in the main syllable (Fig. 4I).

Individuals belonging to Group A were found in Bulgaria, eastern and central Serbia. Individuals belonging to Group B were found in the Pannonian Basin (Pannonian Serbia, Romania, Hungary, Croatia, Austria and Slovakia,), Italy, Montenegro and western Serbia (Dinarides) (Fig. 2). The song of the specimen from Slovenia, which showed characters of both groups, was omitted from the statistical analyses presented in Fig. 4, but was included in PCA analyses (Fig. 7) in order to illustrate its position in a multidimensional context.
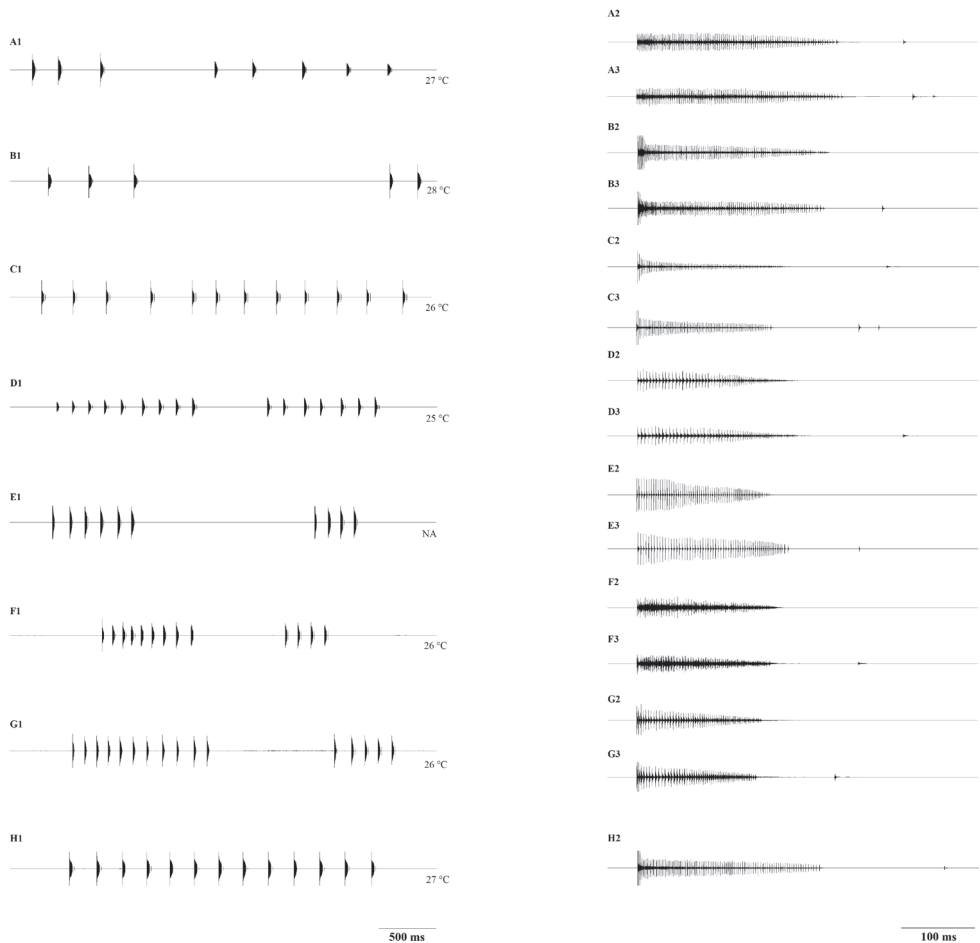
Figure 3. Oscillograms of the male calling song in *Isophya modestior* across the range. Two groups (Group A and Group B) and two more subgroups (Subgroup B1 and Subgroup B2) can be separated on the basis of the calling song. Group A includes oscillograms **A** Lalinac (eastern Serbia, close to type locality) **B** Pinosava (central Serbia); Subgroup B1 includes oscillograms **C** Beočin (Pannonian Serbia) **D** Gudurica (Pannonian Serbia) **E** Carasova (Romania) **F** Mecsek (Hungary) **G** Loipersbach (Austria); Subgroup B2 includes oscillograms **H** Đerekare (Dinaric Alps, Serbia).

In Group A, the main syllable consisted on average of 96.57 ± 2.86 pulses lasting for 338.6 ± 14.06 ms, which corresponds also with another character, the higher number (221 ± 5.61) of stridulatory teeth on a stridulatory file (Figs 5A, 5B) compared to Group B with 164.38 ± 7.02 teeth (Fig. 5C–F). The main syllable in Group B consisted of 72.38 ± 2.80 pulses and lasted 195.01 ± 5.35 ms. The groups differed significantly in syllable length (ANCOVA, $\lambda = -0.4$, $F_{1,49} = 117.3$, $P < 0.001$). There was a significant negative correlation between temperature and syllable length (ANCOVA, $\lambda = -0.4$, $F_{1,54} = 10.66$, $P = 0.002$). Both groups responded to temperature in a similar manner (ANCOVA, $\lambda = -0.4$, $F_{1,54} = 0.03$, $P = 0.85$), but were clearly separated by their syllable duration (Fig. 6).
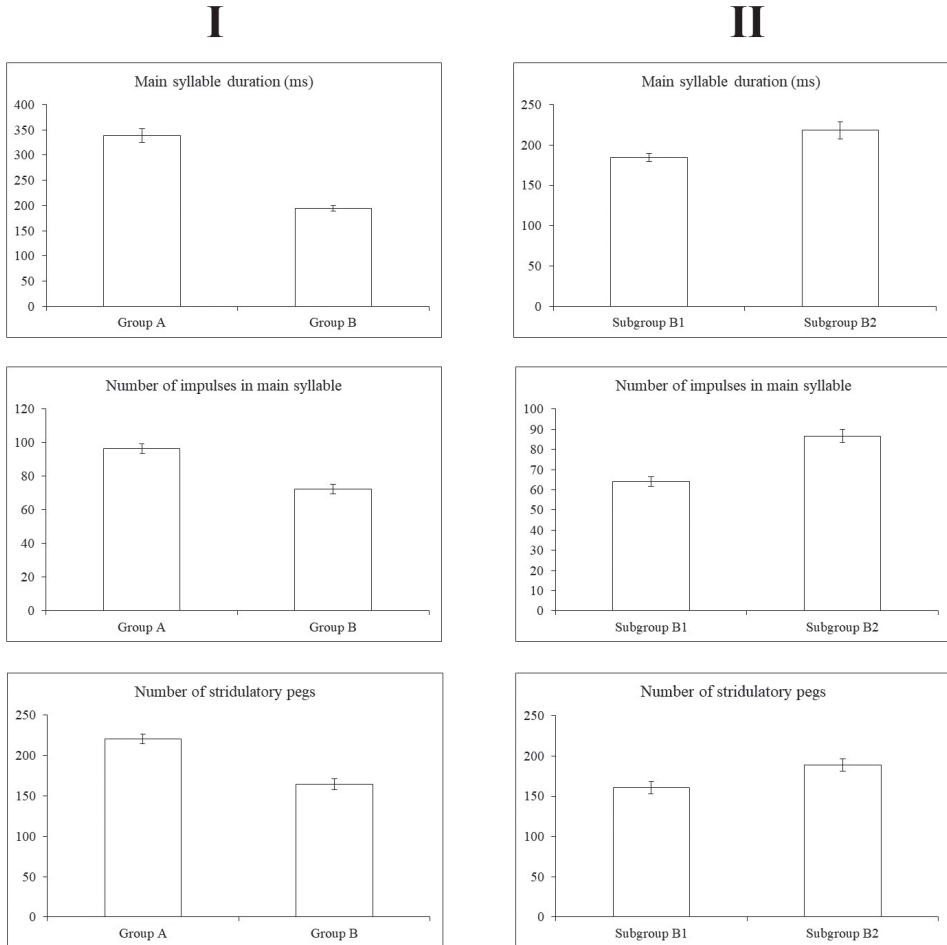
Figure 4. Variability in analyzed characters between the **A** and **B** groups (I) and B1 and B2 subgroups (II).

Additional analyses within Group B showed that specimens could be subdivided into two subgroups (Fig. 4II): B1–Pannonian Basin (northern Serbia, Romania, Hungary, Croatia and Austria) and NE Italy; B2–Montenegro and western Serbia (Dinarides). The main syllable in Subgroup B1 consisted of 64.11 ± 2.52 pulses lasting for 184.42 ± 5.18 ms, while in Subgroup B2 the main syllable consisted of 86.67 ± 3.19 pulses lasting for 218.46 ± 10.60 ms. Furthermore, the number of stridulatory teeth (Figs 5C, 5D) was lower in Subgroup B1 (160.55 ± 7.71) than in Subgroup B2 (188.67 ± 7.86) (Figs 5E, 5F).

The principal component analysis (PCA) illustrates a positive correlation of the number of stridulatory teeth, and number of pulses in the main syllable and syllable duration, all of which have strong loadings on the first axis (Fig. 7). While high numbers in all these characters specify group A, group B shows lower values. These analyses show that specimens with main syllable durations ≤ 250 ms, number of pulses ≤ 87
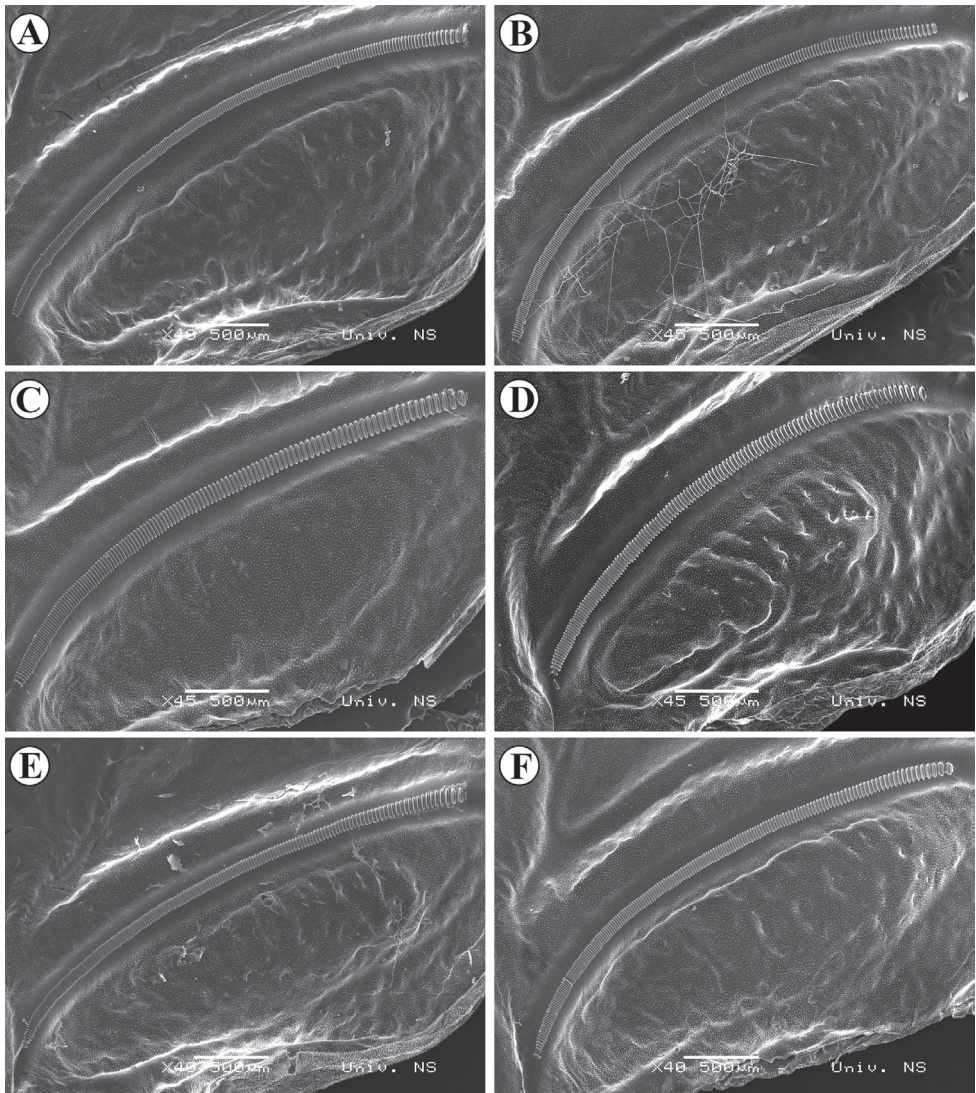
Figure 5. SEM photos of stridulatory files of different groups: Group A **A** Bancarevo (eastern Serbia, type locality) **B** Kladovo (north-eastern Serbia); Subgroup B1 **C** Mesić (Pannonian Serbia) **D** Deronje (Pannonian Serbia); Subgroup B2 **E** Durmitor, Pirlitor (Montenegro / not included in analyzes) **F** Ovčar-Kablar Gorge (western Serbia / not included in analyzes).

and number of stridulatory teeth ≤ 200 belong to group B, while specimens in group A have higher values. Dinaric specimens (subgroup B2) were placed at the upper edge of characters in group B, close to the group A, with the main syllable duration within the range 179–314.7 ms, number of pulses 66.2–94.5 and number of stridulatory teeth 178–204.

The FDA showed that it is possible to discriminate between all three groups in a multivariate context (Fig. 8), with 83.7% of the predicted class memberships being
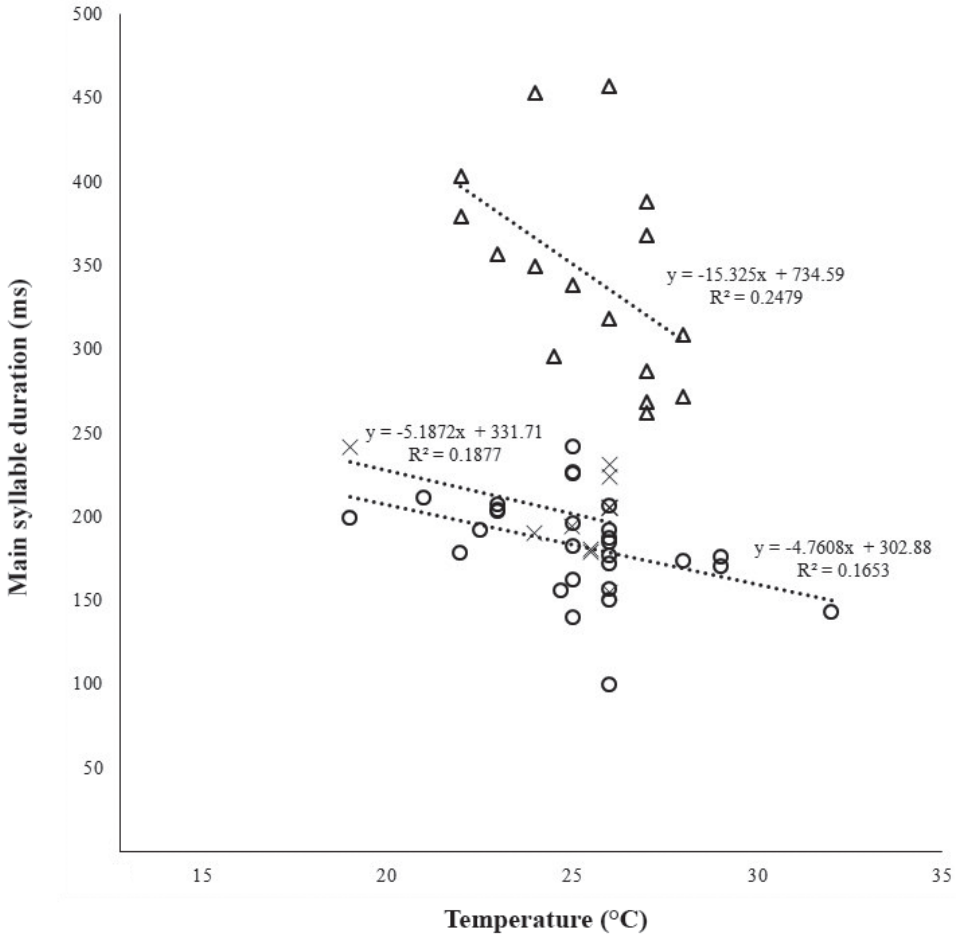
Figure 6. Two-dimensional scatter plot showing the temperature dependence of the main syllable duration between two groups (triangle Group A; circle Group B1; X Group B2).

correct. Within group B, 96.8% of all specimens were assigned to the correct class, while within group A, 83.3% were correctly assigned. Assignments to the subgroups of group B were less accurate, with 88.9% correctly assigned to group B1 and 76.9% to group B2.

Discussion

Our analyses confirm the substantial geographic variation of song characteristics in *Isophya modestior*, separating all samples into two main groups. The first group (A) is distributed on the Balkan Peninsula and represents *Isophya modestior sensu stricto*, while the second group (B) occurs in the Pannonian Basin, Dinarides and NE Italy. The most reliable difference between the groups is the duration of the
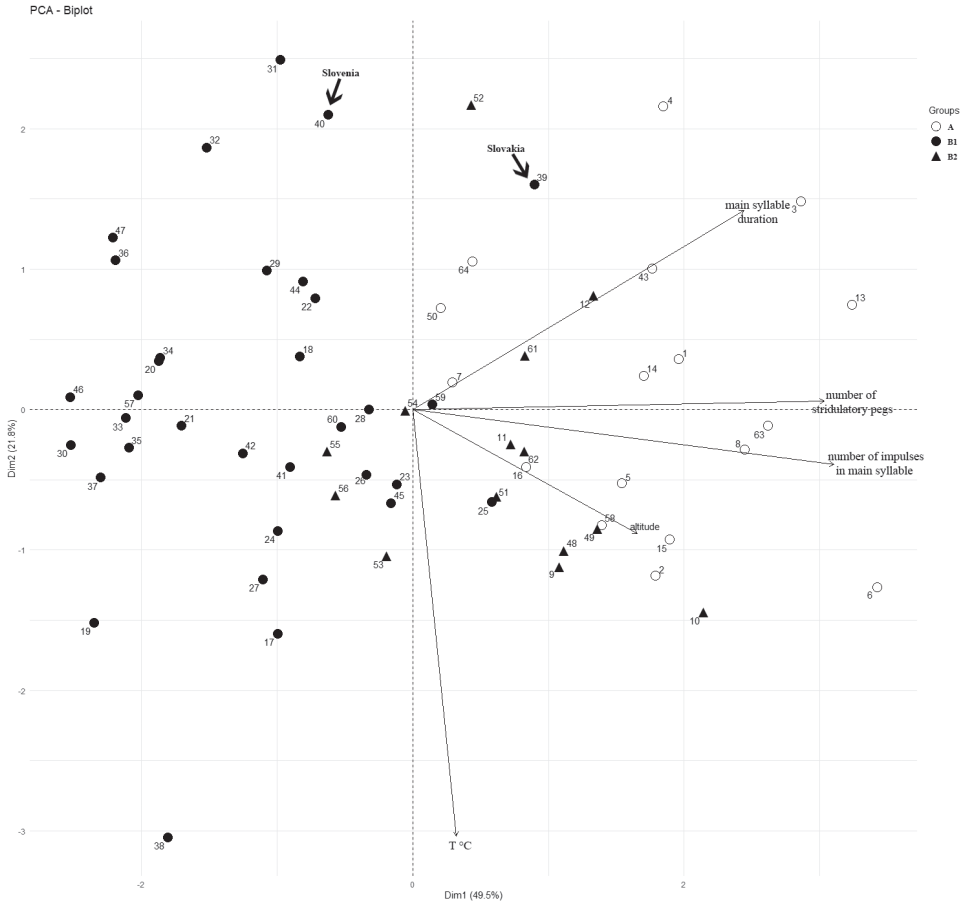
Figure 7. The Principal component analysis (PCA) showing the relationship between analyzed characters and populations (arrow indicates specimens from Slovenia and Slovakia).

main syllable, with group A showing a longer duration, but also a higher number of stridulatory teeth and higher number of pulses in the main syllable than group B. The song of the specimen from Slovenia showed characters of both groups, but the principal component analysis resolved its position in group B, which was presumed based on its locality. Altogether, the two groups showed a clear geographic pattern. The only exception is the specimen from Slovakia (39), which is closer to group A in the PCA plot, while geographically it should belong to group B. This individual had indeed a long main syllable (356 ± 17.05 ms), which is characteristic for group A. However, regarding the number of pulses in the main syllable (86.7 ± 2.58), the specimen fits better in group B. As this specimen was recorded very late in the season (28 July 2016), this might explain the longer duration of the main syllable, since temperature and age are known to have a strong impact on song duration in *Isophya* (Chobanov et al. 2013).
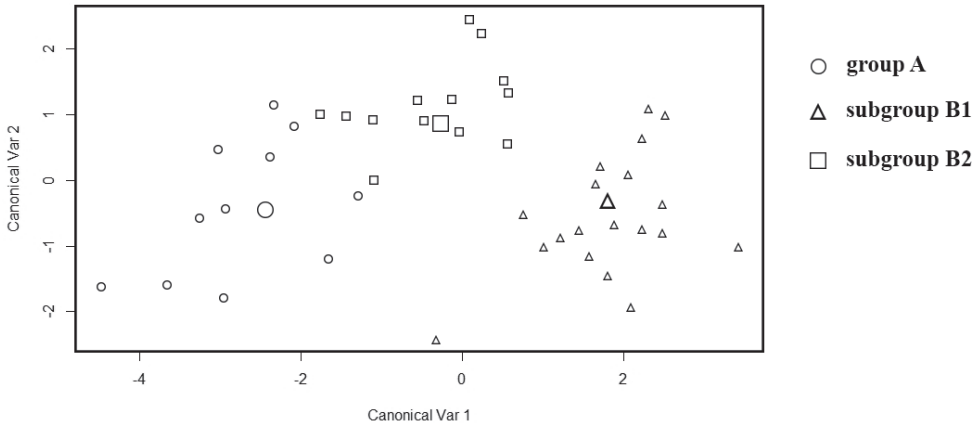
Figure 8. Plot of the two first canonical variables of a fda analysis on the song parameters. Large symbols represent groups centres.

Within group B, the position of two specimens (25 and 59 – Fig. 7) is probably a result of their high number of stridulatory teeth (Fig. 9, see also Suppl. material 1), which was not observed in other analyzed populations. Furthermore, within group B, differences are also present between specimens from the Pannonian Basin (B1) and specimens from the Dinaric area (B2), the latter ones having intermediate song characteristics, closer to group A.

Due to the high variation of song characteristics within group B, our analyses do not allow to conclude whether the geographic structuring of bioacoustic parameters of *Isophya modestior* is a matter of intraspecific variation or whether it reflects the existence of a cryptic species complex. On the other hand, our results support a stronger differentiation between group A and B. Those are mostly split geographically by the Sava-Lower Danube line. Rivers can represent significant barriers for flightless terrestrial insects with low mobility, but also climate-driven vicariances at a local scale could promote lineage diversification in *Isophya* (e.g., Chobanov et al. 2017). For example, the dry conditions in the lowlands of the Balkan Peninsula during Pleistocene Glacial maxima (Wright et al. 2003) may have promoted short-term speciation in mesophilic bush-crickets (Borissov et al. 2021).

Even though bioacoustic analyses represent a strong tool for identification of most of the species within genus *Isophya* (Heller et al. 2004), song parameters within this group may also be a matter of homoplastic/convergent evolution (Chobanov et al. 2017). Orthoptera songs are under strong selection, not only from inter- and intrasexual competition (female choice; e.g. Heller and Hemp 2020), but also from natural selection, e.g. by attracting predators or parasites (e.g. Wagner 1996). Therefore, the result of the present study may be a basis for testing speciation levels in *I. modestior* by involving neutral markers such as DNA sequences or chromosome morphology in order to obtain more insight into the evolution and diversification patterns of the studied populations.

Our study shows that bioacoustic analyses of Orthoptera are still useful to better understand geographic variation within species. Though the European fauna is fairly
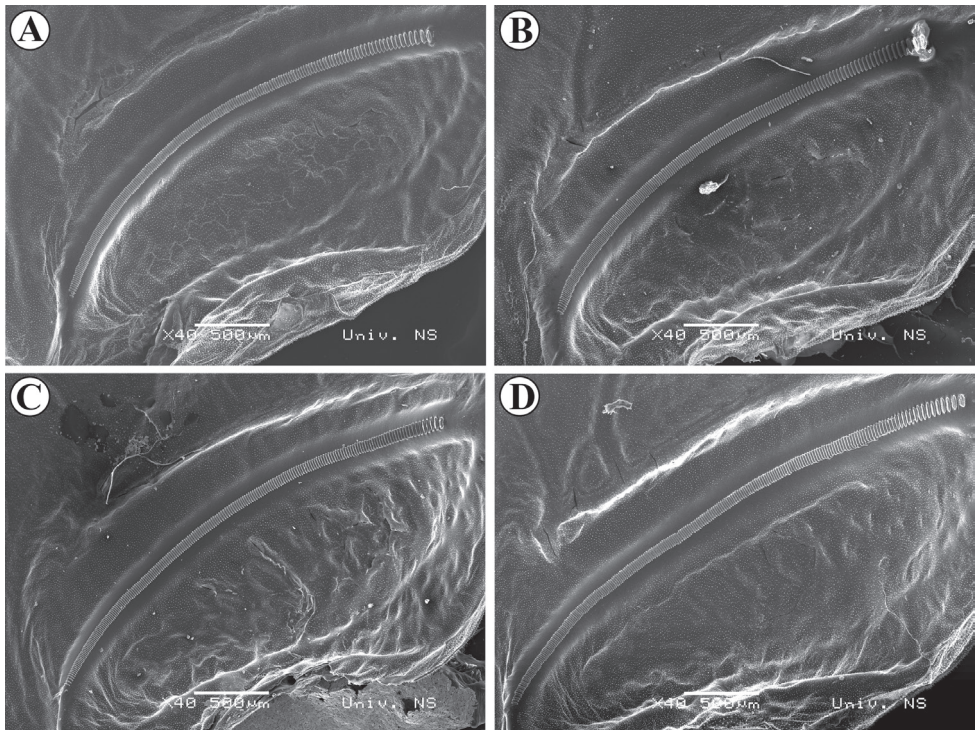
Figure 9. SEM photos of stridulatory files of different specimens from same population (Pannonian Serbia, Fruška Gora Velika Remeta) **A** 192 stridulatory teeth **B** 197 stridulatory teeth **C** 210 stridulatory teeth **D** 239 stridulatory teeth.

well studied compared to other continents, new species of Orthoptera from Europe have been continuously described in recent years (Kleukers et al. 2010; Ingrisch and Pavićević 2010; Iorgu and Iorgu 2010; Orci et al. 2010; Iorgu 2012; Szövényi et al. 2012; Kaya et al. 2012; Chobanov et al. 2014; Chobanov et al. 2015; Tilmans et al. 2016; Olmo-Vidal 2017). The latter particularly concerns the species-rich genera *Isophya* and *Poecilimon* that are still expected to hold further surprises. Discovering new cryptic taxa is, therefore, still realistic in Europe, especially as a result of integrated taxonomic studies. Altogether, our study shows that detailed bioacoustic analyses are useful to understand the geographic structure within species. As bioacoustics is often used in species identification, these data can also help to recognize the species in the field.

Acknowledgements

References

Bernstein SK, Sheeran LK, Wagner RS, Li J, Koda H (2016) The vocal repertoire of Tibetan macaques (*Macaca thibetana*): A quantitative classification. American Journal of Primatology 78(9): 937–949. https://doi.org/10.1002/ajp.22564

Béthoux O, Nel A (2002) Venation pattern and revision of Orthoptera sensu nov. and sister groups. Phylogeny of Paleozoic and Mesozoic Orthoptera sensu nov. Zootaxa 96(1): 1–88. https://doi.org/10.11646/zootaxa.96.1.1

Borissov SB, Hristov GH, Chobanov DP (2021) Phylogeography of the *Poecilimon ampliatus* species group (Orthoptera: Tettigoniidae) in the context of the Pleistocene glacial cycles and the origin of the only thelytokous parthenogenetic phaneropterine bush-cricket. Arthropod Systematics & Phylogeny 79: 401–418. https://doi.org/10.3897/asp.79.e66319

Bradbury JW, Vehrencamp SL (2011) Principles of Animal Communication. 2nd edn. Sunderland (MA): Sinauer. https://doi.org/10.1086/669301

Brizio C, Buzzetti FM, Pavan G (2020) Beyond the audible: Wide band (0–125 kHz) field investigation on Italian Orthoptera (Insecta) songs. Biodiversity Journal 11(2): 443–496. https://doi.org/10.31396/Biodiv.Jour.2020.11.2.443.496

Chobanov DP, Grzywacz B, Iorgu IŞ, Ciplak B, Ilieva MB, Warchałowska Śliwa E (2013) Review of the Balkan *Isophya* (Orthoptera: Phaneropteridae) with particular emphasis on the *Isophya modesta* group and remarks on the systematics of the genus based on morphological and acoustic data. Zootaxa 3658(1): 1–81. https://doi.org/10.11646/zootaxa.3658.1.1

Chobanov DP, Lemonnier-Darcemont M, Darcemont C, Puskás G, Heller KG (2014) *Tettigonia balcanica*, a new species from the Balkan Peninsula (Orthoptera, Tettigoniidae). Entomologia 2(2): 95–106. https://doi.org/10.4081/entomologia.2014.209

Chobanov DP, Kaya S, Çiplak B (2015) Contribution to the taxonomy of *Poecilimon bosphoricus* species group (Orthoptera: Phaneropteridae): two new species from its core range. Zootaxa 3964(1): 63–76. https://doi.org/10.11646/zootaxa.3964.1.3

Chobanov DP, Kaya S, Grzywacz B, Warchałowska-Śliwa E, Çıplak B (2017) The Anatolio-Balkan phylogeographic fault: A snapshot from the genus *Isophya* (Orthoptera, Tettigoniidae). Zoologica Scripta 46(2): 165–179. https://doi.org/10.1111/zsc.12194

Cigliano MM, Braun H, Eades DC, Otte D (2021) Orthoptera Species File. Version 5.0/5.0. [15.09.2021] http://Orthoptera.SpeciesFile.org

Faber A (1928) Die Bestimmung der deutschen Geradflügler (Orthopteren) nach ihren Lautäußerungen. Zeitschrift für wissenschaftliche Insektenbiologie 23: 209–234.

Filer A, Burchardt LS, van Rensburg BJ (2021) Assessing acoustic competition between sibling frog species using rhythm analysis. Ecology and Evolution 11(13): 8814–8830. https://doi.org/10.1002/ece3.7713

Fontana P (1998) L'Ortotterofauna del Monte Summaro (Prealpi Venete, Vicenza) (Insecta, Blattaria, Mantodea, Orthoptera e Dermaptera). Bollettino del Museo Civico di Storia Naturale di Verona 22: 1–64.

Fontana P, Buzzetti FM, Cogo A, Odé B (2002) Guida al riconoscimento e allo studio di cavallette, grilli, mantidi e insetti affini del Veneto. Guide Natura 1, Museo Naturalistico Archeologico di Vicenza, 592 pp. with CD.

Gogala M, Popov AV (1997) Bioacoustcs of singing cicadas of the western Palaearctic: *Cicadetta mediterranea* (Panzer) (Cicadoidea: Tibicinidae). Acta Entomologica Slovenica (Ljubljana) 5(1): 11–24.

Gomboc S, Šegula B (2014) Pojoče kobilice Slovenije/Singing Orthoptera of Slovenia. EGEA, Zavod za naravo, Ljubljana, 240 pp. with DVD.

Gorochov AV, Rasnitsyn AP (2002) Superorder Grylloidea Laicharting, 1781. In: Rasnitsyn AP, Quicke DLJ (Eds) History of insects. Kluwer Academic Publishers, Dordrecht, 293–303. https://doi.org/10.1007/0-306-47577-4

Hall M, Robinson D (2021) Acoustic signalling in Orthoptera. Advances in Insect Physiology 61: 1–99. https://doi.org/10.1016/bs.aiip.2021.09.001

Hastie T, Tibshirani R (2020) Package mda, Version 0.5–2. https://CRAN.R-project.org/package=mda

Heller KG (1988) Bioakustik der europäischen Laubheuschrecken. Ökologie in Forschung und Anwendung 1, 358 pp.

Heller KG (1990) Evolution of song pattern in east Mediterranean Phaneropterinae: constraints by the communication system. In: Bailey WJ, Rentz DCF (Eds) The Tettigoniidae. Biology, systematics and evolution. Crawford House Press, Bathurst, 130–151. https://doi.org/10.1007/978-3-662-02592-5_8

Heller KG, Hemp C (2020) Hyperdiverse songs, duetting, and the roles of intra- and intersexual selection in the acoustic communication of the genus *Eurycorypha* (Orthoptera: Tettigonioidea, Phaneropterinae). Organisms, Diversity & Evolution 20(4): 597–617. https://doi.org/10.1007/s13127-020-00452-1

Heller KG, von Helversen D (1986) Acoustic communication in phanateropterid bushcrickets: Species-specific delay of female stridulatory response and matching male sensory time window. Behavioral Ecology and Sociobiology 18(3): 189–198. https://doi.org/10.1007/BF00290822

Heller KG, Orci KM, Grein G, Ingrisch S (2004) The *Isophya* species of Central and Western Europe (Orthoptera: Tettigonioidea: Phaneropteridae). Tijdschrift voor Entomologie 147(2): 237–258. https://doi.org/10.1163/22119434-900000153

Heller KG, Korsunovskaya O, Massa B, Iorgu IS (2018) High-speed duetting-latency times of the female acoustic response within the bush-cricket genera *Leptophyes* and *Andreiniimon* (Orthoptera, Phaneropteridae). ZooKeys 750: 45–58. https://doi.org/10.3897/zookeys.750.23874

Hochkirch A, Szovenyi G, Chobanov DP, Fontana P, Buzzetti FM, Gomboc S, Ivkovic S, Iorgu IS, Lemonnier-Darcemont M, Puskas G, Zuna-Kratky T, Willemse LPM, Skejo J, Pushkar T, Kristin A, Sirin D, Vedenina V (2016) *Isophya modestior*. The IUCN Red List of Threatened Species 2016: e.T68399393A74525391. https://doi.org/10.2305/IUCN.UK.2016-3.RLTS.T68399393A74525391.en [Accessed on 12 July 2021]

Ingrisch S (1991) Taxonomie der *Isophya*-Arten der Ostalpen (Grylloptera: Phaneropteridae). Mitteilungen der Schweizerische Entomologische Gesellschaft 64: 269–280.

Ingrisch S, Pavićević D (2010) Seven new Tettigoniidae (Orthoptera) and a new Blattellidae (Blattodea) from the Durmitor area of Montenegro with notes on previously known taxa. Zootaxa 2565(1): 1–41. https://doi.org/10.11646/zootaxa.2565.1.1

Ingrisch S, Pavićević D (2012) Faunistics, distribution and stridulation of orthopteroid insects of the Durmitor plateau and thesurrounding canyons. Fauna Balkana 1: 13–120.

Iorgu IŞ (2012) Acoustic analysis reveals a new cryptic bush-cricket in the Carpathian Mountains (Orthoptera, Phaneropteridae). ZooKeys 254: 1–22. https://doi.org/10.3897/zookeys.254.3892

Iorgu, IŞ, Iorgu EI (2010) A new species of *Isophya* (Orthoptera: Phaneropteridae) from the Romanian Carpathian mountains. Travaux du Muséum National d'Histoire Naturelle 'Grigore Antipa' 53: 161–170. https://doi.org/10.2478/v10191-010-0012-9

Iorgu IŞ, Iorgu EI (2012) Song description of Zubovski's bush-cricket, *Isophya zubovskii* (Orthoptera: Phaneropteridae). Travaux du Muséum National d'Histoire Naturelle 'Grigore Antipa' 55(1): 57–63. https://doi.org/10.2478/v10191-012-0006-x

Iorgu IŞ, Iorgu EI, Szövényi G, Orci KM (2017) A new, morphologically cryptic bush-cricket discovered on the basis of its song in the Carpathian Mountains (Insecta, Orthoptera, Tettigoniidae). ZooKeys 680: 57–72. https://doi.org/10.3897/zookeys.680.12835

Jacobs W (1953) Verhaltensbiologische Studien an Feldheuschrecken. Zeitschrift für Tierpsychologie 1: 1–230.

Kaya S, Çiplak B, Chobanov DP, Heller KG (2012) *Poecilimon bosphoricus* group (Orthoptera, Phaneropterinae): Iteration of morpho-taxonomy by song characteristics. Zootaxa 3225(1): 1–71. https://doi.org/10.11646/zootaxa.3225.1.1

Kleukers RMJC, Odé B, Fontana P (2010) Two new cryptic *Leptophyes* species from southern Italy (Orthoptera: Tettigoniidae). Zootaxa 2506(1): 26–42. https://doi.org/10.11646/zootaxa.2506.1.2

Krištín A, Jarčuška B, Kaňuch P (2020) An annotated checklist of crickets, grasshoppers and their allies (Orthoptera) in Slovakia. Zootaxa 4869(2): 207–241. https://doi.org/10.11646/zootaxa.4869.2.3

Nagy B, Heller KG, Orci KM, Szövényi G (2003) Neue Daten zum Vorkommen von *Isophya*-Arten (Orthoptera: Tettigonioidea) im östlichen Alpenvorland. Mitteilungen der Schweizerische Entomologische Gesellschaft 76: 161–172.

Ng NGR, Rheindt FE (2016) Species delimitation in the White-faced Cuckoo-dove (*Turacoena manadensis*) based on bioacoustic data. Avian Research 7(1): e2. https://doi.org/10.1186/s40657-015-0036-8

Olmo-Vidal JM (2017) *Lluciapomaresius nisae*, a new species of Ephippigerini (Orthoptera: Tettigoniidae: Bradyporinae) from the northeast of the Iberian Peninsula. Zootaxa 4221(1): 123–130. https://doi.org/10.11646/zootaxa.4221.1.6

Orci KM (2002) Orthoptera fajcsoportok bioakusztikai és morfometriai vizsgálata [On the bioacoustics and morphology of some species groups of Orthoptera]. PhD dissertation, University of Debrecen, Debrecen, Hungary, 122 pp. [Hungarian with English summary]

Orci KM, Nagy B, Szövényi G, Rácz I, Varga Z (2005) A comparative study on the song and morphology of *Isophya stysi* Čejchan, 1958 and *Isophya modestior* Brunner von Wattenwyl, 1882 (Orthoptera, Tettigoniidae). Zoologischer Anzeiger 244(1): 31–42. https://doi.org/10.1016/j.jcz.2004.11.002

Orci KM, Szövényi G, Nagy B (2010) *Isophya sicula* sp. n. (Orthoptera: Tettigonioidea), a new, morphologically cryptic bush-cricket species from the Eastern Carpathians (Romania) recognized from its peculiar male calling song. Zootaxa 2627(1): 57–68. https://doi.org/10.11646/zootaxa.2627.1.4

R Core Team (2021) R: A language and environment for statistical computing. Version 4.1.2.

Ragge DR, Reynolds WJ (1998) The songs of the grasshoppers and crickets of Western Europe. Colchester: Harley Books, 600 pp.

Senter P (2008) Voices of the past: A review of Paleozoic and Mesozoic animal sounds. Historical Biology 20(4): 255–287. https://doi.org/10.1080/08912960903033327

Sevgili H (2020) *Isophya sonora*, a new bush-cricket species from Eastern Black Sea region of Turkey (Orthoptera: Tettigoniidae; Phaneropterinae). Zootaxa 4860(2): 284–292. https://doi.org/10.11646/zootaxa.4860.2.9

Sweger AL, Uetz GW (2016) Characterizing the vibratory and acoustic signals of the 'puring' wolf spider, *Gladicosa gulosa* (Araneae: Lycosidae). Bioacoustics 25(3): 293–303. https://doi.org/10.1080/09524622.2016.1160328

Szövényi G, Puskás G, Orci KM (2012) *Isophya nagyi*, a new phaneropterid bush-cricket (Orthoptera: Tettigonioidea) from the Eastern Carpathians (Căliman Mountains, North Romania). Zootaxa 3521(1): 67–79. https://doi.org/10.11646/zootaxa.3521.1.5

Tilmans J, Odé B, Willemse L (2016) *Rhacocleis andikithirensis* a new bush-cricket from Greece (Orthoptera: Tettigoniidae: Tettigoniinae). Journal of Orthoptera Research 25(1): 25–38. https://doi.org/10.1665/034.025.0105

Tricas T, Boyle K (2014) Acoustic behaviors in Hawaiian coral reef fish communities. Marine Ecology Progress Series 511: 1–16. https://doi.org/10.3354/meps10930

Venables WN, Ripley BD (2002) Modern Applied Statistics with S. 4th Edn., Springer, New York. https://doi.org/10.1007/978-0-387-21706-2

Wagner Jr WE (1996) Convergent song preferences between female field crickets and acoustically orienting parasitoid flies. Behavioral Ecology 7(3): 279–285. https://doi.org/10.1093/beheco/7.3.279

Wright HE, Ammann B, Stefanova I, Atanassova J, Margalitadze N, Wick L, Blyakharchuk T (2003) Late-glacial and Early-Holocene dry climates from the Balkan Peninsula to Southern Siberia. In: Tonkov S (Ed.) Aspects of palynology and palaeoecology. Pensoft Publishers, Sofia-Moscow, 127–136.

Xie J, Indraswari K, Schwarzkopf L, Towsey M, Zhang J, Roe P (2018) Acoustic classification of frog within-species and species-specific calls. Applied Acoustics 131: 79–86. https://doi.org/10.1016/j.apacoust.2017.10.024

Zhantiev RD, Dubrovin NN (1977) Sound communication in the genus *Isophya* (Orthoptera, Tettigoniidae). Zoologicheskii jurnal 56: 38–51. [in Russian, English abstract]

Supplementary material 1

Table S1

Authors: Slobodan Ivković, Dragan Chobanov, Laslo Horvat, Ionuț Ștefan Iorgu, Axel Hochkirch

Data type: Table (excel file).

Explanation note: Detailed data on analysed specimens and song recordings.

Link: https://doi.org/10.3897/zookeys.1122.85721.suppl1

RESEARCH ARTICLE

ZooKeys
Launched to accelerate biodiversity research

Phylogenetic relationships among the species of the Cameroonian endemic freshwater crab genus *Louisea* Cumberlidge, 1994 (Crustacea, Brachyura, Potamonautidae), with notes on intraspecific morphological variation within two threatened species

Pierre A. Mvogo Ndongo[1,2], Thomas von Rintelen[2], Paul F. Clark[3], Adnan Shahdadi[4], Carine Rosine Tchietchui[5], Neil Cumberlidge[6]

1 *Département de Gestion des Écosystèmes Aquatiques, Institut des Sciences Halieutiques, Université de Douala à Yabassi, PO. Box. 7236 Douala-Bassa, Cameroon* **2** *Museum für Naturkunde, Leibniz Institute for Evolution and Biodiversity Science, Invalidenstrasse 43, 10115 Berlin, Germany* **3** *Department of Life Sciences, The Natural History Museum, London, SW7 5BD, UK* **4** *Department of Marine Biology, Faculty of Marine Sciences and Technology, University of Hormozgan, Bandar Abbas, Iran* **5** *Zoology Unit, Laboratory of Biology and Physiology of Animal Organisms, Faculty of Science, University of Douala, PO Box 24157 Douala, Cameroon* **6** *Department of Biology, Northern Michigan University, Marquette, MI 49855-5376, USA*

Corresponding author: Pierre A. Mvogo Ndongo (mpierrearmand@yahoo.fr)

Citation: Mvogo Ndongo PA, von Rintelen T, Clark PF, Shahdadi A, Tchietchui CR, Cumberlidge N (2022) Phylogenetic relationships among the species of the Cameroonian endemic freshwater crab genus *Louisea* Cumberlidge, 1994 (Crustacea, Brachyura, Potamonautidae), with notes on intraspecific morphological variation within two threatened species. ZooKeys 1122: 125–143. https://doi.org/10.3897/zookeys.1122.85791

Abstract

Louisea Cumberlidge, 1994 (Crustacea, Brachyura, Potamonautidae) currently includes four endemic Cameroonian freshwater crab species whose phylogenetic relationships were previously unresolved. In the present study, phylogenetic analyses are carried out involving three mtDNA loci (COI, 12S rRNA, and 16S rRNA). The COI locus revealed divergence times of 5.6 million years ago (myr) for when *L. balssi* (Bott, 1959) diverged from *L. edeaensis* (Bott, 1969); 4.1 myr for when *L. edeaensis* diverged

from *L. yabassi* Mvogo Ndongo, von Rintelen & Cumberlidge, 2019; and 2.48 myr for when the later species diverged from *L. nkongsamba* Mvogo Ndongo, von Rintelen & Cumberlidge, 2019. Three genetic lineages were found within *L. nkongsamba* that are supported by uncorrected *p*-distances and the haplotype network. Morphological variation in some taxonomically important characters was found within both *L. nkongsamba* and *L. yabassi*. No correlation, however, was found between the morphotypes within these species and the uncovered genetic lineages. Recognition of species boundaries and of subpopulations of species will prove valuable when making informed conservation decisions as part of the development of species action plans for these rare and threatened freshwater crabs.

Introduction

Louisea Cumberlidge, 1994 (Crustacea, Brachyura, Potamonautidae) is endemic to remote Cameroonian forested ecosystems and currently includes four freshwater crab species: *L. balssi* (Bott, 1959), *L. edeaensis* (Bott, 1969), *L. nkongsamba* Mvogo Ndongo, von Rintelen & Cumberlidge, 2019, and *L. yabassi* Mvogo Ndongo, von Rintelen & Cumberlidge, 2019. *Louisea balssi* and *L. edeaensis* have been revised recently based on new material collected in Cameroon (Mvogo Ndongo et al. 2017a, 2018, 2019), while *L. nkongsamba* and *L. yabassi* were recently discovered (Mvogo Ndongo et al. 2019). Other works on Cameroonian freshwater crabs have mainly focused on their taxonomy, phylogenetic relationships, or conservation (Cumberlidge 1999; Daniels et al. 2015; Mvogo Ndongo et al. 2017a, 2017b, 2017c, 2018, 2019, 2020, 2021a; Cumberlidge and Daniels 2022). This is the first study, however, that includes both morphological and molecular data from all known *Louisea* species. The present work also includes new collections of two *Louisea* species from the forested sites in southwestern Cameroon: *L. yabassi* from the Ebo Forest, and *L. nkongsamba* from the Nlonako Ecological Reserve (Mvogo Ndongo et al. 2019, 2021b). These populations are compared with those of *L. balssi* from Kumba and Mount Manengouba (Cumberlidge 1994, 1999; Mvogo Ndongo et al. 2017a, 2017c, 2018, 2019), and of *L. edeaensis* from Yaounde, Edea, and Lake Ossa (Cumberlidge 1994, 1999; Mvogo Ndongo et al. 2017a, 2017c, 2019).

The aim of the present work is to evaluate the phylogenetic relationships within *Louisea* and to estimate the genetic distance between the species using molecular data. Intraspecific variation of some important taxonomic characters within two newly discovered species is also assessed in order to better identify species boundaries within *Louisea*. Accurate species delimitation is necessary for understanding levels of biodiversity, and for adopting effective conservation and sustainable management strategies (Cornetti et al. 2015). The results from this study will be helpful in developing action plans aimed at the conservation of these rare, threatened, and endemic Cameroonian freshwater crab species.

Materials and methods

Sample collection

Four *Louisea* species were collected from four different locations in southwestern Cameroon between 2015 and 2021 (Fig. 1). The species were identified by following Cumberlidge (1994, 1999) and Mvogo Ndongo et al. (2019). Eight specimens of *L. balsi* were collected from 1,958 m a.s.l., Mount Manengouba; 30 specimens of *L. edeaensis* from 90 m a.s.l., Bedimet Island, Lake Ossa; 50 specimens of *L. nkongsamba* from 1000–1400 m a.s.l., Mount Nlonako; and 35 specimens of *L. yabassi* from up to 300 m a.s.l., the Ebo Forest near Yabassi. Specimens of *L. nkongsamba* and *L. yabassi* were studied to clarify intraspecific morphological variation within each species. Specimens were measured; their gender and life stage (juvenile, subadult, and adult) recorded; and their habitat preferences noted. Most of the crabs were released into their natural habitat after recording all relevant morphological data. Only a few whole adult specimens (males and females), as well as one of the walking legs was removed from each of the other selected specimens were preserved in ethanol for further morphological descriptions and molecular analyses. The newly collected specimens were deposited either in the Museum für Naturkunde,
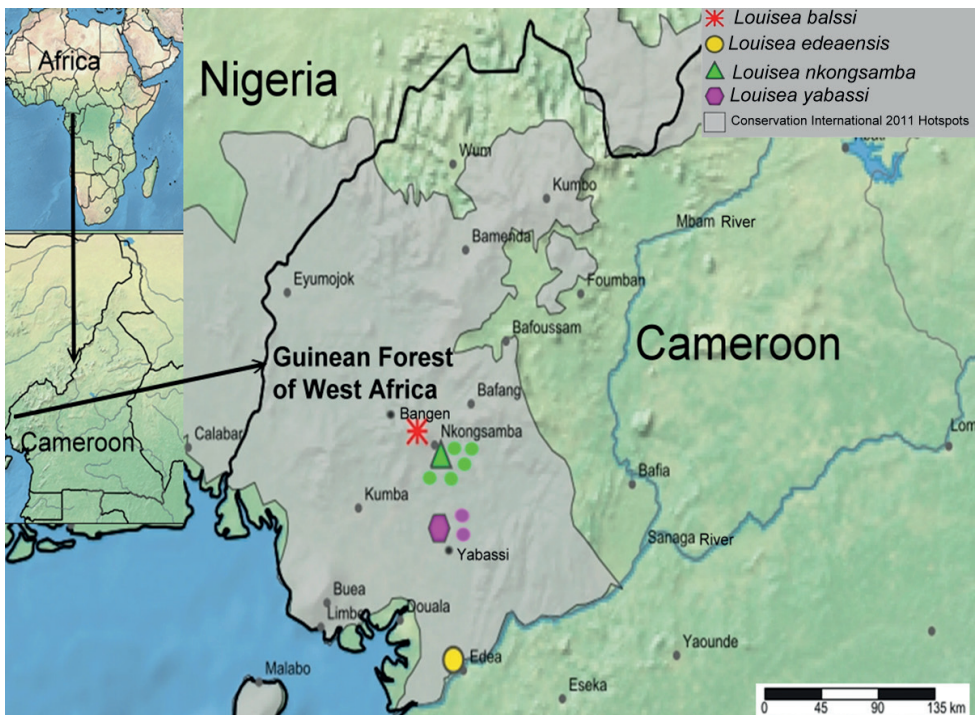
Figure 1. Map of Cameroon showing collection sites of *Louisea* species. *Louisea nkongsamba*: type locality (green triangle), new localities (green circles); *Louisea yabassi*: type locality (purple hexagon), new localities (purple circles).

Berlin, Germany (**ZMB**), or in the Unity of Taxonomy, Production and Sustainable Management of Aquatic Animals, Department of Management of Aquatic Ecosystems, Institut des Sciences Halieutiques, University of Douala, Cameroon (**LABO-PASMAT**).

Morphological analyses

Descriptive morphometrics of *L. edeaensis* and *L. balssi* specimens are given in Mvogo Ndongo et al. (2019: tables 2 and 3, respectively). Measurements (in mm) of the carapace of all the specimens were made with digital callipers. Characters of the carapace, thoracic sternum, chelipeds, and mandibles were examined in detail. The terminology used follows Cumberlidge (1999), and the classification by Cumberlidge and Daniels (2022). Images of the body parts were taken using a Leica microscope (model Z16A POA), and the LAS v. 4 and Helicon Focus v. 6.7.1 software. Post processing was undertaken using Adobe Photoshop CC5. Specimens were sorted according to their stage of development into juveniles, subadults, and adults. Furthermore, the maturity of adults was deciphered by identifying specimens that had undergone the pubertal moult from subadult to adult. The pubertal moult was determined by examining the degree of development of the pleon of a series of juvenile, subadult and adult females. The pleon of juvenile females is undeveloped and resembles the slim pleon of juvenile males; the pleon of subadults is significantly widened and partially covers the thoracic sternum. In comparison, the pleon of adult females is conspicuously enlarged and rounded such that its lateral margins overlap the coxae of the pereiopods, and the telson covers thoracic sternites 1 and 2. The lower limit of the range for the pubertal moult was judged as the CW of the largest non-adult female, while the upper limit of the pubertal moult was the CW of the smallest adult female.

Molecular analyses

Genomic DNA was extracted from a tissue sample of up to 25 mg cut from the pereiopod muscle of 70% ethanol-preserved specimens using the Qiagen DNeasy Blood & Tissue kit following the manufacturer's instructions. Polymerase chain reaction (PCR) was used to amplify three mitochondrial gene fragments: a ~638 bp region of the 16S ribosomal RNA gene (16S rRNA) using primers 16L29 and 16HLeu (Schubart 2009); a ~594 bp region of the 12S ribosomal RNA gene (12S rRNA) using primers 12L4 and 12H2 (Schubart et al. 2006); and a 648 bp region of the protein-coding mitochondrial gene, cytochrome oxidase subunit I gene (COI) using primers LCO-1490 and HCO-2198 (Folmer et al. 1994). PCR was performed in 25 μl volumes containing 1× Taq buffer, 1.5 mM $MgCl_2$, 200 μM each dNTP, 1 U Taq polymerase, ~50–100 mg DNA and ddH_2O up to volume. After an initial denaturation step of 4 min at 94 °C, cycling conditions were 35 cycles at 94 °C for 30 s, 45 °C for 60 s, and 72 °C for 90 s, with a final elongation step of 5 min at 72 °C. The same primers were used in PCR and sequencing. PCR products were sent to Macrogen Europe for purification and cycle sequencing of both strands of each gene. The sequences obtained were proofread manually using Chromas Lite (v. 2.1.1) (Technelysium Pty Ltd, Queensland, Austral-

ia) and aligned with ClustalW (Thompson et al. 1994) implemented in BioEdit 7.0.5 (Hall 1999). New sequences were submitted to the National Center for Biotechnology Information and are available from GenBank under the accession numbers in Table 1. Results from these genes were concatenated into a single alignment, which was then converted into a Nexus file with FaBox (Villesen 2007).

Table 1. Details of mtDNA markers used in the present study for *Louisea* species and outgroup species. Nl = Nlonako; Here = sequence available in the present study; * = Mvogo Ndongo et al. 2019; ** = Mvogo Ndongo et al. 2017c.

Species and sample number	Locality in Cameroon	Population number	Morphotypes (see Tables 3, 4)	Museum/ extraction number	GenBank accession number		
					COI	12S rRNA	16S rRNA
L. nkongsamba (1)	Nlonako, Engugue1382	Population 1	Nl Morphotype 1	ZMB-X21	OP122926	OP133321	OP133281
L. nkongsamba (2)	Nlonako, NgaltongueS1	Population 1	Nl Morphotype 1	ZMB-X26	OP122931	OP133326	OP133286
L. nkongsamba (3)	Nlonako, NgaltongueS1	Population 1	Nl Morphotype 1	ZMB-X27	OP122932	OP133327	OP133287
L. nkongsamba (4)	Nlonako, NgaltongueS1	Population 1	Nl Morphotype 1	ZMB-X28	OP122933	OP133328	OP133288
L. nkongsamba (5)	Nlonako, NgaltongueS1	Population 1	Nl Morphotype 1	ZMB-X29	OP122934	OP133329	OP133289
L. nkongsamba (6)	Nlonako Engugue1462	Population 1	Nl Morphotype 1	ZMB-X31	OP122936	OP133331	OP133291
L. nkongsamba (7)	Nlonako, NgaltongueS2	Population 1	Nl Morphotype 1	ZMB-X36	OP122941	OP133336	OP133296
L. nkongsamba (8)	Nlonako, NgaltongueS2	Population 1	Nl Morphotype 1	ZMB-X37	OP122942	OP133337	OP133297
L. nkongsamba (9)	Nlonako, NgaltongueS2	Population 1	Nl Morphotype 1	ZMB-X38	OP122943	OP133338	OP133298
L. nkongsamba (10)	Nlonako, NgaltongueS2	Population 1	Nl Morphotype 1	ZMB-X39	OP122944	OP133339	OP133299
L. nkongsamba (11)	Nlonako, Eyimba	Population 1	Nl Morphotype 1	ZMB-X41	OP122946	OP133341	OP133301
L. nkongsamba (12)	Nlonako, Nguengue	Population 1	Nl Morphotype 1	ZMB-X46	OP122951	OP133346	OP133306
L. nkongsamba (13)	Nlonako, Nguengue	Population 1	Nl Morphotype 1	ZMB-X47	OP122952	OP133347	OP133307
L. nkongsamba (14)	Nlonako, Nguengue	Population 1	Nl Morphotype 1	ZMB-X48	OP122953	OP133348	OP133308
L. nkongsamba (15)	Nlonako, Engugue1382	Population 2	Nl Morphotype 1	ZMB-X22	OP122927	OP133322	OP133282
L. nkongsamba (16)	Nlonako, Engugue1382	Population 2	Nl Morphotype 1	ZMB-X23	OP122928	OP133323	OP133283
L. nkongsamba (17)	Nlonako, Engugue1382	Population 2	Nl Morphotype 1	ZMB-X24	OP122929	OP133324	OP133284
L. nkongsamba (18)	Nlonako, NgaltongueS1	Population 2	Nl Morphotype 1	ZMB-X30	OP122935	OP133330	OP133290
L. nkongsamba (19)	Nlonako Engugue1462	Population 2	Nl Morphotype 2	ZMB-X32	OP122937	OP133332	OP133292
L. nkongsamba (20)	Nlonako Engugue1462	Population 2	Nl Morphotype 2	ZMB-X33	OP122938	OP133333	OP133293
L. nkongsamba (21)	Nlonako Engugue1462	Population 2	Nl Morphotype 2	ZMB-X34	OP122939	OP133334	OP133294
L. nkongsamba (22)	Nlonako, Eyimba	Population 2	Nl Morphotype 1	ZMB-X42	OP122947	OP133342	OP133302
L. nkongsamba (23)	Nlonako, Eyimba	Population 2	Nl Morphotype 1	ZMB-X43	OP122948	OP133343	OP133303
L. nkongsamba (24)	Nlonako, Eyimba	Population 2	Nl Morphotype 1	ZMB-X44	OP122949	OP133344	OP133304
L. nkongsamba (25)	Nlonako, Nguengue	Population 2	Nl Morphotype 1	ZMB-X49	OP122954	OP133349	OP133309
L. nkongsamba (26)	Nlonako, Nguengue	Population 2	Nl Morphotype 1	ZMB-X50	OP122955	OP133350	OP133310
L. nkongsamba (27)	Nlonako, Engugue1382	Population 3	Nl Morphotype 1	ZMB-X25	OP122930	OP133325	OP133285
L. nkongsamba (28)	Nlonako Engugue1462	Population 3	Nl Morphotype 1	ZMB-X35	OP122940	OP133335	OP133295
L. nkongsamba (29)	Nlonako, NgaltongueS2	Population 3	Nl Morphotype 1	ZMB-X40	OP122945	OP133340	OP133300
L. nkongsamba (30)	Nlonako, Eyimba	Population 3	Nl Morphotype 1	ZMB-X45	OP122950	OP133345	OP133305
L. yabassi (31)	Eboforest Stream no. 1	Population 1	Ebo Morphotype 1	ZMB-X11	OP122956	OP133351	OP133311
L. yabassi (32)	Eboforest Stream no. 1	Population 1	Ebo Morphotype 1	ZMB-X12	OP122957	OP133352	OP133312
L. yabassi (33)	Eboforest Stream no. 1	Population 1	Ebo Morphotype 1	ZMB-X13	OP122958	OP133353	OP133313
L. yabassi (34)	Eboforest Stream no. 1	Population 1	Ebo Morphotype 1	ZMB-X14	OP122959	OP133354	OP133314
L. yabassi (35)	Eboforest Stream no. 1	Population 1	Ebo Morphotype 1	ZMB-X15	OP122960	OP133355	OP133315
L. yabassi (36)	Eboforest Stream no. 2	Population 2	Ebo Morphotype 2	ZMB-X16	OP122961	OP133356	OP133316
L. yabassi (37)	Eboforest Stream no. 2	Population 2	Ebo Morphotype 2	ZMB-X17	OP122962	OP133357	OP133317
L. yabassi (38)	Eboforest Stream no. 2	Population 2	Ebo Morphotype 2	ZMB-X18	OP122963	OP133358	OP133318
L. yabassi (39)	Eboforest Stream no. 2	Population 2	Ebo Morphotype 2	ZMB-X19	OP122964	OP133359	OP133319
L. yabassi (40)	Eboforest Stream no. 2	Population 2	Ebo Morphotype 2	ZMB-X20	OP122965	OP133360	OP133320
L. edeaensis	Lake Ossa, Bedimet Island	Population 1	—	ZMB Crust 30335	MN188068.1*	—	MN217395*
L. edeaensis	Lake Ossa, Bedimet Island	Population 1	—	T351-30	KY964474.1**	KY964479**	KY964472**
L. edeaensis	Lake Ossa, Bedimet Island	Population 1	—	ZMB_Crust 26930	KY964473.1**	KY964478**	—
L. balssi	Manengouba, stream	Population 1	—	ZMB Crust 30319	MN188071.1*	MN217385*	MN217392*
L. balssi	Manengouba, stream	Population 1	—	ZMB Crust.29628	MN188070.1*	MN217384*	MN217391*
Potamonemus man	Bakossi National Park	Population 1	—	ZMB Crust 30327	MN188067.1*	MN217390*	MN217398*
Buea mundemba	Korup National Park	Population 1	—	ZMB Crust 30321	MN188069.1*	MN217388*	MN217396*

Phylogeographic investigations

The COI mitochondrial gene employed here is relatively variable and is commonly used for population genetics, and more recently also for faunal species identification using the barcoding approach (Hebert et al. 2003). This was useful for the examination of the population structure of *L. nkongsamba*, which provides evidence for genetic substructure among the sampling sites in Nlonako Ecological Reserve. These data are critical for the investigation of the historical connectivity among populations of *Louisea* species and are useful for the implementation of the future management of genetic diversity.

Maximum parsimony genotype networks (Templeton et al. 1992) were built with the software PopArt (Leigh and Bryant 2015) in order to graphically depict the genetic distances between mitochondrial genotypes. Haplotype and nucleotide diversities were used to compare genetic diversities among the sampling sites in terms of the number of haplotypes and the genetic distances of these haplotypes. Phylogeographic investigations have been successfully used by several researchers to determine connectivity among populations of other endemic crab species, e.g., *Sesarma fossarum* Schubart, Reimer, Diesel & Türkay, 1997, from the Cockpit Country, Jamaica (see Stemmer and Schubart 2016).

Phylogenetic investigations

The mitochondrial genes (COI, 12S rRNA, 16S rRNA) were used to identify the species boundaries, to examine the evolutionary origins and the relationships within *Louisea* species, and to determine whether morphological and ecological similarities between species are based on convergence or common ancestry. Here two methods of phylogenetic inference were applied to the data set: maximum likelihood (ML) using the software PAUP*, and Bayesian inference (BI) as implemented in MrBayes (v. 3.3; Huelsenbeck and Ronquist 2001) (see Mvogo Ndongo et al. 2017b, 2017c; Fratini et al. 2005). The best evolutionary model was determined with jModeltest v. 2.1.7 (Darriba et al. 2012) based on the Akaike Information Criterion (Posada and Buckley 2004) and resulted in the GTR+I+G (COI), GTR+G (16S rRNA) and HKY+G (12S rRNA) models. ML tree was obtained for each alignment with 1000 bootstrap pseudoreplicates. BI was performed to infer phylogeny by using MrBayes v. 3.2.2 (Huelsenbeck and Ronquist 2001). The Markov Chain Monte Carlo was run with four independent chains for 10,000,000 generations, samplefreq = 500, and burnin = 10,001. Analyses were conducted separately to test for topology congruence.

A total of 138 DNA sequences were obtained, 46 sequences each of COI, 16S rRNA, and 12S rRNA (Table 1). ML and BI trees were constructed for individual gene. The relative tree presented here for ML topology has been reconstructed from the concatenation of the three partial loci (COI, 16S rRNA, and 12S rRNA) into a

single alignment, which was then converted into a Nexus file with FaBox. This tree includes *L. balssi*, *L. edeaensis*, *L. nkongsamba*, and *L. yabassi* as the in-group, and *Potamonemus man* Mvogo Ndongo, von Rintelen & Cumberlidge, 2021a and *Buea mundemba* Mvogo Ndongo, von Rintelen & Cumberlidge in Mvogo Ndongo, von Rintelen, Tomedi-Tabi & Cumberlidge, 2020 as the out-group species.

To estimate clade divergence times based on the COI gene, a Bayesian analysis with the software BEAST v. 2.6.2 (Bouckaert et al. 2019) was conducted using a strict clock model (Yule Model) with a rate of evolution for the COI of 2.33% per million years (my) (10% SD) (following Schubart et al. 1998). Markov chains for 10 million generations were undertaken, sampling every 1000th iteration and discarding the first 25% as burn-in. Overall, 7500 trees were obtained, and these trees were used to calculate the maximum clade credibility tree in TreeAnnotator v. 1.6.1 (part of the BEAST package). The uncorrected *p*-distances (%) was calculated in MEGA 7 (Kumar et al. 2016).

Abbreviations used

a.s.l.	above sea level;
CW	carapace width measured at widest point;
CL	carapace length measured along medial line from anterior to posterior margin;
CH	carapace height measured at maximum height of cephalothorax;
FW	front width measured along anterior frontal margin between inner angles of orbits;
myr	million years ago;
PAMN	Pierre A. Mvogo Ndongo;
S2/3	male sternal sulcus between thoracic sternites 2 and 3;
S3/4	male sternal sulcus between thoracic sternites 3 and 4.

Results

Morphological analyses

Morphometric measurements of *L. yabassi* and *L. nkongsamba* populations are provided in Table 2. The adult size range of *L. yabassi*, based on male and female specimens from the two populations, was determined to be between CW 16.5 and CW 24.0 mm. Subadults of *L. yabassi* ranged from CW 11.0 mm to CW 15.5 mm, whereas juveniles of this species were CW 10.0 mm or less. The adult size range of *L. nkongsamba*, based on male and female specimens from four of the six sites, was between CW 15.8 mm and CW 20.0 mm. Subadults of *L. nkongsamba* ranged from CW 11.5 mm to CW 14.4 mm (two populations, PAMN 02.12.19 and PAMN

10.12.19, consisted entirely of subadults), whereas juveniles of this species measured CW 10.0 mm or less. No major differences were found between the carapace proportions (CW/FW, CL/FW, and CH/FW) of any of the populations of these two species, and these proportions were virtually identical in all cases (Table 2). The difference between the adult size range of *L. yabassi* and *L. nkongsamba* is minor, with the former species growing up to CW 24 mm and the latter species reaching only CW 20 mm.

Differences in certain morphological characters of the specimens of *L. yabassi* from two populations in the Ebo Forest are noteworthy (Table 3). Like *L. yabassi*, *L. nkongsamba* also showed differences in several morphological characters among the specimens from six sites, which are organised here into morphotype 1 (Nlonako Enguegue NO. 1_1462) and morphotype 2 (Nlonako Eyimba, Ngaltongue, Enguegue NO. 2_1382 m, Nguegue) (Table 4). These morphological differences between the two populations/morphotypes of *L. yabassi* and *L. nkongsamba* are also illustrated

Table 2. Morphometric and collection data of specimens of *Louisea yabassi* from Ebo Forest, Cameroon, and *L. nkongsamba* from Nlonako Ecological Reserve, Cameroon. Ad: adult; Sa: subadult, M: male; F: female.

Species	CW/FW mean (*n*)	CL/FW mean (*n*)	CH/FW mean (*n*)	Size range (CW in mm)	Museum number	Locality	Geographic coordinates	Altitude (m a.s.l.)
L. yabassi	2.9 (19)	2.1 (19)	1.3 (19)	Ad M 16.4–20.2	LaboPasmat X100	Ebo Forest, Stream NO. 1	04°25'01.7"N, 010°12'00.8"E	162
L. yabassi				Ad F 12.0–24.1	ZMB Crust 33829	Ebo Forest, Stream NO. 1	04°25'01.7"N, 10°12'00.8"E	162
L. yabassi	2.9 (16)	2.1 (16)	1.3 (16)	Ad M 16.6–21.3	LaboPasmat X101	Ebo Forest, Stream NO. 2	04°24'59.3"N, 010°12'07.7"E	254
L. yabassi				Ad F 17.4–22.5	ZMB Crust.33775	Ebo Forest, Stream NO. 2	04°24'59.3"N, 010°12'07.7"E	254
L. nkongsamba	2.9 (8)	2.1 (8)	1.3 (8)	Ad M 15.8–20.0	LaboPasmat X102	Nlonako, Nguengue	04°54'44.8"N, 009°58'50.0"E	1176
L. nkongsamba	2.9 (5)	2.1 (5)	1.3 (5)	Ad M 12.8–18.5	LaboPasmat X102Y	Nlonako, NgaltongueS2	04°55'20.4"N, 009°57'31.0"E	1180
L. nkongsamba	2.9 (12)	2.1 (12)	1.3 (12)	Ad M 13.8–17.4	LaboPasmat X103	Nlonako, NgaltongueS1	04°55'20.4"N, 009°57'42.6"E	1180
L. nkongsamba	2.9 (10)	2.1 (10)	1.3 (10)	Sa M 11.7–11.8	ZMB Crust.33789	Nlonako, Enguegue1382	04°54'21.6"N, 009°58'20.6"E	1382
L. nkongsamba	2.9 (11)	2.1 (11)	1.3 (11)	Sa M 11.5–14.4	LaboPasmat X104	Nlonako, Eyimba	04°53'30.7"N, 009°59'05.1"E	1194
L. nkongsamba	2.9 (6)	2.1 (6)	1.3 (6)	Ad 12	LaboPasmat X104Y	Nlonako, Enguegue1462	04°54'21.9"N, 009°58'22.4"E	1462
L. nkongsamba				Ad F 14–15	LaboPasmat X105	Nlonako, Enguegue1462	04°54'21.9"N, 009°58'22.4"E	1462
L. nkongsamba				Sa 6.60	LaboPasmat X105Y	Nlonako, Enguegue1462	04°54'21.9"N, 009°58'22.4"E	1462
L. edeaensis	3.0 (21)	2.5 (21)	1.4 (21)	Ad M 14.1–17.5	See Mvogo Ndongo et al. 2019: 143, table 2	Lake Ossa	03°48'56.1"N, 010°03'18.5"E	90
L. edeaensis				Ad F 13.0–19.9	See Mvogo Ndongo et al. 2019: 143, table 2	Lake Ossa	03°48'56.1"N, 010°03'18.5"E	90
L. balssi	2.9 (8)	2.1 (8)	1.2 (8)	Ad M 13.3–16.2	See Mvogo Ndongo et al. 2019: 147, table 3	Manengouba	05°01'56.9"N, 009°49'37.8"E	1958
L. balssi				Ad F 13.3–14.8	See Mvogo Ndongo et al. 2019: 147, table 3	Manengouba	05°01'56.9"N, 009°49'37.8"E	1958

(Figs 2, 3). Despite those morphological differences, there is no genetic support for recognising these differences as indicating different genetic lineages that would warrant formal taxonomic recognition (Figs 4–6).

Table 3. Comparison of selected morphological characters between two populations (morphotypes) of *Louisea yabassi* from Ebo Forest, Cameroon.

Character	Population no. 1 (morphotype 1)	Population no. 2 (morphotype 2)
Epibranchial tooth	reduced to granule (Fig. 2A, C)	small (Fig. 2B, D)
Intermediate tooth between exorbital & epibranchial teeth	distinct, but small (Fig. 2A, C)	relatively large, triangular (Fig. 2B, D)
Major cheliped dactylus	slim, gently arched (Fig. 3F)	slim, almost straight (Fig. 3H)
Cheliped carpus inner margin teeth	both distal and proximal teeth large, positioned some distance from each other (Fig. 3G)	distal tooth larger than proximal tooth, positioned relatively closer to each other (Fig. 3C)
Mandible inferior lateral corner of coxa (biting edge)	lacking pointed tip (Fig. 2G)	with pointed tip (Fig. 2G)
Margin of male sternal sulcus S3	with long setae (Fig. 2E)	lacking setae (Fig. 2F)
Male sternal sulcus S3/4	reduced to 2 deep lateral notches (Fig. 2E)	indiscernible (Fig. 2F)
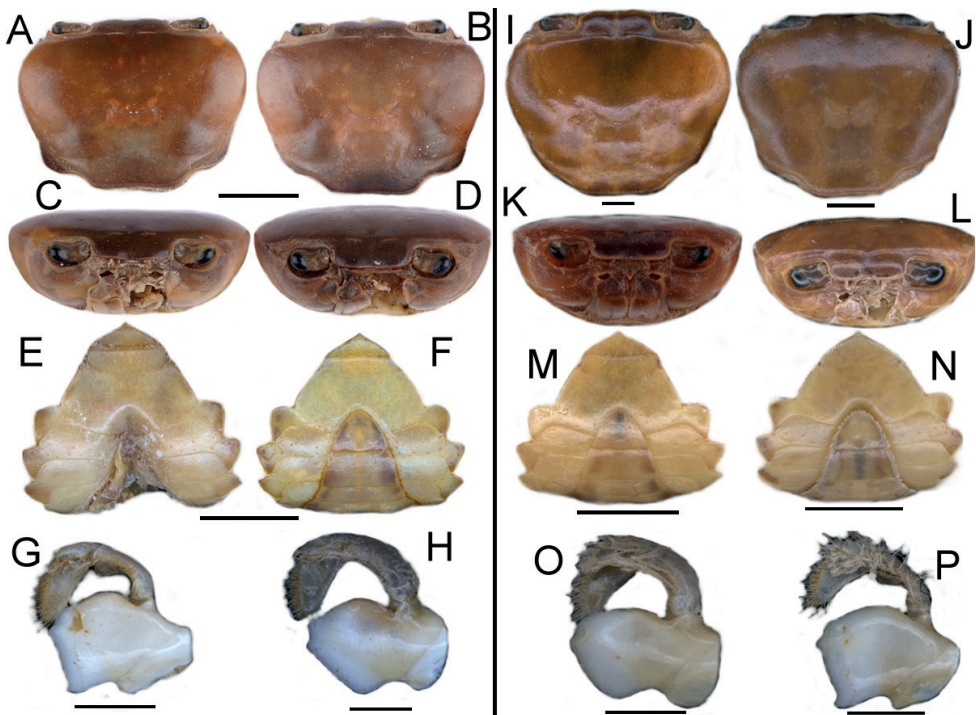
Figure 2. *Louisea yabassi* from Ebo Forest, Cameroon, adult male (CW 20.2 mm) from site no. 1 (**A, C, E, G**), adult male (CW 21.3 mm) from site no. 2 (**B, D, F, H**). *Louisea nkongsamba* from Nlonako, Cameroon, adult male (CW 18.2 mm) from Eyimba (**I, K, M, O**), subadult male (CW 12.0 mm) from Enguegue (site no. 1) (**J, L, M, P**). **A, B, I, J** dorsal view of cephalothorax **C, D, K, L** frontal view of cephalothorax **E, F, M, N** ventral view of thoracic sternum **G, H, O, P** frontal view of left mandible. Scale bars: 8 mm (**A, C, E**); 9 mm (**B, D, F**); 1 mm (**G, H**); 4 mm (**I, K**); 12 mm (**J, M**); 3 mm (**L**); 8 mm (**N**); 2 mm (**O, P**).

Table 4. Comparison of selected morphological characters between two populations (morphotypes) of *Louisea nkongsamba* from Mount Nlonako, Cameroon.

Characters	Morphotype 1 Nlonako Enguegue1462	Morphotype 2 Nlonako Eyimba, Ngaltongue, Enguegue1382, Nguegue and type specimens
Exorbital tooth	relatively large (Fig. 2J, L)	relatively small (Fig. 2I, K)
Epibranchial tooth	small (Fig. 2J, L)	reduced to granule (Fig. 2I, K)
Intermediate tooth between exorbital & epibranchial teeth	relatively large (Fig. 2J, L)	relatively small (Fig. 2I, K)
Lateral margin posterior to epibranchial tooth	lined with small granules (Fig. 2J)	smooth (Fig. 2I)
Postfrontal crest	poorly defined, completely traversing carapace, reaching anterolateral margins at intermediate tooth (Fig. 2J, L)	clearly defined, completely traversing carapace, not reaching anterolateral margins (Fig. 2I, K)
Major cheliped dactylus	slim, straight (Fig. 3A)	slim, gently arched (Fig. 3B)
Cheliped carpus inner margin teeth	distal tooth larger than proximal tooth, both slender, positioned some distance from each other (Fig. 3D)	distal tooth larger than proximal tooth, both robust, positioned relatively closer to each other (Fig. 3E)
Medial inferior margin of cheliped merus	with small but distinct jagged distal tooth angled outward at 60°, followed by numerous granules and small teeth (Fig. 3I)	with large jagged distal tooth angled outward at 90°, followed by numerous granules and small teeth decreasing in size proximally (Fig. 3J)
Mandible inferior lateral corner of coxa (biting edge)	lacking pointed tip (Fig. 2P)	with pointed tip (Fig. 2O)
Male sternal sulcus S3/4	indiscernible except for 2 deep lateral notches (Fig. 2N)	indiscernible, lacking lateral notches (Fig. 2M)

Figure 3. *Louisea nkongsamba* from Nlonako, Cameroon, subadult male (CW 12.0 mm) from Enguegue (site no. 1) (**A, D, I**), adult male (CW 18.2 mm) from Eyimba (**B, E, J**). *Louisea yabassi* from Ebo Forest, Cameroon, adult male (CW 21.3 mm) from site no. 2 (**C, H**), adult male (CW 20.2 mm) from site no. 1 (**F, G**). **A, B, F, H** frontal view of chela **C, D, E, G** cheliped carpus **I, J** cheliped merus. Scale bars: 5 mm (**A–J**).
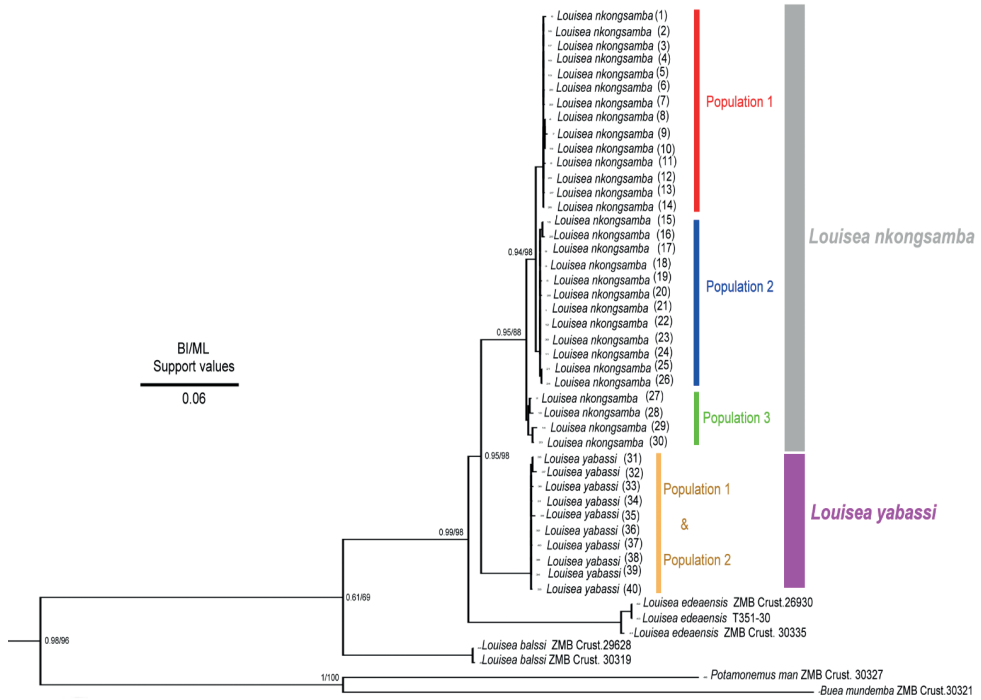
Figure 4. ML tree topology for *Louisea* species of Cameroon, derived from mtDNA sequences corresponding to three mtDNA loci (partial 12S rRNA, 16S rRNA, and COI genes). BI and ML statistical values (%) on the nodes indicate posterior probabilities and bootstrap support, respectively.
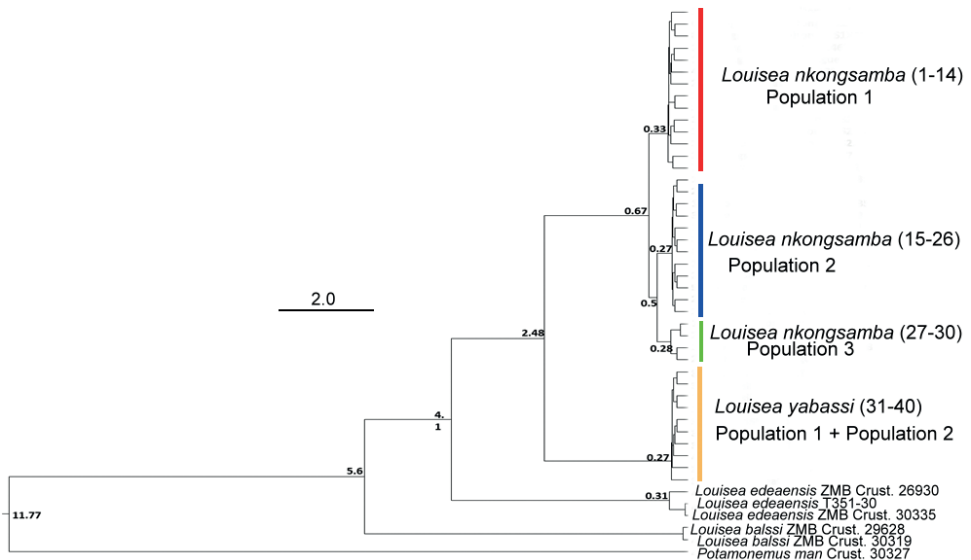
Figure 5. BI tree topology for *Louisea* species of Cameroon, derived from COI mtDNA sequences. Statistical values on the nodes indicate dates in millions of years.
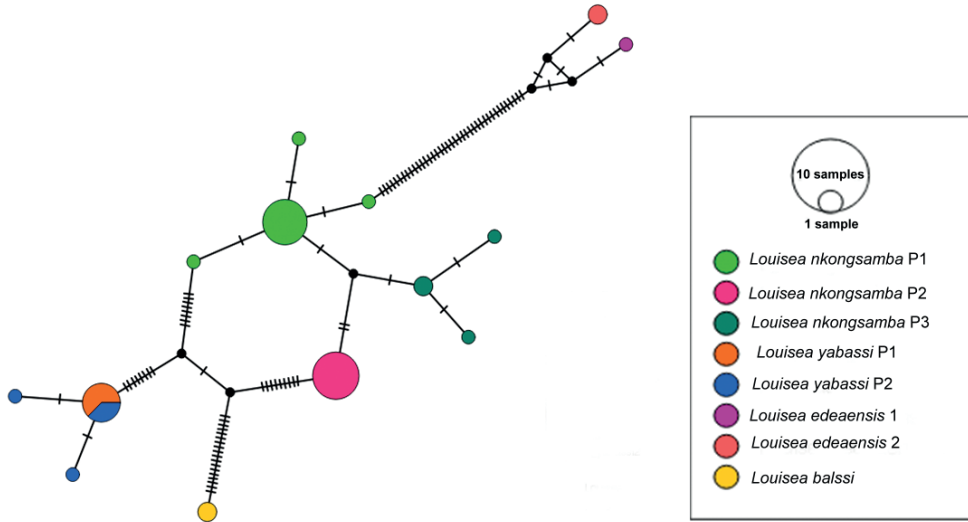
Figure 6. Maximum parsimony genotype networks for *Louisea* species of Cameroon, derived from COI mtDNA sequences. Hatch marks stand for mutation steps.

The pubertal moult estimates indicate that the largest *Louisea* species is *L. yabassi* (CW 24 mm); the smallest species is *L. balssi* (CW 16.2 mm); while the size ranges of *L. edeaensis* and *L. nkongsamba* overlap with each other (~CW 20 mm) in between those of *L. balssi* and *L. yabassi* (Table 2). *Louisea balssi* is a high-altitude species that dwells at 1958 m a.s.l.; *L. nkongsamba* is a submontane species found between 938 and 1462 m a.s.l.; while both *L. edeaensis* and *L. yabassi* are low-altitude crabs, occurring at 90 m a.s.l. and 300 m a.s.l., respectively (see Mvogo Ndongo et al. 2017a, 2017c, 2019, 2021b; Table 2).

Molecular analyses

The present molecular analyses support recognition of three lineages (as population 1, 2, and 3) of *L. nkongsamba* from six sites on Mount Nlonako (Figs 4–6). These distinct lineages, however, do not correlate with the two morphotypes recognised herein for *L. nkongsamba* (Table 4). Population 1 of *L. nkongsamba* included specimens that were collected from all six localities of Mount Nlonako (Tables 1, 5; Fig. 4); population 2 of *L. nkongsamba* comprised specimens that were collected from five out of six sites of Mount Nlonako (Tables 1, 5; Fig. 4); and population 3 of *L. nkongsamba* comprised specimens that were collected from four out of six sites of Mount Nlonako (Tables 1, 5; Fig. 4). Both morphotypes of *L. nkongsamba* are represented in one or the other population (Table 1).

The uncorrected *p*-distance between *Louisea* species pairs reveal that each is well isolated from other taxa assigned to this genus (Table 6). *Louisea nkongsamba* is sister species to *L. yabassi* with relatively low *p*-distance (3.97%) (Table 6); both are sister to *L. edeaensis*. *Louisea balssi* is isolated from *L. edeaensis*, with a sequence divergence of 11.04% (12S rRNA), 10.15% (COI), and 7.77% (16S rRNA) (Table 6); from *L. yabassi*,

with a sequence divergence of 12.94% (12S rRNA), 7.32% (COI), and 5.36% (16S rRNA); and from *L. nkongsamba*, with a sequence divergence of 12.42% (12S rRNA), 7.98% (COI), and 5.04% (16S rRNA) (Table 6). The uncorrected *p*-distances between the three genetic populations of *L. nkongsamba* are given in Table 7. Population 1 of *L. nkongsamba* is sister to population 2, both populations are sister to population 3.

The phylogenetic analysis indicates that *L. balssi* from Mount Manengouba is the ancestral species, while *L. edeaensis* from Lake Ossa is the sister species of the clade that includes *L. yabassi* and *L. nkongsamba* (Fig. 4). Divergence time calculations of *Louisea* species (Fig. 5) showed that the early divergence within the genus occurred during the late Miocene, i.e., *L. balssi* diverged from other species at about 5.6 myr. *Louisea yabassi* and *L. nkongsamba* diverged from *L. edeaensis* at about 4.1 myr, and *L. yabassi* separated from *L. nkongsamba* at about 2.48 myr.

The haplotype network recovered eight haplotypes for *L. nkongsamba* with maximum four mutation steps between the specimens of this species (Fig. 6) and distinguishes between the four *Louisea* species (Fig. 6).

Table 5. Number of individuals of *Louisea nkongsamba* studied per site/population.

Sites	Altitude (m a.s.l.)	Number of individuals in Population 1	Number of individuals in Population 2	Number of individuals in Population 3
Enguegue no. 2	1382	1	3	1
Ngaltongue no. 1	1176	4	1	0
Ngaltongue no. 2	1256	4	0	1
Enguegue no. 1	1462	1	3	1
Nguegue	1211	3	2	0
Eyimba	938	1	3	1
Total		14	12	4

Table 6. Pairwise uncorrected *p*-distances of COI, 16S rRNA, and 12S rRNA partial sequences between the species of *Louisea*.

Louisea species	Uncorrected *p*-distance		
	COI	16S rRNA	12S rRNA
L. nkongsamba and *L. yabassi*	3.97%	2.15%	3.77%
L. nkongsamba and *L. edeaensis*	8.61%	4.33%	4.92%
L. nkongsamba and *L. balssi*	7.98%	5.04%	12.42%
L. edeaensis and *L. yabassi*	8.88%	4.35%	4.27%
L. edeaensis and *L. balssi*	10.15%	7.77%	11.04%
L. yabassi and *L. balssi*	7.32%	5.36%	12.94%

Table 7. Pairwise uncorrected *p*-distances of COI, 16S rRNA, and 12S rRNA partial sequences between the populations of *Louisea nkongsamba*.

Louisea nkongsamba	Uncorrected *p*-distance		
	COI	16S rRNA	12S rRNA
Population 2 and Population 3	0.48%	0.87%	0.95%
Population 2 and Population 1	0.70%	0.20%	0.71%
Population 3 and Population 1	0.52%	0.61%	1.18%

Discussion

Phylogenetic and phylogeographic relationships

The four *Louisea* species recovered here each has a monophyletic clade (Fig. 4) with strong topological statistical support, and high pairwise uncorrected *p*-distance values between species pairs (Table 6). This study, therefore, supports the continued recognition of all four *Louisea* species that are endemic to the southwest Cameroon rainforests. The earliest divergence for *Louisea* species happened at ~5.6 myr (late Miocene; Fig. 5), which corresponds to the dates for cladogenesis within genera provided by Daniels et al. (2015). In contrast, the latest *Louisea* divergence between *L. nkongsamba* and *L. yabassi* seems to have occurred during the late Pliocene (2.48 myr). Similar divergence times were recovered for another Central African freshwater crab species pair, *Sudanonautes aubryi* (H. Milne Edwards, 1853) and *S. floweri* (De Man, 1901) (see Daniels et al. 2015: fig. 3). Even the two morphologically variable *Louisea* species, *L. nkongsamba* and *L. yabassi*, were found in the molecular analyses to have low uncorrected *p*-distance values (Table 6), but both are recognised as distinct (see Mvogo Ndongo et al. 2019).

   Louisea species are found in different habitats within the rainforest zone: *L. balssi* in montane forest streams; *L. nkongsamba* in submontane forest streams; *L. edeaensis* on the islands of a freshwater lake; and *L. yabassi* in lowland forest streams. *Louisea nkongsamba* specimens from cool mountain streams draining the submontane forests of Mt. Nlonako (938–1462 m a.s.l.) are small-bodied with adult males measuring CWs 16–20 mm. *Louisea balssi* adult males from the cool high-altitude streams (1,958 m a.s.l.) draining into the caldera of Mount Manengouba are also noticeably small-bodied (CWs 13.0–16.2 mm). This agrees with the findings of Daniels et al. (2016) who reported that genetic differentiation tends to be somewhat limited in small-bodied montane species of freshwater crabs. Only a limited genetic variation, however, was found in the lowland forest species, *L. edeaensis*. In comparison, the moist tropical rainforests surrounding Mount Manengouba receive a high annual rainfall that has maintained a stable forest ecosystem, even during drier periods in the past when rain forests were replaced by savannas in other parts of Central Africa (Brown and Ab'Saber 1979; Diamond and Hamilton 1980; Mayr and O'Hara 1986; Grubb 1992; Zimkus 2009). Consequently, in such high rainfall areas, *L. balssi* would be sheltered from the harsher effects of rainforest disruption arising from prolonged dry periods in the past, making the Cameroon Highlands a Pleistocene forest refuge for freshwater crab species. Over time, *Louisea* dispersed from its original location around Mount Manengouba into the surrounding forests of southwest Cameroon, including Mount Nlonako. There *L. nkongsamba* evolved and continued to disperse into the forested lowlands around Yabassi and Lake Ossa, where *L. yabassi* and *L. edeaensis* evolved.

Intraspecific morphological variation

The two *L. yabassi* populations from localities ~2–3 km apart in the Ebo Forest genetically form a single clade with little lineage differentiation (Fig. 4; populations 1 and 2), and these individuals show relatively low levels of morphological variation (Table 3). Despite

this, two *L. yabassi* morphotypes could be identified (Table 3). Similarly, the six sampled localities around Mount Nlonako, where *L. nkongsamba* is found, are 4–10 km apart (Tables 2, 5). These individuals of *L. nkongsamba* fall into three genetically recognisable populations (Fig. 4; populations 1–3), which in turn have two distinct morphotypes (Table 4). Populations 1 and 3 consisted of individuals that all belong to morphotype 1, while population 2 included individuals of both morphotypes (Table 1). The high carapace (CH/FW = 1.3) and narrow front width (CW/FW = 2.9) of both *L. yabassi* and *L. nkongsamba* are associated with a semi-terrestrial, air-breathing lifestyle (Cumberlidge 1999). Populations of both species prefer temporary water bodies such as puddles near small permanent streams, as well as damp environments under small stones or in forest floor leaf litter adjacent to streams (Mvogo Ndongo et al. 2017a, 2018, 2019, 2021b). Freshwater crabs have limited dispersal abilities due to the absence of a free-swimming larval phase and their direct development resulting in crab hatchlings; the limited dispersal abilities of the crabs and the restricted movements of the adults in combination with the isolated and fragmentary nature of their wetland habitats might be at least partly responsible for their rich diversity and high endemism (Cumberlidge et al. 2009; Mvogo Ndongo et al. 2021b). The intraspecific morphological and genetic variations observed within *L. yabassi* and *L. nkongsamba* are crucial for adaptation by natural selection, not least because low levels of variation are associated with the extirpation of populations and an increased risk of species extinction (Bolnick et al. 2011; Scheiner and Holt 2012; Forsman 2014).

Acknowledgements

References

Bolnick DI, Amarasekare P, Araújo MS, Bürger R, Levine JM, Novak M, Rudolf VHW, Schreiber SJ, Urban MC, Vasseur DA (2011) Why intraspecific trait variation matters in community ecology. Trends in Ecology & Evolution 26(4): 183–192. https://doi.org/10.1016/j.tree.2011.01.009

Bott R (1959) Potamoniden aus West-Afrika (Crust., Dec.). Bulletin de l'Institut Français d'Afrique Noire. Série A, Sciences Naturelles 21(3): 994–1008.

Bott R (1969) Die Flusskrabben aus Asien und ihre Klassifikation (Crustacea, Decapoda). Senckenbergiana Biologisches 50: 359–366.

Bouckaert R, Vaughan TG, Barido-Sottani J, Duchêne S, Fourment M, Gavryushkina A, Heled J, Jones G, Kühnert D, De Maio N (2019) BEAST 2.5: an advanced software platform for Bayesian evolutionary analysis. PLoS Computational Biology 15(4): e1006650. https://doi.org/10.1371/journal.pcbi.1006650

Brown KS, Ab'Saber AN (1979) Ice-age forest refuges and evolution in the neotropics: Correlation of paleoclimatological, geomorphological and pedological data with modern biological endemism. Paleoclimas 5: 1–30.

Cornetti L, Ficetola GF, Hoban S, Vernesi C (2015) Genetic and ecological data reveal species boundaries between viviparous and oviparous lizard lineages. Heredity 2015(115): 517–526. https://doi.org/10.1038/hdy.2015.54

Cumberlidge N (1994) *Louisea*, a new genus of fresh-water crab (Brachyura, Potamoidea, Potamonautidae) *Globonautes macropus edeaensis* Bott, 1969 from Cameroon. Proceedings of the Biological Society of Washington 107: 122–131.

Cumberlidge N (1999) The freshwater crabs of West Africa, family Potamonautidae. Faune et Flore Tropicales 35: 1–382.

Cumberlidge N, Daniels S (2022) A new multilocus phylogeny reveals overlooked diversity in African freshwater crabs (Brachyura: Potamoidea): a major revision with new higher taxa and genera. Zoological Journal of the Linnean Society 194(4): 1268–1311. https://doi.org/10.1093/zoolinnean/zlab082

Cumberlidge N, Ng PKL, Yeo DCJ, Magalhães C, Campos MR, Alvarez F, Naruse T, Daniels SR, Esser LJ, Attipoe FYK, Clotilde-Ba FL, Darwall W, McIvor A, Ram M, Collen B (2009) Freshwater crabs and the biodiversity crisis: Importance, threats, status, and conservation challenges. Biological Conservation 142(8): 1665–1673. https://doi.org/10.1016/j.biocon.2009.02.038

Daniels SR, Phiri EE, Klaus S, Albrecht C, Cumberlidge N (2015) Multi-locus phylogeny of the Afrotropical freshwater crab fauna reveals historical drainage connectivity and transoceanic dispersal since the Eocene. Systematic Biology 64(4): 549–567. https://doi.org/10.1093/sysbio/syv011

Daniels SR, McCleod C, Carveth C, Mexim KK, Cumberlidge N (2016) Using mtDNA sequence data to explore evolutionary relationships among three West African species of freshwater crabs in the genus *Liberonautes* (Brachyura: Potamoidea: Potamonautidae), with a discussion of conservation implications. Journal of Crustacean Biology 36: 731–739. https://doi.org/10.1163/1937240X-00002460

Darriba D, Taboada GL, Doallo R, Posada D (2012) jModelTest 2: More models, new heuristics and parallel computing. Nature Methods 9(8): 772–772. https://doi.org/10.1038/nmeth.2109

De Man JG (1901) Description of a new freshwater crustacean from the Soudan; followed by some remarks on an allied species. Proceedings of the Zoological Society of London 1901: 94–104.

Diamond AW, Hamilton AC (1980) The distribution of forest passerine birds and Quaternary climatic change in Africa. Journal of Zoology 191(3): 379–402. https://doi.org/10.1111/j.1469-7998.1980.tb01465.x

Folmer O, Black M, Hoeh W, Lutz R, Vrijenhoek R (1994) DNA primers for amplification of mitochondrial cytochrome c oxidase subunit I from diverse metazoan invertebrates. Molecular Marine Biology and Biotechnology 3: 294–299.

Forsman A (2014) Effects of genotypic and phenotypic variation on establishment are important for conservation, invasion, and infection biology. Proceedings of the National Academy of Sciences of the United States of America 111(1): 302–307. https://doi.org/10.1073/pnas.1317745111

Fratini S, Vannini M, Cannicci S, Schubart CD (2005) Tree-climbing crabs: A case of convergent evolution. Evolutionary Ecology Research 7: 219–233.

Grubb P (1992) Refuges and dispersal in the speciation of African forest mammals. In: Prance GT (Ed.) Biological Diversification in the Tropics. Columbia University Press, New York, 537–543.

Hall TA (1999) Bioedit: A user-friendly biological sequence alignment editor and analysis program for windows 95/ 98/NT. Nucleic Acids Symposium Series 41: 95–98.

Hebert PDN, Ratnasingham S, de Waard JR (2003) Barcoding animal life: Cytochrome c oxidase subunit 1 divergences among closely related species. Proceedings of the Royal Society of London of Biological Sciences 270(suppl_1): 96–99. https://doi.org/10.1098/rsbl.2003.0025

Huelsenbeck JP, Ronquist F (2001) MRBAYES: Bayesian inference of phylogenetic trees. Bioinformatics 17(8): 754–755. https://doi.org/10.1093/bioinformatics/17.8.754

Kumar S, Stecher G, Tamura K (2016) MEGA7: Molecular Evolutionary Genetics Analysis version 7.0 for bigger datasets. Molecular Biology and Evolution 33(7): 1870–1874. https://doi.org/10.1093/molbev/msw054

Leigh JW, Bryant D (2015) PopART: Full-feature software for haplotype network construction. Methods in Ecology and Evolution 6(9): 1110–1116. https://doi.org/10.1111/2041-210X.12410

Mayr E, O'Hara RJ (1986) The biogeographic evidence supporting the Pleistocene forest refuge hypothesis. Evolution; International Journal of Organic Evolution 40(1): 55–67. https://doi.org/10.1111/j.1558-5646.1986.tb05717.x

Milne-Edwards H (1853) Observations sur les affinities zoologiques et la classification naturelle des crustacés. Annales des Sciences Naturelles, Zoologie, Série 3 20: 163–228.

Mvogo Ndongo PA, von Rintelen T, Schubart CD, Albrecht C, Tamesse JL, Cumberlidge N (2017a) New data on the taxonomy, ecology, and conservation of the rediscovered *Louisea edeaensis* (Bott, 1969) (Brachyura: Potamoidea: Potamonautidae), an endangered freshwater crab from Cameroon. Zootaxa 4231(2): 273–280. https://doi.org/10.11646/zootaxa.4231.2.9

Mvogo Ndongo PA, Schubart CD, von Rintelen T, Tamesse JL, Cumberlidge N (2017b) Morphological and molecular evidence for a new species of freshwater crab of the genus *Sudanonautes* Bott, 1955 (Brachyura: Potamoidea: Potamonautidae) from Cameroon, with notes on its ecology. Zootaxa 4242(1): 161–173. https://doi.org/10.11646/zootaxa.4242.1.8

Mvogo Ndongo PA, Cumberlidge N, Poettinger TS, von Rintelen T, Tamesse JL, Schubart CD (2017c) Molecular evidence for the assignment of the Cameroonian freshwater crab genus *Louisea* Cumberlidge, 1994, to the Afrotropical subfamily Potamonautinae Bott, 1970 (Crustacea: Potamoidea: Potamonautidae). Zootaxa 4286(3): 439–444. https://doi.org/10.11646/zootaxa.4286.3.12

Mvogo Ndongo PA, von Rintelen T, Albrecht C, Tamesse JL, Cumberlidge N (2018) Lost species in Cameroon: rediscovery of the endangered freshwater crab, *Louisea balssi* (Bott, 1959) (Brachyura: Potamonautidae), with notes on its ecology and conservation. Zootaxa 4231(2): 273–280. https://doi.org/10.11646/zootaxa.4231.2.9

Mvogo Ndongo PA, von Rintelen T, Cumberlidge N (2019) Taxonomic revision of the endemic Cameroonian freshwater crab genus *Louisea* Cumberlidge, 1994 (Crustacea, Decapoda, Brachyura, Potamonautidae), with descriptions of two new species from Nkongsamba and Yabassi. ZooKeys 881: 135–164. https://doi.org/10.3897/zookeys.881.36744

Mvogo Ndongo PA, von Rintelen T, Tomedi-Tabi Eyango M, Cumberlidge N (2020) Morphological and molecular analyses reveal three new endemic species of the freshwater crab genus *Buea* Cumberlidge, Mvogo Ndongo, Clark & Daniels, 2019 (Crustacea: Brachyura: Potamonautidae) from a rainforest biodiversity hotspot in Cameroon, Central Africa. Journal of Crustacean Biology 40(3): 288–300. https://doi.org/10.1093/jcbiol/ruaa019

Mvogo Ndongo PA, von Rintelen T, Cumberlidge N (2021a) A new species of the freshwater crab genus *Potamonemus* Cumberlidge & Clark, 1992 (Crustacea, Potamonautidae) endemic to the forested highlands of southwestern Cameroon, Central Africa. ZooKeys 1017: 111–125. https://doi.org/10.3897/zookeys.1017.60990

Mvogo Ndongo PA, von Rintelen T, Schubart CD, Clark PF, von Rintelen K, Missoup AD, Albrecht C, Rabone M, Ewoukem E, Tamesse JL, Cumberlidge N (2021b) Discovery of two new populations of the rare endemic freshwater crab *Louisea yabassi* Mvogo Ndongo, von Rintelen & Cumberlidge, 2019 (Brachyura: Potamonautidae) from the Ebo Forest near Yabassi in Cameroon, Central Africa, with recommendations for conservation action. Journal of Threatened Taxa 13(6): 18551–18558. https://doi.org/10.11609/jott.6724.13.6.18551-18558

Posada D, Buckley TR (2004) Model selection and model averaging in phylogenetics: Advantages of Akaike information criterion and Bayesian approaches over likelihood ratio tests. Systematic Biology 53(5): 793–808. https://doi.org/10.1080/10635150490522304

Scheiner SM, Holt RD (2012) The genetics of phenotypic plasticity. X. variation versus uncertainty. Ecology and Evolution 2(4): 751–767. https://doi.org/10.1002/ece3.217

Schubart CD (2009) Mitochondrial DNA and decapod phylogenies; the importance of pseudogenes and primer optimization. In: Martin JW, Crandall KA, Felder DL (Eds) Crustacean Issues 18: Decapod Crustacean Phylogenetics. Taylor & Francis/CRC Press, Boca Raton, Florida, 47–65.

Schubart CD, Cannicci S, Vannini M, Fratini S (2006) Molecular phylogeny of grapsoid crabs (Decapoda, Brachyura) and allies based on two mitochondrial genes and a proposal for refraining from current superfamily classification. Journal of Zoological Systematics and Evolutionary Research 44(3): 193–199. https://doi.org/10.1111/j.1439-0469.2006.00354.x

Schubart CD, Reimer J, Diesel R, Türkay M (1997) Taxonomy and ecology of two endemic freshwater crabs from western Jamaica with the description of a new *Sesarma* species (Brachyura: Grapsidae: Sesarminae). Journal of Natural History 31(3): 403–419. https://doi.org/10.1080/00222939700770201

Schubart CD, Diesel R, Hedges S (1998) Rapid evolution to terrestrial life in Jamaican crabs. Nature 393(6683): 363–365. https://doi.org/10.1038/30724

Stemmer M, Schubart CD (2016) Genetic analyses determine connectivity among cave and surface populations of the Jamaican endemic freshwater crab *Sesarma fossarum* in the Cockpit Country. International Journal of Speleology 45(1): 35–41. https://doi.org/10.5038/1827-806X.45.1.1912

Templeton AR, Crandall KA, Sing CF (1992) A cladistic analysis of phenotypic associations with haplotypes inferred from restriction endonuclease mapping and DNA sequence data. III. Cladogram estimation. Genetics 132(2): 619–633. https://doi.org/10.1093/genetics/132.2.619

Thompson JD, Higgins DG, Gibson TJ (1994) Clustal W: Improving the sensitivity of progressive multiples sequence alignments through sequence weighting, position– specific gap penalties and weight matrix choice. Nucleic Acids Research 22(22): 4673–4680. https://doi.org/10.1093/nar/22.22.4673

Villesen P (2007) FaBox: An online toolbox for Fasta sequences. Molecular Ecology Notes 7(6): 965–968. https://doi.org/10.1111/j.1471-8286.2007.01821.x

Zimkus BM (2009) Biogeographical analysis of Cameroonian puddle frogs and description of a new species of *Phrynobatrachus* (Anura: Phrynobatrachidae) endemic to Mount Oku, Cameroon. Zoological Journal of the Linnean Society 157(4): 795–813. https://doi.org/10.1111/j.1096-3642.2009.00579.x

RESEARCH ARTICLE

Taxonomic study on the genus *Xenicotela* Bates from China (Cerambycidae, Lamiinae, Lamiini)

Guanglin Xie[1,2], Maxwell V. L. Barclay[2] , Bin Chen[3]

1 *Institute of Entomology, College of Agriculture, Yangtze University, Jingzhou, Hubei, 434025, China* **2** *Department of Life Sciences, Natural History Museum, London, SW7 5BD, UK* **3** *Chongqing Key Laboratory of Vector Insects, Institute of Entomology and Molecular Biology, Chongqing Normal University, Chongqing, 401331, China*

Corresponding authors: Maxwell V. L. Barclay (m.barclay@nhm.ac.uk), Bin Chen (bin.chen@cqnu.edu.cn)

Citation: Xie G, Barclay MVL, Chen B (2022) Taxonomic study on the genus *Xenicotela* Bates from China (Cerambycidae, Lamiinae, Lamiini). ZooKeys 1122: 145–158. https://doi.org/10.3897/zookeys.1122.86344

Abstract

A taxonomic review of the Chinese species of the genus *Xenicotela* Bates, 1884 is presented. A new species, *Xenicotela griseomaculata* **sp. nov.**, is described from Chongqing, China, and a new combination, *Xenicotela convexicollis* (Gressitt, 1942) **comb. nov.**, is proposed.

Keywords

Introduction

The genus *Xenicotela* was established based on *Xenicotela fuscula* Bates from Higo (Japan), (presently considered a synonym of *Xenicotela pardalina* (Bates, 1884)), as a result of a comparison with the similar genus *Xenolea* Thomson (Bates 1884). Up to now, three species: *X. pardalina* (Bates, 1884), *X. distincta* (Gahan, 1888), and *X. bimaculata* (Pic, 1925) are known from Japan, South Korea, China, Vietnam, Laos, Nepal, and India. Among them, only one species, *X. distincta*, has been recorded in China (Cho et al. 1963; Hubweber et al. 2010; Kariyanna et al. 2017; Lin and Tavakilian 2019; Tavakilian and Chevillotte 2021).

In the present study, a new species, *Xenicotela griseomaculata* sp. nov., is described and illustrated from Chongqing, China. *Monochamus convexicollis* Gressitt, 1942 is transferred to *Xenicotela* based on the examination of the holotype and three specimens from the type locality and its adjacent area.

Materials and methods

Specimens from the following institutional collections were examined and/or photographed in this study:

IZAS Institute of Zoology, Chinese Academy of Sciences, Beijing, China;
NHMUK Natural History Museum, London, UK;
MNHN Muséum National d'Histoire Naturelle, Paris, France;
SWU Southwest University, Chongqing, China;
CQNU Chongqing Normal University, Chongqing, China;
YZU Yangtze University, Jingzhou, China;
GZNULS School of Life Sciences, Guizhou Normal University, Guiyang, China.

The genitalia were prepared by soaking the whole beetle in boiling water for several minutes, then opening the abdomen from the apex along the dorsopleural margin. The genitalia were then removed with fine forceps and ophthalmic scissors, and later cleared in 10% KOH at 80–100 °C for several minutes.

All habitus photographs were taken with a Canon 5D Mark II digital camera equipped with a Canon EF 100mm f/2.8L IS USM lens, and genitalia images were taken with a Leica DFC450 digital camera mounted on a Leica M205A microscope. Images of genitalia were taken by keeping them in glycerin. All images were edited using Adobe Photoshop 2020.

Taxonomy

Genus *Xenicotela* Bates, 1884

Xenicotela Bates, 1884: 242; Matsushita 1933: 346; Breuning 1944: 372; Gressitt 1951: 381; Breuning 1961: 353; Rondon and Breuning 1970: 458; Makihara 2007; Hubweber et al. 2010: 288; Lin and Tavakilian 2019: 324.

Type species. *Xenicotela fuscula* Bates, 1884 (= *Xenicotela pardalis* (Bates, 1884))

Redescription. Body small, elongated. Eyes coarsely faceted. Antennae slender, more than 2.0 times as long as body in male and nearly 2.0 times in female; several basal antennomeres sparsely fringed ventrally, antennomeres III–XI annulated with greyish white to greyish yellow pubescence basally and apically; antennal tubercle moderately elevated;

scape short, rather robust, with a narrow and completely closed cicatrix at apex, distinctly constricted near the apex; antennomere III distinctly longer than fourth, about 2.0 times as long as scape. Pronotum broader than long, anterior and posterior margin with vague transverse grooves, each side with a coniform spine at middle. Elytra elongated, with sub-parallel sides, apices rounded. Prosternal process lower than procoxae, arched, procoxal cavities closed posteriorly. Mesosternal process obliquely sloping anteriorly, not tuberculate, mesocoxal cavities open at side. Metasternum normal in length. Legs moderately long, femora clavate, mesotibia without groove near external apex, claw widely divergent.

Distribution. Japan, South Korea, China, Vietnam, Laos, Nepal, India.

Comments. The genus is characterized by the following combination of characters that distinguishes it from similar genera: antennae with basal several antennomeres (usually five segments) sparsely fringed with short setae ventrally, antennomeres III–XI annulated with greyish white to greyish yellow pubescence basally and apically; scape with a narrow and completely closed cicatrix at apex and distinctly constricted before it; lateral spine of pronotum coniform, short; mesosternal process obliquely sloping anteriorly, not tuberculate; mesotibia without groove near external apex.

Aurivillius (1922) placed the genus *Xenicotela* in the tribe Dorcaschematini. Subsequently, Matsushita (1933) defined the tribe Xenicotelini for the genus according to the following differences on the basis of comparing with tribes Ancylonotini and Prosopocerini: scape with a completely closed apical cicatrix and mesotibia without a groove near the external apex. Breuning (1943) transferred the genus into Agniinii, and Gressitt (1951) placed it in Lamiini. Kariyanna et al. (2017) and Tavakilian and Chevillotte (2021) followed Matsushita's decision and put the genus into Xenicotelini in their Cerambycidae database. In the present study, we follow Breuning's and Gressitt's arrangement, since the characters of *Xenicotela* correspond well with Lamiini.

Xenicotela distincta (Gahan, 1888)
Figs 1, 2, 7, 8, 10, 12, 13, 22, 23

Monohammus distinctus Gahan, 1888: 392; Aurivillius 1922: 95. Type locality: Assam, India.
Xenicotela distincta: Breuning 1944: 373; Gressitt 1951: 382; Rondon and Breuning 1970: 458; Hubweber et al. 2010: 288; Weigel et al. 2013: 288; Kariyanna et al. 2017: 253; Lin and Tavakilian 2019: 324.
Nephelotus 4-maculatus Pic, 1925: 16. Type locality: Tonkin, Vietnam.
Nephelotus tonkineus Pic, 1926: 143. Type locality: Hoa-Binh, Vietnam.
Xenicotela distincta m. *tonkinensis* Breuning, 1944: 373.
Monochamus binigricollis: Wang 1998: 599, misidentification.

Type material examined. *Holotype* of *Monohammus distinctus* Gahan (NHMUK), the label details are shown in Fig. 7. ***Holotype*** of *Nephelotus tonkineus* Pic (MNHN), the label details are shown in Fig. 10.
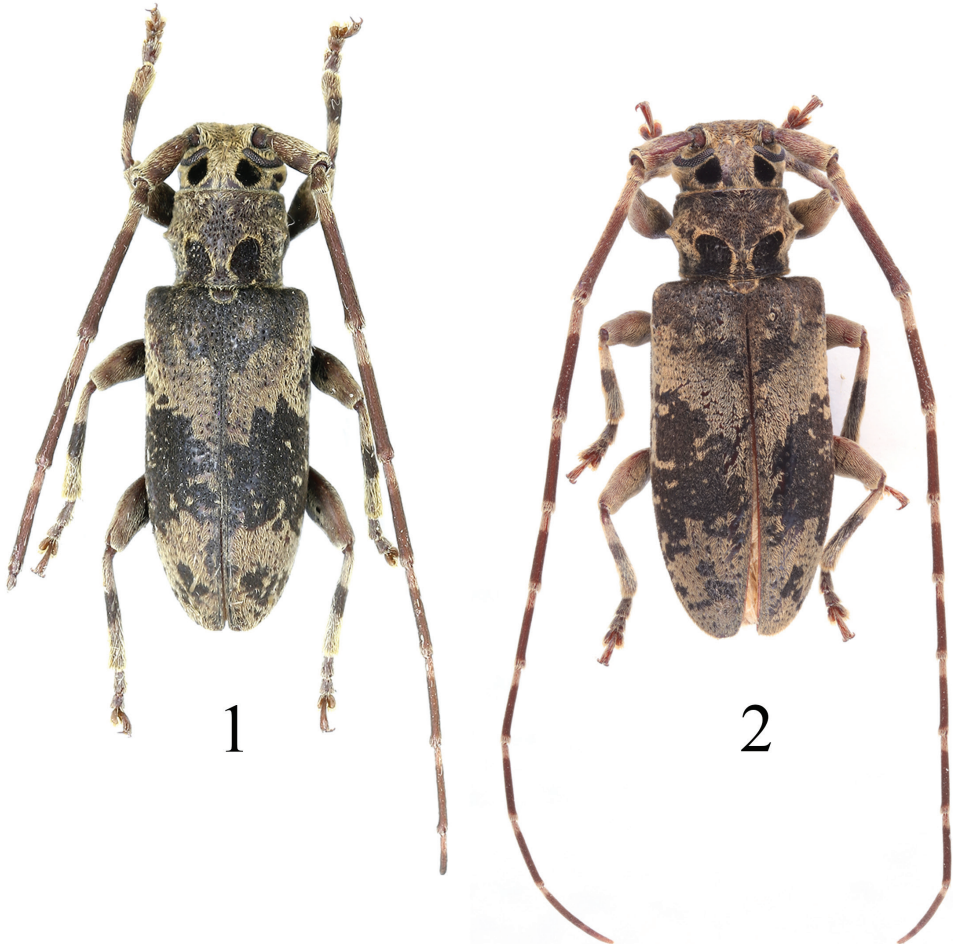
Figures 1, 2. Habitus of *Xenicotela distincta* (Gahan, 1888) **1** male **2** female **1** from Yunnan: Jiangcheng **2** from Guizhou: Ziyun.

Other materials examined. One male, Cʜɪɴᴀ: Yunnan Province, Cangyuan County, Daheishan, alt. 2400 m, May 15, 1980, coll. by Kaiquan Li (SWU); One female, Cʜɪɴᴀ: Guizhou Province, Ziyun County, Nazuo Village, June 8, 2019, coll. by Shulin Yang (GZNULS); one female, Cʜɪɴᴀ: Yunnan Province, Xishuangbanna Prefecture, Danuoyou, May 29, 2008, coll. by Meiying Lin (IZAS); one male, Cʜɪɴᴀ: Yunnan Province, Jiangcheng County, Qushui Township, alt. 564 m, 22°37'1"N, 102°9'49"E, June 8, 2019, coll. by Lanbin Xiang (YZU).

Redescription. Male. Body length 10.0 mm, humeral width 3.4 mm. Body mostly black brown to black, densely clothed with greyish yellow and black pubescence forming markings. Antennae dull reddish brown, scape and extreme apex of pedicel clothed with greyish yellow pubescence, base and extreme apex of antennomeres III–XI annulated with greyish yellow pubescence. Head provided with two slightly quadrate black pubescent spots behind upper lobes of eyes, pronotum also provided with two suboval

black spots of the same texture at the posterior half, distinctly edged with greyish yellow pubescence and widely separated anteriorly. Scutellum bordered by greyish yellow pubescence. Elytra mostly black brown to black at base, with a broad transverse black band intermingled with some irregular small greyish yellow pubescent spots at middle, mostly clothed with greyish yellow pubescence intermingled with some irregular black spots at apex. Ventrites I–IV fringed with long setae at posterior edge. Legs with femora and tibiae black brown medially, with a greyish yellow pubescent ring at base and apex.

Head finely and densely punctate, frons transverse, lower lobe of eyes about as long as gena. Pronotum broader than long, deeply and slightly densely punctate, lateral spine short and small. Scutellum short, ligulate. Elytra elongate, about 2.1 times as long as width across humeri, subparallel in basal two-thirds, gradually narrowed backwards in apical third, apices slightly transversely truncate, surface deeply and slightly coarsely punctate. Legs relatively short, claws divaricate.

Female. Similar to male, body sometimes mostly reddish brown; antennae relatively short; lateral spine of pronotum larger than that of male; elytra about 2.0 times as long as humeral width, median band sometimes interrupted by a sutural pubescent strip.

Male genitalia. Tergite VIII (Figs 12, 13) with both sides relatively circularly converge to apex, apex slightly truncated, clothed with short to medium straight setae along apical and lateral sides. Tegmen (Figs 22, 23) length approximately 1.73 mm, maximum width of ringed part approximately 0.66 mm, each paramere length approximately 0.37 mm, basal width approximately 0.19 mm; parameres widely separated at apex, with length-width ratio of each lobe about 1.95, rounded at apex, about apical two-fifths clothed with sparse setae of different lengths and thicknesses. Median lobe (Figs 22, 23) slightly longer than tegmen, obviously arcuate in lateral view, apical margin of dorsal plate and ventral plate nearly straight; median struts relatively broad, about two-fifths length of median lobe.

Distribution. China (Yunnan, Guizhou), India, Vietnam, Nepal, Laos.

Comments. Wang (1998) first recorded *Monochamus binigricollis* Breuning, 1965 from China based on specimens from Guizhou (Wangmo) and Yunnan (Cangyuan). However, after examination of the specimens, we found that they were misidentified, and actually belong to *X. distincta* (Fig. 8). According to the information currently available, *M. binigricollis* should be excluded from the fauna of China. *M. binigricollis* needs to be transferred to the genus *Xenicotela* Bates. This issue will be discussed and processed in a separate paper.

Xenicotela convexicollis (Gressitt, 1942) comb. nov.

Figs 3, 4, 9, 11, 16–21

Monochamus convexicollis Gressitt, 1942: 83. Type locality: Zhejiang (Tianmushan), China. Gressitt, 1951: 393; Chou 2004: 296; Hubweber et al. 2010: 282; Lin and Tavakilian 2019: 310.

Type material examined. ***Holotype*** (female, IZAS), the label details are shown in Fig. 9.
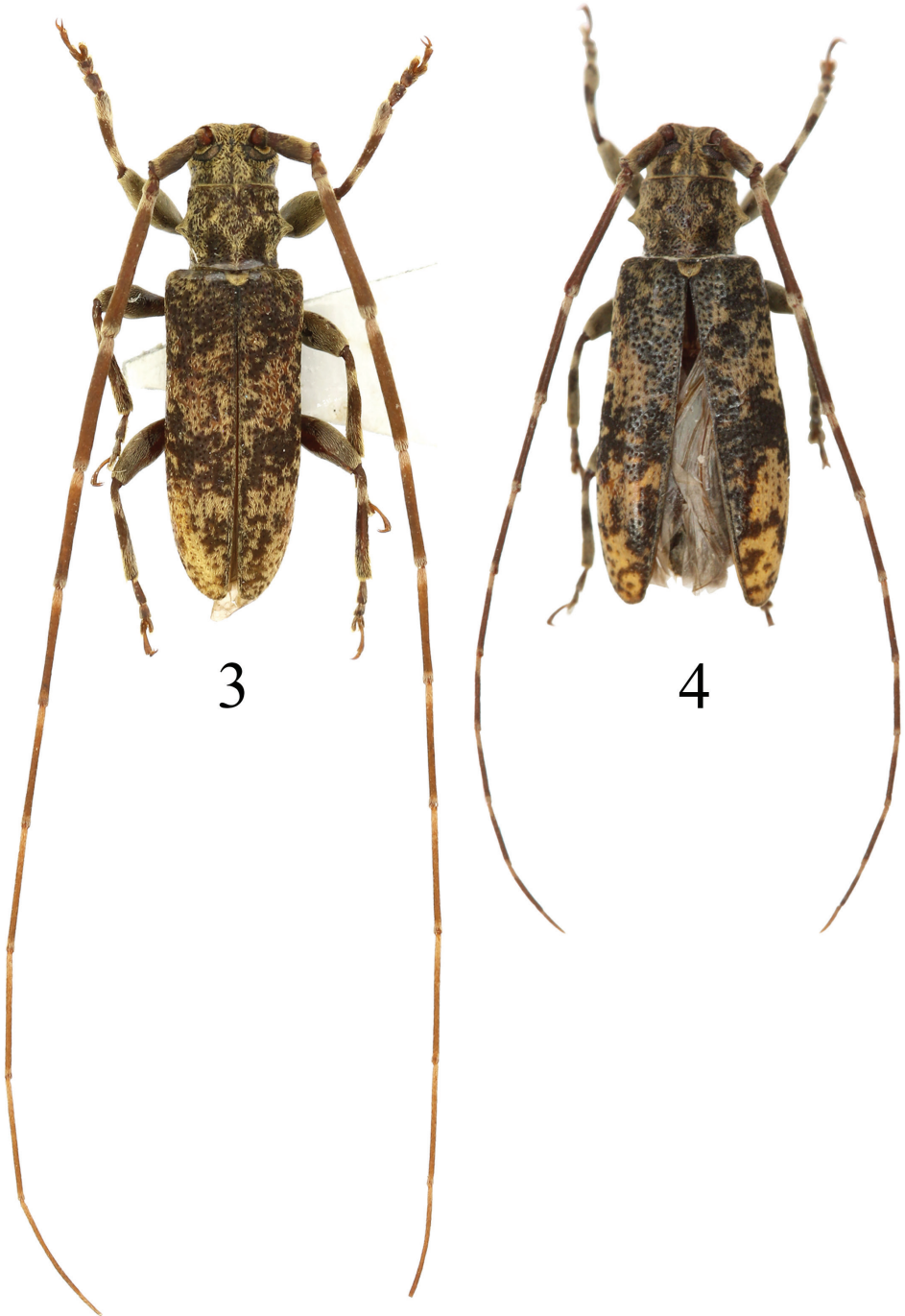
Figures 3, 4. Habitus of *Xenicotela convexicollis* (Gressitt, 1942) comb. nov. **3** male **4** female, from Zhejiang: West Tianmushan

Other materials examined. One male and one female: China, Zhejiang, Lin'an, West Tianmushan, July 13, 2012, collected by Guanglin Xie (YZU); one female: China, Zhejiang, Lin'an, Qingliangfeng, May 22, 2012, collected by Guanglin Xie (YZU).

Redescription. Male. Body length 11.0 mm, humeral width 3.5 mm. Body mostly black brown, clothed with greyish yellow to pale yellow pubescence, with mottled patches of black and yellow on dorsal surface. Maxillary and labial palpi reddish brown. Antennae dull reddish brown, basal four antennomeres and base of fifth antennomere fringed with very sparse greyish yellow setae, antennomeres III–XI densely annulated with greyish yellow pubescence basally and apically, antennomeres III–V weakly thickened. Pronotum with posterior half furnished with two subparallel longitudinal black stripes of which apex of inner edge bent outward, with anterior half provided with two small stripes obliquely extend outward posteriorly (but indistinct on the holotype). Scutellum clothed with pale yellow pubescence. Elytra unevenly clothed with pale yellow pubescence mottled with various black spots, presenting an incomplete black transverse band behind the middle and mostly black at base. Tibiae black brown, clothed with greyish yellow pubescence forming a subbasal and an apical annulus.

Head finely punctate, frons quadrate, slightly bulging; eyes coarsely faceted, lower lobe longer than broad, about as long as gena. Antennae slender, about 2.8 times as long as body; antennal tubercle moderately raised; scape short, slightly swollen medially; antennomere III distinctly longer than antennomere IV, about 2.5 times as long as scape; antennomeres IV–X nearly equal in length. Pronotum transverse, finely punctate, convex, with centre slightly flat; anterior and posterior margins with vague transverse sulci, each side with a conical spine, short and blunt. Scutellum short, ligulate. Elytra elongated, about 2.3 times as long as width across humeri, with subparallel sides and rounded apices; surface coarsely punctate, the punctures gradually becoming finer towards apex; disc slightly raised at center of basal fourth, followed by a weak central depression along suture. Legs moderately long, with femora slightly swollen medially; prefemur stouter than mesofemur and metafemur; mesotibia without a groove near external apex, metafemur reaching the end of third abdominal segment, claw divaricate.

Female. Length 11.0–12.0 mm, humeral width 3.0–3.5 mm. Similar to male, maxillary and labial palpi mostly blackish brown, each side of occiput provided with a black maculation behind upper eye lobe, antennae about 1.8 times as long as body, pronotal lateral spine conical, more cuspidal.

Male genitalia. Tergite VIII (Fig. 11) with both sides converging straight to apex, apex broadly truncated, clothed with short to medium straight setae along apical and lateral sides. Tegmen (Figs 16, 17) length approximately 1.64 mm, maximum width of ringed part approximately 0.52 mm, each paramere length approximately 0.38 mm, basal width approximately 0.17 mm; parameres widely separated at apex, with length-width ratio of each lobe about 2.41, rounded at apex, about apical two-fifths clothed with sparse setae of different lengths and thicknesses. Median lobe (Figs 16, 17) about as long as tegmen, slightly arcuate in lateral view, apical margin of dorsal plate and ventral plate nearly straight; median struts relatively broad, about half length of median lobe.

Female genitalia. Bursa copulatrix (Fig. 21) long, bursiform, slightly expanded apically. Spermatheca (Fig. 21) inserts into the bursa copulatrix at fourth of blind end. Spermathecal duct rather short. Spermathecal capsule approximately S-shaped, tubular, consisting of a basal membranous and an apical strongly sclerotized part, sclerotized tube starts from the second bend and overlaps with membranous part, with blind end slightly curved and expanded. Spermathecal gland located at the joint of membranous and sclerotized part.

Distribution. China (Zhejiang, Taiwan).

Comments. Gressitt (1942) described the species based on a female specimen and originally placed it in the genus *Monochamus* Dejean, 1821. However, after careful examination of the holotype, we conclude that it belongs to the genus *Xenicotela* Bates. This species has the antennae distinctly constricted before the cicatrix, antennomeres III–V clearly fringed with sparse greyish yellow setae ventrally, antennomeres III–XI with the base and extreme apex annulated with greyish yellow pubescence; the pronotum provided with a small, short and conical spine and the mesotibia without a groove, which are well matched with genus *Xenicotela*. Especially, the mesotibia lacks a groove and the antennomeres III–V are clearly fringed with setae, which are obviously different from genus *Monochamus*.

Although the holotype (Fig. 8) does not present black spots on the pronotum, the male and female specimens from the type locality and its adjacent place show distinct black spots on the pronotum (Figs 3, 4). Chou (2004) first recorded this species in Taiwan, China; according to his photographs, there are also distinct black spots on the pronotum. Therefore, we speculate that improper preservation of the holotype may have led to the black spots on the pronotum not being visible.

The species is very similar to *Xenicotela pardalina* (Bates, 1884), however, it can be distinguished from the latter by the lower lobe of the eyes not longer than the gena, and by the elytral base with less light-coloured pubescence, while in *X. pardalina*, the lower lobe is distinctly longer than the gena and the base of elytra is mostly clothed with light-coloured pubescence.

Xenicotela griseomaculata sp. nov.

https://zoobank.org/9BB0B30A-2926-4928-91D7-B349FAAC35B5

灰斑殷天牛

Figs 5, 6, 14, 15, 24, 25

Type material. *Holotype*: male, CHINA: Chongqing, Wuxi County, Xiabao township, Shuanghe Village, 31°21'4"N, 109°11'24"E, July 26, 2019, coll. by Bin Chen. The holotype is temporarily stored in the Entomological Museum of Yangtze University (YZU).

Description. Male. Body length 12.5 mm, humeral width 4.1 mm. Body mostly black, with greyish yellow, greyish white, brown and black pubescence, with slight mottled maculae. Head with greyish yellow pubescence, denser on gena and around the eyes, and with a subrounded black velvet spot on each side of occiput behind
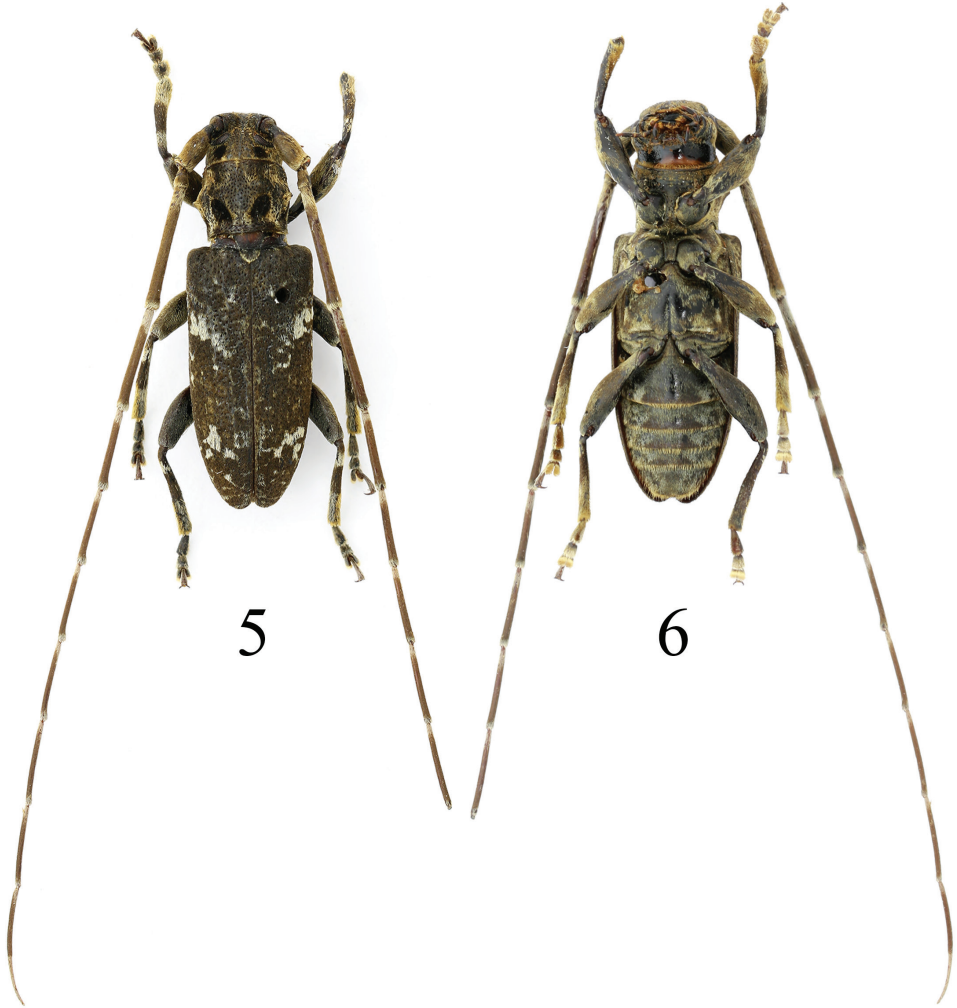
Figure 5, 6. Habitus of *Xenicotela griseomaculata* sp. nov. Holotype, male, from Chongqing: Wuxi.

eyes. Antennae mostly clothed with greyish yellow pubescence, fringed with sparse short greyish yellow setae ventrally from first to fifth antennomere; base of scape naked, black, apex of scape and pedicel with slightly greyish white pubescence, bases and extreme apices from antennomeres III–X, base and apical two-fifths of antennomere XI with greyish white pubescence. Pronotum with pubescence greyish yellow mixed with greyish white and brown giving a mottled appearance, each side behind the middle with an oblong black velvet spot edged with mottle of greyish yellow and greyish white, of which the apices obliquely extended outwards and widely separated from each other, the inner edge curved outwards anteriorly. Scutellum with greyish white pubescence, thicker on edge. Elytra with fine and close greyish yellow to brown pubescence, decorated with greyish white pubescent spots as following:
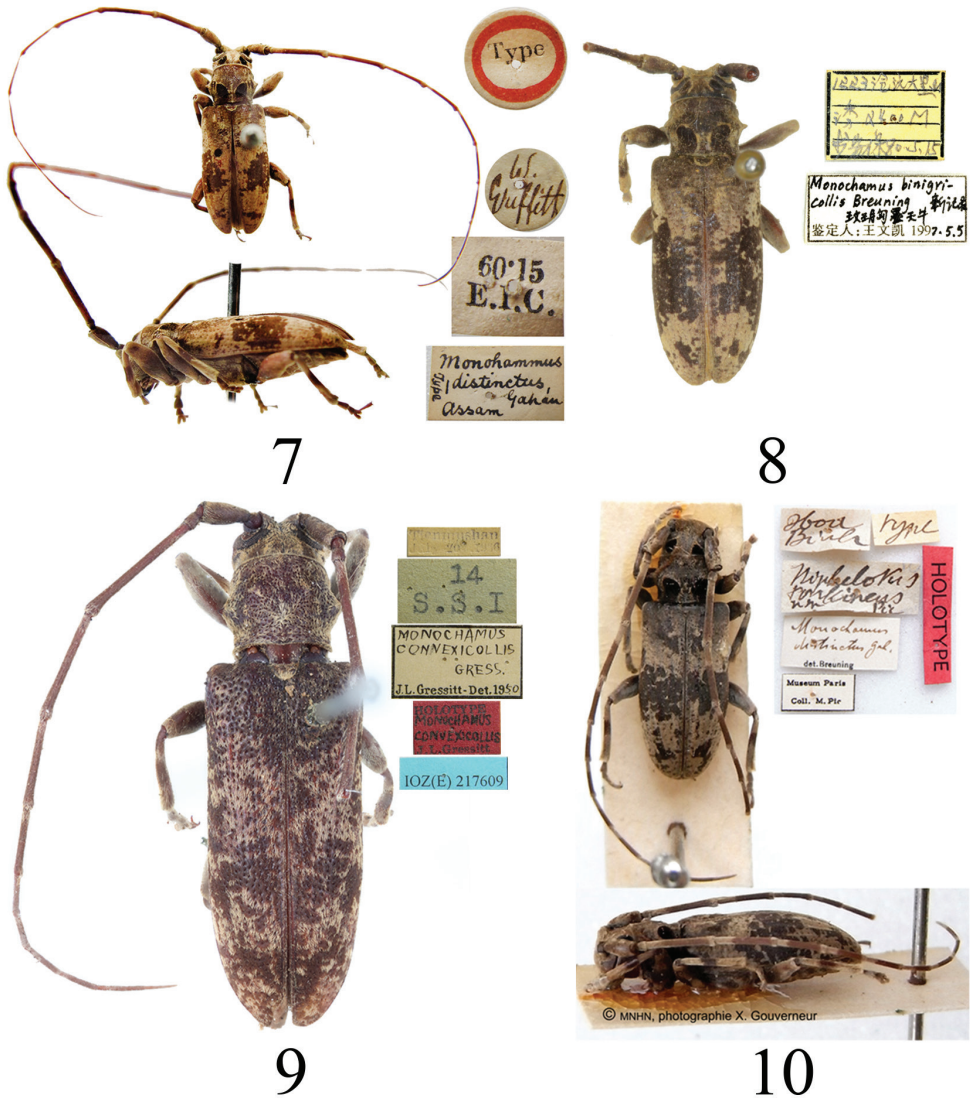
Figures 7–10. Habitus of *Xenicotela* spp. **7** holotype of *Monohammus distinctus* Gahan, 1888 **8** *Xenicotela distincta* (Gahan, 1888) **9** holotype of *Monochamus convexicollis* Gressitt, 1942 **10** holotype of *Nephelotus tonkineus* Pic, 1926.

each elytron with a conspicuous oblique band after basal fourth, and an incomplete transverse band composed of several irregular spots, before and after the two bands scattered with several small irregular spots. Legs mostly with greyish yellow pubescence, femora only the extreme apex slightly greyish white, tibiae with four pubescent rings alternating black and greyish yellow from base to apex. Ventral surface with non-uniform greyish yellow pubescence, posterior margin of each abdominal sternite fringed with ochraceous pubescence.
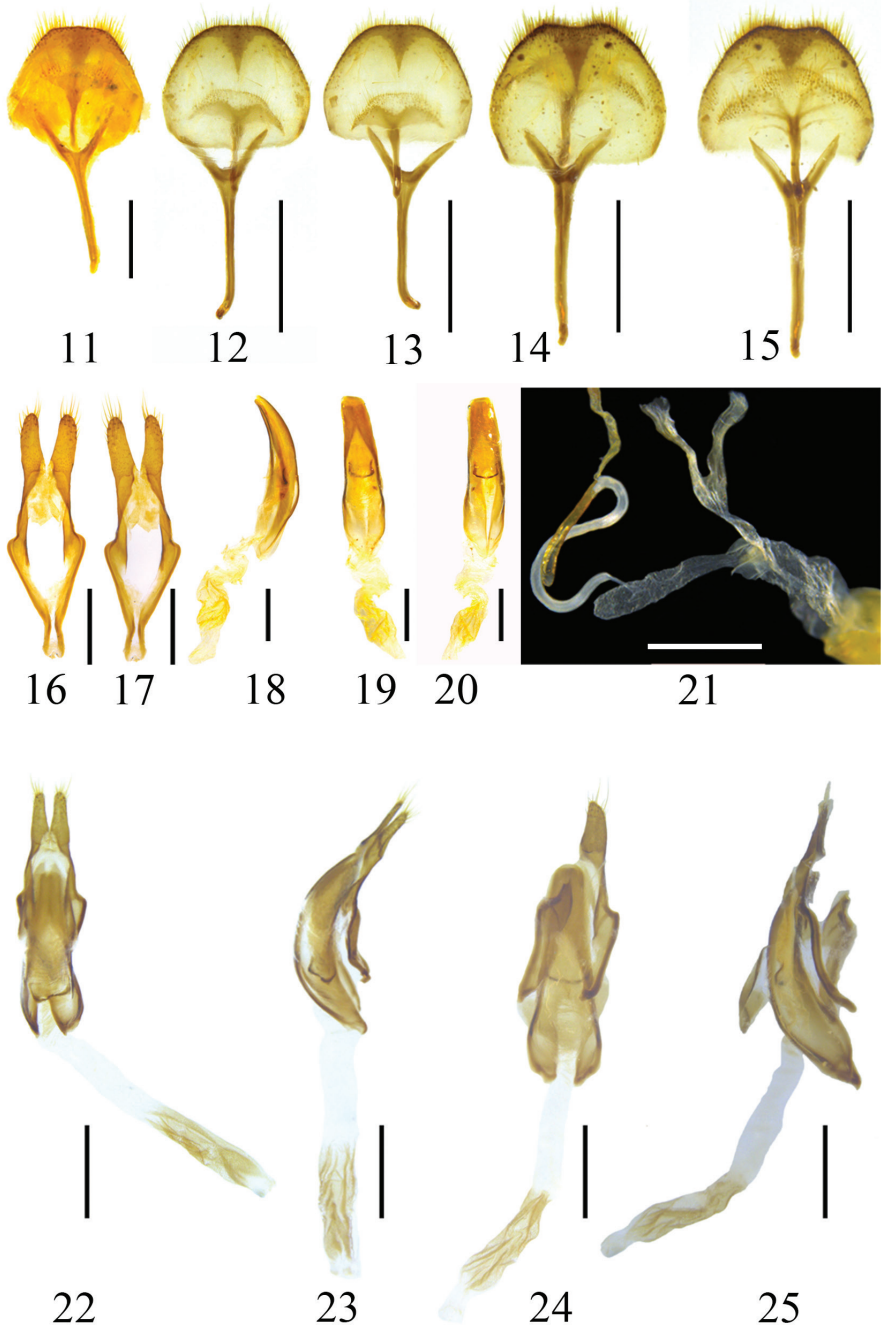
Figures 11–25. Habitus of *Xenicotela* spp. **11–15** tergite VIII with sternites VIII & IX **16, 17** tegmen **18–20** aedeagus **21** female genitalia **22–25** phallus **11, 13, 15, 17, 19, 24** ventral view **12, 14, 16, 20, 22** dorsal view **18, 23, 25** lateral view **11, 16–21** *Xenicotela convexicollis* (Gressitt, 1942) comb. nov. **12, 13, 22, 23** *Xenicotela distincta* (Gahan, 1888) **14, 15, 24, 25** *Xenicotela griseomaculata* sp. nov. Scales: 0.5 mm (**11, 16–20**); 1 mm (**12–15, 21–25**).

Head finely and closely punctate, frons transverse, slightly convex, with a smooth fine longitudinal medium sulcus extending to occiput. Eyes coarsely faceted, lower lobe longer than broad, shorter than gena. Antennae slender, about 2.5 times as long as body; antennal tubercles rather elevated, separated from each other; scape stout, slightly flat, with base strongly decrescent and apex distinctly constricted before cicatrix; antennomere III longest, about 2.5 times as long as scape; antennomere IV longer than antennomere V. Pronotum broader than long, anterior margin subequal to posterior margin; each side with a short spine, coniform, blunt apically; disc slightly convex, finely punctate. Scutellum lingulate. Elytra slightly elongated, about 2.0 times as long as width across humeri, gradually narrowing towards apex, apices individually rounded; surface coarsely punctate on base, gradually finer towards apex, middle of basal fourth slightly longitudinally raised. Ventral surface without distinct punctures, procoxal cavities closed posteriorly, mesocoxal cavities open at side, mesosternal process obliquely sloping anteriorly, not tuberculate; apex of terminal abdominal ventrite nearly straight, emarginate medially. Legs moderately long, femora slightly clavate, claws divaricate.

Male genitalia. Tergite VIII (Figs 14, 15) with both sides relatively circularly converge to apex, apex slightly emarginated, clothed with short to medium straight setae along apical and lateral sides. Tegmen (Figs 24, 25) length approximately 1.92 mm, one paramere length approximately 0.48 mm, basal width approximately 0.26 mm, the length-width ratio of paramere about 1.85, rounded at apex, about apical two-fifths clothed with sparse setae of different lengths and thicknesses (tegmen was damaged during dissection and another paramere was lost). Median lobe (Figs 24, 25) slightly longer than tegmen, slightly arcuate in lateral view, apical margin of dorsal plate and ventral plate nearly straight; median struts relatively broad, about two-fifths length of median lobe.

Female. Unknown.

Distribution. China: Chongqing.

Etymology. The species is named for the pattern of the elytra, with greyish white pubescent maculae.

Comments. The new species is differentiated from the other species of the genus by the elytra with two incomplete greyish white bands. The new species is similar to *M. binigricollis* in general appearance (it will be transferred to the genus *Xenicotela* in a separate work); however, it can be easy distinguished from the latter by each elytron with apical fourth mostly dull dark brown, furnished with an incomplete greyish white band consisting of several pubescent spots of different sizes, instead of mostly light in colour, dotted with dark spots of various sizes and shapes.

References

Aurivillius C (1922) Cerambycidae: Lamiinae I. In: Schenkling S (Ed.) Coleopterorum Catalogus auspiciis et auxilio W. Junk, pars 73, Cerambycidae: Lamiinae. W. Junk, Berlin, 1–322. https://www.biodiversitylibrary.org/page/10202648

Bates H (1884) Longicorn beetles of Japan. Additions, chiefly from the later collections of Mr. George Lewis; and notes on the synonymy, distribution, and habits on the previously known species. Journal of the Linnean Society of London, Zoology 18(106): 205–262. https://doi.org/10.1111/j.1096-3642.1884.tb02047.x

Breuning S (1943) Études sur les Lamiaires (Coleopter, Cerambycidae): Douzième tribu: Agniini Thomson. Novitates Entomologicae, 3ème supplément (89–106): 137–280.

Breuning S (1944) Études sur les Lamiaires (Coleopter, Cerambycidae): Douzième tribu: Agniini Thomson. Novitates Entomologicae, 3ème supplément (107–135): 281–512.

Breuning S (1961) Catalogue des Lamiaires du Monde (Coleoptera, Cérambycidae) 5. Lieferung. Tutzing, Museum G. Frey, 287–382.

Cho PS, Yang SY, Yoon IB (1963) Unrecorded species of Cerambycidae from Korea. The Korean Journal of Zoology 6(1): 3–4. http://www.koreascience.or.kr/article/JAKO196311919895649.pdf

Chou WI (2004) Iconography of longhorn beetles in Taiwan. Owl Press, Taiwan, 408 pp.

Gahan CJ (1888) On new Lamiide Coleoptera belonging to the *Monohammus* Group. The Annals and Magazine of Natural History, Sixth Series, 2(11): 389-401.

Gressitt JL (1942) Nouveaux longicornes de la Chine Orientale. Notes d'Entomologie Chinoise 9(5): 79–97.

Gressitt JL (1951) Longicorn beetles of China. Longicornia 2: 1–667.

Hubweber L, Löbl I, Morati J, Rapuzzi P (2010) Family Cerambycidae Latreille, 1802. Taxa from the People's Republic of China and Japan: tribe Monochamini Gistel, 1848. In: Löbl I, Smetana A (Eds) Catalogue of Palaearctic Coleoptera. Vol. 6. Chrysomeloidea. Apollo Books, Stenstrup, 274–288.

Kariyanna B, Mohan M, Gupta R, Vitali F (2017) The checklist of longhorn beetles (Coleoptera: Cerambycidae) from India. Zootaxa 4345(1): 1–317. https://doi.org/10.11646/zootaxa.4345.1.1

Lin MY, Tavakilian GL (2019) Subfamily Lamiinae Latreille, 1825. In: Lin MY, Yang XK (Eds) Catalogue of Chinese Coleoptera, Vol. 9. Chrysomeloidea. Vesperidae, Disteniidae, Cerambycidae. Science Press, Beijing, 216–408.

Makihara H (2007) Lamiinae: Lamiini. In: Ohbayashi N, Niisato T (Eds) Longicorn beetles of Japan. Tokai University Press, Hadano-shi, 304–308, 576–605.

Matsushita M (1933) Beitrag zur Kenntnis der Cerambyciden des Japanischen Reichs. Journal of the Faculty of Agriculture 34(2): 157–445. https://eprints.lib.hokudai.ac.jp/dspace/bitstream/2115/12697/1/34%282%29_p157-445.pdf

Pic M (1925) Coléoptères exotiques en partie nouveaux (Suite.). L'Échange. Revue Linnéenne 41(422): 15–16.

Pic M (1926) Nouveaux Coléoptères du Tonkin, III. Bulletin de la Société Zoologique de France 51(1): 143–144. https://doi.org/10.3406/bsef.1926.27685

Rondon JA, Breuning S (1970) Lamiines du Laos. Pacific Insects Monograph 24: 315–571.

Tavakilian GJ, Chevillotte H (2021) Titan: base de données internationales sur les Cerambycidae ou Longicornes. http://titan.gbif.fr/index.html [Accessed on 28 April 2022]

Wang WK (1998) New records of Cerambycid-beetles in China (Coleoptera: Cerambycidae). Journal of Southwest Agricultural University 20(5): 597–600.

Weigel A, Meng LZ, Lin MY (2013) Contribution to the Fauna of Longhorn Beetles in the Naban River Watershed National Nature Reserve. Formosa Ecological Company, Taiwan, 219 pp.

RESEARCH ARTICLE

Three new fold-winged crane flies of the genus *Ptychoptera* Meigen, 1803 (Diptera, Ptychopteridae) from southern China

Zehui Kang[1], Gang Gao[1], Xiao Zhang[1], Ding Yang[2], Junping Wang[1]

1 *Shandong Engineering Research Center for Environment-Friendly Agricultural Pest Management, College of Plant Health and Medicine, Qingdao Agricultural University, Qingdao 266109, China* **2** *College of Plant Protection, China Agricultural University, Beijing 100193, China*

Corresponding authors: Zehui Kang (kangzehui1987@163.com), Junping Wang (junpingwang@qau.edu.cn)

Citation: Kang Z, Gao G, Zhang X, Yang D, Wang J (2022) Three new fold-winged crane flies of the genus *Ptychoptera* Meigen, 1803 (Diptera, Ptychopteridae) from southern China. ZooKeys 1122: 159–172. https://doi.org/10.3897/zookeys.1122.86483

Abstract

Three new *Ptychoptera* Meigen, 1803 species from southern China, *P. hekouensis* **sp. nov.**, *P. longa* **sp. nov.**, and *P. xiaohuangshana* **sp. nov.**, are described and illustrated. These new species are mainly distinguished from congeners by their body colors and male genitalia. The genus *Ptychoptera* is recorded from Guangdong, China for the first time. An updated key to all Chinese *Ptychoptera* species is provided.

Keywords

Introduction

The family Ptychopteridae, also known as fold-winged crane flies, is a group of slender tipulid-like flies in the lower Diptera. Ptychopteridae are divided into subfamilies Bittacomorphinae and Ptychopterinae. The genus *Ptychoptera* Meigen, 1803 is the only extant genus in subfamily Ptychopterinae and can be easily distinguished by the antennae in adults with 13 flagellomeres, the wing with M_{1+2} forked, and the gonopod with a simple gonocoxite (Alexander 1981; Rozkošný 1997; Nakamura and Saigusa 2009).

Nineteen *Ptychoptera* species have been known to occur in China. Charles P. Alexander described three *Ptychoptera* species from China during 1924–1937 (Alexander 1924, 1935, 1937). More than half a century later, three new Chinese species were published by Yang and Chen (1995, 1998) and Yang (1996). More recently, 13 species were added to the fauna of China by Kang et al. (2013, 2019), Zhang and Kang (2021), and Shao and Kang (2021).

In the present paper, three *Ptychoptera* species from southern China – *P. hekouensis* sp. nov. from Yunnan Province, *P. longa* sp. nov. from Guizhou Province, and *P. xiaohuangshana* sp. nov. from Guangdong Province – are described and illustrated, recording the genus *Ptychoptera* for the first time from Guangdong. In addition, the key by Zhang and Kang (2021) is updated to include all Chinese species of *Ptychoptera*.

Materials and methods

Adults were collected by entomological net and kept in 75% alcohol. Type specimens are deposited in the Entomological Museum of China Agricultural University, Beijing, China (CAU). Photographs were taken by a Canon EOS-90D and EF 100 mm f/2.8L IS USM. Genitalia were prepared by immersing the apical portion of the abdomen in warm lactic acid for 0.5–1 h. Afterwards, they were examined and illustrations prepared by using a ZEISS Stemi 2000-C stereomicroscope. After examination, the removed abdomen was transferred to fresh glycerine and stored in a microvial pinned to the respective specimen. Morphological terminology is based primarily on McAlpine (1981) and Fasbender (2014).

Taxonomy

Check list of Chinese *Ptychoptera* species

Ptychoptera bannaensis Kang, Yao & Yang, 2013 (Yunnan)
Ptychoptera bellula Alexander, 1937 (Jiangxi, Zhejiang)
Ptychoptera circinans Kang, Xue & Zhang, 2019 (Fujian)
Ptychoptera clitellaria Alexander, 1935 (Sichuan)
Ptychoptera cordata Zhang & Kang, 2021 (Yunnan)
Ptychoptera emeica Kang, Xue & Zhang, 2019 (Sichuan)
Ptychoptera formosensis Alexander, 1924 (Taiwan; Japan)
Ptychoptera gutianshana Yang & Chen, 1995 (Zhejiang)
Ptychoptera hekouensis sp. nov. (Yunnan)
Ptychoptera lii Kang, Yao & Yang, 2013 (Guizhou)
Ptychoptera longa sp. nov. (Guizhou)
Ptychoptera longwangshana Yang & Chen, 1998 (Zhejiang)
Ptychoptera lucida Kang, Xue & Zhang, 2019 (Xinjiang)
Ptychoptera lushuiensis Kang, Yao & Yang, 2013 (Yunnan)
Ptychoptera qinggouensis Kang, Yao & Yang, 2013 (Neimenggu)

Ptychoptera separata Kang, Xue & Zhang, 2019 (Xizang)
Ptychoptera tianmushana Shao & Kang, 2021 (Zhejiang)
Ptychoptera wangae Kang, Yao & Yang, 2013 (Yunnan)
Ptychoptera xiaohuangshana sp. nov. (Guangdong)
Ptychoptera xinglongshana Yang, 1996 (Gansu)
Ptychoptera yankovskiana Alexander, 1945 (Neimenggu; Korea)
Ptychoptera yunnanica Zhang & Kang, 2021 (Yunnan)

Updated key to *Ptychoptera* from China

1　　Wing with r-m arising from R_{4+5} after Rs fork, Rs not longer than r-m **2**
–　　ing with r-m arising from Rs before or at Rs fork, Rs at least 1.5 times length of r-m (Fig. 2a–c) **10**
2　　Mesopleuron mostly brown (Fig. 1c, e); epandrial clasper brown ....
　　...***P. circinans***
–　　Mesopleuron uniformly yellow (Fig. 1a); epandrial clasper uniformly yellow ......
　　..**3**
3　　Gonostylus long and slender, about 1.5 times length of gonocoxite ....
　　...***P. bannaensis***
–　　Gonostylus short, as long as gonocoxite (Fig. 4b, h)...**4**
4　　Postnotum dark brown with a large yellow spot **5**
–　　Postnotum uniformly black..**6**
5　　Wing with spots at forks of R_{1+2}, R_{4+5} and M_{1+2} forming a band (Fig. 2c); abdomen with first tergum yellow with caudal 1/5 light brown; subapical spine of epandrium absent (Fig. 2b); anterior lobe of basal lobe of gonostylus not bilobate, medial lobe of basal lobe of gonostylus not bilobate; apical process of paramere semilunar, apex expanding outward...***P. cordata***
–　　Wing with spots at forks of R_{1+2}, R_{4+5} and M_{1+2} separated (Fig. 2b); abdomen with first tergum dark brown with basal 1/5 yellow; subapical spine of epandrium transverse conical; anterior lobe of basal lobe of gonostylus bilobate, medial lobe of basal lobe of gonostylus bilobate; apical process of paramere hook-shaped, apex incurved..***P. yunnanica***
6　　Wing with a distinct spot at fork of R_{4+5}, spots at forks of R_{1+2} and M_{1+2} weak and nearly invisible ....***P. lii***
–　　Wing with three distinct spots at forks of R_{1+2}, R_{4+5} and M_{1+2}, separated or forming a band..**7**
7　　Second tergum anterior margin yellow with a median brown spot; medial lobe of basal lobe of gonostylus slender, finger-shaped ....***P. lushuiensis***
–　　Second tergum anterior margin yellow brown; medial lobe of basal lobe of gonostylus board, tongue-shaped **8**
8　　Abdomen with 5th and 6th terga mostly yellow, 6th and 7th sterna yellow; apical stylus of gonostylus finger-shaped (Nakamura and Saigusa 2009) ....***P. formosensis***
–　　Abdomen with 5th and 6th terga dark brown, 6th and 7th sterna mostly brown; apical stylus of gonostylus hook-shaped **9**

9   Sixth and 7th sterna yellow, tip of surstylus curved up when viewed from the lateral side, retrose basal projection on inner side with tip bilobate, paramere with a pair of hook-shaped projections and a pair of conical projections, subapical sclerite of aedeagus serrated with five teeth ....***P. tianmushana***

–   Sixth and 7th sterna mostly brown, tip of surstylus not curved up when viewed from the lateral side, retrose basal projection on inner side not bilobate at tip, paramere with a pair of slender L-shaped projections, subapical sclerite of aedeagus serrated with two teeth .... ***P. emeica***

10   Mesopleuron uniformly yellow **11**

–   Mesopleuron mostly brown or black..**14**

11   Wing with bands and clouds (Fig. 2b, c)...**13**

–   Wing without band or cloud...**12**

12   Scutellum uniformly yellow brown; 2nd tergum mostly yellow with posterior margin brown; epandrial clasper without papillary projection on inner side; medial lobe of basal lobe of gonostylus semicircular ....***P. wangae***

–   Scutellum mostly brownish black, middle area yellow (Fig. 1b); 2nd tergum mostly brownish black with middle area yellow; epandrial clasper with two papillary projections on inner side (Fig. 4a); medial lobe of basal lobe of gonostylus ear-shaped (Fig. 4b) ....***P. hekouensis* sp.nov.**

13   Base of Rs with an elliptic cloud; abdomen with sterna yellow ....***P. qinggouensis***

–   Base of Rs without cloud; abdomen with sterna black (Alexander 1935)............. .... ***P. clitellaria***

14   Epandrial lobes merged with epandrial claspers (Fig. 4a, g) **15**

–   Epandrial lobes not merged with epandrial claspers (Fig. 4d) **20**

15   Wing with r-m separated from fork of Rs by longer than its own length; epandrial claspers short and blunt .... ***P. separata***

–   Wing with r-m close to fork of Rs; epandrial claspers slender.........................**16**

16   Wing with an elliptic cloud at middle of CuA$_1$ (Fig. 2c) **17**

–   Wing without an elliptic cloud at middle of CuA$_1$ **19**

17   Epandrial clasper without a curved finger-shaped projection interiorly............**18**

–   Epandrial clasper with a curved finger-shaped projection interiorly (Fig. 4g)....... ....***P. xiaohuangshana* sp. nov.**

18   Epandrial claspers curved downward, tip bifurcated....................***P. gutianshana***

–   Epandrial claspers straight, tip not bifurcated....................................***P. bellula***

19   Gonostylus much longer than gonocoxite ....***P. xinglongshana***

–   Gonostylus not longer than gonocoxite..................................***P. longwangshana***

20   Epandrium bilobed, epandrial claspers not merged basally.............................**21**

–   Epandrium not bilobed, epandrial claspers merged basally (Fig. 4d) ....***P. longa* sp. nov.**

21   Abdomen with 2nd and 3rd terga brownish black; epandrial claspers finger-shaped and broad basally, curved inwards at middle..***P. lucida***

–   Abdomen with 2nd and 3rd terga mostly yellow; epandrial claspers flat and acinaciform, middle of inner edge slightly swollen................................***P. yankovskiana***

Ptychoptera hekouensis **Kang, Gao & Zhang, sp. nov.**
https://zoobank.org/97105AE4-40AD-46BC-A51F-1E5A7E48A464
Figs 1a, b, 2a, 3a, 4a–c, 5a–c

Diagnosis. Scutellum mostly brownish black, middle area yellow; wing marked with small brown marks at base of Rs, tip of R_1, base of R_{2+3}, fork of R_{4+5}, r-m, and fork of M_{1+2}; epandrial clasper tapering and slightly curved distally to the middle, inner side with two papillary projections; medial lobe of basal lobe of gonostylus ear-shaped.

Description. Male. Body length 8.0 mm, wing length 9.0 mm.

Vertex and frons black; face and clypeus yellow with brown hairs; gena yellow with a black elliptical spot medially, hairs on gena dark brown; occiput yellow. Compound eyes black without pubescence. Scape, pedicel and basal 1/2 of 1st flagellomere yellow, remaining flagellomeres dark brown; hairs dark brown. Proboscis yellow with brown hairs. Palpus yellow with last segment gradually darked apically, hairs brown.

Thorax (Fig. 1a, b). Pronotum and propleuron yellow. Prescutum mostly brownish black, anterior margin with lateral area yellow; scutum and paratergite mostly brownish black, posterior margin yellow; scutellum mostly brownish black, middle area yellow with a patch of dense brown hairs; postnotum yellow. Mesopleuron uniformly yellow. Coxae and trochanters yellow. Wing (Fig. 2a) 3.3 times as long as wide, subhyaline, apical 1/2 slightly brown, marked with small brown marks at base of Rs, tip of R_1, base of R_{2+3}, fork of R_{4+5}, r-m, and fork of M_{1+2}. Veins brown; Sc ending in C exceeding basal 1/3 of R_{2+3}; Rs straight, 4 times the length of r-m; r-m arise from Rs. Wing with setae below fold in cell cua_2, and over tip 1/3 of wing. Halter and prehaltere pale yellow with brown hairs.

Abdomen. First tergum yellow with caudal 1/3 brownish black, 2nd tergum brownish black with middle area yellow, 3rd tergum yellow with caudal 1/3 brownish black, 4th tergum yellow with caudal 1/2 black, 5th to 7th terga black; first to 4th sterna yellow, 5th to 7th sterna black; hairs on abdomen yellow.

Male genitalia (Figs 3a, 4a–c, 5a–c) black except caudal 1/2 of epandrial clasper brownish yellow. Epandrium (Fig. 4a) bilobed, epandrial lobe narrow, epandrial clasper tapering and slightly curved distally to the middle, inner side with two papillary projections, with brown long hairs; epiproct V-shaped, with short hairs. Gonocoxite (Fig. 4b) long and stout, 2 times as long as wide, basal apodeme small; apical process of paramere triangular, apex semilunar. Gonostylus (Fig. 4b): anterior lobe of basal lobe of gonostylus elliptic with dense short hairs; medial lobe of basal lobe of gonostylus ear-shaped with dense short hairs; secondary lobe of apical stylus of gonostylus finger-shaped, slightly curved distally with several long hairs; tertiary lobe of apical stylus of gonostylus triangular, pointed apically; apical stylus of gonostylus finger-shaped, swollen distally with long hairs. Hypandrium (Fig. 4c): basal division of hypandrium dumbbell-shaped basally with dense long hairs posteriorly; spathate lobe of hypandrium triangular with several long hairs; lateral extension of terminal division of hypandrium elliptic with dense long hairs on posterior 1/2; terminal division of hypandrium papillary. Aedeagus (Fig. 5a–c): subapical sclerite tongue-shaped, apex of subapical sclerite round; aedeagal sclerites with apex laterally compressed, with dorsal corner extended dorsoanterior,
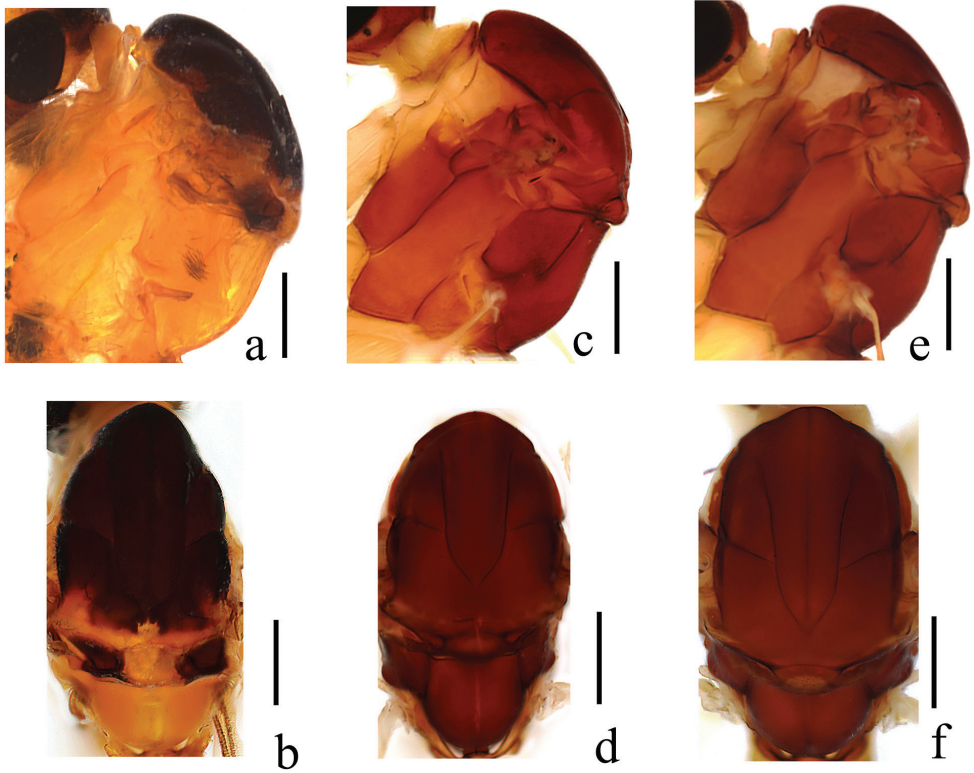
Figure 1. Thoraxes of new *Ptychoptera* species **a** *P. hekouensis*, dorsal view **b** *P. hekouensis*, lateral view **c** *P. longa*, dorsal view **d** *P. longa*, lateral view **e** *P. xiaohuangshana*, dorsal view **f** *P. xiaohuangshana*, lateral view. Scale bars: 0.5 mm.

curved sided and convergent; lateral ejaculatory processes with base narrow, extended anterolaterally; sperm sac subspherical; ejaculatory apodeme flag-like, closely associated with aedeagal sclerites, larger than sperm sac, paralleling anterior margin of sperm sac.

Female. Unknown.

Material examined. China·1♂, *holotype*; Yunnan Province, Hekou District, Nanxi Town; 132 m; 22 May 2009; T. Zhang leg.; CAU·1♂, *paratype*; same collection data as holotype; CAU.

Distribution. China (Yunnan).

Etymology. Specific name *hekouensis* (adjective, feminine) referring to the type locality, Hekou.

Remarks. This new species is similar to *P. wangae* from China but can be separated from the latter by the scutellum mostly brownish black with middle area yellow, the 2nd tergum mostly brownish black with middle area yellow, the epandrial clasper with two papillary projections on inner side, and the medial lobe of basal lobe of gonostylus ear-shaped. In *P. wangae*, the scutellum is uniformly yellow brown, the 2nd tergum is mostly yellow with posterior margin brown, the epandrial clasper does not have papillary projection on inner side, and the medial lobe of basal lobe of gonostylus is semicircular (Kang et al. 2013).
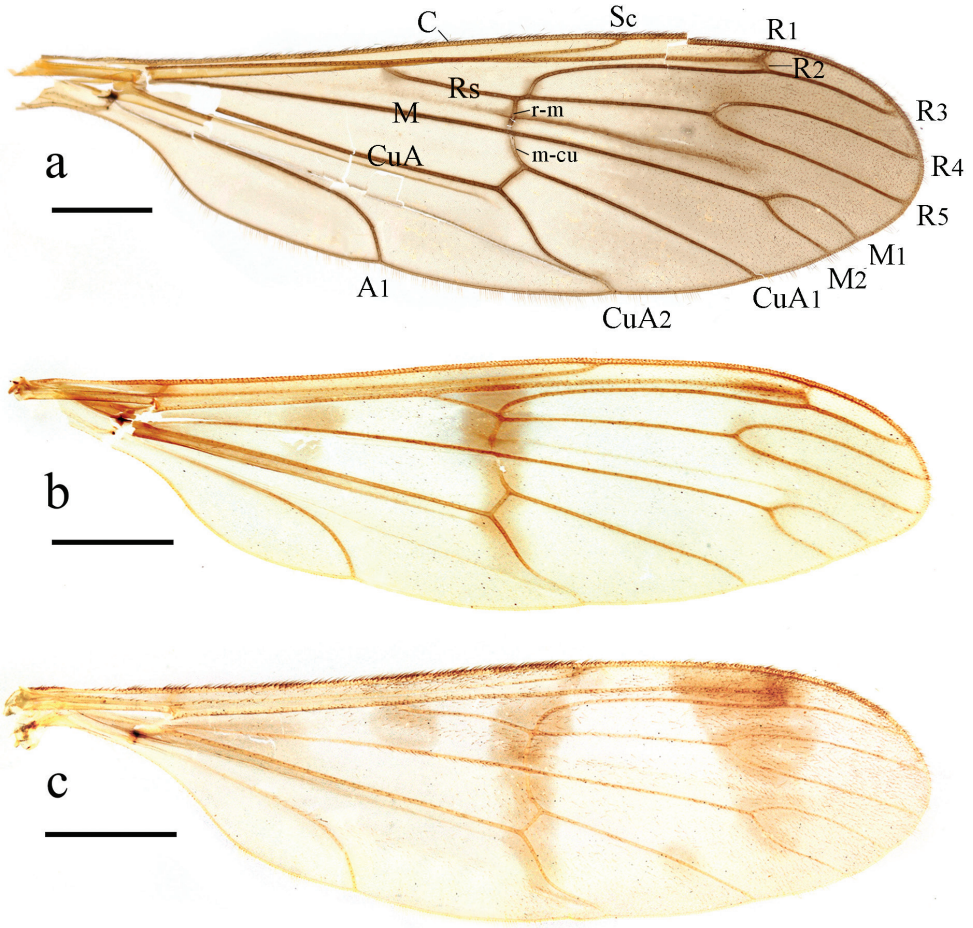
Figure 2. Wings of new *Ptychoptera* species **a** *P. hekouensis* **b** *P. longa* **c** *P. xiaohuangshana*. Scale bars: 1.0 mm.

Ptychoptera longa Kang, Gao & Zhang, sp. nov.

https://zoobank.org/E6BFCB06-E52C-452F-94AF-9C2A725CB967
Figs 1c, d, 2b, 3b, 4d–f, 5d–f

Diagnosis. Mesopleuron mostly brown, except upper 1/2 of anepisternum yellow; wing marked with four brown marks and one brown band; epandrium not bilobed, epandrial lobe rectangle; epandrial clasper finger-shaped, merged basally, basal 1/2 broad and rectangle, apical 1/2 narrowing bilaterally; secondary lobe of apical stylus of gonostylus sickle-shaped; terminal division of hypandrium elliptic.

Description. Male. Body length 7.5 mm, wing length 7.5 mm.

Vertex and frons brown; face and clypeus yellow with brown hairs; gena yellow with a black elliptical spot medially, hairs on gena brown; occiput yellow. Compound eyes black without pubescence. Scape and pedicel yellow, flagellomeres light yellow; hairs on antenna brown. Proboscis yellow with brown hairs. Palpus yellow with brown hairs.
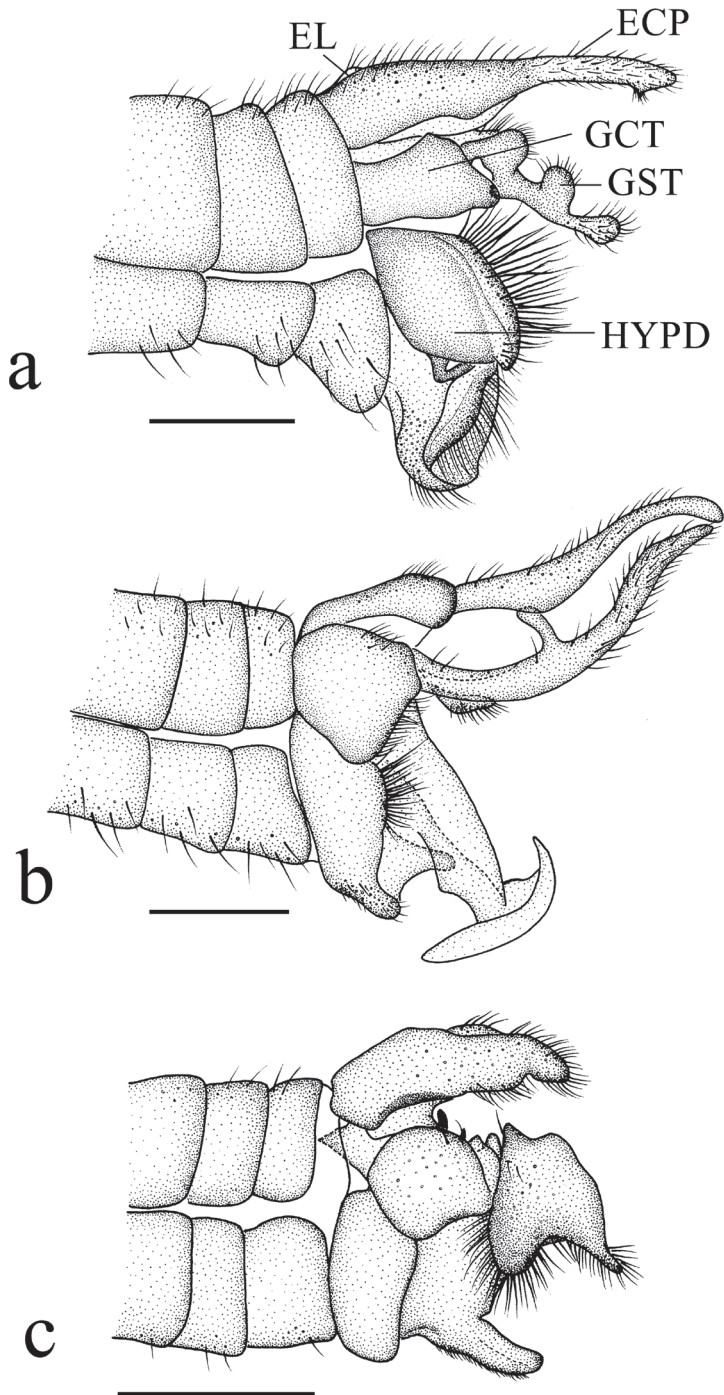
Figure 3. Male genitalia of new *Ptychoptera* species **a** *P. hekouensis* **b** *P. longa* **c** *P. xiaohuangshana*. Scale bars: 0.5 mm. (ECP = epandrial clasper, EL = epandrial lobe, GCT = gonocoxite, GST = gonostylus, HYPD = hypandrium).
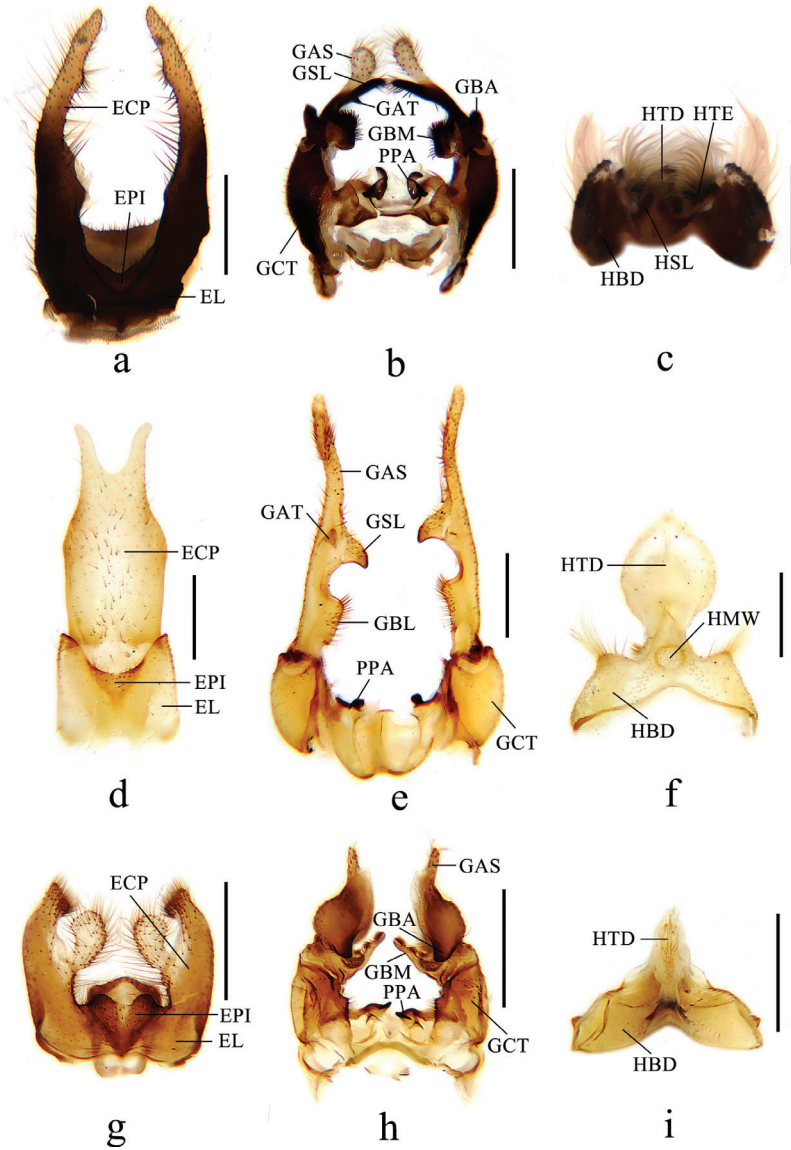
Figure 4. Details of male genitalia of new *Ptychoptera* species **a** epandrium of *P. hekouensis*, dorsal view **b** gonocoxite and gonostylus of *P. hekouensis*, dorsal view **c** hypandrium of *P. hekouensis*, ventral view **d** epandrium of *P. longa*, dorsal view **e** gonocoxite and gonostylus of *P. longa*, dorsal view **f** hypandrium of *P. longa*, ventral view **g** epandrium of *P. xiaohuangshana*, dorsal view **h** gonocoxite and gonostylus of *P. xiaohuangshana*, dorsal view **i** hypandrium of *P. xiaohuangshana*, ventral view. Scale bars: 0.4 mm. (ECP = epandrial clasper, EL = epandrial lobe, EPI = epiproct, GAS = apical stylus of gonostylus, GBA = anterior lobe of basal lobe of gonostylus, GBL = basal lobe of gonostylus, GBM = medial lobe of basal lobe of gonostylus, GCT = gonocoxite, GSL = secondary lobe of apical stylus of gonostylus, GAT = tertiary lobe of apical stylus of gonostylus, HBD = basal division of hypandrium, HMW = membranous window of terminal division of hypandrium, HSL = spathate lobe of hypandrium, HTD = terminal division of hypandrium, HTE = lateral extension of terminal division of hypandrium, PPA = apical process of paramere).

Thorax (Fig. 1c, d). Pronotum light brown; propleuron yellow. Prescutum, scutum and paratergite uniformly brown; scutellum mostly brown, middle area yellowish brown; postnotum brown, laterotergite with a patch of dense brown hairs. Mesopleuron mostly brown, except upper ½ of anepisternum yellow. Coxae and trochanters yellow. Wing (Fig. 2b) 3.8 times as long as wide, subhyaline, marked with four brown marks and one brown band as follows: four elliptic brown marks at base of cell R, tip of R_1, fork of R_{4+5}, and fork of M_{1+2}; one brown band extending from anterior margin of wing, covering base of R_{2+3} and r-m, to the bend in distal section of CuA_2. Veins brown; Sc ending in C at level of basal 1/3 of R_{2+3}; Rs straight, 2 times the length of r-m; r-m arise from R_{4+5}. Wing with setae over Sc and Rs, at and below fold in cell cua_2, and over tip 1/2 of wing (sparse before forks of R_{4+5} and M_{1+2}). Halter and prehaltere pale yellow with light brown hairs.

Abdomen. First tergum brown with basal 1/3 yellow, 2nd tergum brown with middle 1/3 yellow, 3rd tergum yellow with caudal 1/3 brown, 4th to 6th terga brown, 7th tergum brown with posterior margin yellow; first to 3rd sterna yellow, 4th to 6th sterna brown with posterior margin yellow, 7th sternum yellow; hairs on abdomen brown.

Male genitalia (Figs 3b, 4d–f, 5d–f) yellow. Epandrium (Fig. 4d) not bilobed, epandrial lobe rectangle, posterior margin with U-shaped concave; epandrial clasper finger-shaped, merged basally, basal 1/2 broad and rectangle, apical 1/2 narrowing bilaterally, with short brown hairs; epiproct triangular with short hairs. Gonocoxite (Fig. 4e) short and stout, 1.5 times as long as wide, basal apodeme small; apical process of paramere papillary, apex with hooked projection. Gonostylus (Fig. 4e): basal lobe of gonostylus ear-shaped with dense short hairs on inner side; secondary lobe of apical stylus of gonostylus sickle-shaped with short hairs; tertiary lobe of apical stylus of gonostylus triangular, round apically; apical stylus of gonostylus long and slender, finger-shaped with short hairs. Hypandrium (Fig. 4f): basal division of hypandrium trapeziform, anterior margin with V-shaped concave, posterior margin with dense long hairs; membranous window of terminal division circular; terminal division of hypandrium elliptic. Aedeagus (Fig. 5d–f): subapical sclerite rectangular, apex of subapical sclerite slightly concave; aedeagal sclerites with apex laterally compressed, with dorsal corner extended dorsoanterior, curved sided and convergent, base broad; lateral ejaculatory processes with base straight, narrow, extended straight anterolaterally; sperm sac subspherical; ejaculatory apodeme flag-like, closely associated with aedeagal sclerites, larger than sperm sac, paralleling anterior margin of sperm sac.

Female. Unknown.

Material examined. Сhina·1♂, *holotype*; Guizhou Province, Suiyang District, Kuankuoshui National Nature Reserve; 11 Aug. 2010; S. Liu leg.; CAU·1♂, *paratype*; same collection data as holotype; CAU.

Distribution. China (Guizhou).

Etymology. Specific name from Latin *longa* (adjective, feminine, meaning "long"), referring to the long epandrial clasper.

Remarks. This new species is similar to *P. yankovskiana* from China and Korea but can be separated from the latter by first tergum brown with basal 1/3 yellow, the epandrium not bilobed, and the epandrial claspers merged basally. In *P. yankovskiana*, the first tergum is uniformly dark brown, the epandrium is bilobed and the epandrial claspers is not merged basally (Kang et al. 2019).

Ptychoptera xiaohuangshana Kang, Gao & Zhang, sp. nov.

https://zoobank.org/564AC7EB-55BD-46AA-8474-8F99541D9028
Figs 1e, f, 2c, 3c, 4g–i, 5g–i

Diagnosis. Mesopleuron mostly brown, except upper 1/2 of anepisternum yellow; wing marked with three brown marks and two brown bands; epandrial clasper with a curved finger-shaped projection interiorly; anterior lobe of basal lobe of gonostylus nose-shaped; medial lobe of basal lobe of gonostylus toothbrush-shaped.

Description. Male. Body length 7.0 mm, wing length 7.0 mm.

Vertex and frons brown; face and clypeus yellow with light brown hairs; gena yellow with a black elliptical spot medially, hairs on gena brown; occiput yellow. Compound eyes black without pubescence. Scape and pedicel yellow, flagellomeres light yellow; hairs on antenna brown. Proboscis light yellow with light yellow hairs. Palpus light yellow with light yellow hairs.

Thorax (Fig. 1e, f). Pronotum and propleuron light brown. Prescutum, scutum, and paratergite uniformly brown; scutellum mostly brown, middle area yellowish brown; postnotum brown, laterotergite with a patch of dense brown hairs. Mesopleuron mostly brown, except upper ½ of anepisternum yellow. Coxae and trochanters yellow; femora yellow with brown ring apically; hairs on legs brown. Wing (Fig. 2c) 3.8 times as long as wide, subhyaline, marked with three brown marks and two brown bands as follows: one triangular brown mark at base of M, two elliptic brown marks at base of Rs and at midlength of CuA_1; median band extending from anterior margin of wing, covering base of R_{2+3} and r-m, to the bend in distal section of CuA_2; subapical band extending from anterior margin of wing, covering tip of R_1, R_2, and fork of R_{4+5}, to fork of M_{1+2}. Veins brown; Sc ending in C not at level of basal third of R_{2+3}; Rs slightly curved medially, 4.1 times the length of r-m; r-m arise from Rs. Wing with setae over Sc and Rs, at and below fold in cell cua_2, and over tip 1/2 of wing (slightly sparse before forks of R_{4+5} and M_{1+2}). Halter and prehaltere pale yellow with light brown hairs.

Abdomen. First tergum light brown, 2nd tergum light brown with middle 1/3 yellow, 3rd tergum yellow caudal 1/2 light brown, 4th to 6th terga light brown, 7th tergum yellow with basal 1/3 light brown; first to 3rd sterna yellow, 4th to 6th sterna light brown with posterior margin yellow, 7th sternum yellow with basal 1/3 light brown; hairs on abdomen light brown.

Male genitalia (Figs 3c, 4g–i, 5g–i) brown. Epandrium (Fig. 4g) bilobed, epandrial lobe semicircular; epandrial clasper broad basally, with a curved finger-shaped projection interiorly, finger-shaped projection basally narrow, apically swollen, with uniformly long hairs; epandrial clasper narrowed medially and slightly curved ventrally, slightly swollen and flat apically, with dense long hairs; epiproct triangular, with two papillary projections posteriorly, with short hairs. Gonocoxite (Fig. 4h) broad, 2 times as long as wide, inner side with a triangular projection medially, with dense hairs; basal apodeme small; apical process of paramere hooked. Gonostylus (Fig. 4h): anterior lobe of basal lobe of gonostylus nose-shaped with several long hairs; medial lobe of basal lobe of gonostylus toothbrush-shaped, with a hairy semilunar lobe basally and a hairy papillary projection medially; apical stylus of gonostylus finger-shaped with short hairs. Hypandrium (Fig. 4i):
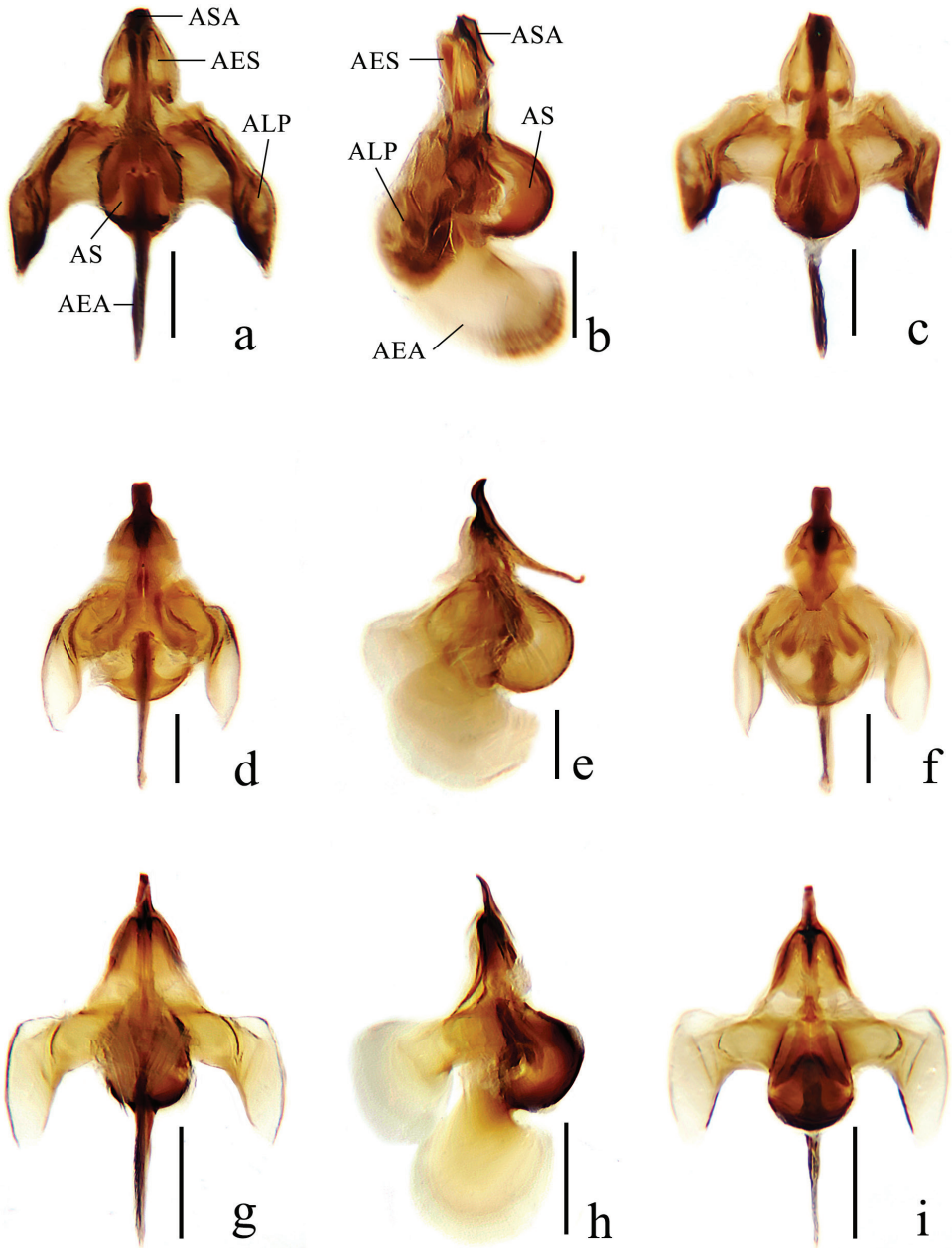
Figure 5. Aedeagi of new *Ptychoptera* species **a** *P. hekouensis*, dorsal view **b** *P. hekouensis*, lateral view **c** *P. hekouensis*, ventral view **d** *P. longa*, dorsal view **e** *P. longa*, lateral view **f** *P. longa*, ventral view **g** *P. xiaohuangshana*, dorsal view **h** *P. xiaohuangshana*, lateral view **i** *P. xiaohuangshana*, ventral view. Scale bars: 0.2 mm. (AEA = ejaculatory apodeme, AES = aedeagal sclerite, ALP = lateral ejaculatory process, AS = sperm sac, ASA = subapical sclerite of aedeagus).

basal division of hypandrium triangular, anterior margin with V-shaped concave; terminal division of hypandrium gourd-shaped with dense short hairs. Aedeagus (Fig. 5g–i): subapical sclerite triangular, apex of subapical sclerite flat; aedeagal sclerites with apex laterally compressed, with dorsal corner extended dorsoanterior, curved sided and convergent, base broad; lateral ejaculatory processes with base straight, extended straight anterolaterally; sperm sac subspherical; ejaculatory apodeme flag-like, closely associated with aedeagal sclerites, larger than sperm sac, paralleling anterior margin of sperm sac.

Female. Unknown.

Material examined. China·1♂, ***holotype***; Guangdong Province, Ruyuan District, Nanling National Forest Park, Mount Xiaohuangshan; 24 Aug. 2010; T. Zhang leg.; CAU·1♂, ***paratype***; same collection data as holotype; CAU.

Distribution. China (Guangdong).

Etymology. Specific name *xiaohuangshana* (adjective, feminine) referring to the type locality, Mount Xiaohuangshan.

Remarks. This new species is similar to *P. bellula* from China but can be separated from the latter by the 2nd tergum light brown with middle 1/3 yellow, the epandrial clasper with a curved finger-shaped projection interiorly, the epiproct with two papillary projections posteriorly, and the medial lobe of basal lobe of gonostylus toothbrush-shaped. In *P. bellula*, the 2nd tergum is black with base yellow, the epandrial clasper does not have a curved finger-shaped projection interiorly, the epiproct have a strongly haired papillary projection posteriorly, and the medial lobe of basal lobe of gonostylus is semilunar (Alexander 1937; Krzeminski and Zwick 1993).

Acknowledgements

References

Alexander CP (1924) Undescribed species of Japanese Ptychopteridae (Diptera). Insecutor Inscitiae Menstruus 9: 80–83.

Alexander CP (1935) New or little-known Tipulidae from eastern Asia (Diptera). XXIII–XXVII. Philippine Journal of Science 56: 339–372.

Alexander CP (1937) New species of Ptychopteridae (Diptera). Bulletin of the Brooklyn Entomological Society 32: 140–143.

Alexander CP (1945) Undescribed species of crane-flies from northern Korea (Diptera, Tipuloidea). Transactions of the Royal Entomological Society of London 95(4): 227–246. https://doi.org/10.1111/j.1365-2311.1945.tb00261.x

Alexander CP (1981) Ptychopteridae. In: McAlpine JF, Peterson BV, Shewell GE, Teskey HJ, Vockeroth JR, Wood DM (Eds) Manual of Nearctic Diptera (Vol. I). Agriculture Canada Monograph 27. Agriculture Canada, Ottawa, 325–328.

Fasbender A (2014) Phylogeny and diversity of the phantom crane flies (Diptera: Ptychopteridae). PhD Dissertation, Iowa State University, Ames, 855 pp.

Kang ZH, Yao G, Yang D (2013) Five new species of *Ptychoptera* Meigen with a key to species from China (Diptera: Ptychopteridae). Zootaxa 3682(4): 541–555. https://doi.org/10.11646/zootaxa.3682.4.5

Kang ZH, Xue ZX, Zhang X (2019) New species and record of *Ptychoptera* Meigen, 1803 (Diptera: Ptychopteridae) from China. Zootaxa 4648(3): 455–4723. https://doi.org/10.11646/zootaxa.4648.3.3

Krzeminski W, Zwick P (1993) New and little known Ptychopteridae (Diptera) from the Palaearctic region. Aquatic Insects 15(2): 65–87. https://doi.org/10.1080/01650429309361504

McAlpine JF (1981) Morphology and terminology: Adults. In: McAlpine JF, Peterson BV, Shewell GE, Teskey HJ, Vockeroth JR, Wood DM (Eds) Manual of Nearctic Diptera Vol. 1. Agriculture Canada Monograph 27. Agriculture Canada, Ottawa, 9–63.

Meigen JW (1803) Versuch einer neuen Gattungs-Eintheilung der europaischen zweiflugligen Insekten. Magazin für Insektenkunde (Illiger) 2: 259–281.

Nakamura T, Saigusa T (2009) Taxonomic study of the family Ptychopteridae of Japan (Diptera). Zoosymposia 3(1): 273–303. https://doi.org/10.11646/zoosymposia.3.1.23

Rozkošný R (1997) Family Ptychopteridae. In: Papp L, Darvas B (Eds) Contributions to a Manual of Palaearctic Diptera (with Special Reference to Flies of Economic Importance), Volume 2: Nematocera and Lower Brachycera. Science Herald, Budapest, 291–297.

Shao JQ, Kang ZH (2021) New species of the genus *Ptychoptera* Meigen, 1803 (Diptera, Ptychopteridae) from Zhejiang, China with an updated key to Chinese species. ZooKeys 1070: 87–99. https://doi.org/10.3897/zookeys.1070.67779

Yang JK (1996) New record of family Ptychopteridae in Xinglongshan (Diptera: Ptychopteridae). In: Wang X (Ed.) Resources Background Investigation of Gansu Xinglongshan National Nature Reserve. Gansu Minorities Press, Gansu, 288–289.

Yang JK, Chen HY (1995) Diptera: Ptychopteridae. In: Zhu T (Ed.) Insects and Macrofungi of Gutianshan, Zhejiang. Zhejiang Scientech Press, Hangzhou, 180–182.

Yang JK, Chen HY (1998) Diptera: Ptychopteridae. In: Wu H (Ed.) Insects of Longwangshan Nature Reserve. China Forestry Publishing House, Beijing, 240–241.

Zhang X, Kang ZH (2021) Two new species of the genus *Ptychoptera* Meigen, 1803 (Diptera, Ptychopteridae) from Yunnan, China with remarks on the distribution of Chinese species. ZooKeys 1070: 73–86. https://doi.org/10.3897/zookeys.1070.58859

CORRIGENDA

Corrigenda: Harding LE (2022) Available names for *Rangifer* (Mammalia, Artiodactyla, Cervidae) species and subspecies. ZooKeys 1119: 117–151. https://doi.org/10.3897/zookeys.1119.80233

Lee Harding[1]

1 *Canadian Wildlife Service (retired), Delta, Canada*

Corresponding author: Lee Harding (leeharding@shaw.ca)

Citation: Harding L (2022) Corrigenda: Harding LE (2022) Available names for *Rangifer* (Mammalia, Artiodactyla, Cervidae) species and subspecies. ZooKeys 1119: 117–151. https://doi.org/10.3897/zookeys.1119.80233. ZooKeys 1122: 173–174. https://doi.org/10.3897/zookeys.1122.94672

As a result of copy-editing cut-and-paste errors, incorrect authorities were given in two cases.

The corrected authorities are:

R[*angifer*] *platyrhynchus* (Vrolich, 1828).
Rangifer groenlandicus (Borowski, 1780) as Greenland Caribou (Kellogg 1932). Linnaeus (1767) gave *groenlandicus* as a junior synonym for circumpolar *R. tarandus*.

The Taxonomic Conclusions were not affected and the Synonymy (suppl. material 1) is correct.

References

Borowski GH (1780) Gemeinnüzzige Naturgeschichte des Thierreichs : darinn die merkwürdigsten und nüzlichsten Thiere in systematischer Ordnung beschrieben, und die Geschlechter in Abbildungen nach der Natur vorgestellet werden. Vol. 1 Part 4,Gottlieb August Lange, Berlin and Stralsund, 360 pp. https://doi.org/10.5962/bhl.title.40486

Kellogg R (1932) New names for mammals proposed by Borowski in 1780 and 1781. Proceedings of the Biological Society of Washington 45: 147–148.

Linné [Linnæus] C (1767) Systema naturae per regna tria naturae, secundum classes, ordines, genera, species, cum characteribus, differentiis, synonymis, locis Editio 12. Vol. Tomus I Editio duodecima,Vindobonae, Upsalla, Sweden, 1327 pp. https://doi.org/10.5962/bhl.title.156772

Vrolich [Vrolik] W (1828) Rendier. In: Nieuwe Verhandelingen der eerste Klasse van het Koninklijk-Nederlandsche Instituut van Wetenschappen, Letterkunde en Schoone Kunsten te Amsterdam. Amsterdam, 160.